IGNITION CHARACTERISTICS OF PLASTICS

by

HILARY E. THOMSON

DOCTOR OF PHILOSOPHY

University of Edinburgh

1988

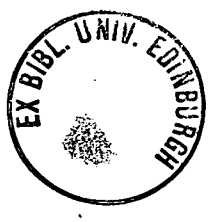

DECLARATION

It is declared that this thesis and the results therein contained are the work of the author, herself, and have been produced under the supervision of Dr D.D. Drysdale.

Hilary E. Thomson
Edinburgh
May, 1988

Greville, Fulke, First Baron Brooke (1554-1628)

"Fire and people do in this agree,
They both good servants, both ill masters be"

'Inquisition upon Fame'

IN MEMORY OF ROSS A.M. THOMSON, BSc, PhD, CChem, FRSC.

ACKNOWLEDGEMENTS

The author wishes to express her gratitude to the following persons for their invaluable contributions to this work:

Dr D. Drysdale for his supervision, advice and encouragement throughout the period of research.

Mr L. Russel for technical assistance with apparatus design and construction.

Mr A. M^{c} Innes for advice on construction of electronic circuitry.

Mr R. O'Donnel for production of photographs contained in this thesis.

Dr D. Sheen for provision of TGA apparatus at Strathclyde University.

The Micro Support Unit (Physical Sciences) for their advice on the production of this thesis.

Finally, my husband, Andrew, for his proof reading and forbearance.

This work was supported by grants from the Home Office, the Fire Research and Training Trust and the IBM Corporation.

ABSTRACT

The piloted ignition of a range of common thermoplastics has been studied by exposing horizontal samples (65 x 65 x 6mm thick) to irradiance levels in the range 10-40kW/m^2. Fine thermocouples attached to the exposed and rear faces allowed continuous monitoring of surface temperatures. A small H_2 pilot flame was applied at 4 second intervals and the times to sustained ignition and the corresponding surface temperatures were recorded. Within the limits of experimental error and with the exception of PMMA at the lowest heat flux, ignition temperature showed no systematic dependence on radiation intensity or spectral characteristics of the source, although separate experiments indicated a dependence on surface area when this was reduced to less than ca 4cm^2. Ignition delay times proved to be dependent not only on radiant intensity but also on spectral characteristics of the source and various other experimental variables. Similar observations were made when these experiments were repeated in the ISO ignitability apparatus.

A theoretical model for piloted ignition based on the numerical solution of heat transfer equations for a semi-infinite solid and with critical firepoint temperature as the criterion for ignition was developed. Improved predictive results were obtained by adapting the model to incorporate the effects of diathermancy and source emission/sample absorption interactions.

An experimental rig was designed and constructed which allowed sample weight to be monitored continuously during experiments. The minimum rate of evolution of decomposition products necessary to support flashing and sustained ignition by pilot was determined for the range of thermoplastics studied previously. These results are significantly lower than results reported elsewhere. This may be

attributed to differences in the convective heat transfer coefficient at the surface in the various experimental rigs.

The effect of two different fire retardant systems on ignition was investigated by determining the firepoint temperature, ignition delay time and critical mass flux at piloted ignition for three fire retarded plastics and comparing these with the equivalent values for the unmodified parent materials. Limiting oxygen index (LOI) values were also determined. The fire retarded modifications exhibited higher values in all four measured parameters than their untreated counterparts.

TABLE OF CONTENTS

TABLE OF CONTENTS

TABLES

TABLES (cont.)

CHAPTER 5 DISCUSSION (cont.)

FIGURES

FIGURES (cont.)

NOMENCLATURE

A	Arrhenius factor
A'	Sample area (m^2)
c	Thermal capacity (J/kg.K)
C	Conversion factor (equation 2.3) (g/mV)
e_λ	Monochromatic emissivity
E	Internal energy (kJ/g)
E_A	Activation energy (J/mole)
f	Fuel/air ratio
f_s	Heat flux into solid (kW/m^2)
F_o	Fourier number
h	Convective heat transfer coefficient ($W/m^2.K$)
H	Enthalpy (kJ/g)
ΔH_c	Heat of combustion (kJ/g)
k	Thermal conductivity (W/m.K)
l	Thickness (m)
L	Latent heat of gasification (J/g)
LOI	Limiting oxygen index
m	Mass flow rate (g/s)
n	An integer
N	Newtonian cooling constant (h.k)
Q"	Incident radiant heat flux (kW/m^2)
Q''_{ext}	External heat flux absorbed at surface (kW/m^2)
Q''_{loss}	Heat loss expressed as flux through surface (kW/m^2)
r	Reflectance
r	Stoichiometric ratio
R	Ideal gas constant
R_x	Heater coil radius (m)
S	Sensible heat transfer rate as defined in equation 1.34
t	Time (s)
Δt	Time increment duration (s)
T	Temperature (C or K)
ΔT	Temperature differential
u	Absorption of energy by diathermancy
V	Chart paper speed (m)
W	Volatile content ($\rho_o-\rho_f$) (g/m^3)
x	Distance (m)

NOMENCLATURE (cont.)

Δx	Increment thickness (m)

Greek Symbols

α	Thermal diffusivity ($k/\rho c$) (m^2/s)
$\bar{\alpha}$	Absorptance
$\bar{\alpha}_\lambda$	Monochromatic absorptance
β	Volumetric expansion coefficient (equation 1.1)
β	Dimensionless group ($\beta=h(\alpha t)^{\frac{1}{2}}$ (equation 1.18)
ε	Emissivity
λ	Wavelength (μm)
$\Delta\lambda$	Wavelength increment (μm)
ρ	Density (g/m^3)
σ	Stefan-Boltzmann constant ($5.67\times10^{-8} W/m^2.K^4$)

Subscripts

cr	Critical
f	Flame, final
fl	Flashpoint
g	Gas phase
ig	Ignition
m	Mean
x	In the x-direction
0	Ambient, initial
∞	Final value

Superscripts

"	Per unit area

CHAPTER 1

INTRODUCTION

CHAPTER 1
INTRODUCTION

1.1 BACKGROUND

In the history of mankind, fire has proved both a blessing and a curse. Adequately controlled, it provides a highly beneficial source of heat and power to meet a variety of industrial and domestic requirements. Conversely, the consequences of unwanted fires are often devastating in terms of human suffering and material damage. In the United Kingdom alone, some 1000 people die and more than £400 million worth of property are lost each year (U.K. Fire Statistics (1984)). With our ever increasing use of synthetic materials in place of the traditional cellulose based natural products has come the urgent need to understand the behaviour of these man-made substitutes in fire situations and to predict the associated risk.

The earliest reference found relating to investigation of the fire hazards of plastic materials was contained in a report by Stokes and Weber (1917) entitled "Effects of heat on celluloid and similar materials" which stated that

> 'in 1907, at the request of the Steamboat Inspection Service, the Bureau of Standards made a careful study of celluloid and other pyroxylin plastics and afterwards carried out an investigation of their properties with special reference to the hazard connected with their use and transport.'

The concept of flammability has direct applicabilty to combustible gases and liquids, whose fire properties can be quantified in terms of flammability limits (Zabetakis (1965)) and flashpoints (Burgoyne & Williams-Leir (1949), Burgoyne, Roberts & Alexander (1967)), respectively. However there is no equivalent

parameter for the quantification of fire risk relating to a combustible solid. The fire properties of solids tend to be dependent not only on the chemical nature of the material but also on its physical and geometrical form and on the fire environment to which it is exposed. Thus, "flammability" of a solid must take into account the total system in which sample variables and the (potential) fire environment are defined.

1.2 FIRE TESTING

1.2.1 Tests Available

Four types of test relating to assessment of material behaviour in the fire situation can be identified.

- **Ad hoc tests** are generally large scale mock ups devised in response to a particular incident and deal with one specific situation. They lack standardization and the results require careful interpretation and have limited validity when applied to alternative situations.

- **Hazard assessment tests** are small scale laboratory procedures relating to one or more aspects of fire identified after extensive study of the fire problem. They are less specific than ad hoc tests but tend to be apparatus dependent.

- **Quality assurance tests** measure one characteristic with the aim of ensuring that product composition or design remains consistent, for example, the limiting oxygen index test (ASTM D 2863-77 (1977)) is often used in this context.

- **Basic property tests** measure a property or characteristic of materials, such as calorific value, by an established technique. The information provided by these tests can be used only if it is possible to accurately model real situations on the basis of fundamental parameters. In the future, such tests and related models should relegate hazard assessment tests to a position of much lesser importance than that which they occupy at present.

A fire can be divided into three phases (Figure 1.1): the initiating fire, the fully developed fire and the decaying fire.

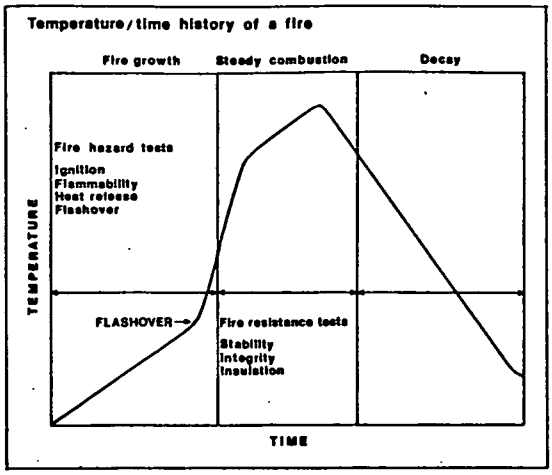

Figure 1.1 Stages in the development of fire.

Experience shows that combustible materials always burn in a fully developed fire. Thus, in estimating fire hazard, only the early stages of combustion up to the point of flashover are relevant. This phase consists of ignition, flame spread, heat release and flashover along with various side effects including smoke release, toxicity and corrosivity of fire gases. In the real situation, these phenomena are influenced by a vast number of interactive parameters such as type, duration and intensity of ignition source, type, form, properties and geometry of the combustibles, ventilation, etc. This degree of complexity is impossible to reproduce in the laboratory .and, consequently, hazard assessment tests do not give accurate predictions about material behaviour in the real fire situation. Since the early 1970s all British Standards describing fire tests have included the following cautionary note:

> 'This standard should be used to measure and describe the the properties of materials, products or assemblies in response to heat and flame under controlled laboratory conditions and should not be used to describe or appraise the fire hazard or fire risk of materials, products or assemblies under actual conditions. However, results of this test may be used as elements of a fire risk assessment which takes into account all of the factors which are pertinent to an assessment of the fire hazard of a particular end use.'

A classic example of the limitations of small scale fire tests is described by Emmons (1974) who compared the rating of twenty four different wall lining materials as obtained in the fire testing laboratories of six European countries, viz., Germany, Belgium, Denmark, France, the Netherlands and U.K. A plot of rating by each country versus the average rating produced a scatter about the expected 45^{0} line which was little better than random. Indeed, a phenolic foam wall board was graded best (out of twenty four) in the German test and worst in the Danish test. It seems incredible that this should have happened, particularly as the results of these tests were being used to assess behaviour on the full scale. Nevertheless, judicious use of standard tests can provide valuable information on the comparative risks associated with various materials. Kishore and Mohandas (1982a) have reviewed some of the more common test methods available, outlining their advantages and disadvantages.

The Building Regulations of most countries stipulate certain minimum requirements for building materials based on their performance in a range of standard fire tests applicable to a particular country. In general, these hazard assessment tests may be subdivided into four broad categories:

1. Ignitability.
2. Flame spread.
3. Heat release.
4. Miscellaneous eg smoke release, flashover, toxicity.

Only categories (1) and (2) relate directly to ignition and some of the more common tests applicable in Britain and the United States within these two sections are listed below (Troitzsch (1982)).

1.2.1.1 Ignitability Tests

Ignition (spontaneous or piloted) is the fundamental process in our understanding of fire and results from the exposure of a combustible material to radiative, convective and/or conductive heating. Ignition not only represents the initial event in any fire but is also the mechanism involved in flame spread, fire growth and the phenomenon known as flashover in compartments. Hence, ignitability is a common feature of fire tests.

Early ignitability tests were generally based on furnace exposure to determine an ignition temperature, an example being the test furnace developed by Setchkin (1949). Subsequently, ignition by flame impingement was investigated, for example BS476: Part 5 (1979). Testing for radiant ignitability is a relatively new approach motivated by the realisation that imposed radiant flux is one of the most important features of room fire development. In such tests, ignition delay times under a range of imposed heat fluxes or alternatively, the minimum heat flux required for ignition, are generally determined.

The ISO ignitability apparatus (ISO 5657-86 (1986)), under development since the early 1970s, represented the first widely used apparatus designed specifically for testing radiant ignitability. More recently, substantial work on radiant ignitability has been carried out by Babrauskas and Parker (1987) using the cone calorimeter which has been put forward by the American Society for Testing and Materials Committee as the basis of a proposed standard.

BS476: Part 5 "Ignitability Test": This test is carried out by exposing one face of a vertical test specimen to a 10mm long gas flame for 10 seconds. The extent of flaming during pilot flame application and for 10 seconds afterwards is noted.

ASTM D 1929-77 "Ignition Properties of Plastics": The Setchkin furnace (Setchkin (1949)), as described in section 1.3.3, is used to determine self- and flash-ignition temperatures with low (25mm/s), moderate (50mm/s) and high (100mm/s) airflow rates and a temperature rise of 600^{0}C/h. This test is mentioned in special cases in the United States Building Regulations, for example, UBC Section 5207 states that domelights must not fall out of their holders at temperatures less than 200^{0}F below their flash-ignition temperature as determined by UBC Standard No.52-3 (= ASTM D 1929).

1.2.1.2 Flammability Tests

Flame spread is critical to the rate at which a fire will develop. In an enclosure, the attainment of fully developed burning requires growth of the fire beyond a certain critical size capable of producing high temperatures (typically $>600^{0}$C) at ceiling level. Therefore, it is important to consider flame spread over combustible materials as a basic component of fire growth. The process of flame spread (Figure 1.3) may be equated to an advancing ignition front where the leading edge of the flame acts as both the source of heat and the pilot. Consequently, the non-steady state heat transfer problems involved in flame spread are similar to those encountered in the pilot ignition of solids.

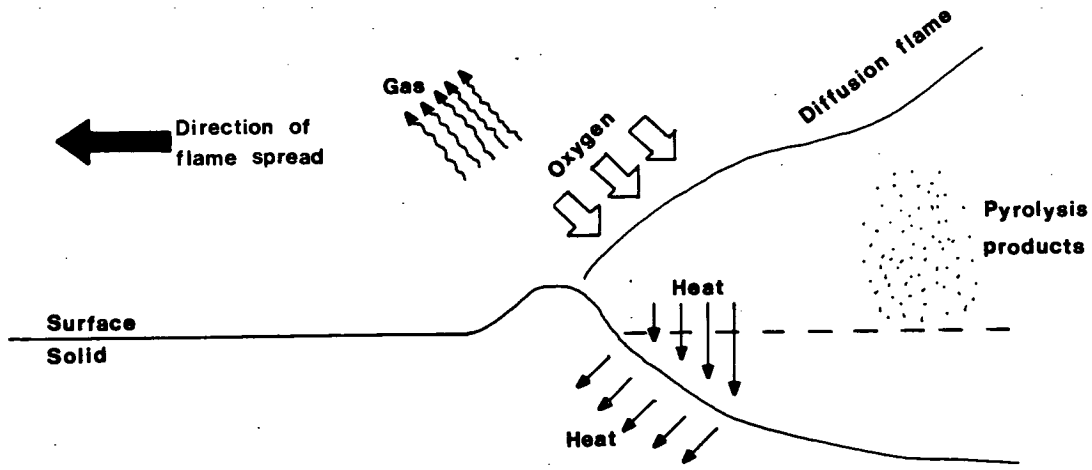

Figure 1.3 Mechanism of flame spread after Akita (1978)

Work on the spread of laminar diffusion flames over solid combustibles has been carried out by several investigators including de Ris (1969), Fernandez-Pello & Williams (1977) and Frey & T'ien (1979). Quintiere (1981) analysed flame spread results from a potential test method apparatus (Robertson (1979)) using a mathematical model developed for the general case of transient flame spread with external radiant heating. This approach is based on fire parameters such as flame heat transfer rate and length rather than on fundamental properties. Similar analyses were carried out by Rockett (1974) for vertical downward flame spread.

The British Standards Institution (BSI) and the American Society for Testing and Materials (ASTM) Committee have developed certain specific tests intended to indicate the relative flammability of materials:

BS476: Part 7 "Surface Spread of Flame Test for Materials": This test involves placing a sample (900mm x 230mm) in a holder with its long axis at right angles to the edge of a gas fired radiant panel (at approximately 800^{o}C). A vertical luminous gas flame is applied at the hotter end of the sample for 60 seconds and the spread of flame away from the pilot source along the sample is observed as a function of time. The material is classified as Class 1,2,3 or 4 on this basis. Class 1 materials are subsequently subjected to BS476: Part 6 "Fire propagation test" and those that meet the stringent requirements of this test are designated class 0.

It has been recognised that some plastics cannot be tested by the surface spread of flame method since they fall out of the holder. These materials are required to pass the fire performance tests of BS2782.

BS2782: Part 5 "Miscellaneous Methods" Method 508 A "Rate of Burning": The specimen (150mm x 13mm x 1.5mm), with reference lines at 25mm and 125mm

parallel to the free end, is clamped with its longitudinal axis horizontal and its short edge inclined at 45^{o} to horizontal. A non-luminous alcohol or bunsen flame is applied to the free end for 10 seconds. The times at which the first and second reference lines are reached by the flame are noted and the rate of burning is computed in mm/minute.

Method 508 C "Flammability of Thin PVC Sheeting": The specimen (550mm x 35mm) is stretched over a semi-circular frame. Absolute alcohol (0.1ml) in a copper cup at one end of the sample is ignited. After the flames extinguish, the extent of burning is noted.

Method 508 D "Alcohol Cup Test": Specimens (150mm x 150mm) inclined at 45^{o} to horizontal are exposed to an alcohol flame which is situated 25mm beneath the lower surface of the specimen and burns for approximately 45s. After the flames extinguish, afterflame and afterglow times are noted and the area of char is estimated.

ASTM E162-78 "Flammability of Materials Using a Radiant Heat Energy Source": This method provides a laboratory test procedure for measuring and comparing the surface flammability of materials at an angle of 30^{o} to vertical when exposed to a prescribed level of radiant heat energy from a radiant panel. The sample size is 150 x 460 mm and should be representative, to the extent possible, of the material being evaluated. A flame spread index is calculated from measured flame spread.

ASTM D 2859-76 "Methenamine Pill Test": This test relates to floor coverings. A steel plate with a 205mm diameter cut-out is laid over the specimen (230mm x 230mm). A methenamine tablet, placed at the centre of the exposed area of

specimen, is ignited. The test continues until flames extinguish or reach the inner edge of the steel plate. The area over which char extends is noted.

ASTM D635-77 "Rate of Burning and/or Extent of Burning of Self-Supporting Plastics in a Horizontal Position": In this test, a bar of the material being evaluated is is supported horizontally at one end. The free end is exposed to a specified gas flame for 30 seconds. Time and extent of burning are reported if the specimen does not burn to the 100mm mark. An average burning rate is reported for a material if it burns beyond the reference mark.

ASTM D 568-77 "Rate of Burning of Plastics in a Vertical Position": The sample is suspended vertically from a clamp and a 25mm flame is applied to the lower edge for a maximum of 15 seconds until the specimen ignites. An average burning rate is reported if the sample burns up to the 350mm reference mark and if the reference mark is not reached then burning time and extent of burning are noted.

ASTM E 84-79a "Surface Burning Characteristics of Building Materials" (Steiner Tunnel Test): This test was originally developed to compare wood and wood products. The specimen (7.6m x 0.51m) forms the ceiling of a tunnel furnace and a flame (2.3 l/min of methane) impinges on the underside of the sample at one end. Surface spread of flame (and also heat contribution and smoke yield) are compared with the behaviour of the standard materials, asbestos cement and red oak flooring and a "flame spread classification" (FSC) is determined.

USA Building Codes prohibit the use of lining materials with FSC>25 in certain locations. This is based on experience with traditional materials where there is an apparent correlation between FSC and behaviour of materials in the large scale corner test (Fang (1975)). However, no such correlation exists for a range of fire

retarded polyurethane foams for some of which FSC < 30 (Table 1.1)

Table 1.1

Data of D'Souza and McGuire (1977)

Material type and form	Condition	Flashover time (min)	FSC
Natural Fiberboard	----------	0.60	129.4
Polyurethane board	with foil	0.75	35.9
Polyurethane board	without foil	0.37	18.0

Clearly, certain low density synthetics which pass the stringent requirements of the Building Codes pose a major hazard in the fire situation. This is indicative of the complexity of fire testing and emphasises the need for a sound understanding of fire dynamics and a rational approach to assessment of fire hazard. It is also important to remember that several of the fire tests currently in use were developed for traditional materials, such as wood, and may not be equally applicable to modern synthetic materials which tend to deform, melt and drip during heating.

1.2.2 Requirements of a Fire Test

Malhotra (1975) published a paper which discussed the design of fire tests and identified the most important features of a "well designed test" which are listed below.

1. Environmental conditions: The test should reproduce the heating regime source, thermal feedback, oxygen supply, movement and dispersal of combustion products as is likely to be experienced in practice.

2. Range of applicability: The environmental conditions should be capable of variation to increase the applicability of the test.

3. Material representation: The modelling of the material should be such as to exclude effects of size, the presence of joints and junctions.

4. Flexibility: The test should be capable of reproducing different orientations in which the product can be used.

5. Reproducibility, repeatability and discrimination should be of an acceptable level depending upon the nature of the test.

6. Ease of operation: Small tests should be capable of single handed operation in no more than two hours, even complex tests should not take more than one day.

7. Meaningful expression of results: The results should be expressed objectively in units which make comparison easy. Descriptive phraselogy should be avoided.

Despite the diversity of the tests in common use, none matches up to these criteria. The International Standards Organisation (ISO) is currently developing a new range of tests which take advantage of increased knowledge of fire dynamics and have the aim of promoting worldwide standards to facilitate the exchange of goods and services and to encourage mutual cooperation between countries. One such test is ISO 5657-1986 (the "ISO ignitability test") which is described previously and relates to the piloted ignition of materials exposed to radiation. An aim of the present work has been to investigate this test in detail, identify any possible limitations in its applicability and in so doing to gain a better understanding of the processes involved in ignition.

1.3 LITERATURE REVIEW

1.3.1 Identification of Area of Interest

Martin (1965), in a discussion of ignition of cellulosic materials, identified three areas in the ignition behaviour of organic solids which were dependent on the level of incident heat flux and the thickness of the exposed solid. In the first case, the solid was too thin (or alternatively, the heat flux level too low) to maintain a temperature gradient and ignition was governed by convective heat loss and turbulent mixing. The concentration of flammable volatiles in the pyrolysis gas/air mixture was frequently too low for flaming to occur, and glowing ignition was the usual result.

At the other extreme, where the irradiance level was very high, ablation effects predominated. Energy was absorbed at the heated surface so rapidly that pyrolysis of the surface layer was complete before heat could penetrate the material. Flaming ignition resulted but unless exposure was continued after ignition, there was insufficient energy absorption by the material to sustain ignition and the flame self-extinguished.

In the intermediate region, between convection and ablation controlled regions, Martin identified a region he described as being diffusion controlled. Ignition behaviour was determined by diffusion of heat into the interior of the material. Pyrolysis then occured at depth and volatiles flowed back out through the heated surface where they ignited and burned. Thus, from the practical viewpoint of fire hazard assessment, the diffusion controlled ignition region is of greatest interest, has received the most attention and is the area with which this study is concerned.

1.3.2 Criteria for Ignition

A review of the literature has revealed two basic approaches to investigation of the ignition behaviour of solid fuels. These are (i) experimental techniques and (ii) mathematical analyses of processes involved in ignition. In many cases, the two overlap as mathematical correlations are frequently sought for experimental results. In general, the material is heated by either (i) radiation, (ii) convection (Kashiwagi et al. (1971)) or (iii) direct flame impingement (Hunter and Hoshall (1980), Clark (1983a,b,1984)). Convective heating is considered to be by a flow of hot gases directed at the specimen without the nearby presence of a flame. However, this mode of heating is not common in fire testing because of practical difficulties, non-uniformity of flux and also since convective heating has been shown to be less important in real fires than radiative heating (de Ris (1979)). The major disadvantage of using direct flame impingement is that the heat flux thus produced is again highly non uniform and, as a result, is difficult to analyse mathematically. Consequently, radiation is the preferred mode of heating for ignitability tests.

A substantial proportion of the pre-1970 work on ignition focussed on wood and other cellulosic materials. Although the present study is concerned only with the ignition of plastics which have considerably different characteristics from cellulosic materials, the earlier work on wood is still relevant in defining the general concepts of ignitability.

Irrespective of the type of combustible considered, identification of certain key criteria for ignition has proved necessary. One of the most commonly used is that of critical surface temperature. This approach assumes that sustained ignition is only possible when the surface temperature exceeds some critical value (T_{ig}),

frequently referred to as the firepoint temperature. For piloted ignition, this is the lowest temperature at which ignition of decomposition products by a pilot source results in sustained burning at the surface. This is a similar concept to the firepoint of a combustible liquid except that it refers to surface rather than bulk temperature as measured in the Cleveland Open Cup Apparatus (ASTM D 92-78 (1978)). Also, in the case of liquids, the generation of volatiles tends to be a simple reversible evaporation process resulting in a vapour with the same molecular composition as the liquid. However, with solids, the volatiles are produced as a result of thermal decomposition of high molecular weight polymers which gives rise to a complex mixture of degradation products of relatively low molecular weight. Nevertheless, firepoint as a limiting condition for ignition is common to both solids and liquids.

Lawson and Simms (1952) suggested that ignition of wood might depend upon the temperature of the exposed surface being raised to a critical value but did not specify a figure. Simms (1960) published results of experiments on the spontaneous ignition of wood exposed to radiation from a gas fired panel, a tungsten filament lamp and a carbon arc. He used a fairly simple heat transfer model to correlate his experimental results and obtained a theoretical value of $525^{o}C$ for the critical temperature for spontaneous ignition. Simms and Law (1967) subsequently reported calculated temperatures of $380^{o}C$ for piloted ignition and $540^{o}C$ for spontaneous ignition of wood samples exposed to radiation from a radiant panel.

Weatherford and Sheppard (1965) and Martin (1965) among others (see Kanury (1972)) subsequently emphasised the importance of heating history and temperature gradient within the solid at the instant of ignition.

Weatherford and Sheppard (1965) proposed an alternative thermal criterion for sustained ignition of cellulosic materials also based on surface temperature. They examined the pilot ignition of a plane slab heated symmetrically from both sides by convection and observed that the surface temperature history was not perceptibly different from that exhibited by a semi-infinite slab during the early stages of the heating process. Eventually, however, the surface temperature of a finite thickness slab begins to depart more and more rapidly from that which would be expected for an infinitely thick slab.

The experimental times to sustained pilot ignition obtained by Bamford et al. (1946) for symmetrical heating by flame impingement appeared to correlate with departures of the calculated surface temperature from the infinite thickness case as observed by Weatherford and Sheppard. Weatherford and Sheppard also noted that computed surface temperature history curves for one sided heating indicated a critical slab thickness above which the surface temperature never exceeded that corresponding to an infinitely thick slab. This critical thickness was in approximate agreement with the experimental observation of Bamford et al. that slabs greater than 0.3cm thick could not sustain piloted ignition by one sided heating.

On the basis of these results, Weatherford and Sheppard suggested that a qualitative criterion for sustained ignition could be that the surface temperature must increase perceptibly more rapidly than would that of an infinitely thick slab. This is analogous to stating that the surface must receive sufficient feedback heat from within the slab to perceptibly alter its temperature history relative to that of an infinitely thick slab.

Another proposed criterion for ignition is critical fuel mass flux. This can be interpreted in terms of a critical mass flow of volatiles sufficient to support a nascent flame capable of losing heat to the surface without the flame temperature being reduced to a value below which the flame is extinguished. This provides a method of quantifying ignition and extinction conditions in terms of basic properties of the solid and its decomposition products. The existance of a minimum critical rate of production of fuel vapours at the point at which a combustible solid could be ignited was first suggested by Bamford et al. (1946). They reported that for the ignition of vertical samples of wood (deal, oak and pine), a theoretical minimum rate of evolution of gases of $2.5 \times 10^{-4} g/cm^2.s$ was required.

Kanury (1977) compared mass flow rate of the volatiles with the rate of air entrainment into the plume rising from the hot surface. He assumed (incorrectly) that the plume temperature was equal to the limiting flame temperature rather than the surface temperature and carried out calculations based on fuel/air mass ratios to explain the significance of the values for critical mass flux obtained by Bamford et al.(1946). He estimated the free convectively induced air mass flux by $\rho_g(g\alpha_g\beta\Delta T)^{1/3}$ and used the following relationship (equation 1.1) to obtain critical mass flux (m''_{cr}) in terms of the fuel/air ratio (f).

$$f = m''_{cr}/\rho_g(\alpha_g\beta\Delta T)^{1/3} \qquad (1.1)$$

where ρ_g is gas phase density ($1x10\text{-}3g/cm^3$), α_g is gas thermal diffusivity ($0.2cm^2/s$), β is the volumetric expansion coefficient and ΔT is gas phase temperature differential ($\beta\Delta T \simeq 4$). Hence $m''_{cr} = 1x10^{-2}.f$. Kanury determined from combustion literature that for most hydrocarbon and carbohydrate products possible in cellulose pyrolysis, the lower flammability limit of the fuel/air ratio (f^*)

lies between $1x10^{-2}$ and $4x10^{-2}$. Therefore, if the mixture above the surface is to attain the lower flammability limit, f must be greater than f^*, ie m''_{cr} must lie between $1x10^{-4}$ and $4x10^{-4}$g/cm^2.s. This is a necessary condition for ignition of the volatiles to occur (possibly to give flashing ignition) but, in isolation, is insufficient to define the limiting criterion for sustained pilot ignition. This relates to a comparison of closed cup (ASTM D93-80 (1980)) and open cup flashpoint (ASTM D92-78 (1978)) measurements for combustible liquids. At the closed cup flashpoint, the vapour pressure of the liquid corresponds to the lower flammability limit of the vapour in air. At the open cup flashpoint, however, vapour diffuses away from the liquid and the occurence of ignition depends on the height of the ignition source above the surface (Burgoyne, Roberts and Alexander (1967), Glassman and Dryer (1981)). Sustained ignition then requires a higher bulk temperature which corresponds to a vapour pressure in excess of the stoichiometric mixture in air.

Various other criteria for ignition have been suggested, including minimum critical radiant heat flux. However, it is expected that this factor will be sensitive to changes in surface heat losses brought about by alterations to the geometry and orientation of that surface. Lawson and Simms (1952) estimated the limiting flux for ignition of vertical samples of wood by extrapolating a plot of Q" versus $Q''/t_{ig}^{1/2}$ to $t_{ig}=\infty$, where t_{ig} is the time to ignition under a radiant heat flux, Q". They deduced a minimum flux for piloted ignition of wood of approximately 12kW/m^2. Similar results were obtained by Koohyar et al.(1968b), and Tewarson and Pion (1978) for horizontal samples. Quintiere (1981) consistently deduced higher values than Lawson and Simms (1952) and Tewarson and Pion (1978) for minimum flux, both by using measurements of flame spread over different

surfaces under a range of radiant heat fluxes and by direct ignition data. There is limited evidence that the pilot ignition of certain composites may be possible at even lower fluxes. Examples of this include fabrics stretched over insulating substrates such as cotton batting (Alvares (1975)) and materials exhibiting delamination which effectively insulates the surface lamina from the bulk of the material by a layer of air (Rasbash and Drysdale (1983)).

Sauer (1956) proposed critical char depth as a criterion for ignition of wood. He assumed that charring begins at any depth when the volatile content there, W, falls to a certain value, W_c. Dimensionless correlations of weight loss and char depth were then prepared. Previously, Williams (1953) found that a damage function of the form

$$W_c = \int_0^t \exp(E_A/RT).dt \qquad (1.2)$$

gave an adequate correlation for charring, but commented that it was extremely complex to use. This theory was based on a suggestion by F.C. Henriques (1947) for correlating thermal damage to skin.

Several investigators have questioned the validity of applying a single criterion to the definition of ignition. Lawrence (1950) attempted to determine whether the fixed temperature criterion was sufficient to describe ignition or whether a critical rate of production of volatiles was also necessary. He assumed that the irradiated solid was opaque and that there was no significant chemical heating. He then calculated that the rate of production of volatiles at ignition was always more than twice the critical level (2.5×10^{-4} g/cm^2.s) suggested by Bamford et al. (1946) as necessary for continued burning. His results were successfully correlated in terms of ignition occuring when the surface temperature reached 500^{0}C. Therefore, he assumed that the rate of production of volatiles was never a critical factor.

However, at rates of heating close to the threshold for ignition it is possible that the supply of volatiles would be exhausted before the surface reached $500^{o}C$ and Lawrence's conclusion of a fixed ignition temperature would be invalidated.

Rasbash (1975), in his application of the firepoint equation, identified four interdependent criteria for sustained ignition by a pilot. These comprised:

1. Critical surface temperature.
2. Critical rate of convective heat transfer from flame to solid.
3. Critical rate of emission of volatiles.
4. Critical flame temperature (Roberts and Quince (1973)).

This approach is discussed in greater detail in Section 1.3.4.

While several proposed criteria for ignition exist, these have little value unless they can be validated by experimental observations. Once validated, these criteria may then be usefully applied to theoretical modelling of the ignition process.

1.3.3 Experimental Approach

One of the most frequently adopted criteria for ignition is that of attainment of a critical surface temperature (the "firepoint temperature"). Another commonly applied criterion is that of minimum flowrate of volatiles.

Critical Surface Temperature

Surface temperature is not easily measured without special equipment and techniques and, predictably, there are substantial differences in the reported ignition temperatures by various investigators (Table 1.2).

Table 1.2

Firepoint temperatures of PMMA

INVESTIGATOR	IGNITION TEMPERATURE(^{o}C)	
	Piloted	Spontaneous
Delmonte & Azam (1943)	-	620
Schoenborn & Weaver (1947)	-	146
Setchkin (1949)	280,300	430,450
Kashiwagi (1979a)	360-400	370-410
Deepak & Drysdale (1983)	270	-
Beyler (1985)	313	-
Thomson & Drysdale (1987)	309	-

Historically, several different experimental methods have been adopted to obtain temperature measurements. Delmonte and Azam (1943) placed small plastic samples (12.5mm x 1.5mm x 25mm) in contact with fused sodium hydroxide heated to known temperature in a furnace (25^{o}C intervals). They obtained two temperatures for spontaneous ignition: (i) an instantaneous temperature where the sample ignited in less than 1 second and (ii) a minimum temperature where the sample ignited within 10 seconds of contact. This technique is necessarily somewhat inaccurate because of the 25^{o}C temperature intervals considered. In addition there is the problem of the unknown effect of molten sodium hydroxide on the polymers in question.

Several investigators have relied on thermocouple measurements of temperature. Schoenborn and Weaver (1947) took small bar shaped samples (12.5mm x

12.5mm x 31mm) of various plastics and placed them in an electric furnace which had previously stabilized at a known high temperature. A standard 30 B and S type thermocouple was inserted into a hole (2.25mm diameter) drilled on the centre line of the major axis of each sample. For all materials, a series of samples was prepared, each with a different hole depth. Time and temperature measurements were recorded for the samples during the test and a plot of time versus temperature was obtained. These plots showed a distinct "break point" (change in slope) which was deduced by the authors to indicate the local temperature at a given position within the sample when surface ignition began. A plot of break point versus distance between thermocouple junction and surface produced a curve which could be extrapolated back to zero distance (specimen surface). The temperature obtained from this extrapolation was arbitrarily defined as the apparent surface temperature at the moment of ignition.

Results obtained in this investigation indicated that for most materials, surface temperature at ignition as well as ignition delay time was dependent on the rate of heating (ie furnace temperature). Air flow to the furnace was restricted and ignition of the sample was delayed until sufficient volatiles were present and could form a flammable mixture with the contained air. Furthermore, this treatment assumes that the position of the sample surface remains constant during a test and takes no account of those materials which melt and deform during heating. In general, the results for surface temperature at ignition obtained in this study are substantially lower than equivalent results reported by other investigators (Table 1.2). A critical discussion of this work was carried out by Setchkin (1948).

Fons (1950) reported ignition temperature measurements with thermocouples placed in 9mm diameter pine wood specimens at positions 0.5 and 0.667 of the

radius from the centre. The specimens were placed in a furnace at 521°C (1150°F) until the wood caught fire. A surface temperature of 343°C (650°F) for the spontaneous ignition of wood was calculated using the transient heat flow equations for inert solid cylinders.

Setchkin (1949) developed a test furnace which fulfilled the following requirements:-

1. The temperature of air passing the specimen was uniform and constant.
2. The airflow was steady and adjustable.
3. The specimen was in a stream of air of known temperature, was visible from the outside and was easily removable.

Two test methods were applied:

- **Rising temperature** where a furnace heating rate of 500°C/hour was applied until a temperature of 750°C was attained, or until ignition occured either spontaneously or as a result of pilot application. Materials which failed to ignite under this regime were designated incombustible.
- **Steady temperature** where the sample was inserted into the furnace which had previously been stabilized at a known temperature. The sample was then bathed by a stream of air (0.91-12.2m/s, depending on the material). The furnace temperature was progressively raised and the test repeated until ignition occurred. The sample temperature (surface or within) was measured by a thermocouple placed on or inserted into the sample. The air temperature was also recorded.

The rising temperature method tends to produce slow decomposition and it is possible that higher ignition temperatures will be obtained than are actually characteristic of the test material. The second method introduces several problems. A thermocouple inserted into the specimen below the surface cannot indicate the actual surface temperature whereas a surface mounted thermocouple will be subjected to incident radiation and, unless very fine, will record a higher

temperature than exists at the surface. Setchkin advocated the use of an air flow rate suitable for the particular specimen, "in accordance with the trend of the exothermic reaction". This indicates a dependency of ignition on the rate of oxidative degradation. Therefore, tests performed at constant air rate would produce ignition temperatures that were higher or lower than those obtained using the ideal rates reported by Setchkin for any particular material. Conversely, it would not be possible to compare the relative fire hazard of materials by ignition temperature if different air rates were used. Subsequently, variants of this furnace were utilised by Patten (1961) and by the American Society for Testing and Materials Committee for incorporation into ASTM D1929 (1977) and E136 (1979).

Hunter et al. (1977) pioneered the "moving wire technique" for studying the ignition and extinction of solids. This method involves the substrate, in the form of a coating on a wire, being moved at controlled speed through a stationary ignition source. At given wire speed, the surface temperature varies with longitudinal position, being a maximum at the "downstream" edge of the heat source where ignition occurs. The surface temperature of the moving substrate is determined by one of two methods. The first employs a thermocouple in rubbing contact with the substrate, while the second involves the use of thermal paints (in the non-burning regions). The authors conclude that "ignition temperature is independent of a number of the secondary variables plaguing flammability studies" and suggest that information of direct applicability to real, practical systems can be gathered in the scientifically simpler moving wire system.

Several investigators (Gardon (1953), Kashiwagi (1979a,b), Deepak & Drysdale (1983), Beckel and Matthews (1984), Atreya et al.(1986)) have relied on surface

mounted thermocouples to measure firepoint temperature.

Gardon (1953) published temperature versus time curves for natural and black-inked wood samples in various positions. Surface temperature was sensed with 0.025mm diameter, spot-welded Chromel-Alumel thermocouples lightly sprung against the irradiated surface of the wood.

Kashiwagi (1979a) obtained surface temperature measurements for horizontal samples of polymethylmethacrylate and red oak (under conditions of piloted and spontaneous ignition) exposed to radiation from a CO_2 laser in the range 70 to 180kW/m^2 using surface mounted 25μm diameter chromel-alumel thermocouples. For PMMA, he found that surface temperature at ignition was in the range of 375 to 410^{0}C and remained fairly constant over the range considered, for both pilot and spontaneous ignition. However, for red oak, the surface temperature at ignition increased from 400^{0}C at 160kW/m^2 to 575^{0}C at 80kW/m^2 for auto-ignition and from 420^{0}C at 150kW/m^{2}to 500^{0}C at 70kW/m^2 for piloted ignition.

Deepak and Drysdale (1983) recorded surface temperature at piloted ignition for horizontal specimens of an unidentified brand of polymethylmethacrylate using fine chromel-alumel thermocouples cemented to the sample surface with a Perspex cement ("Tensol"). Firepoint temperatures of around 270-280^{0}C were recorded.

Beckel and Matthews (1984) recorded the surface temperature of polyoxymethylene at spontaneous ignition in an opposed flow diffusion flame system using R-type platinum/rhodium thermocouples with a bead diameter of 250μm. They determined that the surface temperature at spontaneous ignition for

POM was about 390±20°C and appeared to be independent of incident flux.

Atreya et al.(1986) utilised fine chromel-alumel thermocouples to measure the surface temperature of vertical and horizontal samples of red oak and mahogany at piloted ignition. Thermocouple junctions were slid into very fine incisions made in the surface of the samples, the remainder of the thermocouple being secured with a little wood glue. They deduced that for mahogany an average ignition temperature of 375°C adequately represented both horizontal and vertical modes while for red oak, the average ignition temperature was 365°C.

Unfortunately, the use of surface mounted thermocouples is plagued by problems with conduction errors and thermal contact. There also exists the possibility that the thermocouple itself will absorb incident radiation and record a higher temperature than actually exists at the surface. These problems are avoided by placing the thermocouple within the sample (see Schoenborn and Weaver (1947) and Martin (1965)) but estimation of surface temperature from the extrapolation of temperatures measured at depth tends to be inaccurate.

An alternative means of determining surface temperature is to use an optical method such as infrared pyrometry. Alvares (1963) made surface temperature measurements of blackened alpha cellulose exposed to radiation from a carbon arc source, using an infrared pyrometer with a 3.41μm narrow band pass filter. The arc radiation was restricted to less than 2.5μm wavelength by a 12mm thick Plexiglas window. Temperatures in the range 600 - 650°C were reported at spontaneous ignition.

Smith and King (1970) measured the spontaneous and piloted ignition temperatures of several cellulosics, black rubber and polyurethane foam exposed

to radiation (5 to 105 kW/m^2) from two quartz lamps by means of a long wavelength infrared pyrometer. Their results are listed in Table 1.3.

Table 1.3

Firepoint temperatures (Smith and King (1970))

MATERIAL	PILOTED T_{ig} (^oC)		UNPILOTED T_{ig} (^oC)	
	Average	Range	Average	Range
Pine block	408	343-571	488	416-566
Pine dowel	341	302-382	659	454-732
Oak dowel	351	285-404	NF	NF
Box cardboard	322	302-366	636	538-749
Newspaper	283	232-338	292	271-363
White canvas	335	299-368	NF	NF
Cotton cloth	327	266-416	439	388-546
Black rubber	421	316-502	653	638-688
P.U. foam	294	154-416	378	360-399

In these experiments, surface temperature at ignition was observed to decrease with increasing radiant heat flux for the cellulosic materials but this trend was less obvious for black rubber and polyurethane foam.

Koohyar (1968a) determined the surface temperatures of several types of wood during heating to ignition. A radiometer at about 75^o to the normal and with a correction for reflected irradiance was used. Spontaneous ignition for one sided heating was reported at 330-495^{o}C, average 402^{o}C and piloted ignition was at

a certain critical value. In subsequent work, Tewarson and Pion (1978) determined m''_{cr} for a large number of materials, including standard cellular plastics, under conditions of both forced and natural convection. Their results ranged from 2.5g/m^2.s for polyethylene to 7.6g/m^2.s for PE/42%Cl under conditions of forced convection and 1.9g/m^2.s to 6.5g/m^2.s for the same two materials under conditions of natural convection. No information is given concerning the reproducibility of these data or their dependence on such experimental parameters as incident heat flux, sample dimensions, oxygen concentration and position of pilot ignition source with respect to the sample surface.

Deepak and Drysdale (1983) reported preliminary critical mass flux values for PMMA of around 4.0g/m^2.s using a transducer to detect mass loss. The apparatus used in this investigation was similar to that employed by Tewarson and Pion (1978). The full results of this study are reported in a paper by Rasbash et al. (1986). The critical mass flux at ignition was found to increase by about 25-30% with increased heat flux from 12-20kW/m^2 and apparently levels out at higher fluxes. The effect of air flow rate and oxygen concentration on the value of critical volatile mass flux was also investigated.

Kishore and Mohandas (1982b) examined the spontaneous ignition behaviour of polystyrene heated in a furnace. They determined percentage weight loss before ignition and also rate of weight loss at ignition of small cylinders of polystyrene, 1.1cm in diameter and 250mg weight, at several furnace temperatures. They deduced that there was a fair correlation between the above two weight loss parameters and that there was a relationship between log (rate of weight loss at ignition) and inverse furnace temperature (K^{-1}) which could be mathematically

represented as

$$\text{Rate of weight loss} = A.\exp(E_A/T) \qquad (1.3)$$

In general, however, there have been very few attempts to obtain the necessary experimental data to test the concept of critical mass flux. Those values of mass flux at ignition which have been obtained tend to be scattered and there is an insufficient data base for any meaningful comparative study to be made.

1.3.4 Mathematical Modelling of Ignition

Mathematical descriptions of ignition range from the very complex equation for which no solution exists to the unrealistically simplistic approach in which more factors are neglected than are considered (see Welker (1970)). Most start with a basic energy balance equation for the solid combustible material. Generally, the system is considered to be one-dimensional and the gaseous volatiles are assumed to be in temperature equilibrium with the solid. The energy balance then becomes

$$\frac{\partial}{\partial x}\left(k\frac{\partial T}{\partial x}\right) + \bar{\alpha}_{av}Q''.\exp(-\bar{\alpha}_{av}x) + \frac{\partial(C_g m''T)}{\partial x} = \frac{\partial(\rho H)}{\partial t} \qquad (1.4)$$

Equation 1.4 cannot be solved in the closed form and there are insufficient data available to attempt a numerical solution. However, if certain simplifying assumptions are made, the equation may be solved either numerically or mathematically. First, assume that the sample is opaque, ie none of the radiation incident on the exposed surface penetrates into the interior of the solid. Thus, the second term in equation 1.4 relating to diathermanous heating disappears from the energy balance.

Next, assume that the mass flow within the solid term is negligible. This assumption is valid if

$$m''C_g l/k \ll 1 \qquad (1.5)$$

where $m''C_g l/k$ is a form of the Peclet number. Kanury and Blackshear (1970) have postulated that the requirement of equation 1.5 is not generally met for cellulosic materials if l is taken as the specimen thickness. However, if l is taken to be the thickness of the reaction and char zone, the Peclet number is much smaller for heating rates where ignition occurs relatively quickly. This seems to be a reasonable approximation since one would predict little gas flow within the solid except through the reaction and char zone. The lack of cellular structure in synthetic polymers would be expected to hinder flow of pyrolysis products from within the solid which implies that the mass flow term is probably of even lesser significance for synthetic polymers than for wood.

Finally, assume constant sample dimensions, ie no expansion or shrinkage during heating or pyrolysis. The final term in equation 1.4 then becomes

$$\frac{\partial(\rho H)}{\partial t} = \frac{\partial(\rho E)}{\partial t} \qquad (1.6)$$

Equation 1.4 can now be rewritten as

$$\frac{\partial}{\partial x}\left(k\frac{\partial T}{\partial x}\right) = \frac{\partial(\rho E)}{\partial t} \qquad (1.7)$$

for which a numerical solution can be found provided that data are available for k, ρ and E. Havens (1968) based his solid phase model for ignition of thermally thick cellulose on equation 1.7. The initial condition is given by

$$T = T_o \quad \text{for } t \leq 0 \qquad (1.8)$$

and the boundary conditions are

$$\frac{\partial T}{\partial x} = 0 \quad \text{for } x \to \infty \qquad (1.9a)$$

and

$$-k\frac{\partial T}{\partial x} = \bar{\alpha}_{av}\dot{Q}'' - h(T_s - T_o) - \varepsilon\sigma T_s^4 \quad \text{for } x=0 \qquad (1.9b)$$

Assuming that E is a direct function of temperature only

$$\frac{\partial E}{\partial t} = \frac{\partial E}{\partial T}.\frac{\partial T}{\partial t} \qquad (1.10)$$

Havens obtained values of $\partial E/\partial T$ from differential scanning calorimetry measurements and then solved equation 1.7 numerically with the appropriate boundary conditions. He was able to calculate a theoretical temperature profile and weight loss for hollow cylindrical pine samples heated at the inside surface.

While equation 1.7 is amenable to numerical solution, it cannot be solved in the closed form. Hence, it is usually modified to separate the sensible heat terms from the decomposition heat terms. Thus,

$$\frac{\partial(\rho E)}{\partial t} = \rho\frac{\partial E}{\partial t} + E\frac{\partial \rho}{\partial t} \qquad (1.11)$$

The internal energy term is assumed to be made up of two parts, a sensible heat term, cT, and a term related to the energy required for pyrolysis, L_v. Both L_v and c are usually assumed to be constant and the sensible heat effects attendant to density changes are usually ignored as being negligible. Thus,

$$\frac{\partial}{\partial x}\left(k\frac{\partial T}{\partial x}\right) = \rho c\frac{\partial T}{\partial t} + L_v\frac{\partial \rho}{\partial t} \qquad (1.12)$$

The term $\partial\rho/\partial t$ represents the sample weight loss rate. If pyrolysis is assumed to follow a first order decomposition process, then

$$\frac{\partial \rho}{\partial t} = W.A.\exp(-E_A/RT) \qquad (1.13)$$

Equations 1.12 and 1.13 can be solved by numerical techniques assuming that experimental values of the thermal and kinetic parameters are available. However, the lack of a completely acceptable criterion or set of criteria to define ignition means that equations 1.12 and 1.13 cannot be used to predict ignition times under any given set of boundary conditions. Two approximate criteria commonly used

are the attainment of a minimum volatile flowrate or the attainment of a given surface temperature.

Combination of equations 1.12 and 1.13 gives

$$k\frac{\partial^2 T}{\partial x^2} = \rho c\frac{\partial T}{\partial t} + W.L_v.A.\exp(-E_A/RT) \qquad (1.14)$$

Bamford et al. (1946) used equation 1.14 with the boundary condition

$$-k\frac{\partial T}{\partial x} = h(T_f-T_s) + \sigma(\varepsilon_f T_f^4-\varepsilon_s T_s^4) \qquad (1.15)$$

which is essentially the same as equation 1.9(b) except that the sample was surrounded by flame. They solved the equation numerically using an electical analogue technique and obtained a value of 2.5×10^{-4} g/cm^2.s as the critical mass flux for the piloted ignition of wood.

Weatherford and Sheppard (1947) subsequently solved Bamford et al.'s model numerically with a digital computer in a manner analogous to the graphical method devised by Schmidt (see for example, Drysdale (1985)). The values of wood properties reported by Bamford et al. (1946) were employed. The computed results indicated that increment thickness was critical. In computations for low thermal conductivity materials, excessive increment thickness apparently generated undulations in the theoretical vapour generation rate curve. An apparent maximum allowable increment thickness of between 1.25 and 2.5mm for the parameters used in these calculations was deduced. Weatherford and Sheppard concluded that "the computations reported by Bamford et al. did not accurately represent the mathematical model upon which they were based" because the slab thickness increments ranged from 1.25 to 5.00mm. They showed that a specific fuel generation rate in isolation was a necessary but not an adequate criterion for ignition as had been proposed by Bamford et al.

Minimum weight loss rate as a criterion for ignition has been used considerably less often than attainment of a given surface temperature. Many investigators adopting the critical surface temperature criterion have chosen to simplify the mathematical model even further by assuming that the sample is inert and has constant thermal properties. Equation 1.14 then becomes

$$k\frac{\partial^2 T}{\partial x^2} = \rho c\frac{\partial T}{\partial t} \qquad (1.16)$$

The exact form of equation 1.16 depends on the boundary conditions applied to it. Generally, only one surface of the sample is heated. Energy is supplied by any combination of conduction, convection and radiation. Energy losses at the surface include reflection of incident radiation, convective losses and reradiation from the heated surface. Reflection losses are often neglected. Reradiation losses cause the boundary condition equations to be non-linear and so are often neglected in the solution of equation 1.16 which introduces a significant source of error. The unheated surface is generally assumed to be well insulated or, alternatively, the sample is considered to be infinitely thick so that no heat loss occurs at the rear surface. Hence, equation 1.16 has only been solved for simplified boundary conditions. Simms (1960, 1962, 1963) used equation 1.16 as his basic equation for heat transfer but included convective cooling losses at the exposed surface in the boundary equation. Both the thin slab (linear temperature gradient) and the semi-infinite solid, under conditions of pilot and spontaneous ignition, were considered.

Thin Slab

$$\frac{Q''t}{2l\rho cT_m} = \frac{Nt/\rho cl}{1-\exp(-Nt/\rho cl)} \qquad (1.17)$$

where 2l is slab thickness, T_m is mean temperature and N is the Newtonian

cooling constant = hk

Semi-infinite Solid

$$\frac{Q''t}{\rho c(\alpha t)^{\frac{1}{2}}T_s} = \frac{Nt/\rho c(\alpha t)^{\frac{1}{2}}}{1-\exp(\beta^2 \mathrm{erfc}\beta)} \qquad (1.18)$$

where α is thermal diffusivity and β is a dimensionless group obtained from Biot and Fourier numbers ($\beta = h(\alpha t)^{\frac{1}{2}}$).

The results were plotted in terms of two dimensionless variables. For a semi-infinite solid these are the energy modulus, $Q''t/\rho c(\alpha t)^{\frac{1}{2}}T_s$ which represents the ratio of the energy received by the surface to the heat content of the specimen at ignition and the cooling modulus, $(Nt/\rho c(\alpha t)^{\frac{1}{2}}$, which represents the ratio of energy lost by cooling to the heat content. When the cooling modulus tends to zero, then from equation 1.18

$$\frac{Q''t}{\rho c(\alpha t)^{\frac{1}{2}}T_s} \rightarrow \frac{\pi^{\frac{1}{2}}}{2} \qquad (1.19)$$

Equation 1.19 gives an approximate value for T_s at small values of the cooling modulus and an appropriate value can be chosen for the Newtonian cooling constant,N for that temperature range. The value of T_s can then be adjusted to give the best fit between experimental points and equation 1.18.

Simms & Law (1967) correlated ignition data for wet and dry woods in a similar manner on the basis of equations 1.17, 1.18 and 1.19. It was necessary to obtain values for the two unmeasured parameters, h and T_s. For piloted ignition, they used values of T_s of 360°C and h of 36W/m^2.K. For spontaneous ignition, they used T_s of 525°C and h of 58.6W/m^2.K. It should be noted that the convective coefficients used by Simms in his work are significantly higher than those used by other investigators. For example, Alvares et al. (1969) used 11.7W/m^2.K based on

free convection heat transfer theory. It is possible that the large value of h required for correlation by Simms was due to the neglecting of heat loss effects from reflection of incident radiation and reradiation from the surface.

Equation 1.16 can also be solved assuming that the exposed surface is subjected to a constant radiant heat flux so that the boundary conditions are

$$-k\frac{\partial T}{\partial x} = \bar{\alpha}Q'' \quad \text{for } x=0 \tag{1.20a}$$

and

$$\frac{\partial T}{\partial x} = 0 \quad \text{for } x \to \infty \tag{1.20b}$$

where x is distance into the solid. Carslaw and Jaeger (1959) give the solution for the exposed surface temperature as

$$T_s = T_o + \frac{2\bar{\alpha}Q''t^{\frac{1}{2}}}{(k\rho c)^{\frac{1}{2}}} \sum_0^\infty \left(\text{ierfc}\frac{2nl}{2(\alpha t)^{\frac{1}{2}}} + \text{ierfc}\frac{(2n+2)l}{2(\alpha t)^{\frac{1}{2}}}\right) \tag{1.21}$$

If ignition is assumed to occur when a given surface temperature (T_{ig}) is attained, equation 1.21 can be solved to obtain

$$t_{ig} = \frac{(k\rho c)(T_{ig}-T_o)^2}{4(\bar{\alpha}Q'')^2 \Sigma^2} \tag{1.22}$$

where Σ represents the summation of terms in the brackets of equation 1.21. Equation 1.22 indicates four groups of variables important in the ignition process. These are

- $(k\rho c)$, thermal inertia, which represents the conduction of heat away from the exposed surface (k) and the retention of sensible heat within the solid (ρc).
- $(T_{ig}-T_0)$, surface temperature rise, which represents an assumed ignition criterion.
- $\bar{\alpha}_{av}Q''$, absorbed flux, which represents the rate of heating.
- Σ, which represents the dimensionless thickness of the material with respect to the duration of heating.

Hallman (1971) used equation 1.22 as the basis of an empirical relationship to correlate his ignition data (ignition delay time and corresponding incident heat flux) and proposed that

$$t_{ig} = \frac{160\,(T_{ig}-T_o)^{1.04}\,(k\rho c)^{0.75}}{(\bar{\alpha}Q'')^2} \qquad (1.23)$$

Equation 1.23 does not represent his data for specific materials particularly well, presumably because the correlation was optimised as the best fit for all the plastics tested rather than for any one in particular.

All the models described up to this point refer to ignition under relatively low levels of incident radiant heat flux as being a solid phase phenomenon. However, Mutoh et al. (1979) carried out an experimental study on the radiative ignition of polymethylmethacrylate and found that ignition delay time changed discontinuously at a certain critical radiant flux (60W/cm^2 for PMMA). For a radiant flux above this critical value, ignition was observed to occur at the plume axis away from the PMMA surface and for a radiant heat flux below the critical value, it was observed to occur near the PMMA surface close to the plume boundary. This would suggest that ignition under high levels of incident radiation is a gas phase rather than a solid phase phenomenon.

Alvares and Martin (1971) and Ohlemiller and Summerfield (1971) proposed models for ignition under high radiant heat flux levels in which chemical reactions in the gas phase between the fuel gas and oxygen were assumed. Ohlemiller and Summerfield (1971) obtained a simplified solution for the ignition delay time (t_{ig}) of polymers exposed to radiation from a CO_2 laser by decoupling the conduction and in depth absorption of radiation terms for the solid, thus obtaining

$$t_{ig} = t_{cd} + \frac{\rho c\,(T_{ig}-T_o)}{\bar{\alpha}(1-r)Q''} + \frac{\pi\bar{\alpha}}{4}\cdot\left(\rho c\,(T_{ig}-T_o)/(1-r)Q''\right)^2 \qquad (1.24)$$

where T_{cd} is the time for diffusional and chemical processes in the gas phase and r is reflectance.

In addition, several investigators (Deverall and Lai (1969), Linan and Williams (1971,1972), Kashiwagi (1974), Kindelan and Williams (1975,1977), and Atreya and Wichman (1987) have produced generalised theoretical analyses of radiative ignition in which a combination of gas phase and solid phase phenomena are considered.

Deverall and Lai (1969) developed a model involving both the gas and solid phase based on the criterion that for cellulosic materials, the threshold for ignition occurs when the irradiance is twice the heat flux required for pyrolysis less the heat conducted into the solid, all evaluated at the solid fuel surface.

$$\left.Q''\right|_{x=0} = \left.2L_v m''\right|_{x=0} - \left.k\frac{\partial T}{\partial x}\right|_{x=0} \qquad (1.25)$$

This equation provides a necessary condition but not a sufficient condition for ignition. It does not predict when ignition will occur although ignition time and temperature are required to calculate the heat conduction term.

Kindelan and Williams (1975,1977) divided the polymer gasification process into three stages: an inert heat up followed by a short transition to steady state gasification. According to their model, gas phase ignition can occur either during the transition stage or during steady state gasification.

Kashiwagi (1974) based his model for spontaneous ignition on a hypothetical plastic material exposed to an incident radiant heat flux. The model includes the effects of gas phase reaction and a finite value of the absorption coefficient of the

solid (diathermancy). Figure 1.4 shows a schematic representation of this model which is highly nonlinear and involves complex couplings which make the equations amenable to numerical solution only. He concluded that there are lower and upper limits in the value of the pyrolysis activation energy for ignition with given values of the gas phase activation energy and frequency factor. This is also true for the gas phase activation energy with given values of the pyrolysis activation energy and frequency factor.

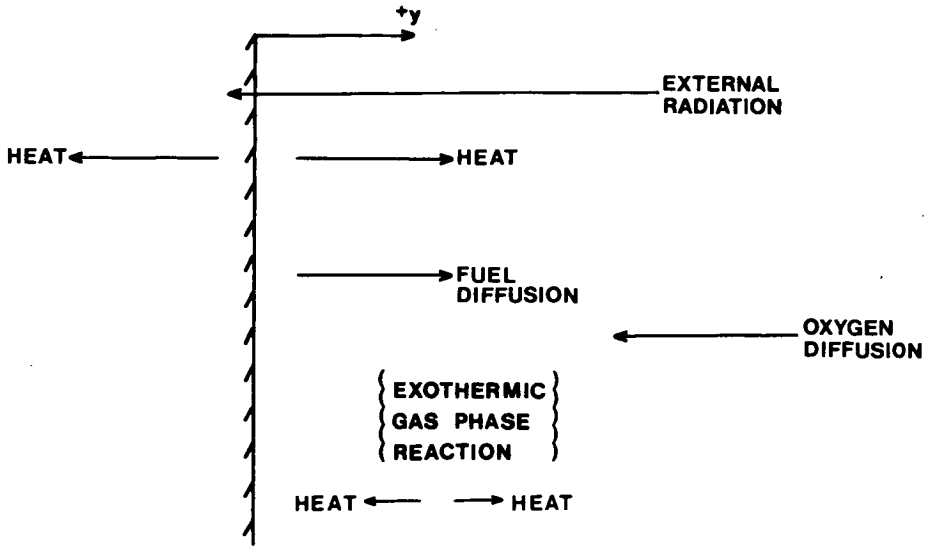

Figure 1.4 Kashiwagi's model

Atreya & Wichman (1987) have developed an approximate analytical model for the piloted ignition of cellulosic solids which may also be applied to plastics. The model is based on the following observations: (i) critical conditions at ignition are achieved solely by external radiation and surface radiant emission plays a dominant role in determining the surface temperature at ignition and (ii) although the heat lost by the flame to the solid at the instant of ignition is significant and may cause thermal quenching, its contribution to the enthalpy rise of the solid is negligible. Further simplifications include the concepts of nearly constant limit diffusion flame temperature at extinction and the nearly constant heat of combustion of oxygen for most hydrocarbons. Several of these observations were

first made by Rasbash (1975) and are discussed in some detail in his work on "firepoint theory".

The model by Atreya & Wichman attempts to :

1. Establish a relationship between critical surface temperature and critical fuel mass flux at ignition.

2. Determine the critical surface temperature at ignition from gas phase considerations.

Equations are derived for mass balance, energy balance and decomposition kinetics within the solid phase and for energy balance in the gas phase. The parameters within these equations are then "nondimensionalised" to produce the following equations:

Mass balance:

$$\frac{\partial m}{\partial x} = \frac{\partial \rho}{\partial t} \tag{1.26}$$

Energy balance:

$$\rho \frac{\partial T}{\partial t} = \frac{\partial}{\partial x}\left(k \frac{\partial T}{\partial x}\right) \tag{1.27}$$

Decomposition kinetics:

$$\frac{\partial \rho}{\partial t} = -A.W.\exp(-E_A/RT) \tag{1.28}$$

with initial and boundary conditions;

$$T(x,0) = T(\infty,t) = \rho(x,0) = 1$$

$$m(\infty,t) = 0 \tag{1.29}$$

$$-k\frac{\partial T}{\partial x}(0,t) = 1-H(T_S-1) - \sigma(T_S^4-1)$$

where $H=hT_0/\bar{\alpha}Q''$, m is fuel mass, ρ_f is final char density and A is the pre-exponential factor.

Solution of this nonlinear set of equations yields the transient temperature and density distributions inside the solid. An exact analytical solution was not possible because of the highly nonlinear nature of the problem, hence approximate integral methods were employed.

Equation 1.30 describes the solid phase process.

$$m \simeq \frac{A(1-\rho_f)T_s^2}{f_s E_A}.\exp(-E_A/T_s)\{1-\frac{\exp(-E_A(1-1/T_s))}{T_s^2}\} \qquad (1.30)$$

while equation 1.31 describes the gas phase process.

$$m \simeq \frac{rY_{O\infty}H(T_f-T_s)}{\Delta H-(T_f-1)-rY_{O\infty}(T_f-T_s)} \qquad (1.31)$$

where T_f is the normalised limit flame temperature, ΔH is the normalised heat of combustion of air and $Y_{0,\infty}$ is the oxygen mass fraction.

If the curves corresponding to 1.30 and 1.31 are plotted, the intercept is the ignition point which yields a unique solution for fuel mass flux and surface temperature at ignition. This model provides limited justification for the use of critical surface temperature and critical fuel mass flux at ignition.

Rasbash (1975) took a completely different approach to the problem of ignition. He assumed the existence of a firepoint temperature for piloted ignition and produced a relationship based on generalization of the theory of extinction of a fire by cooling the fuel. He assumed quasi steady state conditions and identified the firepoint condition mathematically by an equation describing heat and mass balance at the surface of the solid (equation 1.32).

$$S = (\phi\Delta H_c - L_v).m''_{cr} + Q''_{ext} - Q''_{loss} \qquad (1.32)$$

Where S is the "net sensible heat entering the fuel" (equal to zero in the quasi steady state), ϕ is the maximum fraction of the heat of combustion that can be lost

from the flame to the surface without extinction of the flame, ΔH_c is the heat of combustion of the volatiles, L_v is the heat required to produce the volatiles, m''_{cr} is the critical mass flux of volatiles at the firepoint, Q''_{ext} is the external heat flux absorbed at the surface and Q''_{loss} is the heat loss expressed as a flux through the surface. Rasbash used equation 1.32 to identify the condition for sustained ignition at the surface and stated that if S is negative, the surface will cool and the flame will go out but if S is positive, the surface temperature will rise and the flame will strengthen and develop towards steady burning. Further data on surface temperature, critical mass flux and heat transfer conditions at the surface are required to test the validity of this theory.

Studies of thermal degradation and ignition have resulted in a better understanding of the fundamental processes involved. However, it is still not possible to predict, with any degree of confidence, whether ignition will occur under given conditions, when ignition will occur and if ignition will be sustained, unless there are experimental data available to support the mathematical approach. This is analogous to stating that, thus far, mathematical models have been successful only at the correlational level. Further progress towards realistic predictive models requires a much greater examination of the assumptions and criteria inherent in the correlations.

1.4 RADIATIVE IGNITION OF A COMBUSTIBLE SOLID

1.4.1 Scenario

In room fires, radiative heating plays a more important role in spread of fire than does convective heating (deRis (1979)). Figure 1.5 shows schematically the heat transfer model and possible decomposition processes when a polymer is exposed to radiation. Part of the incident radiation (Q") will be reflected, part transmitted and the remainder absorbed by the irradiated material. Of that portion initially absorbed, part will be re-radiated, part will be lost by convective cooling effects and the remainder will be retained within the material. The proportion of energy absorbed is primarily dependent on the absorptance characteristics of the material surface and the spectral distribution of the incident source. The amount of initially absorbed energy which is retained in the material and contributes to temperature rise is determined by the thermal properties and physical thickness of the irradiated material.

1.4.2 Factors Affecting Ignition by Radiation

In general, factors affecting ignition may be classified into 2 broad categories.

1. Material considerations
2. Environmental parameters

1.4.2.1 Material Considerations

It is possible to identify several material properties which influence ease of ignition. For example, if the heat of volatilization (L_v) is high or the heat of combustion (ΔH_c) small, then the material will be difficult to ignite. Thermally stable materials which have high degradation temperatures will exhibit greater

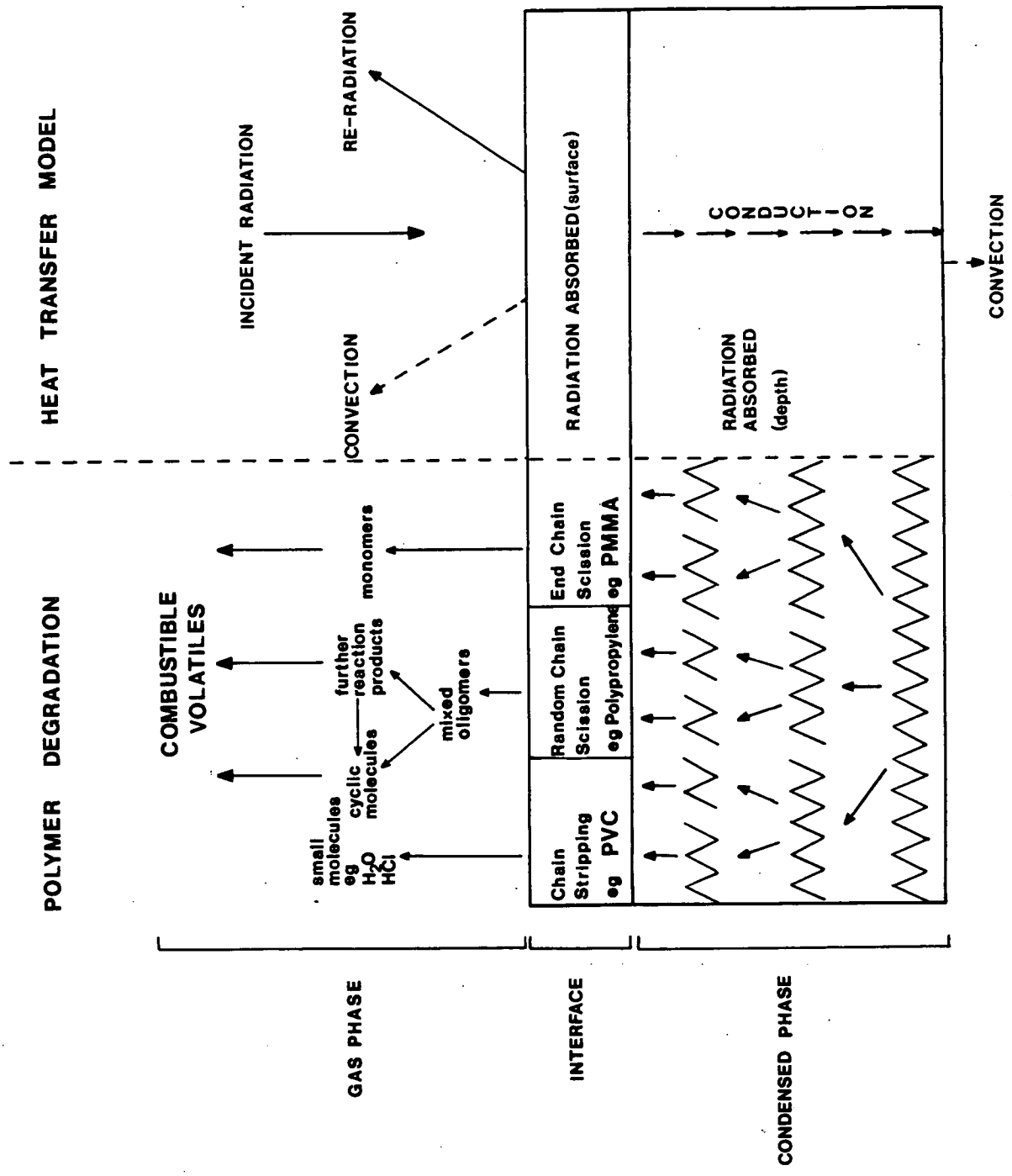

Figure 1.5 Schematic representation of polymer exposed to radiation

radiative heat losses at the firepoint than those with lower degradation temperatures. Char forming materials develop a layer of char which insulates the fuel below resulting in higher temperatures being required at the char surface to maintain the flow of volatiles.

Thermal inertia ($k\rho c$) plays an dominant role in the rate of heating of a thick solid (Table 1.4). The surface temperature of materials with small thermal inertia responds more rapidly to an imposed heat flux than that of materials with large thermal inertia. This is clearly demonstrated by the thermal heat up model based on the constant heating of a thermally thick, opaque solid (Carslaw & Jaeger (1959)) with an assumed constant surface ignition temperature which yields a simple analytical expression for ignition delay time (equation 1.22) and indicates that ignition delay time is directly proportional to thermal inertia.

Table 1.4

Materials exposed to a radiant flux of 25kW/m^2

MATERIAL	THERMAL INERTIA (W^2S/M^4K^4)	IGNITION TEMPERATURE / IGNITION TIME ($^oC/s$)*
PS	$1.7x10^5$	3.3
PMMA	$3.2x10^5$	2.7
POM	$7.7x10^5$	1.5

* Data from Thomson and Drysdale (1987)

It is possible to modify several of the above properties by the addition of extraneous materials, in particular fire retardants, to the combustible solid. For

example, bromine and chlorine containing fire retardants release halogen into the gas phase along with the volatiles and render them less reactive. Borates and phosphates added to cellulosic materials promote a degradation reaction which creates a greater yield of char and a higher proportion of CO_2 and H_2O in the volatiles thus reducing ΔH_c. Alumina trihydrate is often used as a filler for polyesters. This increases the thermal inertia and effectively lowers ΔH_c as water vapour is released with the volatiles.

Kashiwagi et al. (1986) investigated the differences in polymethylmethacrylate degradation characteristics and their effects on its fire properties for two different commercial brands of PMMA. They attributed the small differences found to inter brand property variations such as molecular weight, impurities, addition of plasticisers and uv absorbers, etc.

Another important factor affecting the ignition process is surface absorptivity. Most organic materials reflect varying proportions of the incident energy in in the near visible region from 0.3 to 1.0μm. Both Gardon (1953) and Williams (1953) used heat balances to estimate values for absorbed energy by wood. Gardon calculated apparent absorptivities in the range 44-70% and Williams in a comparable study reported the corresponding value for birch to be 66%. Both these calculations ignored the effect of chemical reactions. The heat balances were obtained from measured sample temperatures. Simms (1960) observed that the absorptivity of wood is dependent on exposure time. He deduced empirical absorption factors corresponding to different exposure times by comparing the intensities of irradition required to ignite the natural material with those required when the material is artificially blackened by carbon black.

Hallman, Welker and Sliepcevich (1972, 1974, 1976, 1977, 1978) have carried out substantial work on absorptance characteristics of a variety of commercial plastics. Reflectance measurements were obtained using spectrophotometers over the wavelength range 0.3 to 10μm. Absorptance values were obtained by means of Kirchoff's Law (Equation 1.33).

$$\bar{\alpha}_\lambda + r_\lambda = 1 \qquad (1.33)$$

Where $\bar{\alpha}_\lambda$ is monochromatic absorptance and r_λ is monochromatic reflectance.

The average absorptances of the polymers over the monochromatic wavelength span of the heat sources were represented by the equation

$$\alpha_{av} = \frac{\int_{\lambda 1}^{\lambda 2} \bar{\alpha}_\lambda e_\lambda . d\lambda}{\int_{\lambda 1}^{\lambda 2} e_\lambda . d\lambda} \qquad (1.34)$$

where e_λ is monochromatic emissivity of source and λ is wavelength.

Equation 1.34 was converted to a trapezoidal rule summation (equation 1.35) for use in a computer program.

$$\bar{\alpha}_{av} = \frac{\Sigma \bar{\alpha}_\lambda e_\lambda \Delta\lambda}{\Sigma e_\lambda \Delta\lambda} \qquad (1.35)$$

Hallman et al. quote average absorptance values for various polymers under a variety of radiation sources. The limits of integration are the wavelengths which include "significant" amounts of source energy. It was observed that certain dark coloured materials such as black Plexiglas exhibited essentially blackbody behaviour and consequently, very little difference in average absorptance with different radiation sources was detected. Conversely, materials exhibiting several discrete peaks in their infrared absorption spectra (see Figure 1.6) were found to have average absorptances strongly dependent on the nature of the source. For

example, the average absorptance of clear Plexiglas was found to vary from 0.85 for a blackbody radiation source at 1000^{o}K to 0.25 for a blackbody radiation source at 3500^{o}K.

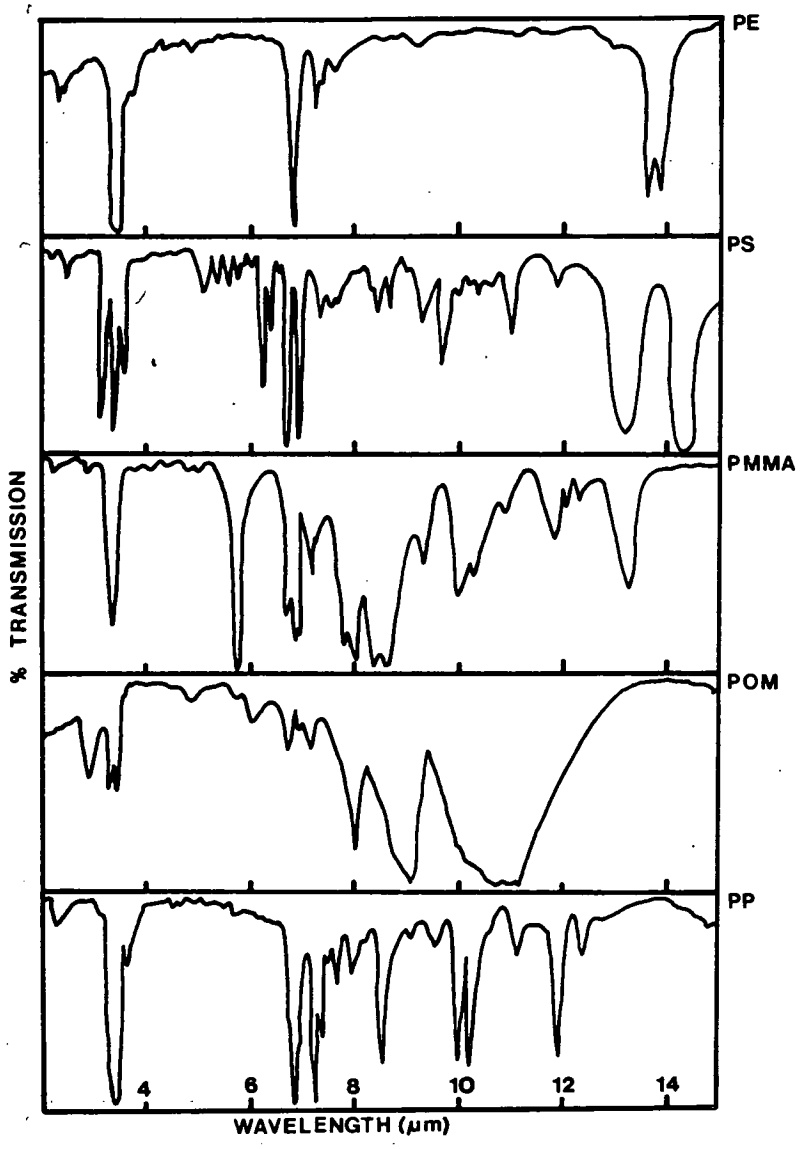

Figure 1.6 IR absorption spectra.

The effect of diathermancy on the temperature rise of solids is still uncertain. Conventionally, the Lambert-Beer attenuation law is used to calculate the energy absorption, u.

$$u = \bar{\alpha}_{av} Q''.\exp(-\bar{\alpha}_{av} x) \qquad (1.36)$$

However, with highly reflecting diathermanous materials which produce indepth

scattering, u cannot be expressed as simply as in equation 1.36 (Simms (1962)).

1.4.2.2 Environmental Parameters

Ignition is also strongly dependent on various experimental parameters, the most obvious of these being rate of heating. Aside from the variations in composition of the pyrolysis products obtained under different heating rates, there is a predictable relationship between heating rate and ignition delay time.

Lawson and Simms (1952) and Koohyar (1968b) showed that there is a critical heat flux below which a combustible solid cannot be ignited. Theoretically, the time required for the surface temperature to reach the ignition temperature increases asymptotically to infinity as the external radiation is reduced. This asymptotic value can be found from the surface energy balance for an inert solid expressed as:-

$$-k\frac{\partial T}{\partial x} = Q'' - h(T_S - T_O) - \varepsilon\sigma(T_S^4 - T_O^4) \qquad (1.37)$$

If surface temperature (T_s) is replaced by ignition temperature (T_{ig}) then as time tends to infinity so the left hand side of equation 1.37 tends to zero. Hence the minimum radiant heat flux for ignition is given by:-

$$Q''_{min} = h(T_{ig} - T_O) + \varepsilon\sigma(T_{ig}^4 - T_O^4) \qquad (1.38)$$

Several discrepancies in the results obtained by different investigators may be partially explained in terms of variations in experimental method and apparatus. Factors such as nature and position of pilot source may affect ignition. In general, there are three common types of pilot source (viz. flame, spark and glowing wire). Ideally the pilot will be situated in the region of highest volatile concentration, will not contribute to the incident radiation and will be sufficiently energetic to initiate combustion. Any deviations from this situation would be expected to produce inconsistencies in the results. Simms (1962) investigated the effect of pilot

flame position on ignition and found a dependency. Some investigators have attempted to avoid this problem by use of a pilot source "large enough to preclude effects of pilot position on ignition time" (Hallman et al. (1972))

The configuration and situation of the apparatus may also have an effect on ignition. These features will affect the airflow around the sample which would be expected to influence the formation of a flammable volatile/air mixture in the vicinity of the sample surface. An imposed air flow or one induced by an extract system could also influence air flow patterns and result in cooling of the heated surface.

Sample orientation should be taken into account. A horizontal sample exposed to radiation experiences uniform entrainment of air from all sides and the surface temperature is essentially uniform over the exposed area. However, with a vertical sample, entrainment of air is non-uniform and a well defined boundary layer is formed. This results in a pronounced surface temperature gradient from top to bottom of the sample (Atreya et al. (1986),Kashiwagi (1982)).

Both sample area and thickness may be expected to have some effect on ignitability (Simms et al. (1957)). Simms (1960) investigated the effect of sample area on ignition in some detail and observed that the effect was smaller when irradiance was high. For areas in excess of $0.01m^2$, the increase in ignition time is typically only 10% over that for a specimen of infinite area. In practical terms, the ideal specimen should be of such an area as to exhibit one dimensional heat transfer and to eliminate edge effects. If a specimen is thermally thick (physical thickness in excess of $2(\alpha t)^{\frac{1}{2}}$) then further increase in thickness would not be expected to have any effect on ignition. However, thinner samples would be

expected to exhibit a dependency on thickness and also on the nature of the backing material.

The most variable feature of ignition experiments tends to be the radiation source. The nature of the incident radiation has a significant effect on ignition. In accidental fires, the radiation source will generally be a fire in the vicinity of the target object. If the fire is sufficiently small and the flames are optically thin, a substantial portion of the emitted radiation will be within two narrow wavelength intervals characteristic of H_2O and CO_2 around 2.7 and 4.4μm, respectively (Hallman (1971)). In the case of a large fire with luminous diffusion flames containing large amounts of incandescent carbon, radiation from the soot will result in the dominance of essentially grey-body radiation. However, experimentally a large variety of radiant sources have been employed by different investigators.

Bamford et al. (1946) utilised a vertical electric heater composed of twenty one one kilowatt elements. Lawson and Simms (1952) obtained uniform irradiances over an area in excess of $60cm^2$ using a gas fired surface combustion heater. Simms (1960,1961) compared the ignition of thick and thin cellulosic materials and blackened fibreboard under three different radiation sources. These were a tungsten filament lamp with ellipsoidal mirror for focussing, a carbon arc source and a gas fired radiant panel. Simms and Coiley (1963) calculated an effective emissivity of 0.7 for a gas fired panel with an absolute effective blackbody temperature of 1150^0K.

Koohyar et al. (1968a,b) designed an ignition cabinet which used buoyant diffusion flames from liquid fuels as the radiation source. However,they observed

difficulties in distinguishing between spontaneous and piloted ignition when the flames were very close to the sample surface.

Hallman (1971) compared ignition of various plastics and rubbers under radiation from benzene flames with that from a tungsten lamp. Hallman et al. (1972,1974,1976,1977,1978) carried out a systematic investigation into the effect of radiation source on polymer ignition. They considered blackbody radiation sources at six temperatures between 1000^{o}K and 3500^{o}K, flame radiation and solar radiation. They have also compared the carbon arc and radiant panel as radiant heat sources.

The radiant source utilised by Clark (1984b) consisted of a flat spiral helix of resistance wire supported on a ceramic form so that the radiating area was effectively a circular plate 75mm in diameter. An average radiant heat flux of 17 kW/m^2 was produced.

Radiation sources currently in favour include the conical radiant heater (Heselden (1976)) consisting of a coiled electrical element and found in standard apparatus such as the ISO Ignitability Test apparatus (ISO 5657-86 (1986)) and the cone calorimeter (Babrauskas and Parker (1987)). The CO_2 laser has also been widely used recently since mathematical analysis of the results is considerably simplified by consideration of a monochromatic radiation source (Ohlemiller and Summerfield (1971), Kashiwagi (1979a,b), Mutoh et al (1979), Niioka and Williams (1979), Beckel and Mattews (1984)).

Each radiation source has its own characteristic spectral output which may differ considerably from an equal intensity output from an alternative source (Figure 1.7). Electrical heaters generally show near grey-body emission and a high

emissivity (Heselden (1976)). Gas-fired radiant panels, which typically operate around 900°C, derive a significant portion of their radiation from the ceramic face and thus exhibit discrete molecular wavelength peaks superimposed on a grey-body continuum (Comeford (1972), Simms and Miller (1963)). High temperature lamps (2000 - 3000°C) have a substantially different spectral output from sources operating at lower temperatures. CO_2 lasers exhibit essentially monochromatic radiation around 10.6μm. The spectral output of a flame consists of characteristic molecular peaks including those at 4.4 and 2.7μm corresponding to CO_2 and H_2O, respectively.

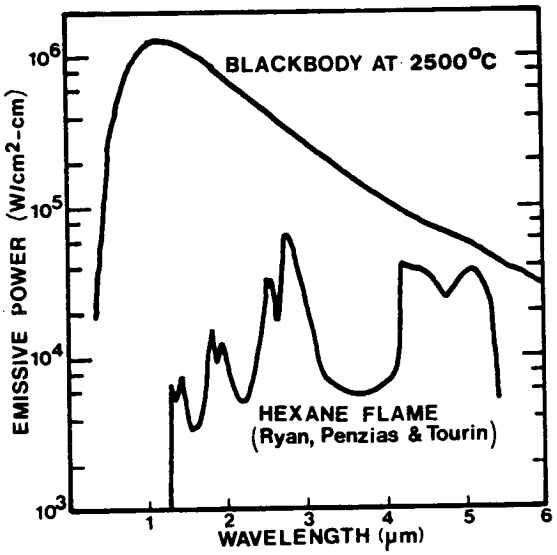

Figure 1.7 Characteristic spectral outputs (Hallman et al. (1972))

The importance of the variations in spectral output is dependent on the absorptivity of the surface to be ignited. For materials whose radiant absorptance is independent of wavelength, source variation is immaterial but the majority of materials show a variety of characteristic absorption peaks in the infrared region. Optimum absorption of energy occurs at wavelengths where the sample shows strong absorptivity and the source shows a complimentary high emissivity.

1.5 OBJECTIVES OF THE RESEARCH

This project was undertaken with the aim of systematically investigating the processes involved in the ignition of plastics under exposure to low level radiation. In particular, it was intended to establish the validity of defining ignition by the criteria of critical surface temperature and/or critical mass flux of volatiles. It was also intended to accumulate sufficient mass loss data to fully test the "firepoint equation" (Rasbash (1975))

The effect of various material and environmental factors on ignition was considered with a view to identifying potential inconsistencies between existing ignitability tests. The ISO ignitability test was studied in detail and modifications were made to allow measurement of surface temperature. It was hoped that the potential of the ISO ignitability test for fire hazard assesssment could be gauged on the basis of experimental results.

The development of a correlational computer model for piloted ignition in conjunction with the experimental work was deemed to be useful.

CHAPTER 2

EXPERIMENTAL

CHAPTER 2
EXPERIMENTAL

2.1 INTRODUCTION

The initial objective of the experimental work has been to identify and measure properties of polymeric materials which could be classed as fundamental to the ignition process. The dependency of these measurements on the experimental and environmental parameters discussed previously was investigated. The properties selected for study were ignition delay time, firepoint temperature and critical mass flux of volatiles at the firepoint. Appendix B identifies the materials studied which were all of commercial origin and were not pre-conditioned in any way.

2.2 IGNITION DELAY TIME AND FIREPOINT TEMPERATURE

2.2.1 E.U. and ISO Ignitability Apparatus

Firepoint temperatures and ignition delay times were measured in each of two types of ignition apparatus:

1. The Edinburgh University (E.U.) apparatus.
2. The ISO ignitability apparatus.

In both cases, horizontal samples were exposed to radiation from a conical heater. However, several differences in configuration and mode of operation existed between the two sets of apparatus (Table 2.1). Comparison of equivalent results from each test rig enabled observations on apparatus dependency to be made.

Table 2.1

Comparison of E.U. and ISO ignitability apparatus

FEATURE	E.U. APPARATUS	ISO APPARATUS
1. Pilot	Non-luminous H_2 diffusion flame at end of horizontal swing arm (manual).	Luminous premixed propane flame applied at regular intervals by "nodding duck" system (mechanical).
2. Location	In laboratory with partial, all-round screening.	In open-fronted fume cupboard.
3. Sample mounting	Sample surface 25mm above surroundings. Sample edges totally enclosed by sample holder. Sample backed by Kaowool board.	Sample surface flush with surroundings. Sample edges exposed. Sample backed by Supalux.
4. Heat flux	Heater at fixed temperature. Heat flux varied by altering position of heater.	Heater in fixed position. Heat flux varied by altering heater temperature.
5. Sample size	65mm x 65mm.	165mm x 165mm.

2.2.1.1 Edinburgh University (E.U.) Ignition Apparatus

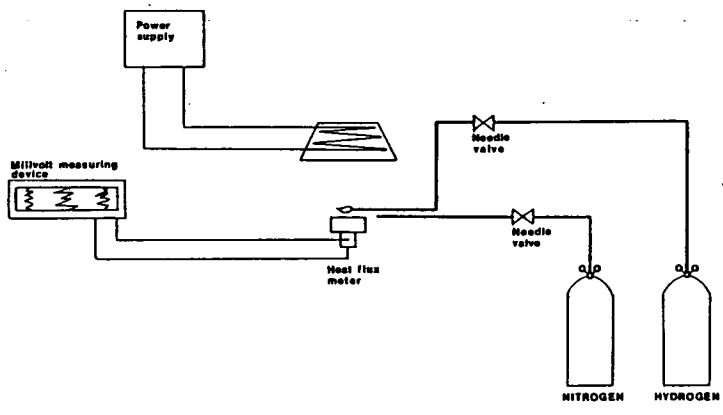

Figure 2.1 E.U. ignition apparatus (schematic)

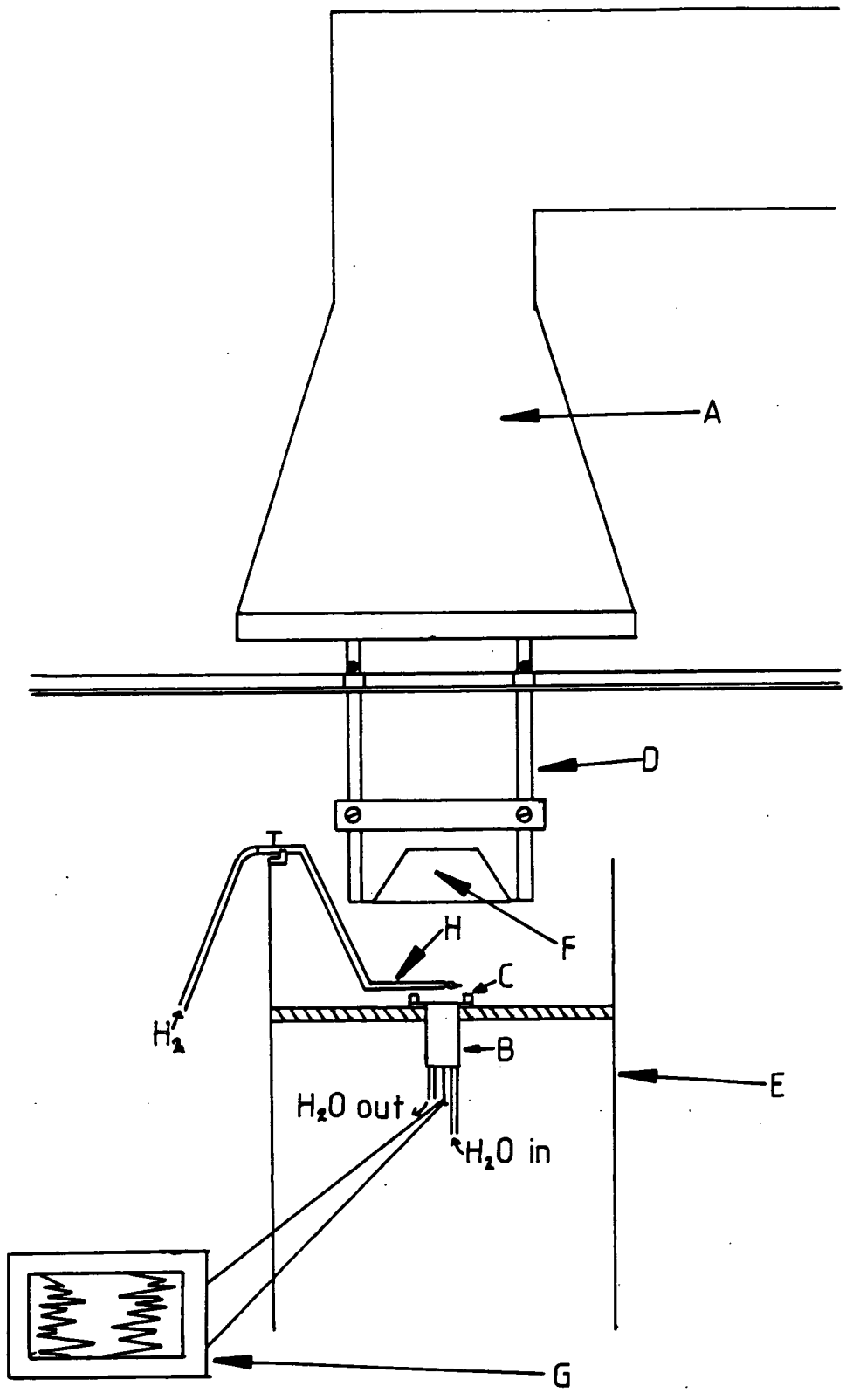

Figure 2.2 E.U. ignition apparatus
A, extract hood; B, heat flux meter; C, guide rails; D, support rods; E, draught shield; F, radiant conical heater; G, pen chart recorder.

Description: The ignition apparatus used in the first phase of this work evolved from a rig designed by Deepak and Drysdale (1983). A conical radiant heater (Stanton Redcroft Limited) composed of nine concentric turns of electrical heating element and similar to that incorporated in the ISO Ignitability Test apparatus (ISO 5657-86 (1986)) was used to provide radiant heat. The range of radiant heat fluxes (10-40kW/m^2) was achieved by setting the heater to its maximum temperature (1050^{o}K) and adjusting its height above the sample surface to one of a number of set levels determined by the spacing of adjustment holes in the support rods, ie constant heater temperature/variable heater position (Figure 2.3).

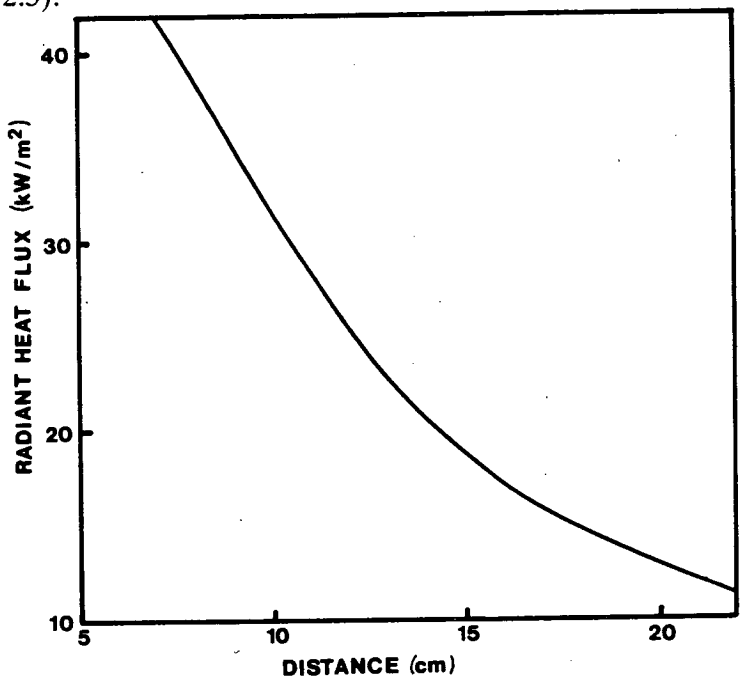

Figure 2.3 Heater position versus radiant heat flux.

The radiation intensity in the plane of the sample surface was measured using a blackened Gardon type heat flux meter (see Wraight (1971)) which had previously been calibrated against a secondary standard at the Fire Research Station, Borehamwood (Figure 2.4). The voltage output from the heat flux meter was recorded on one channel of a six channel pen chart recorder (Watnabe

Multicorder) with a full scale deflection setting of 1mV.

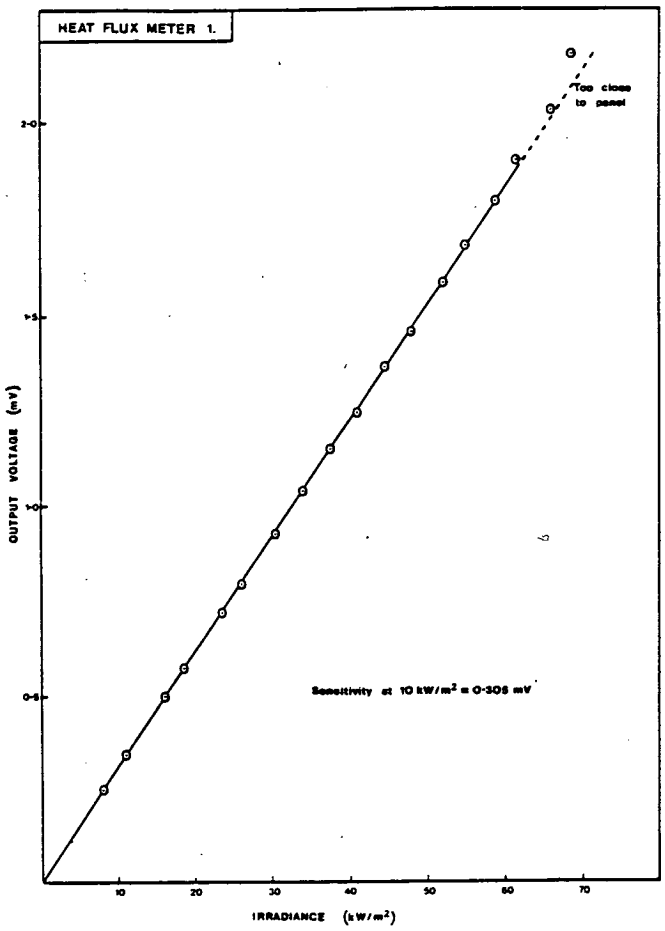

Figure 2.4 Calibration chart for heat flux meter.

Uniformity of flux was verified in a very crude manner by exposing a sheet of white card (300mm x 300mm) to radiation from the conical heater and observing the development of char on the surface of the card. A more quantitative investigation was then carried out in which the heat flux meter was traversed across a horizontal plane and the heat flux at several positions was measured (Figure 2.5). Within a radius of 30mm from the centre (equivalent to sample area of exposure), the radiation intensity was found to decrease by less than 0.5%, whilst at 50mm from the centre, radiation intensity was approximately 1.5% reduced.

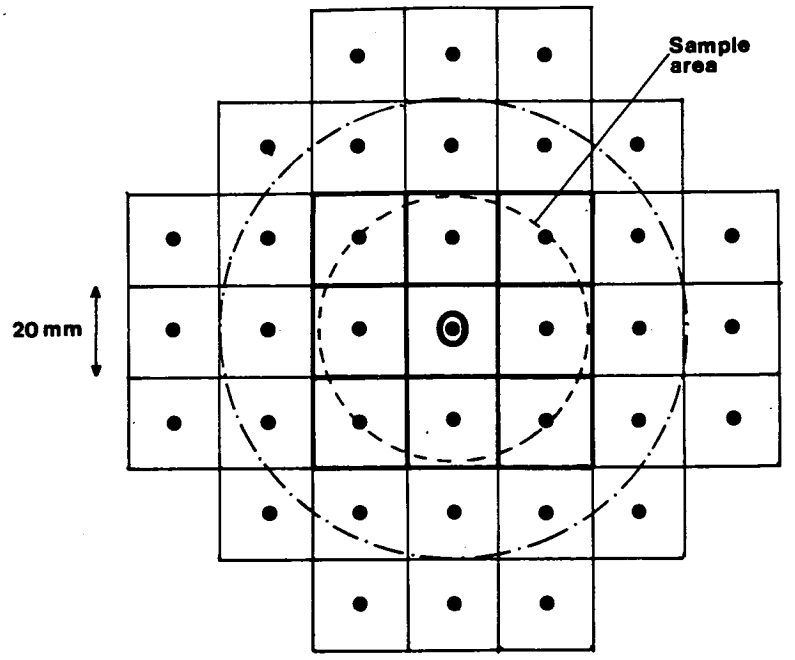

Figure 2.5 Measurement of heat flux profile.

During a normal series of experiments, the heat flux meter was located in a lower position directly below the centre of the heater thus allowing the reproducibility and stability of the heater output to be monitored between runs without interfering with the sample positioning. The apparatus was completely surrounded by a draught shield of mild steel and was located beneath an extract hood.

Method: The samples (65mm x 65mm x 6mm thick) were wrapped in aluminium foil. The sample holder, which was constructed from 0.6mm stainless steel, allowed exposure of a circular area 60mm in diameter (Figure 2.6). A small rectangle of foil was removed from the centre of the rear face of the sample to permit a thermocouple junction to be attached. The sample was then placed in the holder and the foil peeled away from the exposed circular area. A second thermocouple was attached to the centre of the exposed sample surface. The sample was held in position in the holder by a tightly fitting Kaowool backing board. The heater was allowed to equilibrate for approximately 20 minutes until

the heat flux meter in its raised position gave a steady output which was noted. The heat flux meter was then dropped to its lower position and the sample was quickly placed in position using the fixed guide rails. On observation of the evolution of volatiles, a small, non-luminous hydrogen diffusion flame (6mm long) at the end of a swing arm formed from a length of copper tubing (internal diameter 2mm) was passed across the sample surface at 4 second intervals until sustained burning occurred or until 15 minutes had elapsed. Flames were quenched by directing a stream of nitrogen across the sample surface. The specimen holder was then withdrawn from the apparatus and the thermocouple "hot" junctions removed from the samples before solidification of the polymer prevented their easy removal. Results of these experiments are included in Table 4.2.

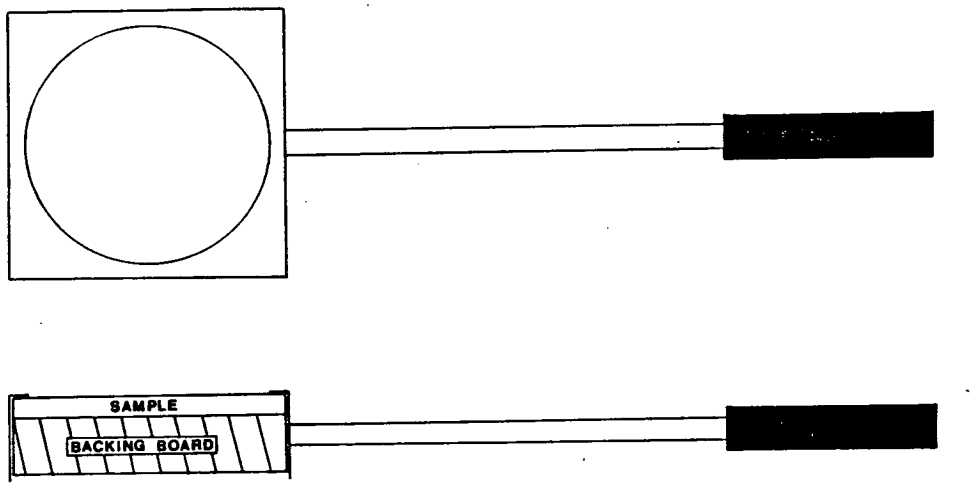

Figure 2.6 Sample holder

2.2.1.2 ISO Ignitability Test Apparatus (Figures 2.7 and 2.8)

Description: The rig consisted of a support framework which allowed the test specimen to be clamped horizontally between a pressing plate and a masking plate such that a defined area (disc 150mm in diameter) of the upper surface of the

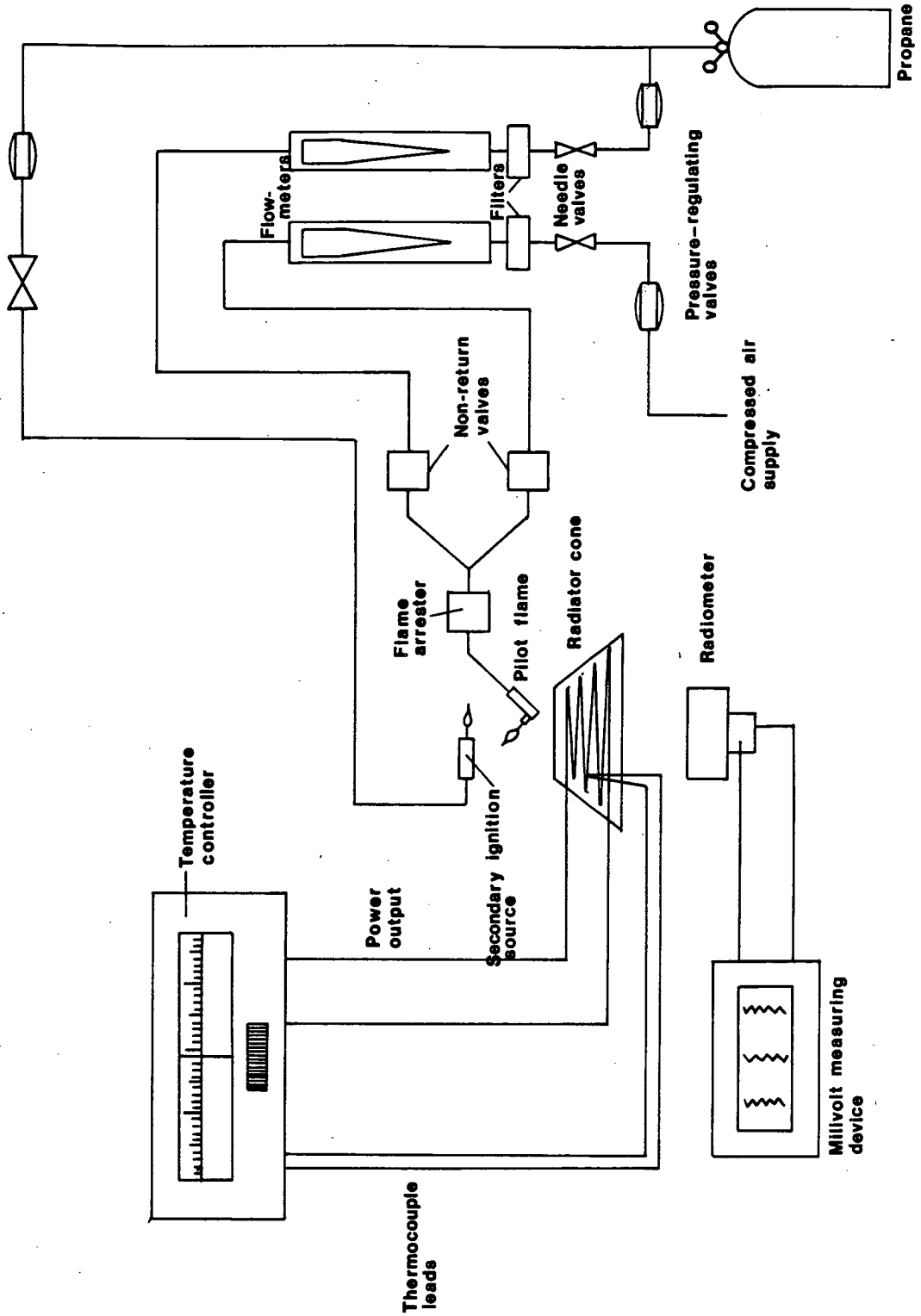

Figure 2.7 ISO ignitability apparatus (schematic)

specimen was exposed to radiation. Radiation was provided by a radiant conical heater powered by a voltage stabilised source with heater element temperature feedback control. The range of radiant heat fluxes (10-50kW/m^2) was achieved by maintaining a fixed heater position and altering the heater temperature by adjusting the supply voltage from the stabilised source. An automated pilot flame application mechanism brought a small premixed propane flame at 4 second intervals through the centre of the radiator cone to a position 10mm above the centre of the specimen surface. A screening plate was used to shield the specimen during its insertion into the apparatus.

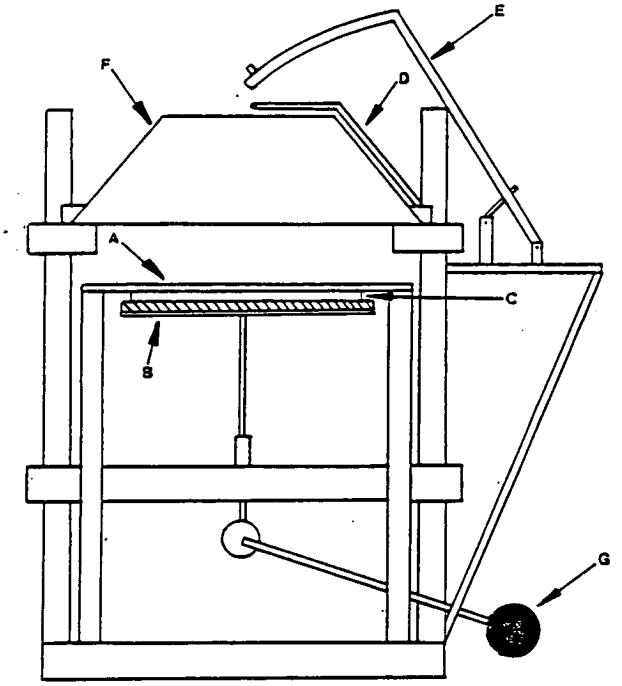

A, masking plate
B, pressing plate
C, sample
D, fixed flame
E, pilot flame applicator
F, radiant conical heater
G, counterweight

Figure 2.8 ISO ignitability apparatus.

Method: Samples (165mm x 165mm x 6mm thick)were wrapped in aluminium foil. A disc of foil 150mm in diameter was removed from the upper surface of the samples and a small central area(~1cm^2) at the rear of the sample was also exposed. Fine K type thermocouples were attached to the centres of upper and rear sample surfaces. The samples, backed by Supalux board, were placed on the

insertion and location tray (Figure 2.9).

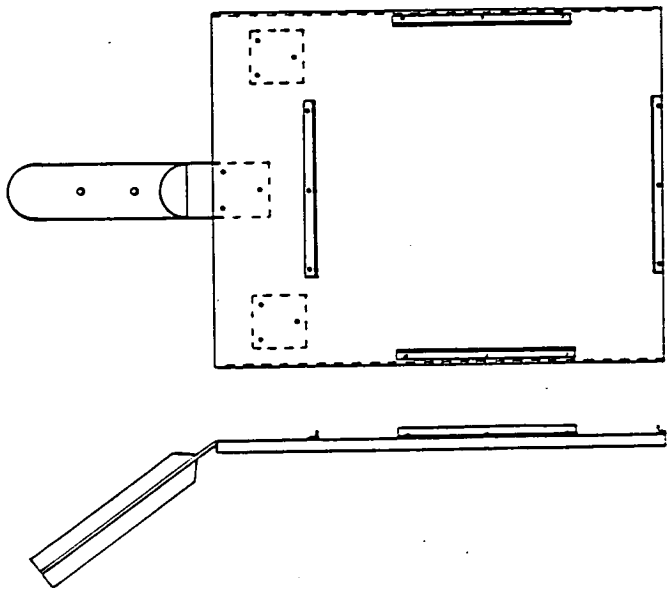

Figure 2.9 Insertion and location tray.

The screening plate was placed on top of the masking plate and the pilot flame application mechanism started. The pressing plate was lowered to allow insertion of the specimen and then released to hold the specimen against the masking plate. The screening plate was subsequently removed and timing commenced. Timing was terminated either when sustained surface ignition occurred or alternatively after 15 minutes of testing if no ignition occurred in this time. Flames were quenched by placing the extinguishing board on top of the masking plate. The thermocouple "hot" junction was then removed from the sample surface before solidification of the polymer occured. Results of these experiments are included in Table 4.2.

2.2.2 Thermocouple Techniques

Very fine chromel/alumel (T_1/T_2, K type) thermocouple "hot" junctions were formed from 0.06mm thermocouple wires. The junctions were either silver soldered and the bead hammered flat or spot welded. The reference junction

(silver soldered) and remainder of the thermocouple wiring was constructed from 0.38mm wires. The "hot" junction was attached to the larger diameter wiring by means of a type K thermocouple line plug and socket. This permitted the easy removal of samples with the "hot" junctions still attached at the end of an experiment and allowed selective replacement of the "hot" junction when necessary. The reference junction was placed in melting ice and the "hot" junction attached to the centre of the sample surface using the appropriate adhesive where available (eg "Tensol" for polymethylmethacrylate) or alternatively by local heating of the material and lightly pressing the junction into the surface (Table 2.2).

Table 2.2

Thermocouple attachments

MATERIAL	METHOD OF ATTACHMENT
Polymethylmethacrylate (PX)	A
Polymethylmethacrylate (FINN)	A
Polyoxymethylene (POM)	B
Polypropylene (PP)	B
Polyethylene (PE)	B
Polystyrene (PS)	A

A indicates thermocouple attached by adhesive

B indicates thermocouple attached by local melting of material

The thermocouple outputs were monitored continuously by means of two of the six channels of the pen chart recorder (Watanabe Multicorder) on full scale

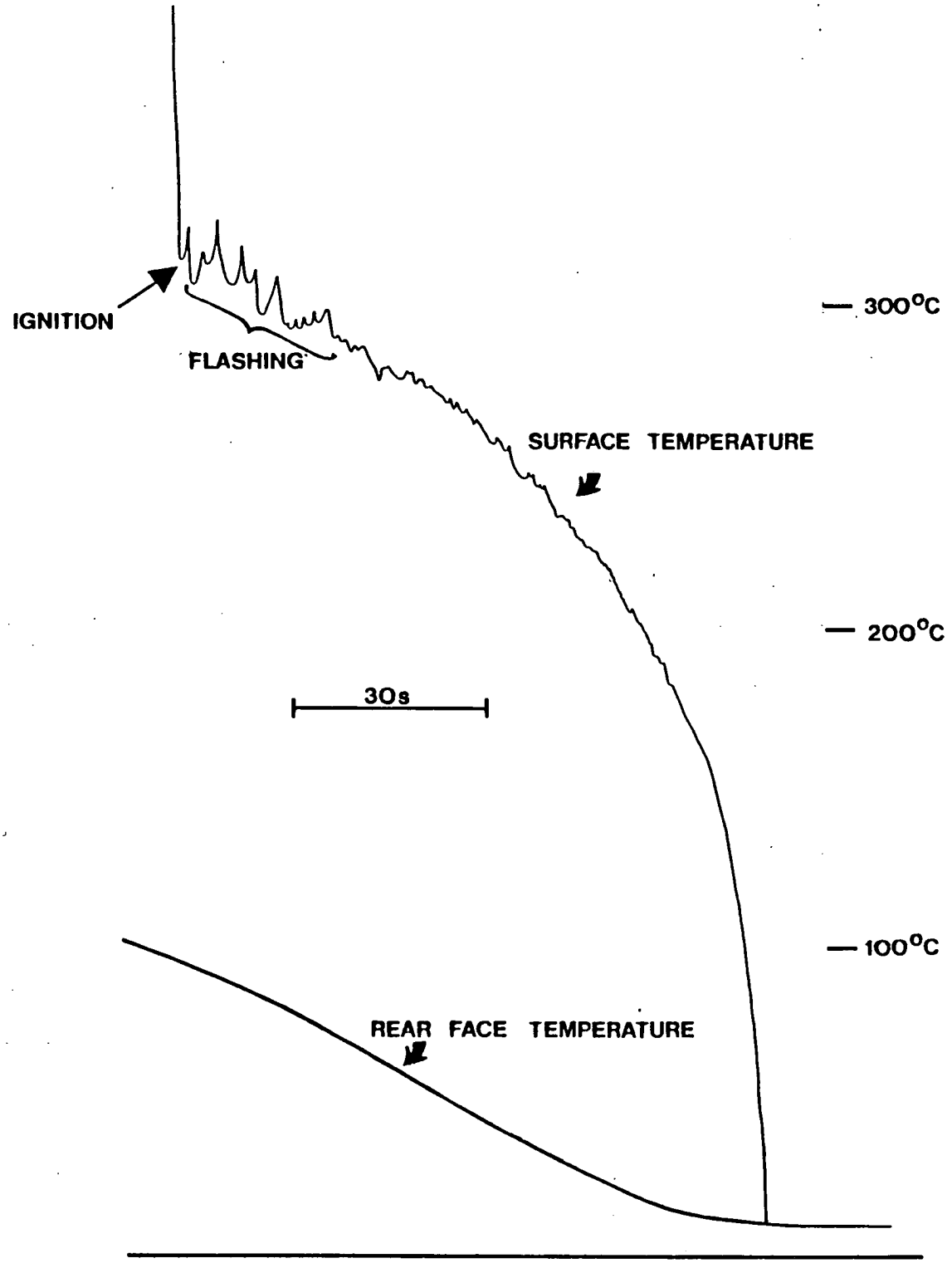

Figure 2.10 Typical surface temperature-time curve (PX@30 kW/m^2)

deflection settings of 20mV. E.m.f. values were converted to temperature using standard tables (BS4937 Part 4 (1977) Type K) and temperature-time curves were plotted. "Hot" junctions were replaced after a maximum of five usages since there was a tendency for the junction to become brittle and fail during a run if heated and cooled repeatedly. Calibration of the thermocouples was checked regularly between experiments by use of a reference temperature of 100°C (boiling water).

Maintenance of close contact between the thermocouple junction and the sample surface proved difficult. There was a tendency for the junction either to lift off the surface completely, characterised by a sudden increase in "noise" on the thermocouple output, or alternatively to sink into the polymer melt, resulting in a very sluggish response by the thermocouple after ignition. This was a particular problem for the hydrocarbon polymers (PE,PP and PS) with their low melt viscosities, and for all materials exposed to low heat fluxes with correspondingly long heating times. All temperature-time traces with excess noise or sluggish response to ignition were rejected. Figure 2.10 shows a typical, acceptable temperature-time plot. The chart paper speed, which was verified regularly, was varied according to the intensity of the imposed incident radiation in order to produce traces within a fairly uniform length range. At minimum flux a speed setting of 30mm/minute was used and at maximum flux a setting of 120mm/minute was used. A small constant voltage was applied to one of the spare channels on the chart recorder and an "interupt" switch was used to mark the start and end point of an experimental run on this trace. The ignition delay time was determined by converting the distance between markers on the chart trace to time. Various arrangements for thermocouple attachment were tested and the most successful which was subsequently adopted for all temperature

measurements is shown in Figure 2.11. Experiments at each radiation level were repeated until six acceptable temperature traces were obtained. Firepoint temperature and ignition delay time for a particular radiant heat flux level were quoted as the mean value (with one standard deviation in parenthesis) of the six determinations obtained (see Table 4.2).

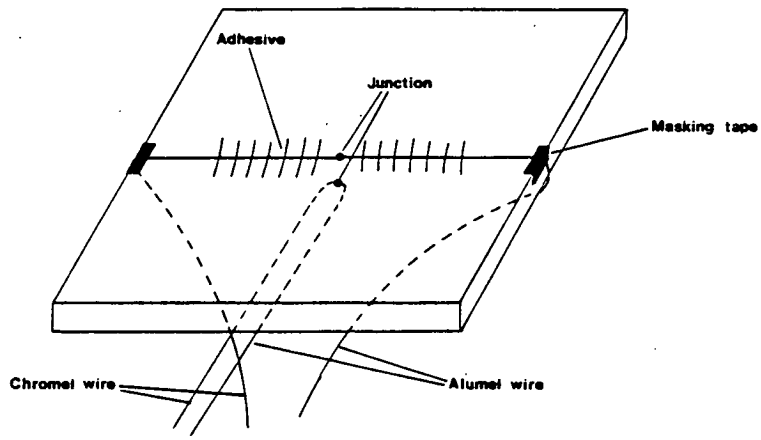

Figure 2.11 Instrumentation of sample

2.2.3 Factors Affecting Ignition

Preliminary experiments were carried out in the Edinburgh University ignition apparatus on four common materials (chipboard, hardboard, nylon carpet and glass-reinforced polyester) for the purpose of familiarisation with the apparatus. Ignition delay time was measured at four different heat fluxes but no attempt was made to obtain surface temperature measurements. These results were then compared with ignition delay times recorded for the same four materials in the ISO Ignitability Test apparatus at the Fire Research Station, Borehamwood (Table 4.1). The latter results formed part of a large scale study ("Round Robin") on the reproducibility of results obtained in the ISO Ignitability Test by several laboratories and operators (Heselden and Wraight (1984)).

Variations in the two sets of results were found and so the effect of apparatus

dependency was subsequently investigated in greater detail. Complete sets of results for ignition delay time and firepoint temperature were obtained as described previously from the E.U. rig for three brands of polymethylmethacrylate (Finnacryl, Perspex and an unidentified brand), polyoxymethylene, polyethylene, polypropylene and polystyrene at a minimum of five different radiant heat fluxes ranging from 10-40kW/m^2. All results quoted are based on the mean value of a minimum of six replicates. Similar measurements were then obtained for six of these seven materials using the ISO Ignitability Test apparatus at Fire Research Station, Borehamwood (Table 4.2). Since the operator was the same in both instances, any differences in the results may be attributed to variations between the two sets of apparatus.

It was decided to investigate these inter-apparatus differences systematically in the E.U. apparatus.

Effect on Ignition of Variation in Nature and position of the pilot source: This factor was investigated by comparing firepoint temperatures and ignition delay times for ICI Perspex as obtained previously under the following experimental conditions:

1. 25kW/m^2. H_2 pilot flame 0.5cm above centre of sample surface.
2. 25kW/m^2. Spark pilot 0.5cm above centre of sample surface.
3. 25kW/m^2. H_2 pilot flame 1.0cm above centre of sample surface.
4. 25kW/m^2. Spark pilot 1.0cm above centre of sample surface.
5. 25kW/m^2. H_2 pilot flame 2.0cm above centre of sample surface.
6. 25kW/m^2. Spark pilot 2.0cm above centre of sample surface.

The results are given in Table 4.3.

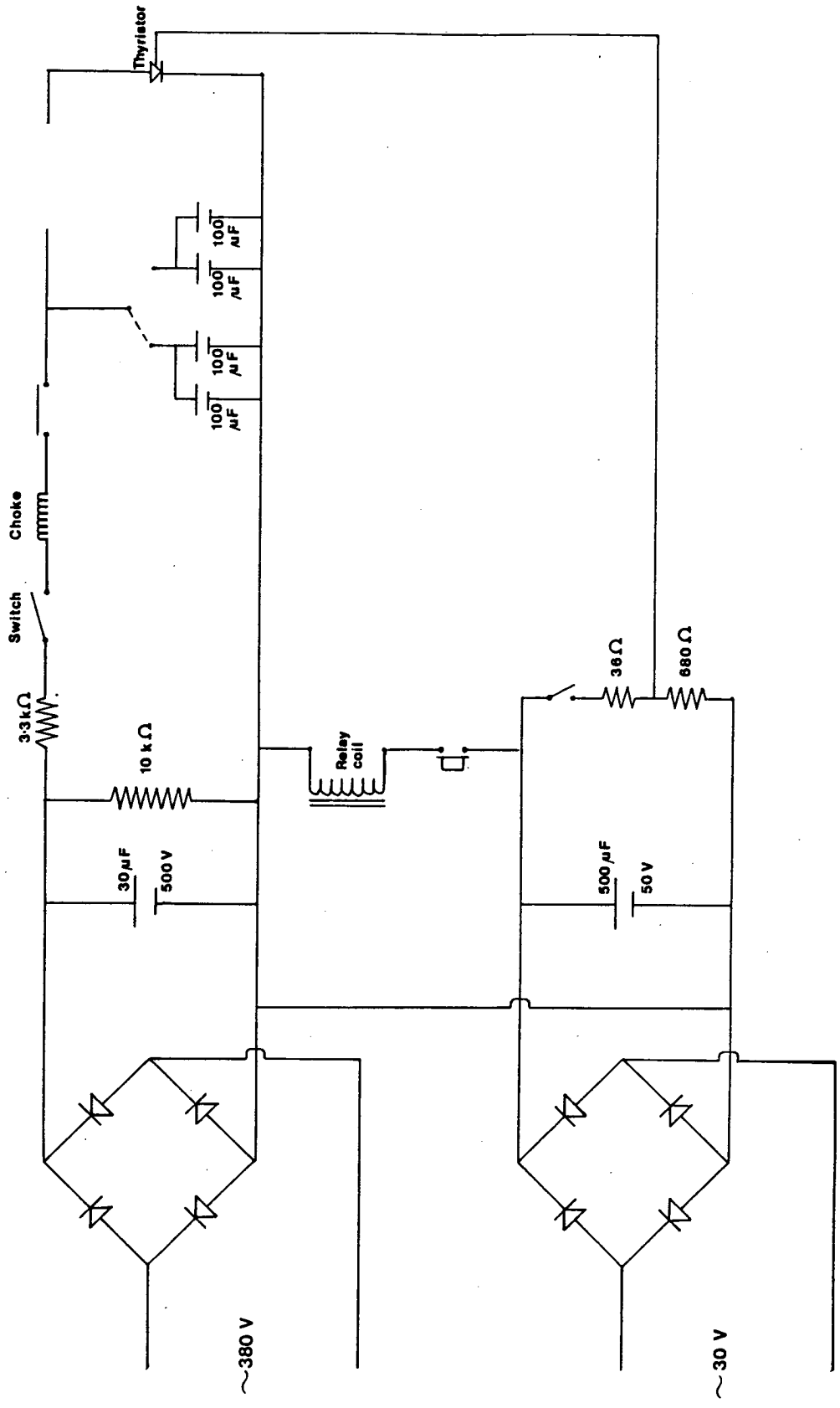

Figure 2.12 Circuit diagram for spark generator

The spark was generated using the electronic circuit shown in Figure 2.12. The electrodes were formed from tungsten rod (diameter 1mm) and the gap between points of the electrodes was bridged by a 3mm length of graphite rod (diameter 1mm).

Effect on Ignition of Airflow: Firepoint temperature and ignition delay time were obtained for Finnacryl and polypropylene at 25kW/m^2 with the extract system activated and subsequently inactivated. Comparison of results (Table 4.4) indicated whether or not a small induced airflow affected ignition.

Effect on Ignition of Sample Mounting: An alternative method of sample mounting was constructed for the E.U. rig which left the edges of the sample exposed (Figure 2.13).

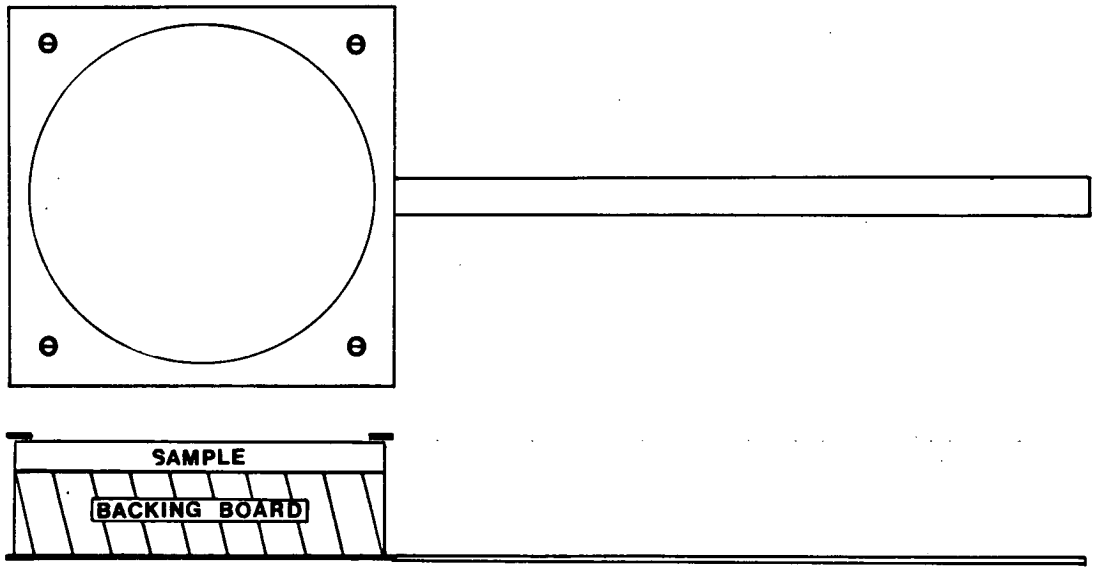

Figure 2.13 Alternative sample holder.

This system involved the sandwiching of a foil-wrapped sample and backing board between two 2mm steel plates (65mm x 65mm), the uppermost of which allowed exposure of an area of sample surface 60mm in diameter. The arrangement was

held rigid by a nut and bolt holding the plates together at each corner. Firepoint temperature, edge temperature and ignition delay time for Perspex at 25kW/m^2 using both methods of sample restraint were determined and compared (Table 4.5).

Effect on Ignition of Varying the Radiation Source: One major difference between the ISO Ignitability Test apparatus and the E.U. apparatus is in the method of achieving a range of radiant heat fluxes. In both cases, a similar conical radiant heater is utilised but in the ISO rig, the heater is in a fixed position and the radiant heat flux is varied by adjusting the heater temperature. This has the effect of altering the spectral distribution of the source. In the E.U. rig, heat flux is varied by setting the heater temperature to a fixed maximum value and adjusting the separation between source and sample which results in a constant spectral output for all heat fluxes.

Perspex and polypropylene were selected for further investigation in the E.U. rig. Times to ignition and firepoint temperature for these two materials obtained in the preliminary experiments with the E.U. ignitability apparatus, ie constant heater temperature/variable heater position were compared with results for equivalent radiant heat fluxes obtained by changing the heater temperature while maintaining a fixed heater position (lower edge 6cm above sample surface), ie procedure used in ISO ignitability test. The results of these experiments are given in Table 4.6.

Heater element temperature measurements at each radiant heat flux setting were made using a Minolta/Land Cyclops 52 infrared thermometer. A thermocouple was placed in contact with the heating element which was set at its maximum

temperature and the infrared thermometer was focused on the same area of the element. The emissivity setting on the thermometer was adjusted until the temperature reading coincided with the temperature recorded by the thermocouple. The value of emissivity thus obtained (95%) was assumed to remain constant for all temperature settings. A significant temperature gradient between the hottest and coolest turns of the heating element was observed (Figure 2.14).

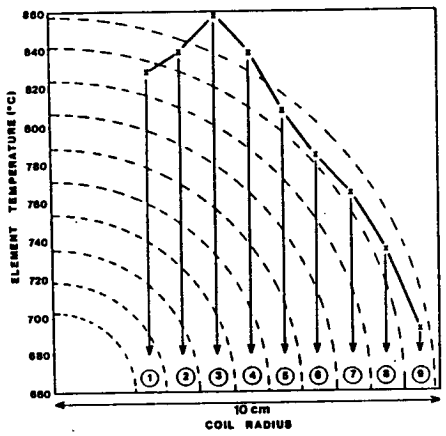

Figure 2.14 Temperature distribution of coil

Hence the temperature of each turn of the coiled element was determined and an average heater temperature based on the radius of each turn and the corresponding temperature was calculated as follows:

$$T_{av} = \frac{\sum_{x=1}^{x=9} R_x T_x}{\sum_{x=1}^{x=9} R_x} \qquad (2.1)$$

where T_{av} is average heater temperature, T_x is temperature of coil x and R_x is radius of coil x.

Figure 2.15 shows a plot of average heater temperature versus radiant heat flux with the heater in its lowest position.

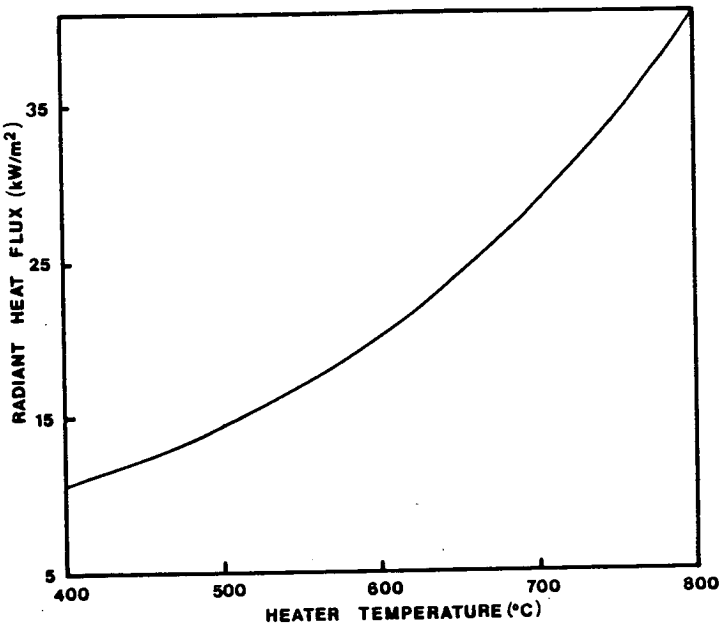

Figure 2.15 Heater temperature versus heat flux

Figure 2.16 shows the difference in spectral output between black bodies at temperatures of approximately $400^{o}C$ and $800^{o}C$ respectively, ie the minimum and maximum average heater temperatures used in this series of experiments.

In an attempt to simplify the investigation into source emission/sample absorption interactions, the E.U. apparatus was modified to incorporate a 12W, continuous wave CO_2 laser (Edinburgh Instruments Ltd.) in place of the radiant conical heater (Figure 2.17). This produced a narrow beam of essentially monochromatic radiation at a wavelength of around 10.6μm. As previously, a horizontal sample was exposed to radiation perpendicular to its surface. The laser beam was diverged by passing it through a zinc selenide meniscus lens and then deflected through 90^{o} onto the sample using a gold coated mirror. This arrangement ensured that there would be no deposition of decomposition products onto the optics of the laser. The average flux created by the Gaussian distribution of energy across the laser beam over the area of irradiation approximately 1.6cm in

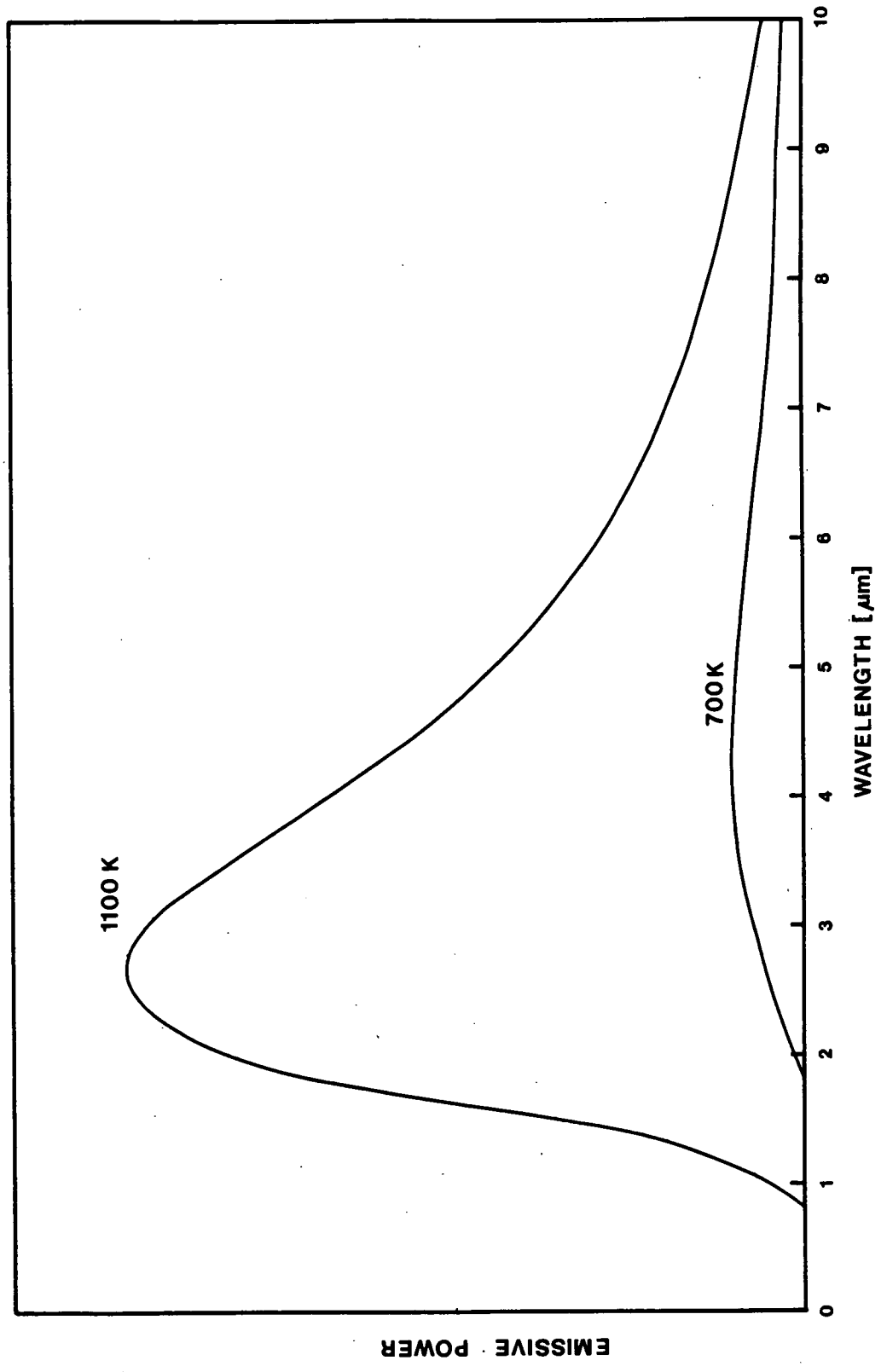

Figure 2.16 Blackbody spectral outputs

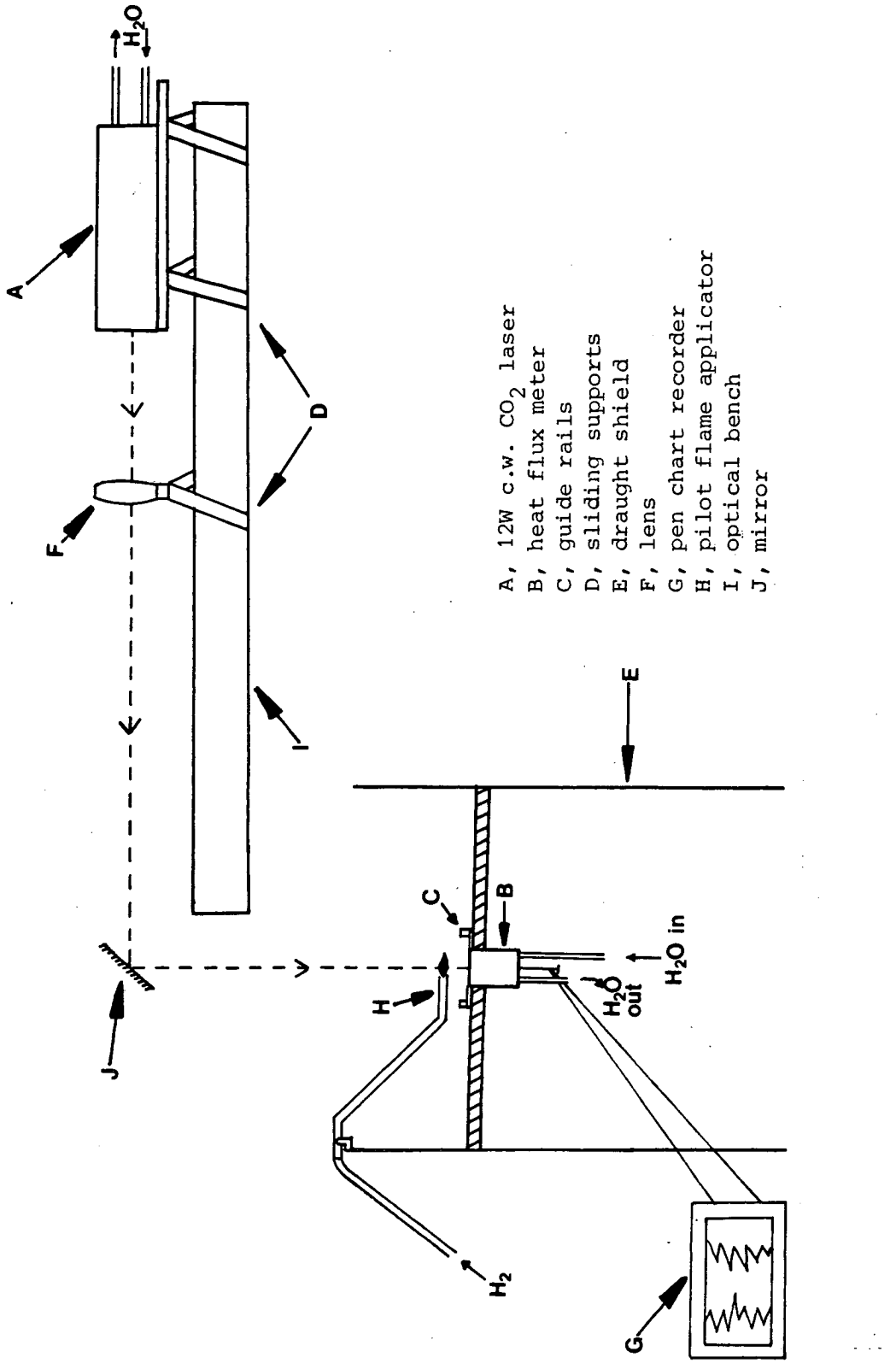

Figure 2.17 E.U. firepoint temperature apparatus incorporating laser

diameter was measured as 34kW/m^2. The method of pilot flame application was identical to previous experiments. Ignition delay time and firepoint temperature were recorded for Perspex and compared with results obtained previously for Perspex under a radiant heat flux of 34kW/m^2 produced by the conical heater (Table 4.7). It was appreciated that a direct comparison of results was not justifiable because of the large difference in areas of irradiation between laser and conical heater experiments (2cm^2 and 28cm^2, respectively). This prompted the next series of experiments.

Effect on Ignition of Sample Dimensions: A series of experiments was carried out to permit the direct comparison of results obtained using the laser source with those obtained using the conical heater (maximum temperature). The maximum area of irradiation from the laser at 34kW/m^2 was 2cm^2. Therefore it was deemed necessary to irradiate a comparable area using the conical heater. A sample of Perspex (65mm x 65mm x 6mm thick) was wrapped in aluminium foil, placed in the holder and a small central area exposed by removing a square of foil (14mm x 14mm). A thermocouple was attached in the usual way and the surface exposed to 34kW/m^2 from the conical heater. The temperature of the foil was also monitored by attaching a thermocouple to its underside and was found never to exceed 100^{0}C. Ignition delay time and firepoint temperature were recorded as previously. Further experiments were carried out in which small squares of Perspex (14mm x 14mm x 6mm thick) were flush mounted in (a) foil-covered Kaowool board and (b) blackened Kaowool board (65mm x 65mm x 25mm thick). Samples of this configuration were exposed to radiation from the conical heater and also to radiation from the laser. Ignition delay times and firepoint temperatures were recorded (Table 4.7)

The effect of sample thickness on ignition was also considered. The requirement for thermal thickness was taken as being:

$$x > 2(\alpha t)^{\frac{1}{2}} \qquad (2.2)$$

where x is sample thickness, t is time of heating and α is thermal diffusivity ($k/\rho c$).

The ignition delay times and firepoint temperatures obtained at 24kW/m^2 for samples of 6mm thick Perspex (thermally thick) were compared with equivalent results for 3mm and 1mm thick samples of Perspex sheeting. One would predict that ignition of samples which were not thermally thick for the duration of the experiment would show a dependency on the nature of the backing material. Hence previous results obtained at 24kW/m^2 for 6mm, 3mm and 1mm Perspex samples backed by Kaowool board were compared with equivalent results of experiments conducted on similar samples backed by Supalux board. The radiant heat flux was then reduced to 17kW/m^2 and the measurements on 6mm thick Perspex samples (not thermally thick) backed by both Kaowool board and Supalux were repeated. The results are given in Table 4.8.

Effect on Ignition of Specimen Absorptivity: It was recognised that each plastic would have its own characteristic absorption spectrum and, hence, the interaction of each plastic with any one specific radiation source would be unique to that plastic.

Thin films of each of the thermoplastics were produced by the methods indicated in Table 2.3.

Table 2.3

Preparation of Samples for IR Spectroscopy

MATERIAL	METHOD OF PREPARATION
PX	Reprecipitation from chloroform
FINN	Reprecipitation from chloroform
PS	Reprecipitation from benzene
PP	Thin film drawn from melt
PE	Thin film drawn from melt
POM	KBr disc

Infrared absorption spectra were run for the six materials and compared (Figure 1.6).

Theoretically, sample absorption/source emission interactions should cease to be a relevant factor in the consideration of the ignition of a material exhibiting black body behaviour (absorptivity of unity at all wavelengths). Black Perspex was identified as being a readily available material which most closely approached black body behavior. A radiant heat flux of 25kW/m^2 was selected. Four different combinations of heater temperature and heater position were used to produce this heat flux and in each case, ignition delay time and firepoint temperature were measured as previously for both colourless and black ICI Perspex (Table 4.9).

Having investigated in some detail the validity of using critical surface temperature at firepoint as a criterion for ignition, it was decided to attempt a theoretical calculation of surface temperature (Chapter 3.).

2.3 MASS LOSS MEASUREMENTS

2.3.1 Critical Mass Flux at Ignition

Previous work at Edinburgh University on measurement of mass loss rate (Lygate (1979), Deepak and Drysdale (1983), Dawes (1983), Drysdale and Mazhar (1979)) using a load cell to detect changes in sample weight proved cumbersome and produced results which were very susceptible to external vibrations and air movement. The load cell also proved to be sensitive to temperature as heat was conducted down the sample support rod (Lygate (1979)). In view of the problems encountered with the load cell, the apparatus was redesigned (Figure 2.18 and 2.19).

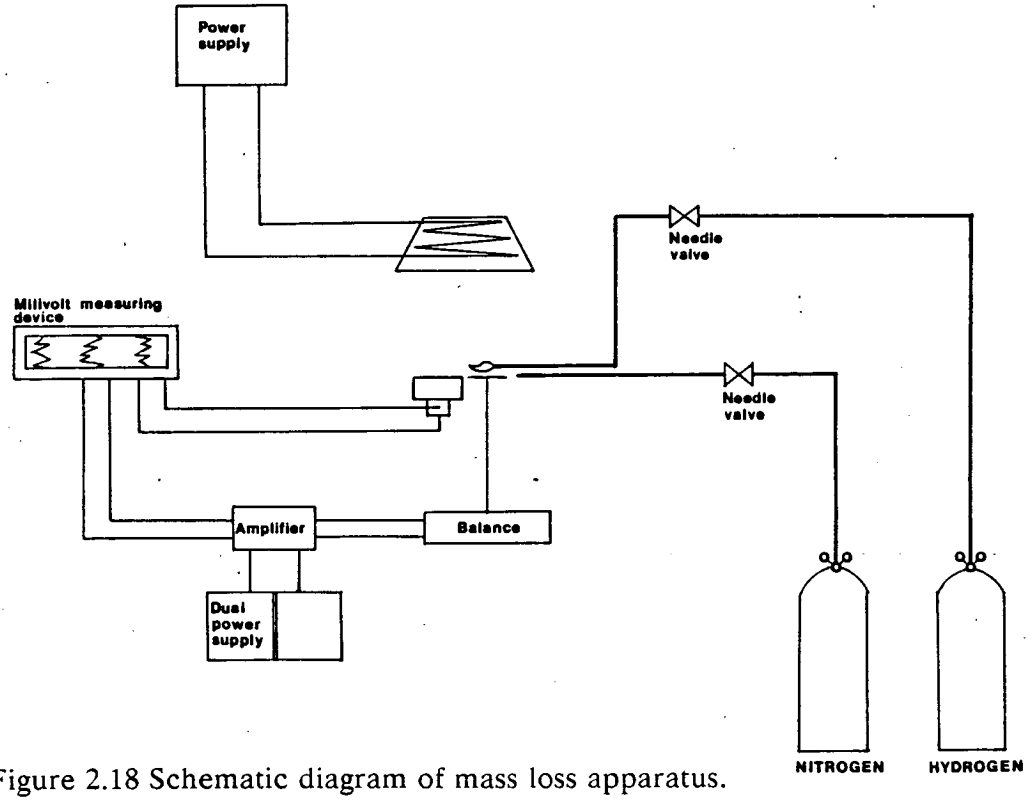

Figure 2.18 Schematic diagram of mass loss apparatus.

A Sartorius top loading electronic balance (Model L610) was selected for use in this phase of the project because of its high sensitivity over the weight range required and also because of the relative simplicity of obtaining a continuous

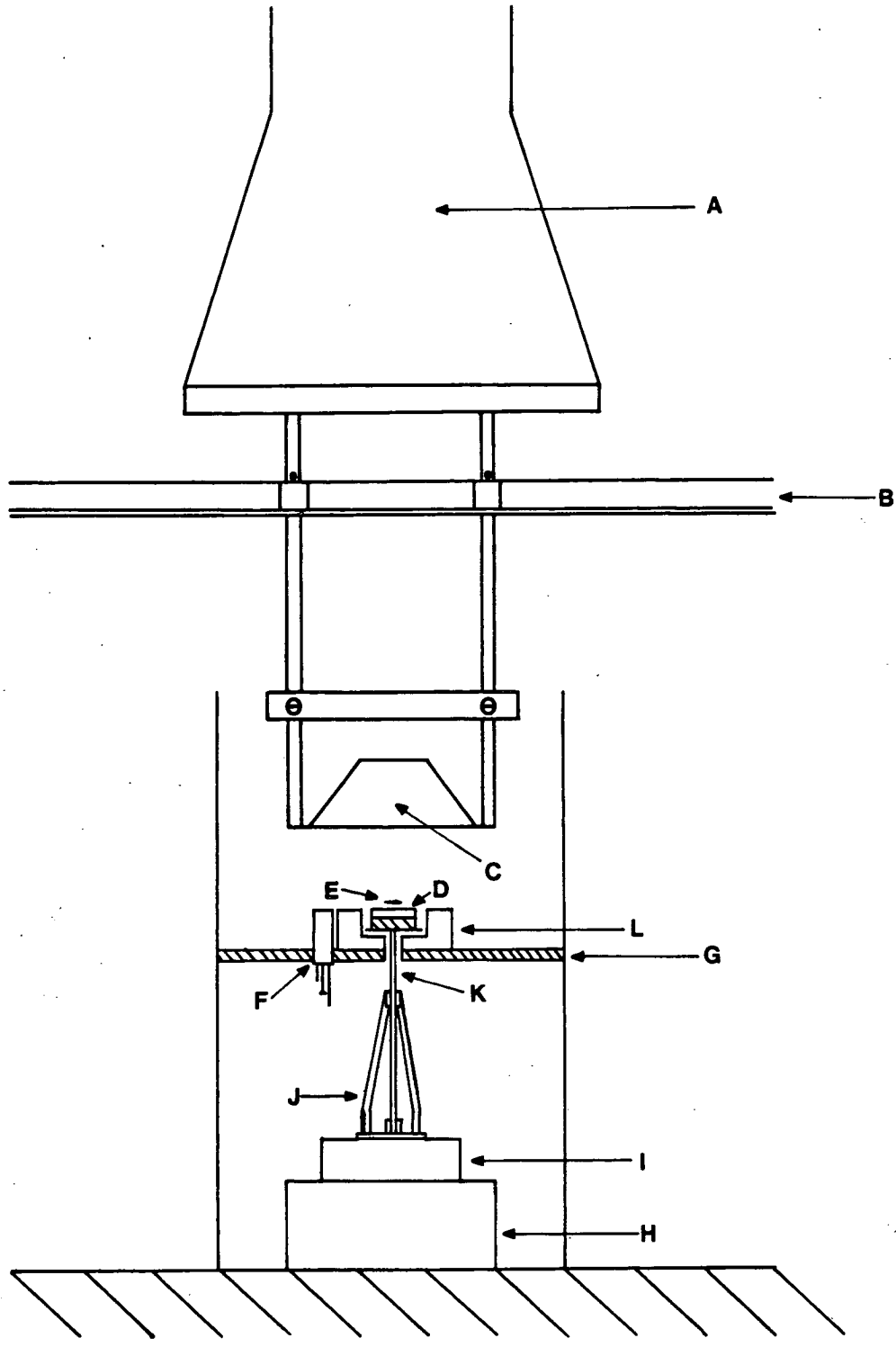

Figure 2.19 Mass loss apparatus

A, extract hood; B, support bar; C, radiant conical heater; D, sample; E, spark generator; F, heat flux meter; G, Kaowool board platform; H, concrete plinth; I, electronic balance; J, tripod; K, glass rod.

analogue voltage output corresponding to weight from this particular model. A lightweight aluminium tripod which fitted closely over the top pan of the balance was constructed to support the sample mounting device. This consisted of a circular aluminium platform (60mm diameter x 1mm thick) attached to a 35cm length of glass rod as shown in Figure (2.20).

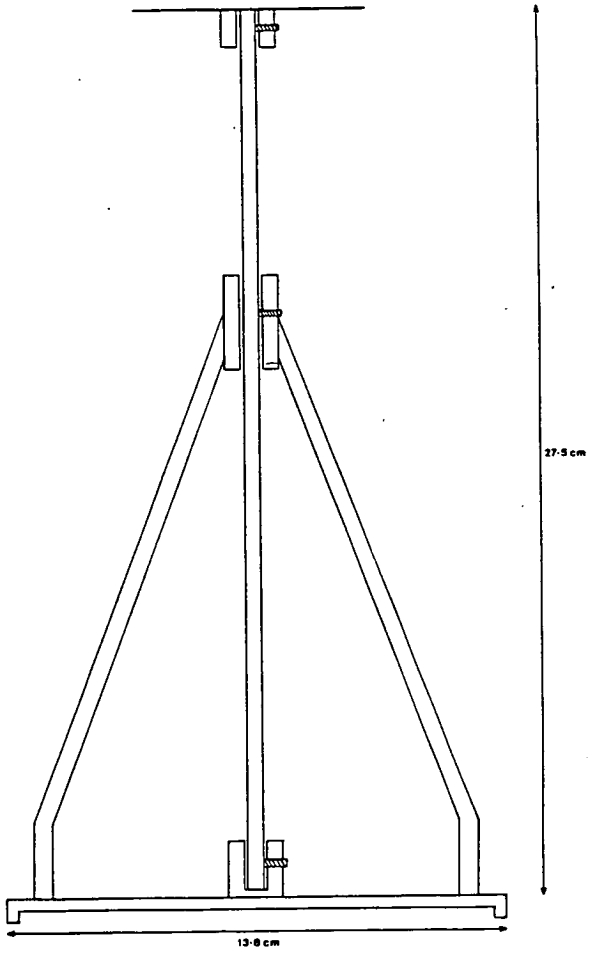

Figure 2.20 Tripod and platform.

A calibration chart for the balance of voltage versus weight was produced using precision weights (Figure 2.21). Increase in voltage was directly proportional to decrease in weight. Although the total weight of sample, mounting platform and tripod was in excess of 80g, the actual change in total weight (due to sample decomposition) was seldom more than 500mg. Consequently, it was more advantageous to monitor weight loss on a sensitive scale (10-20mV f.s.d.) than it

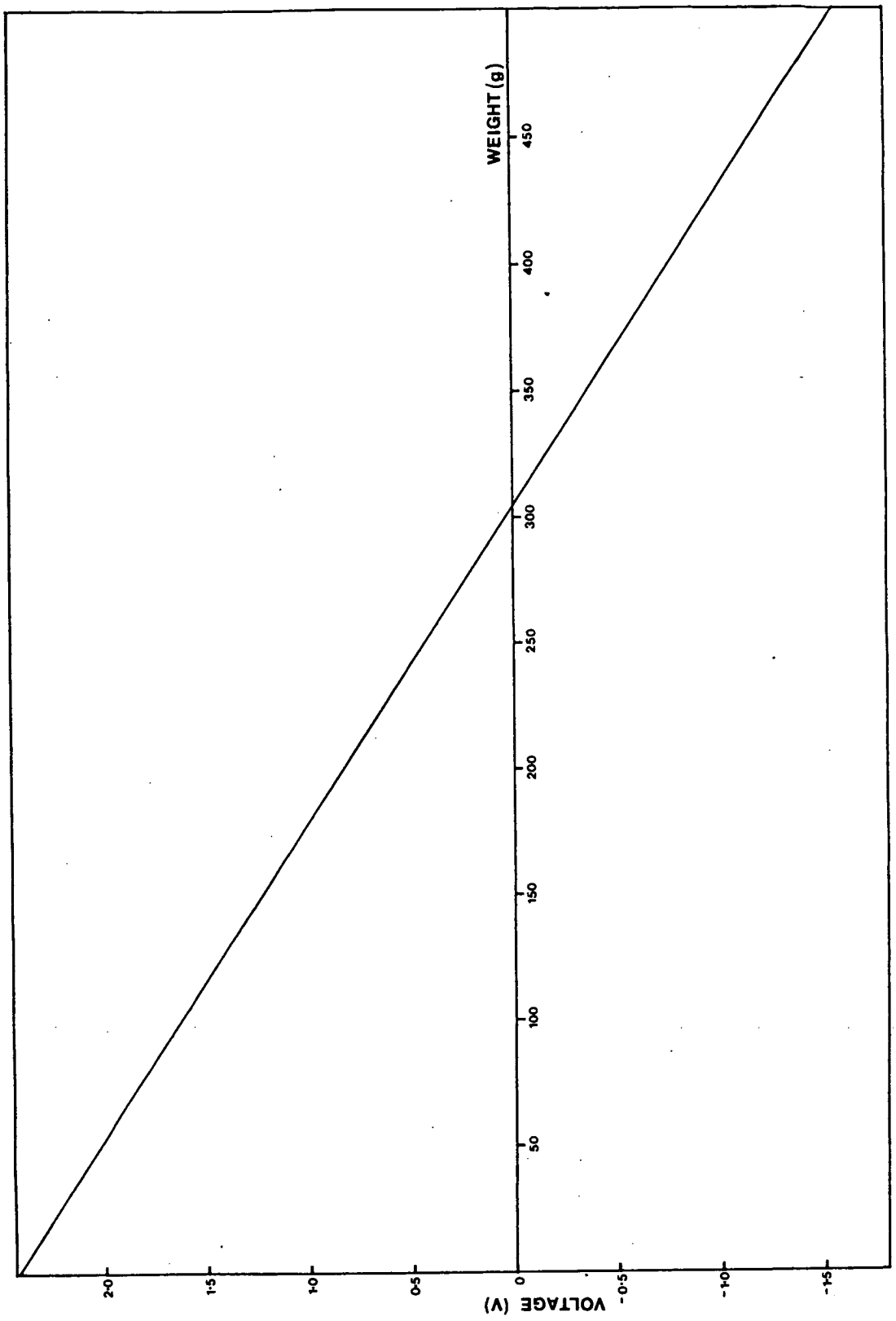

Figure 2.21 Calibration chart for balance

was to consider change in total weight on an insensitive scale (5V f.s.d.). Thus, an electronic device was developed (Figure 2.22) which allowed the initial "dead" weight of sample, platform and tripod to be tared. This enabled the output voltage to be set to zero at the start of each experiment. Output voltage was monitored continuously through one channel of a multichannel pen chart recorder.

Foil wrapped samples (65mm x 65mm x 6mm thick) backed by Kaowool board, were placed in a stainless steel holder which allowed exposure of a circular area of sample 60mm in diameter. The foil was peeled away from this area and the sample in its holder was placed centrally on the aluminium platform. A heat shield was positioned between the sample and the heater to protect the sample until the heater had equilibrated. This was monitored by means of a heat flux meter set to one side of the sample and in the same horizontal plane as the sample. During equilibration, the heater was moved to a position centered on the heat flux meter to allow the radiant heat flux level to be accurately determined. The heater was then repositioned directly above the sample before the start of an experiment. The output voltage corresponding to weight was set to zero by adjustment of the potentiometer arrangement shown in Figure 2.22. The heat shield was removed and timing commenced. On observation of the evolution of volatiles, a hydrogen pilot flame was applied at 4 second intervals as in the previous temperature measurement experiments.

The quality of the initial mass loss curves was poor because of excessive "noise". This was apparently due to the sensitivity of the system to extraneous vibration and, in particular, buoyancy-induced air movement. Attempts to smooth the traces by use of high value capacitors across the output terminals proved ineffectual. Various attempts to shield the platform were made, the most

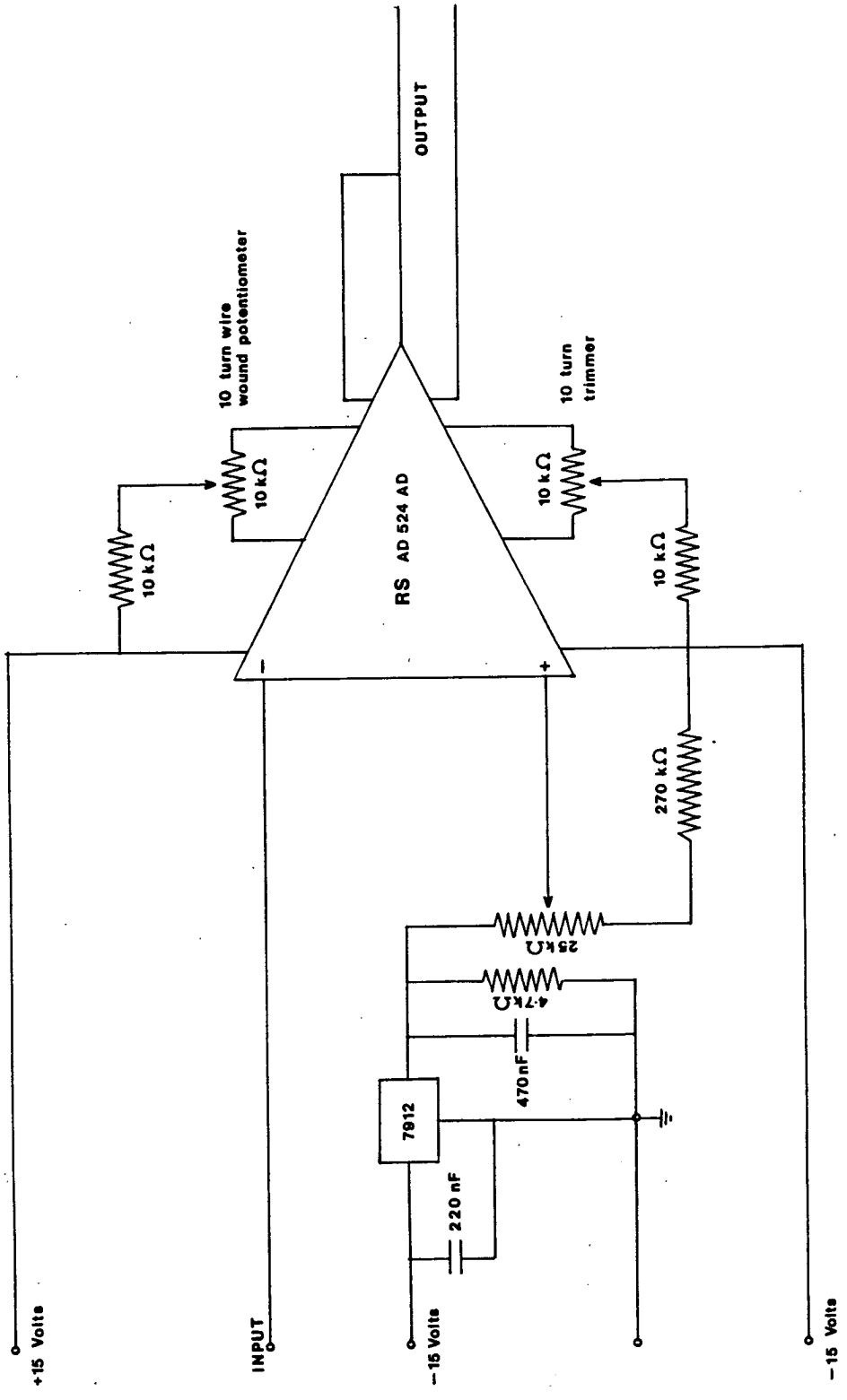

Figure 2.22 Circuit diagram for potentiometer arrangement

successful of these being complete shielding of the exposed portion of the platform and sample holder with a Supalux collar to a level flush with the exposed sample surface. A 7cm high steel cylinder (diameter 16cm) was placed around the sample on top of the collar (Figure 2.23).

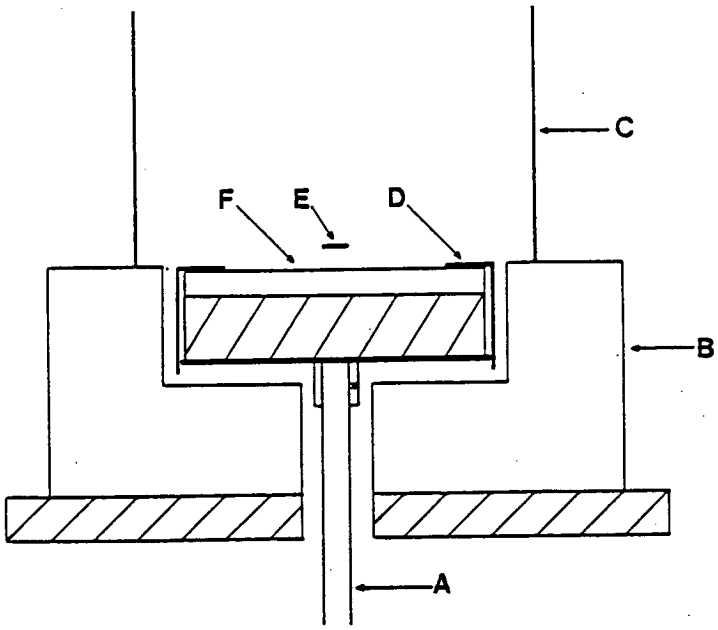

A, glass rod
B, Supalux collar
C, draught shield
D, sample holder
E, spark generator
F, sample

Figure 2.23 Shielding arrangement.

The hydrogen flame pilot source was replaced by the spark generator described earlier (Figure 2.12). The quality of the traces obtained was considerably improved. Figure 2.24 shows a typical mass loss-time curve.

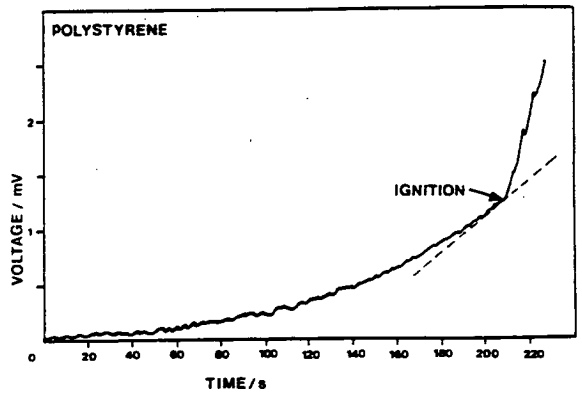

Figure 2.24 Mass loss-time curve

The critical mass flux (m''_{cr}) is derived from the gradient of the curve, dy/dx, at the instant of ignition (which is marked on the chart recorder output by means of an interrupt switch).

$$m''_{cr} = \frac{dy}{dx}.\frac{CV}{A'} \qquad (2.3)$$

where m''_{cr} is the critical mass flux($g/m^2.s$), x is length measured on chart paper (mm), C is the conversion factor 0.12563 (g/mV), V is the chart speed (mm/s) and A' is the exposed sample area (m^2). A cubic expression was fitted to the mass loss curve data up to the point of ignition. Differentiation of the equation allowed the gradient, dy/dx to be calculated at the point of ignition and m''_{cr} was then calculated using equation 2.3.

Critical mass fluxes were determined for six of the materials studied previously (Table 4.11). Results for P.E. at the lowest heat flux were discarded due to a lack of reproducibility resulting from the non-uniformity of char formation. Measurements were made under four different radiant heat fluxes for each material. In addition the effect of varying the heater temperature was examined by varying the heat flux in the two ways described previously (ie constant temperature/variable height and variable temperature/constant height).

2.3.2 Thermogravimetric Analysis

Thermogravimetry is a technique in which the change in the weight of a substance is recorded as a function of temperature or time. The basic requirement is a precision balance with a furnace programmed for a linear rise of temperature with time. The results may be presented in the form of (i) a thermogravimetric curve (Figure 2.25(a)), in which weight change is recorded as a function of temperature or time or (ii) a derivative thermogravimetric (DTG) curve (Figure 2.25(b)) where

the first derivative of the TG curve is plotted with respect to temperature or time.

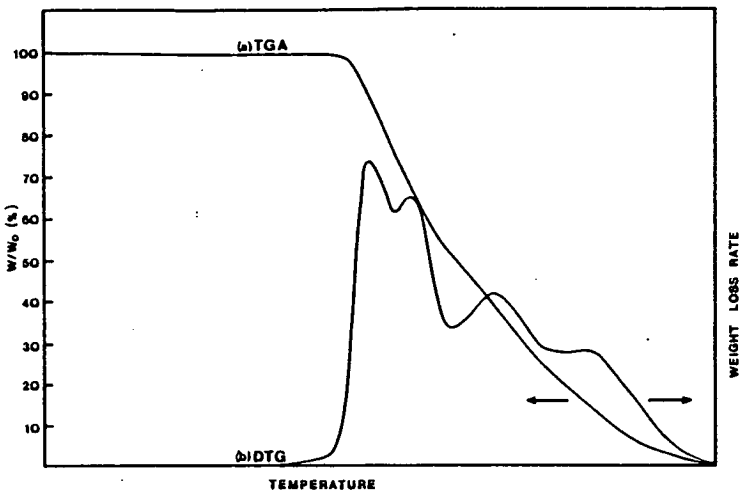

Figure 2.25 Typical TGA and DTA curves.

The following features of the TG curve should be noted:

1. Horizontal portions indicate regions of zero weight change.
2. Curved portions indicate weight loss.
3. The TG curve is quantitative, hence, calculations on compound stoichiometry can be made at any given temperature.
4. The ordinate scale may take several forms, eg percentage weight loss, percentage of total weight, true weight scale, molecular weight units.

Description: The apparatus used for the thermogravimetric measurements was a modified Stanton Redcroft TR-02 thermal balance (shown schematically in Figure 2.26). Samples were placed in a small platinum crucible which was then positioned in the sample well of the alumina head block assembly. A Pt/13% Rh-Pt thermocouple located at the base of the sample well allowed the sample temperature to be followed accurately throughout an experiment. The alumina head block was supported on an alumina riser rod connected to the electronic balance which provided continuous monitoring of sample weight. This whole

assembly was situated within a cylindrical furnace which could be raised or lowered to allow easy access to the sample holder.

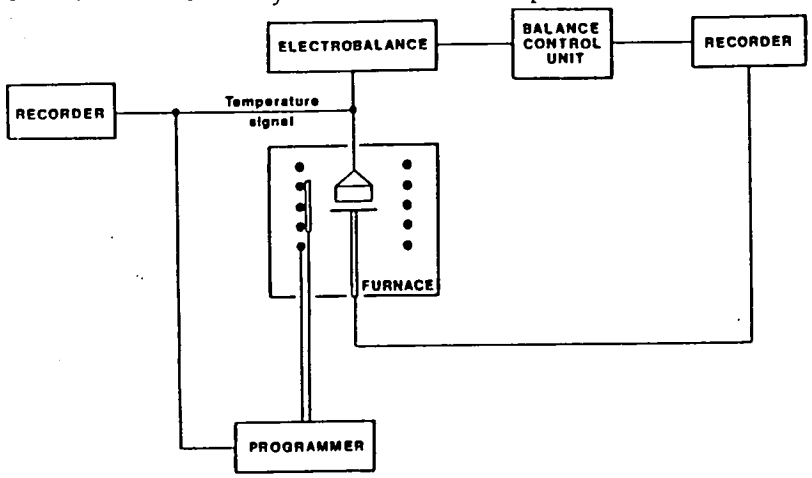

Figure 2.26 Schematic diagram of thermal balance

Method: The crucible was heated in a furnace at 1000°C to constant weight and then kept in a desiccator until required. If an empty crucible is heated in the TGA apparatus, there is generally an apparent change in weight with increasing temperature. This is caused by the interaction of several factors including air buoyancy, convection effects within the furnace, crucible geometry, radiation effects etc. Consequently, it was necessary to determine the apparent weight change with respect to temperature of the crucible used in this series of experiments and apply it as a correction curve (Figure 2.27) in all subsequent experiments in order to obtain the true weight change occuring in a sample. Therefore, the correction curve was specific to the precise conditions under which subsequent experiments were to be carried out, eg atmosphere, heating rate etc.

A sample of approximately 25 mg of the powdered polymer was accurately weighed and placed in the crucible which was then positioned in the sample well of the alumina head assembly. The weight of sample and crucible was balanced by the addition of small weights to the front pan of the balance. The balance was

then actioned, the furnace lowered into position and the apparatus allowed to run for approximately 15 minutes to give a steady reference weight line. The furnace programmer unit was set to a heating rate of 6^{o}C/minute and a maximum furnace temperature of 450^{o}C. The recorder chart speeds were set at 2.5cm/minute and the furnace heating program was commenced. Separate traces of sample temperature with respect to time and of sample weight with respect to time were produced. The two traces were combined and the correction curve applied to produce a plot of percentage of initial weight versus sample temperature. DTG was not available with this apparatus and so degradation rates were estimated from the gradients of the TGA curves at the corresponding times.

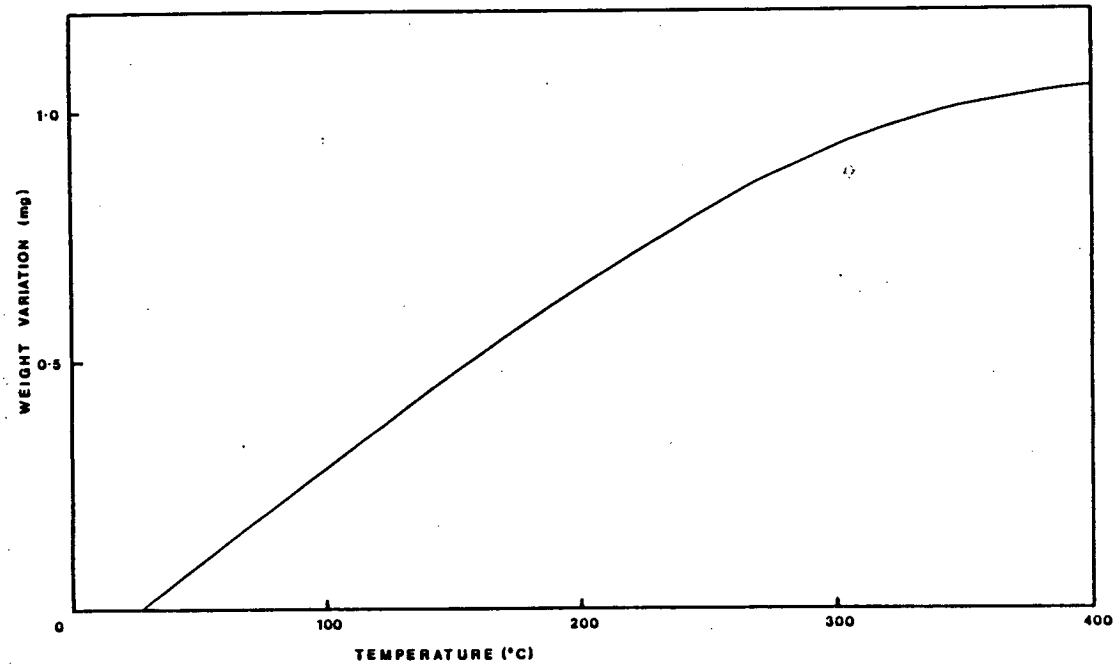

Figure 2.27 Correction curve

2.4 FIRE RETARDANCY

2.4.1 Commercial Fire Retarded Plastics

It is possible to render many plastics less susceptible to fire by the addition of a fire retardant system during manufacture. With regard to fire retardant

compounds, the ultimate aim of the manufacturer is to achieve a plastic/retardant combination which strikes the optimum balance between cost and improved performance in fire situations. The extent to which this has been achieved was assessed by investigation of the ignition behaviour of commercially available fire retarded versions of polymethylmethacrylate, polypropylene and polystyrene. Ignition delay times, firepoint temperatures and critical mass fluxes were determined, as described previously, over a range of radiant heat fluxes. These were compared with equivalent results for the unmodified parent polymers (Tables 4.14 and 4.15) and tentative conclusions as to mode of action of the fire retardant species were drawn. In addition, the limiting oxygen index (LOI) which is the traditional method of assessing efficiency of a fire retardant system was determined for each material as described below.

2.4.2 Limiting Oxygen Index Test

Limiting oxygen index (LOI) is a measure of the minimum volume concentration of oxygen in a flowing stream of oxygen and nitrogen required to maintain candle-like burning of a sample under specified conditions.

$$LOI = \frac{[O_2].100}{[O_2]+[N_2]} \qquad (2.24)$$

LOI as a measure of flammability has now been incorporated into standard tests ASTM D2863 (1977) and BS 2782-141 (1978). However, the concept as applied to organic polymers and other solid materials was first developed by Fenimore and Martin (1966) as a result of an idea proposed by Simmons and Wolfhard (1957) for gaseous and liquid fuels.

Limiting Oxygen Index Apparatus

Description: LOI values were determined using the Stanton Redcroft Module FTA as shown schematically in Figure 2.28. This equipment consists of three sections.

1. The gas supply system comprising filters, digital valves, a mixing chamber and a flowmeter. It was possible to vary the gas stream composition from 0-100% oxygen whilst still maintaining a constant overall gas flow rate of 18 l/minute.

2. The oxygen analysing system with analogue and digital meters which indicate the percentage of oxygen in the gas stream.

3. The test column which is made of heat resistant glass tubing and contains the specimen holder.

Sample Preparation: All tests were run on 6mm thick specimens. The samples were approximately 10mm x 120mm x 6mm and were not preconditioned in any way.

Method: A strip of the material being tested was placed vertically in the holder and the test column was replaced around it. The gas supply was turned on and the oxygen concentration adjusted to approximately 25% while maintaining an overall gas flow rate of 18 l/minute. The sample was ignited at the uppermost tip by application of a flame (25mm long) from a butane torch for approximately 20 seconds until flaming was well established. If the sample continued to burn for three minutes or alternatively burned past the 50mm mark then the oxygen concentration was reduced. Conversely, if the sample was extinguished in less than that time or burning covered a smaller area then the oxygen concentration was increased. The limiting oxygen concentration was always approached from both sides and was taken to be the point at which extinction occurred as nearly as possible at the specified time and length. LOI measurements were repeated six

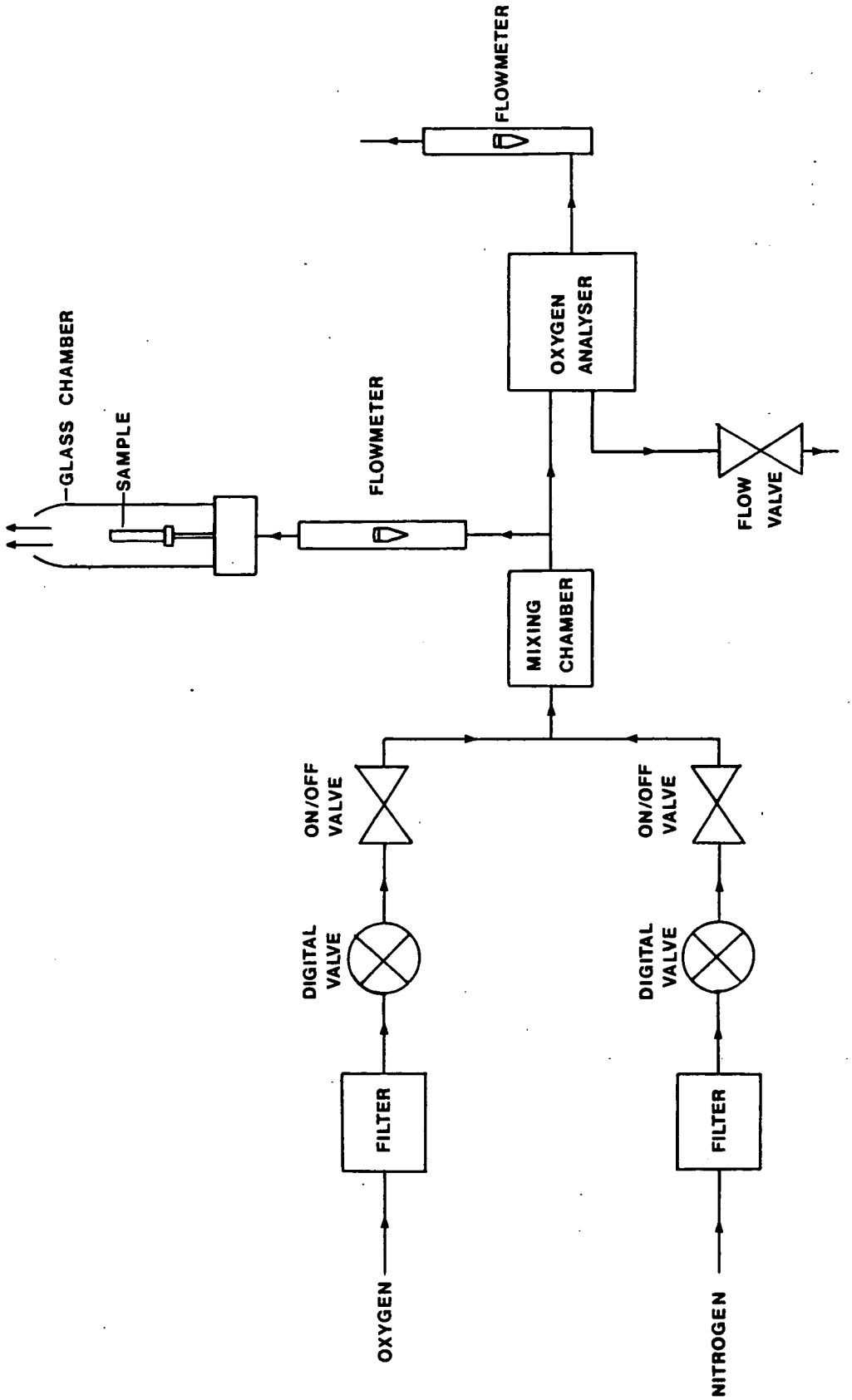

Figure 2.28 Limiting oxygen index (LOI) test apparatus

times for each material. The results are given in Table 4.13.

CHAPTER 3

COMPUTER MODEL

CHAPTER 3
COMPUTER MODEL

3.1 SIMPLISTIC APPROACH

The simplest mathematical model describing the ignition of combustible solids treats the solid as an opaque, chemically inert material exposed to a uniform heat flux with unspecified spectral charateristics. The solid is considered to be either an infinite slab or alternatively, a semi-infinite solid which allows the heat transfer process to be considered in a single dimension perpendicular to the exposed face.

$$t_{ig} = f\{T_{ig}, \bar{\alpha}, k, \rho, c, Q''\} \qquad (3.1)$$

Ignition is generally assumed to occur when a certain critical surface temperature is achieved. This approach has enabled various boundary conditions to be explored. Kanury (1972) attempted to derive analytical solutions to a number of situations and was able to classify various types of behaviour. However, it is obvious that this model is an over-simplification and some of the underlying assumptions are invalid. If the model is to aid the greater understanding of the ignition process and have any potential as a tool for predicting the occurence of ignition then clearly a more realistic set of assumptions are required.

3.2 E.U. MODEL

3.2.1 Basic Version

The E.U. model is illustrated schematically in Figure 3.1. In view of the complexity of the heat transfer problem, it was decided to develop a numerical analysis model analogous to the Schmidt graphical method and based on a semi-infinite solid exposed to a uniform heat flux perpendicular to one face. Whilst this approach is physically unrealistic, it was felt to be a useful starting

point for development work.

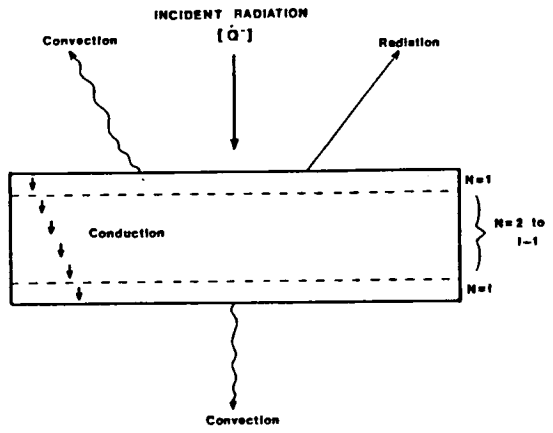

Figure 3.1 Schematic diagram of E.U. model

The numerical solution is based on a semi-infinite solid or thick slab consisting of several thin elements. It is assumed that thermal equilibrium is established within alternate pairs of adjacent elements which results in an approach well suited to computer solution. One such technique is the explicit finite difference method when conduction equation (equation 1.16) is replaced by

$$\frac{1}{(\Delta x)^2}\left(T(x+\Delta x,t) - 2T(x,t) + T(x-\Delta x,t)\right) = \frac{1}{\alpha \Delta t}\left(T(x,t+\Delta t) - T(x,t)\right) \qquad (3.2)$$

where Δx and Δt are the space and time increments respectively (Holman (1976)). The temperature at position x and time, $t+\Delta t$ (ie $T(x,t+\Delta t)$)can be derived from the above equation, provided that the temperature at positions x, $x+\Delta x$ and $x-\Delta x$ at time t are known.

In the E.U. model, the solid is considered to consist of a series of thin elements (thickness Δx) from $N=1$ to i as illustrated in Figure 3.1. The net heat transfer to the surface element ($N=1$) and subsequent transfer of heat to sub-surface elements by conduction is calculated on the basis that a quasi-steady state is achieved at the end of each short time interval (duration Δt). A computer

program was written to calculate the temperature of each element (N=1 to i) at the end of every time interval from t=0 to JΔt. Equation 3.3 provides the only constraint on the magnitude of Δt and Δx for a one dimensional problem.

$$\text{Fourier number, } F_o = (k/\rho c)\Delta t/\Delta x^2 < 0.5 \qquad (3.3)$$

The flow chart for this program is shown in Figure 3.2. An average value for surface absorptivity ($\bar{\alpha}_{av}$), independent of wavelength, is assumed. Values of $\bar{\alpha}_{av}$ for the various materials exposed to radiation from a blackbody source at 1000^0K as determined by Hallman, Welker and Sliepcevich (1977) are used (Table 3.1). The amount of incident radiation absorbed is assumed to be directly proportional to the value of the "average" surface absorptivity and it is further assumed that any incident radiation not absorbed is reflected, ie there is no transmission with absorption at depth of incident radiation.

Table 3.1

Average absorptances (Hallman et al (1977))

MATERIAL	ABSORPTIVITY AT BLACKBODY TEMPERATURE		
	1000^0K	1500^0K	2000^0K
PMMA	0.85	0.69	0.54
POM	0.92	0.86	0.78
PP	0.87	0.83	0.78
PE	0.92	0.88	0.82
PS	0.75	0.60	0.46

Thermal properties (k,ρ,c) are taken to be independent of temperature. The relevant equations in the numerical model are as follows:

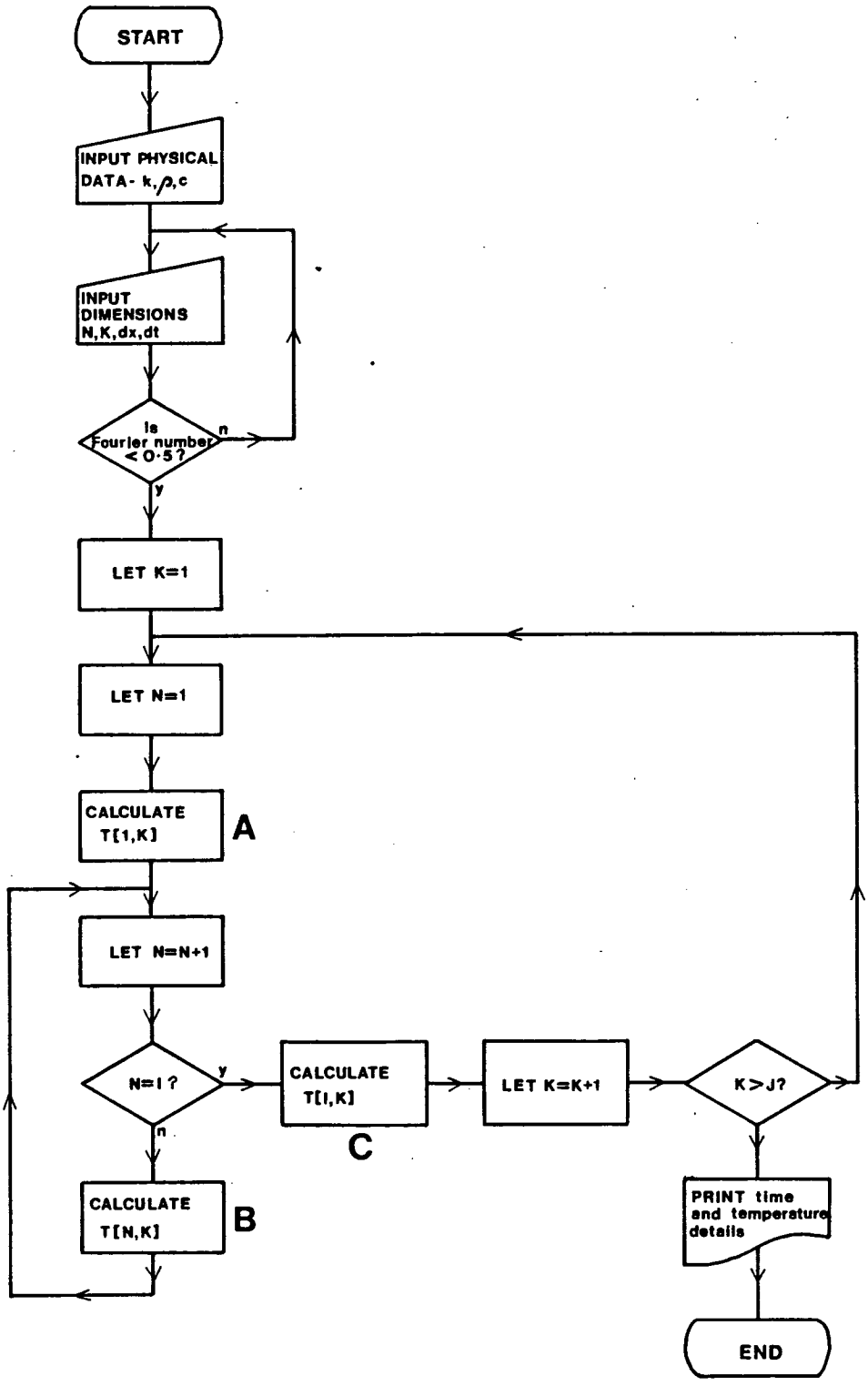

Figure 3.2 Flow chart for basic model

Conduction

$$q''_x = -k\frac{\partial T}{\partial x} \tag{3.4}$$

Convection

$$q'' = h\Delta T \tag{3.5}$$

Radiation

$$q'' = \varepsilon\sigma T^4 \tag{3.6}$$

Energy Balance

$$(Q''_{in}-Q''_{out})\Delta t = \rho c\Delta x\Delta T \tag{3.7}$$

A. For uppermost element (N=1)

$$\text{Heat flux in } (Q''_{in}) = Q''\bar{\alpha}_{av} \tag{3.8a}$$

$$\text{Heat flux out } (Q''_{out}) = \varepsilon\sigma T(1,K-1)^4 + h(T(1,K-1)-ZO) + \frac{k}{\partial x}(T(1,K-1)-T(2,K-1)) \tag{3.8b}$$

Substituting equations 3.8 into equation 3.7 gives:

$$T(1,K-1) + \frac{\Delta t}{\rho c\Delta x}(Q''\bar{\alpha}_{av}-\varepsilon\sigma T(1,K-1)^4 - h(T(1,K-1)-ZO) -\frac{k}{\Delta x}(T(1,K-1)-T(2,K-1))) = T(1,K) \tag{3.9}$$

B. For intermediate elements (N=2 to I-1)

$$\text{Heat flux in } (Q''_{in}) = \frac{k}{\Delta x}(T(N-1,K-1)-T(N,K-1)) \tag{3.10a}$$

$$\text{Heat flux out } (Q''_{out}) = \frac{k}{\Delta x}(T(N,K-1)-T(N+1,K-1)) \tag{3.10b}$$

Substituting equations 3.10 into equation 3.7 gives:

$$T(N,K-1) + \frac{\Delta tk}{\rho c\Delta x^2}(T(N-1,K-1)-2T(N,K-1)+T(N+1,K-1)) = T(N,K) \tag{3.11}$$

C. For the rearmost element (N=I)

$$\text{Heat flux in } (Q''_{in}) = \frac{k}{\Delta x}(T(I-1,K-1)-T(I,K-1)) \tag{3.12}$$

$$\text{Heat flux out } (Q''_{out}) = h(T(I,K-1)-ZO) \tag{3.12b}$$

Substituting equations 3.12 into equation 3.7 gives:

$$T(I,K-1) + \frac{\Delta t}{\rho c \Delta x}\left(\frac{k}{\Delta x}(T(I-1,K-1)-T(I,K-1))\right. \\ \left. - h(T(I,K-1)-ZO)\right) = T(I,K) \qquad (3.13)$$

It was possible to fit the theoretical temperature-time curves to the corresponding experimental curves by manipulating the values chosen for the various parameters, however, this was not satisfactory because unrealistic values of h and $\bar{\alpha}_{av}$ had to be selected to obtain good fit.

3.2.2 Modification 1.

The above equations were modified to include radiation absorption at depth. For simplicity, it was assumed that the radiation "reflected" in the previous basic model was instead transmitted through element N=1 and partially absorbed in element N=2, etc. The rate of radiation absorption (q''_r) in element N can be shown to be

$$q''_r = \bar{\alpha}_{av}(1-\bar{\alpha}_{av})^{N-1}.Q'' \qquad (3.14)$$

The relevant equations from the previous model then become:

A. Element N=1

Equation unaffected by this modification.

B. Elements N=2 to I-1

$$T(N,K-1) + \frac{\Delta t}{\rho c \Delta x}\left(Q''\bar{\alpha}_{av}(1-\bar{\alpha}_{av})^{N-1}\right. \\ \left. + \frac{k}{\Delta x}(T(N-1,K-1)-2T(N,K-1)+T(N+1,K-1))\right) = T(N,K) \qquad (3.15)$$

C. Element N=I

$$T(I,K-1) + \frac{\Delta t}{\rho c \Delta x}(Q''\bar{\alpha}_{av}(1-\bar{\alpha}_{av})^{I-1} + \frac{k}{\Delta x}(T(I-1,K-1) - T(I,K-1)) - h(T(I,K-1)-ZO)) = T(I,K) \quad (3.16)$$

This modification allowed a more realistic fit to be made between the theoretical and experimental results at high heat fluxes, although, it was not possible to account for the observed variation in time to ignition depending on the temperature of the radiant source.

3.2.3 Modification 2.

The wavelength dependency of source radiant intensity and that of radiation absorption by the solid was taken into account. Because of the difficulty of obtaining an emission spectrum from the radiant heater, it was assumed to be a blackbody emitter and data for the ratio $\int_0^{\lambda} E_{b\lambda}.d\lambda / \int_0^{\infty} E_{b\lambda}.d\lambda$, ie $E_{0-\lambda}/E_{0-\infty}$ as a function of temperature were taken from the table of radiation functions given in Appendix C (Dunkle (1954)). Hence, the fraction of total energy of radiation contained within a narrow wavelength band, $\Delta\lambda$, is given by:-

$$\frac{E_{\Delta\lambda}}{E_{0-\infty}} = \frac{E_{0-(\lambda+\Delta\lambda)}}{E_{0-\infty}} - \frac{E_{0-\lambda}}{E_{0-\infty}} \quad (3.17)$$

Therefore, $Q''.E_{\Delta\lambda}/E_{0-\infty}$ is that fraction of the total radiant heat flux contributed by a small wavelength increment, $\Delta\lambda$. If the absorptivity of the sample over the corresponding small wavelength increment is $\bar{\alpha}_{\lambda}$, then the radiant heat flux absorbed within each small wavelength increment is given by:-

$$q_{\lambda} = Q''\bar{\alpha}_{\lambda}\frac{E_{\Delta\lambda}}{E_{0-\infty}} \quad (3.18)$$

and the total radiant heat flux absorbed in the surface layer (N=1) is given by:-

$$Q''_{abs} = \sum_{o}^{\infty} Q''\bar{\alpha}_{\lambda}\frac{E_{\Delta\lambda}}{E_{0-\infty}} \quad (3.19)$$

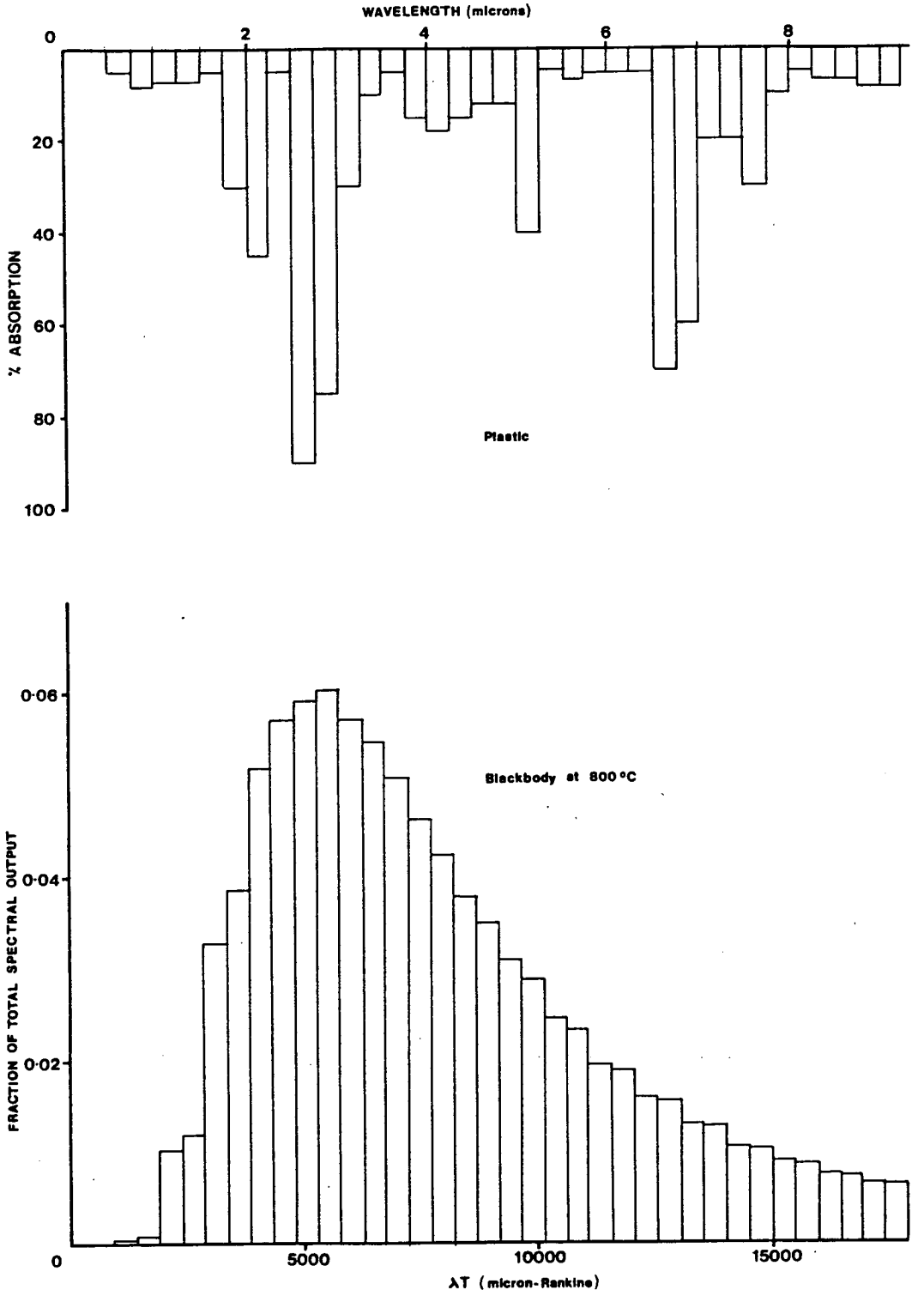

Figure 3.3 Source emission/sample absorption relationship .

The relevant equations in the new model are as follows.

A. Element N=1

$$T(1,K-1) + \frac{\Delta t}{\rho c \Delta x}\left(\sum_1^u Q''\bar{\alpha}_\lambda E_{\Delta\lambda} - h(T(1,K-1)-ZO)\right. \qquad (3.20)$$
$$\left. - \varepsilon\sigma(T(1,K-1)^4 - \frac{k}{\Delta x}(T(1,K-1)-T(2,K-1))\right) = T(1,K)$$

The net energy absorbed in all other elements, ie N> 1 is given by:-

$$Q''_{abs} = \sum_0^\infty Q''\frac{E_{\Delta\lambda}}{E_{0-\infty}}\bar{\alpha}_\lambda(1-\bar{\alpha}_\lambda)^{N-1} \qquad (3.21)$$

B. Elements N=2 to I-1

$$T(N,K-1) + \frac{\Delta t}{\rho c \Delta x}\left(\sum_1^u Q''\bar{\alpha}_\lambda\frac{E_{\Delta\lambda}}{E_{0-\infty}}(1-\bar{\alpha}_\lambda)^{N-1}\right. \qquad (3.22)$$
$$\left. + \frac{k}{\Delta x}(T(N-1,K-1)-2T(N,K-1)-T(N+1,K-1))\right) = T(N,K)$$

C. Element N=I

$$T(I,K-1) + \frac{\Delta t}{\rho c \Delta x}\left(\sum_1^u Q''\bar{\alpha}_\lambda\frac{E_{\Delta\lambda}}{E_{0-\infty}}(1-\bar{\alpha}_\lambda)^{I-1}\right. \qquad (3.23)$$
$$\left. + \frac{k}{\Delta x}(T(I-1,K-1)-T(I,K-1)) - h(T(I,K-1)-ZO)\right) = T(I,K)$$

This modification allows for differences in response when the source temperature is varied. Simplifications include consideration of the source as a blackbody and translation of the absorption spectrum into a series of very narrow rectangular strips (width, $\Delta\lambda$, height, $\bar{\alpha}_\lambda$) each with a discrete absorptivity value as illustrated in Figure 3.3. In this version, the time taken for the sample to attain a given temperature (generally, the experimentally determined firepoint temperature) is calculated.

Further details of the computer programs used in this work are given in Appendix D.

CHAPTER 4

RESULTS

CHAPTER 4
RESULTS

All results quoted are based on a minimum of six replicates. One standard deviation is given in parenthesis after the mean value. Unless otherwise stated, all results derive from the authors own experimental work.

Table 4.1 compares ignition delay times measured in the E.U. apparatus for chipboard, hardboard, nylon carpet and glass reinforced polyester with equivalent measurements made by an unspecified operator in the ISO Ignitability Test apparatus at the Fire Research Station, Borehamwood. The results have been plotted in Figure 4.1 in order to facilitate comparison.

Table 4.2 and Figures 4.2 and 4.3 show ignition delay time, firepoint temperature and corresponding rear face temperature for various plastics as measured in both the E.U. and ISO apparatus. With the exception of Perspex in the ISO apparatus, all these experiments were carried out by the author as outlined in Chapter 2.

Table 4.3 indicates the effect of pilot source type and position on firepoint temperature and ignition delay time for Perspex under a radiant heat flux of $25kW/m^2$.

Table 4.4 shows the results of experiments carried out on Perspex and polypropylene under a radiant heat flux of $25kW/m^2$ with the extract fan switched on and subsequently switched off.

The influence of sample mounting method on ignition is illustrated in Table 4.5. Ignition delay time, firepoint temperature and edge temperature are recorded for Perspex exposed to $25kW/m^2$ in both the original sample holder (sample edges

enclosed) and the modified sample holder (sample edges exposed).

In Table 4.6 and Figures 4.4 and 4.5, ignition delay times and firepoint temperatures of Perspex and polypropylene under several radiation intensities from a fixed temperature/variable position source are compared with results from equivalent experiments using a fixed position/variable temperature radiant source. This enables a estimate of the importance of source emission/sample absorption interactions to be made.

Table 4.7 compares ignition delay time and firepoint temperature for Perspex exposed to laser irradiation with the results of various equivalent area of exposure experiments using the conical heater. In all cases, the radiation intensity was $34kW/m^2$.

Table 4.8 gives the results of experiments on 6mm, 3mm and 1mm thick Perspex samples, backed by both Supalux and Kaowool board, and exposed to a radiation intensity of $24kW/m^2$. At this heat flux, only the 6mm samples are thermally thick for the duration of the experiment. Results are also given for 6mm samples exposed to a radiation intensity of $17kW/m^2$ at which point these samples cease to be thermally thick.

Table 4.9 contrasts the behaviour of black and colourless Perspex under four different heater temperature/position combinations, each resulting in a radiant heat flux of $25kW/m^2$.

In Table 4.10, predicted firepoint temperatures obtained from the basic E.U. model and the modified version which takes account of diathermancy are quoted for minimum and maximum radiant heat fluxes. Mean values of the

experimental ignition delay times are used to determine the end point in the models and average absorptances for the materials under radiation from a blackbody source at $1000^{0}K$ are taken from the data of Hallman et al (1977) (see Table 3.1). Figure 4.6 shows the theoretical temperature-time curves obtained in each version of the model compared with the experimental temperature-time curve for Perspex under a radiant heat flux of $29kW/m^{2}$.

Mass loss measurements on the unmodified plastics studied are given in Table 4.11 and Figure 4.7. These include mass flux at both flashpoint and firepoint and are based on six acceptible mass loss curves.

Table 4.12 gives the activation energies of the decomposition process as calculated from thermogravimetric analysis studies using the Broido (1969) method (see Appendix E).

Results of the limiting oxygen index test on the six unmodified and three fire retarded plastics are given in Table 4.13. A mean value is calculated from the results of six individul tests.

Tables 4.14 and 4.15 and Figures 4.8, 4.9 and 4.10 compare ignition delay time, firepoint temperature and mass flux at ignition for the three fire retarded plastics and their equivalent unmodified parent materials.

Table 4.1

Round Robin materials

SAMPLE MATERIAL	E.U. APPARATUS Q" (kW/m^2)	t_{ig} (s)	ISO APPARATUS Q" (kW/m^2)	t_{ig} (s)
Chipboard	17	294(9)	20	282(16)
"	23	143(5)	30	93(5)
"	28	91(7)	40	44(2)
"	33	64(4)		
"	39	41(4)		
Hardboard	17	238(7)	20	216(3)
"	23	153(7)	30	101(5)
"	28	107(6)	40	61(3)
"	33	78(2)		
"	39	46(2)		
Nylon carpet	17	85(8)	20	NI
"	23	70(6)	30	81(9)
"	28	57(3)	40	44(2)
"	33	47(3)		
"	39	36(2)		
Glass reinforced polyester	17	139(14)	20	123(35)
"	23	70(10)	30	47(4)
"	28	48(7)	40	30(3)
"	33	41(4)		
"	39	32(2)		

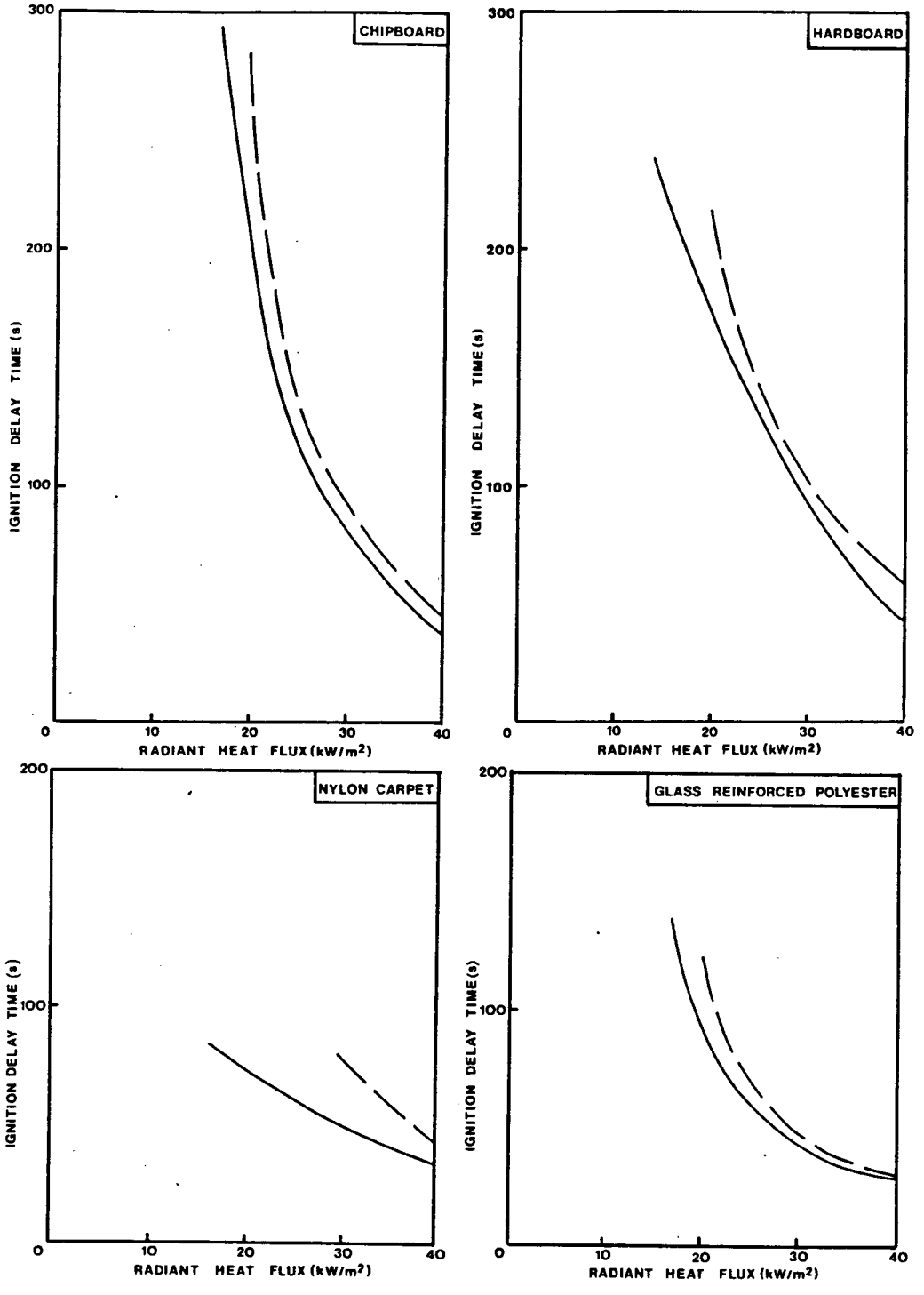

Figure 4.1 Ignition delay times (Round Robin materials)

ISO - - - -, E.U. ————

Table 4.2

Surface temperature measurements

(a) Perspex

	E.U. APPARATUS			ISO APPARATUS		
Q" (kW/m^2)	t_{ig} (s)	T_{ig} (^oC)	T_{rear} (^oC)	t_{ig} (s)	T_{ig} (^oC)	T_{rear} (^oC)
12.5	**671(67)**	**284(3)**	**186(5)**	752(19)	280(13)	193(3)
14	**461(59)**	**300(2)**	**162(4)**	-	-	-
15	-	-	-	475(30)	308(3)	188(7)
17	**288(11)**	**306(1)**	**144(6)**	-	-	-
20	-	-	-	214(9)	302(2)	141(12)
20.5	**173(11)**	**311(1)**	**126(4)**	-	-	-
24	**115(4)**	**311(2)**	**104(3)**	-	-	-
30*	**67(4)**	**311(1)**	**87(2)**	82(3)	313(3)	87(8)
37.5*	**39(2)**	**312(3)**	**66(4)**	-	-	-
40*	-	-	-	48(2)	325(4)	63(1)
50*	-	-	-	32(1)	328(8)	43(2)

Table 4.2(cont.)

(b) Finnacryl

	E.U. APPARATUS			ISO APPARATUS		
Q" (kW/m^2)	t_{ig} (s)	T_{ig} (^oC)	T_{rear} (^oC)	t_{ig} (s)	T_{ig} (^oC)	T_{rear} (^oC)
10	-	-	-	1334(70)	276(3)	223(5)
13	**1125(37)**	**238(4)**	**165(5)**	-	-	-
15	**391(16)**	**NA**	**NA**	423(25)	NA	NA
18.5	**227(5)**	**301(3)**	**141(3)**	-	-	-
20	-	-	-	208(7)	306(4)	136(4)
22	**148(8)**	**311(5)**	**129(3)**	-	-	-
25.5	**99(1)**	**306(5)**	**107(4)**	-	-	-
29	**80(4)**	**308(4)**	**81(6)**	-	-	-
30*	-	-	-	74(2)	306(3)	82(3)
38*	**42(1)**	**317(5)**	**45(5)**	-	-	-
40*	-	-	-	43(3)	308(4)	47(5)
50*	-	-	-	28(2)	314(6)	39(2)

Table 4.2 (cont.)

(c) PMMA (unidentified)

	E.U. APPARATUS			ISO APPARATUS		
Q" (kW/m^2)	t_{ig} (s)	T_{ig} (^oC)	T_{rear} (^oC)	t_{ig} (s)	T_{ig} (^oC)	T_{rear} (^oC)
13	**582(18)**	**259(4)**	**176(6)**	-	-	-
15	**296(10)**	**275(5)**	**154(6)**	-	-	-
18.5	**187(6)**	**277(4)**	**130(4)**	-	-	-
22	**123(5)**	**280(2)**	**108(5)**	-	-	-
25.5*	**82(3)**	**280(2)**	**98(3)**	-	-	-
29*	**63(2)**	**284(3)**	**83(3)**	-	-	-

Table 4.2 (cont.)

(d) Polyoxymethylene

	E.U. APPARATUS			ISO APPARATUS		
Q" (kW/m^2)	t_{ig} (s)	T_{ig} (^oC)	T_{rear} (^oC)	t_{ig} (s)	T_{ig} (^oC)	T_{rear} (^oC)
14	-	-	-	763(16)	NA	NA
15.5	**492(14)**	**NA**	**NA**	-	-	-
17	**386(11)**	**NA**	**NA**	-	-	-
20	-	-	-	300(4)	288(3)	141(3)
21	**248(10)**	**277(5)**	**133(4)**	-	-	-
25	**184(4)**	**278(7)**	**114(6)**	-	-	-
28	**138(3)**	**282(6)**	**104(6)**	-	-	-
30	-	-	-	139(6)	293(4)	105(4)
34	**79(4)**	**288(8)**	**85(4)**	-	-	-
37.5	**56(4)**	**286(6)**	**76(5)**	-	-	-
40	-	-	-	78(4)	296(5)	80(4)
50	-	-	-	54(2)	290(5)	60(5)

Table 4.2 (cont.)

(e) Polypropylene

	E.U. APPARATUS			ISO APPARATUS		
Q" (kW/m^2)	t_{ig} (s)	T_{ig} (^oC)	T_{rear} (^oC)	t_{ig} (s)	T_{ig} (^oC)	T_{rear} (^oC)
13	**625(22)**	**328(3)**	**162(7)**	-	-	-
15	-	-	-	502(34)	NA	NA
17	**417(7)**	**339(7)**	**146(6)**	-	-	-
20	**335(19)**	**336(5)**	**138(6)**	239(29)	332(6)	140(8)
23	**229(6)**	**334(4)**	**124(6)**	-	-	-
29	**104(4)**	**341(6)**	**100(4)**	-	-	-
30	-	-	-	104(8)	333(4)	101(5)
37*	**52(1)**	**332(3)**	**79(5)**	-	-	-
40*	-	-	-	57(2)	335(4)	72(3)
50*	-	-	-	46(2)	345(4)	62(5)

Table 4.2 (cont.)

(f) Polyethylene

	E.U. APPARATUS			ISO APPARATUS		
Q" (kW/m^2)	t_{ig} (s)	T_{ig} (^{o}C)	T_{rear} (^{o}C)	t_{ig} (s)	T_{ig} (^{o}C)	T_{rear} (^{o}C)
19	**524(85)**	**360(4)**	**248(6)**	-	-	-
20	-	-	-	838(274)	NA	NA
23	**315(13)**	**362(6)**	**205(8)**	-	-	-
27	**223(5)**	**362(3)**	**170(5)**	-	-	-
29	**172(4)**	**364(4)**	**144(5)**	-	-	-
30	-	-	-	221(12)	NA	NA
34	**114(8)**	**365(3)**	**128(4)**	-	-	-
39	**85(3)**	**367(5)**	**113(4)**	-	-	-
40	-	-	-	104(6)	NA	NA
50	-	-	-	73(5)	NA	NA

Table 4.2 (cont.)

(g) Polystyrene

	E.U. APPARATUS			ISO APPARATUS		
Q" (kW/m^2)	t_{ig} (s)	T_{ig} (^oC)	T_{rear} (^oC)	t_{ig} (s)	T_{ig} (^oC)	T_{rear} (^oC)
15.5	**354(27)**	**360(8)**	**230(7)**	-	-	-
19	**236(20)**	**369(4)**	**207(6)**	-	-	-
20	-	-	-	312(10)	357(5)	211(5)
28*	**102(6)**	**361(5)**	**157(6)**	-	-	-
30	-	-	-	150(8)	352(11)	163(8)
34*	**67(1)**	**358(4)**	**136(5)**	-	-	-
40*	**45(3)**	**368(6)**	**118(6)**	80(5)	356(6)	125(4)
50*	-	-	-	40(3)	363(6)	91(5)

* Indicates that sample is thermally thick for duration of experiment

Figures in bold represent results from E.U. apparatus

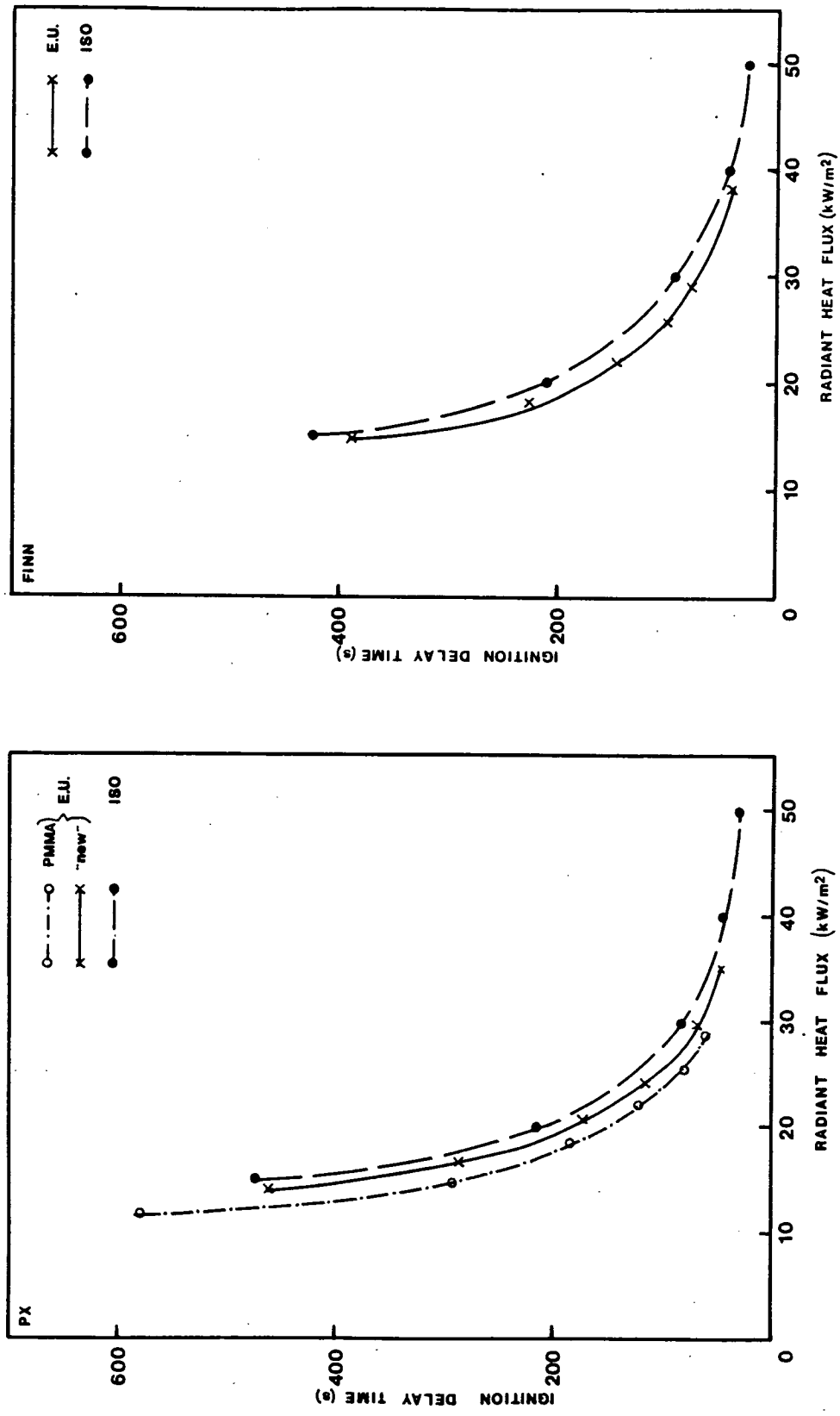

Figure 4.2 Comparison of ignition delay times in E.U. and ISO apparatus

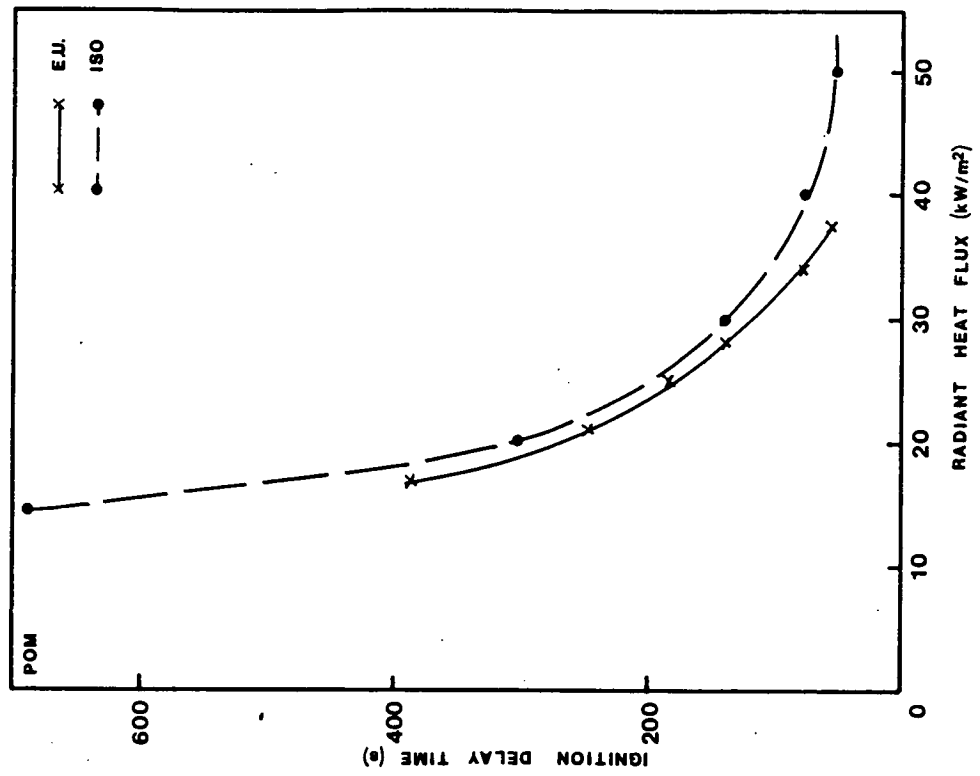

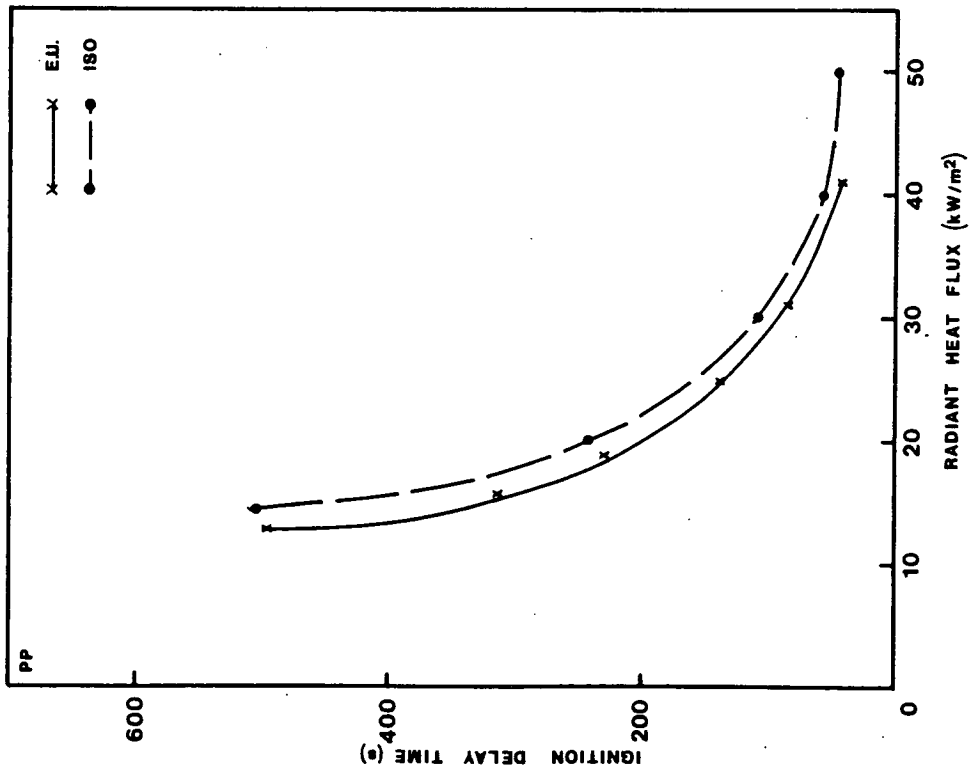

Figure 4.2 (cont.)

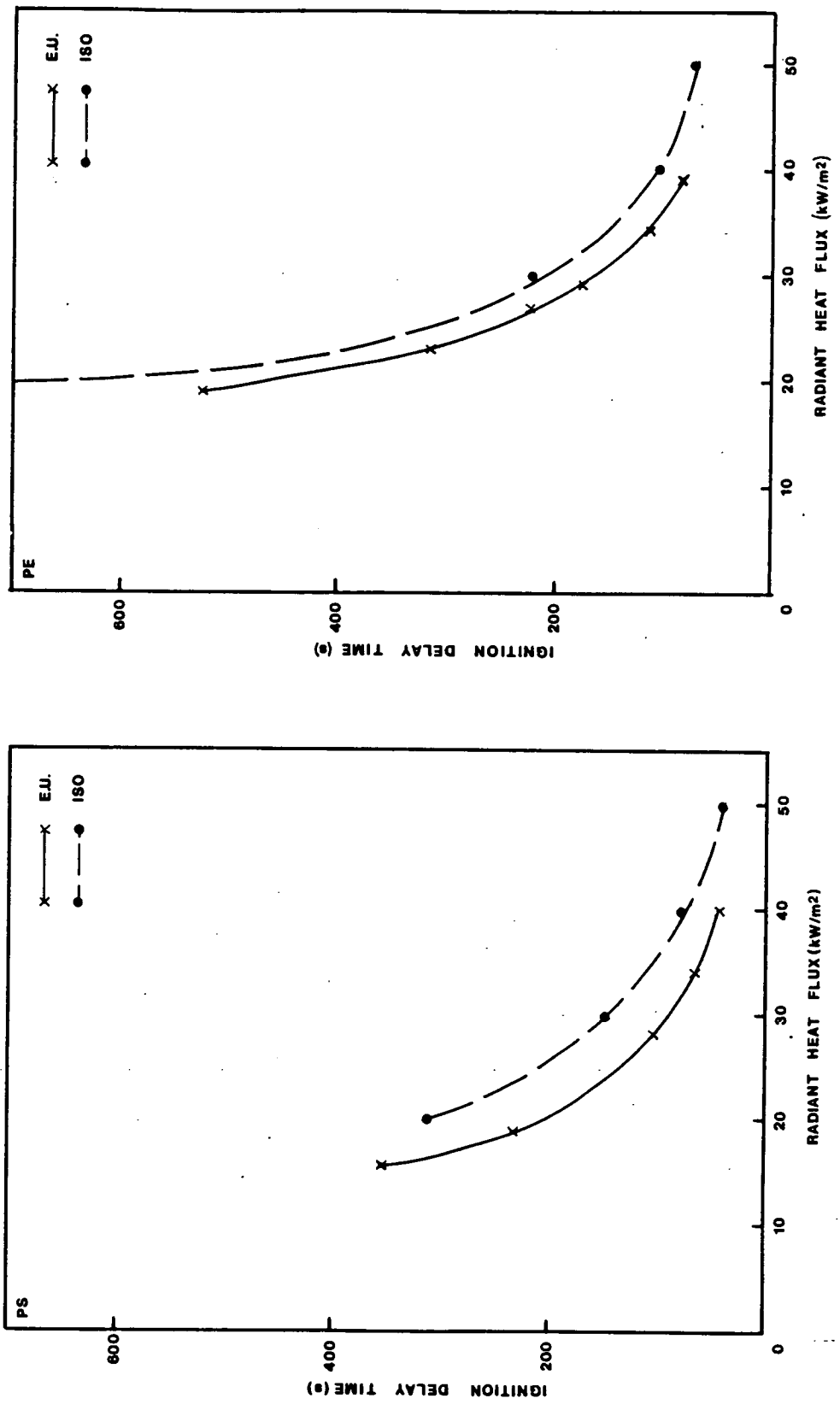

Figure 4.2 (cont.)

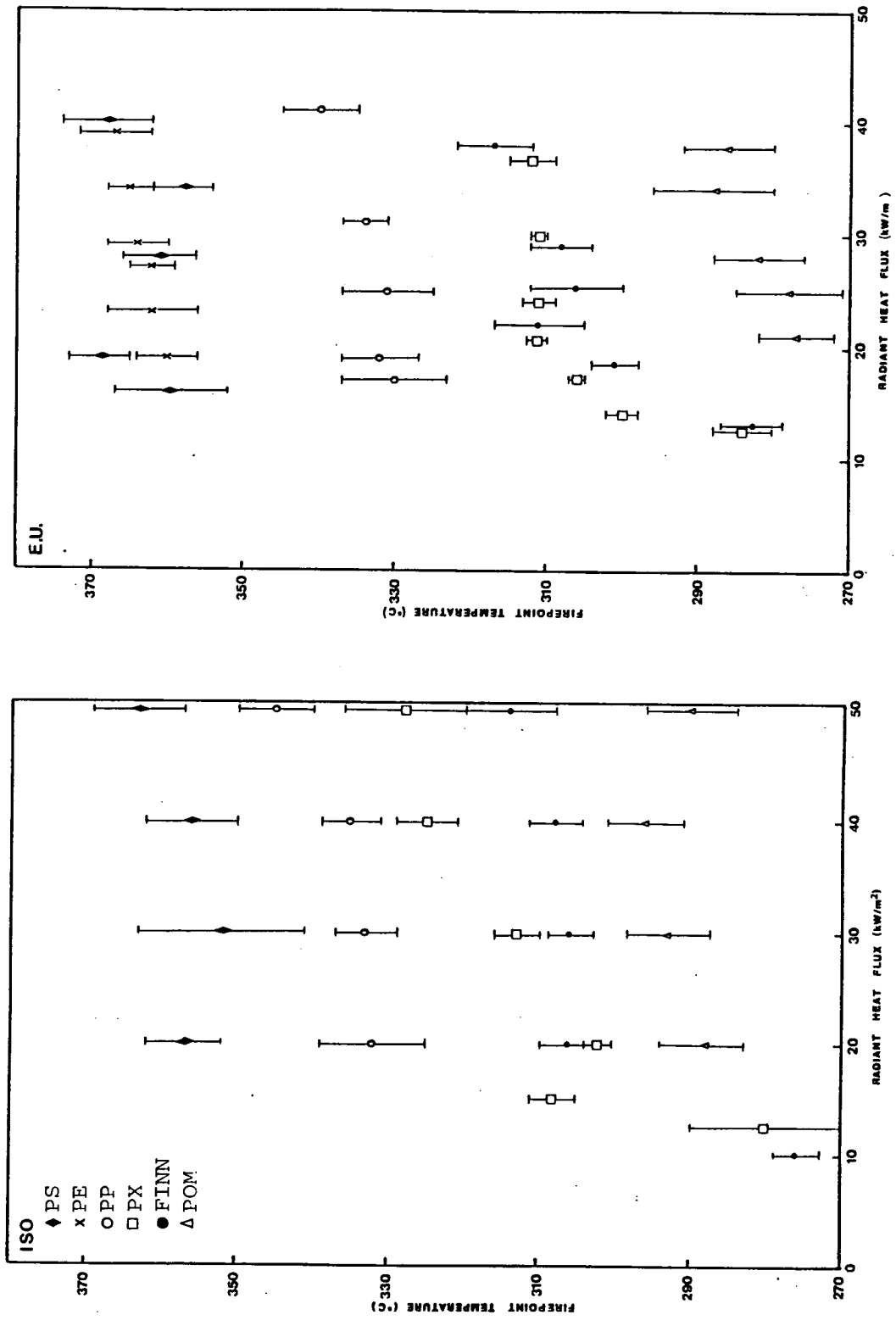

Figure 4.3 Comparison of firepoint temperatures in E.U. and ISO apparatus

TABLE 4.3

Variation in nature and position of pilot

PILOT TYPE		POSITION (cm)		
		0.5	1.0	2.0
Moving H_2 flame:	t_{ig}	110(6)	105(5)	124(8)
	T_{ig}	308(3)	311(3)	310(5)
Central H_2 flame:	t_{ig}	68(9)	95(4)	118(8)
	T_{ig}	324(8)	317(6)	312(3)
Spark:	t_{ig}	116(4)	112(6)	135(5)
	T_{ig}	312(4)	309(2)	314(3)

Table 4.4

Effect of airflow induced by extract fan

AIRFLOW	PERSPEX		POLYPROPYLENE	
	t_{ig}(s)	T_{ig}(^{o}C)	t_{ig}(s)	T_{ig}(^{o}C)
Extract fan "on"	105(5)	311(3)	181(7)	338(4)
Extract fan "off"	111(7)	312(5)	175(5)	334(6)

Table 4.5

Effect on ignition of sample mounting

RESTRAINT	t_{ig} (s)	T_{ig} (^{o}C)	T_{edge} (^{o}C)
Sample holder	115(6)	311(2)	305(4)
Mounting plates	131(7)	314(4)	260(6)

Table 4.6

Effect on ignition of varying source temperature

(a) Perspex

RADIANT HEAT FLUX (kW/m^2)	HEATING REGIME A		HEATING REGIME B	
	t_{ig}(s)	T_{ig}(^oC)	t_{ig}(s)	T_{ig}(^oC)
14	325(12)	288(2)	461(59)	300(2)
17	220(7)	312(1)	288(11)	306(1)
20.5	141(8)	306(4)	173(11)	311(1)
24	95(5)	307(3)	115(4)	311(1)
30	55(2)	306(3)	67(4)	311(1)
37.5	39(2)	312(3)	39(2)	312(3)

(b) Polypropylene

RADIANT HEAT FLUX (kW/m^2)	HEATING REGIME A		HEATING REGIME B	
	t_{ig}(s)	T_{ig}(^oC)	t_{ig}(s)	T_{ig}(^oC)
13	496(8)	317(3)	625(22)	328(3)
17	255(4)	320(5)	417(10)	339(2)
20	156(4)	314(5)	335(19)	330(5)
23	112(6)	330(5)	229(6)	334(4)
29	67(2)	325(3)	104(4)	341(6)
37	52(1)	332(3)	52(1)	332(3)

A is fixed heater position/variable temperature regime.

B is variable heater position/fixed temperature regime.

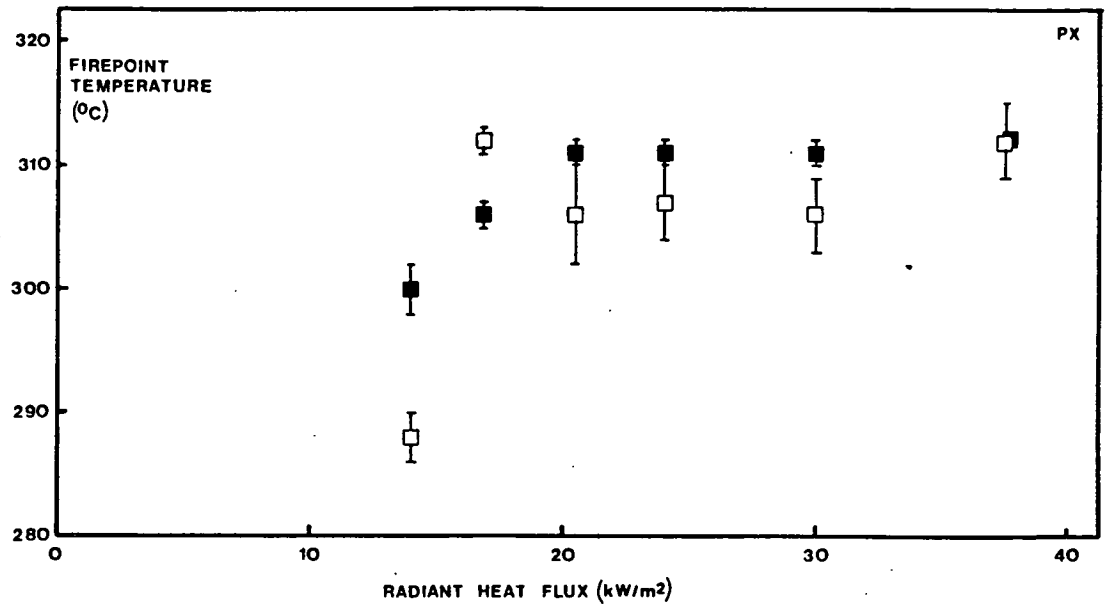

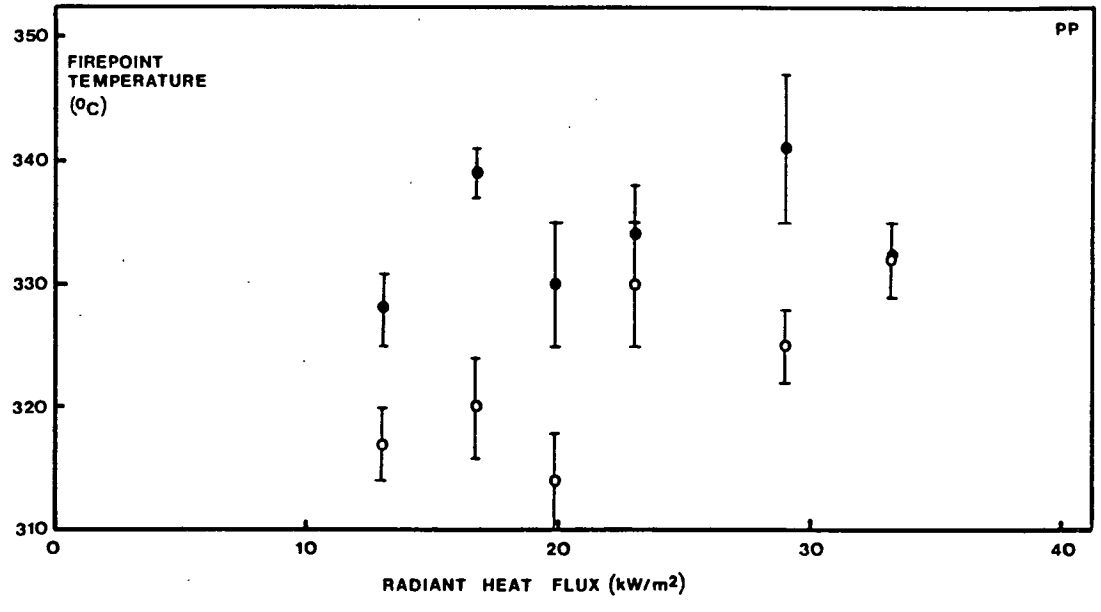

Figure 4.4 Comparison of firepoint temperatures under heating regimes A and B

Open symbols represent regime A
Closed symbols represent regime B

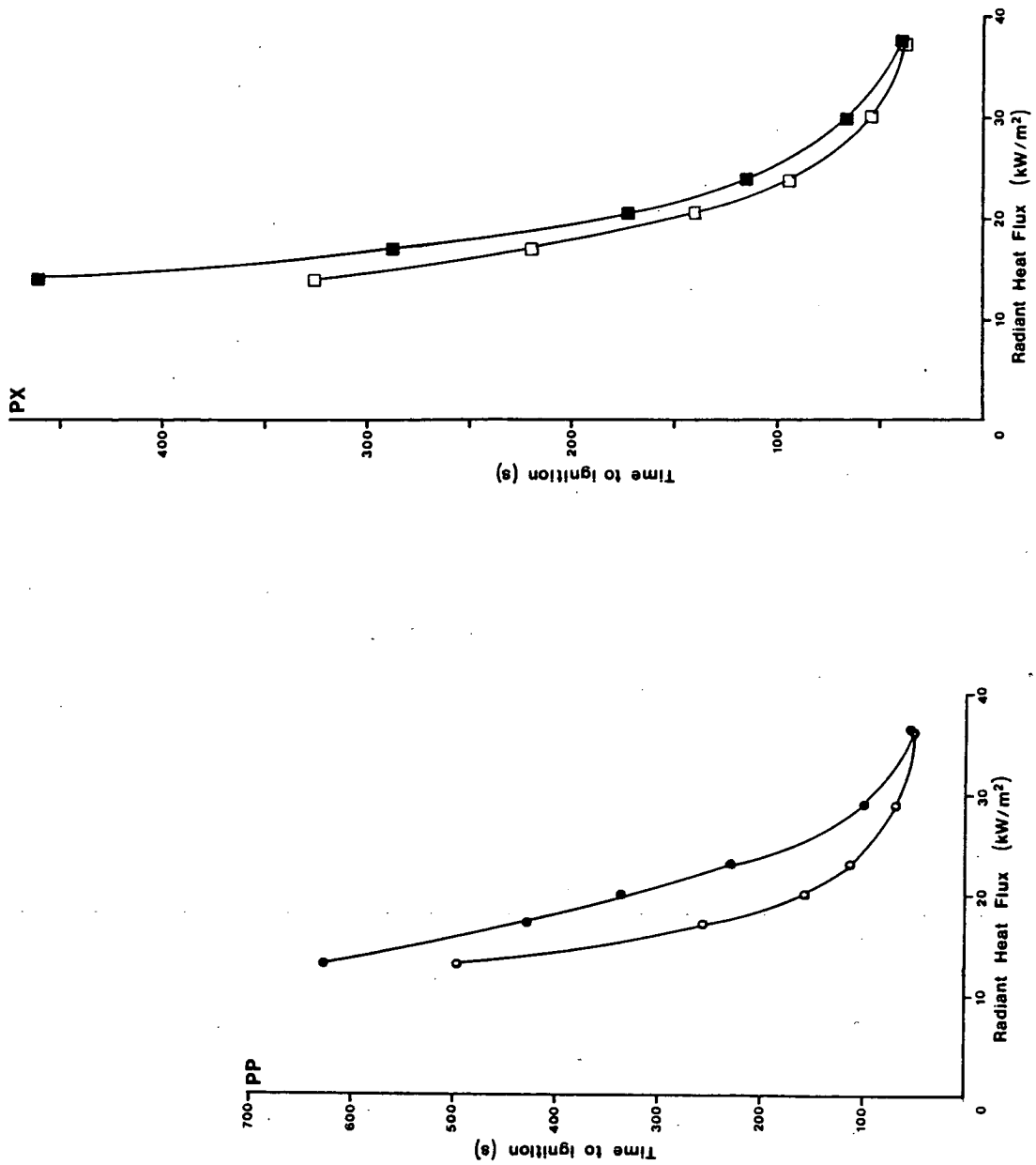

Figure 4.5 Comparison of ignition delay times under heating regimes A and B

Open symbols represent regime A
Closed symbols represent regime B

Table 4.7

Area effects with laser and conical heater

SAMPLE DESCRIPTION	SOURCE	t_{ig}(s)	T_{ig}(^{o}C)
65mm square sample in metal holder	Laser	327(20)	320(7)
19mm square sample mounted in Kaowool board	Laser	224(11)	334(5)
65mm square sample in metal holder	Radiant conical heater	54(3)	312(3)
65mm square sample in metal holder with foil template exposing 19mm square	Radiant conical heater	60(4)	338(4)
19mm square sample mounted in foiled Kaowool board	Radiant conical heater	68(5)	335(4)
19mm square sample mounted in blackened Kaowool board	Radiant conical heater	39(5)	305(5)
165mm square sample tested in ISO rig at F.R.S.	Radiant conical heater	64(2)	306(3)

Table 4.8

Effect of thickness and backing on ignition of Perspex

SAMPLE THICKNESS (mm)	Q" (kW/m^2)	BACKING MATERIAL Supalux Board		Kaowool Board	
		t_{ig} (s)	T_{ig} (^oC)	t_{ig} (s)	T_{ig} (^oC)
6	24	115(4)	311(1)	111(6)	312(2)
3	24	90(6)	306(4)	78(5)	304(3)
1	24	87(10)	304(9)	73(9)	306(10)
6	17	288(11)	306(1)	224(15)	310(3)

Table 4.9

Comparison of black and colourless Perspex

AVERAGE HEATER TEMPERATURE(^oC)	BLACK PERSPEX		C'LESS PERSPEX	
	t_{ig}	T_{ig}(^oC)	t_{ig}(s)	T_{ig}(^oC)
795	128(9)	307(3)	163(10)	308(3)
740	134(10)	311(4)	155(8)	310(3)
643	120(12)	314(3)	146(7)	311(2)
450	124(9)	312(4)	128(7)	313(4)

Table 4.10

Predicted firepoint temperatures (°C)

MATERIAL	HEAT FLUX (kW/m^2)	A		B		C	
		T_{ig}	T_r	T_{ig}	T_r	T_{ig}	T_r
PX	12.5	284	186	294	221	326	256
"	37.5	312	66	290	28	315	33
FINN	13	283	165	311	245	343	288
"	38	317	45	288	39	315	47
POM	21	277	133	319	243	338	253
"	37.5	286	76	266	79	281	86
PP	13	328	162	301	237	329	267
"	37	332	79	312	54	338	63
PE	19	360	248	376	317	396	339
"	39	367	113	352	147	370	158
PS	15.5	360	230	309	189	367	254
"	40	368	118	359	33	412	49

A Experimental values

B Predicted values from basic model

C Predicted values from modification 1.

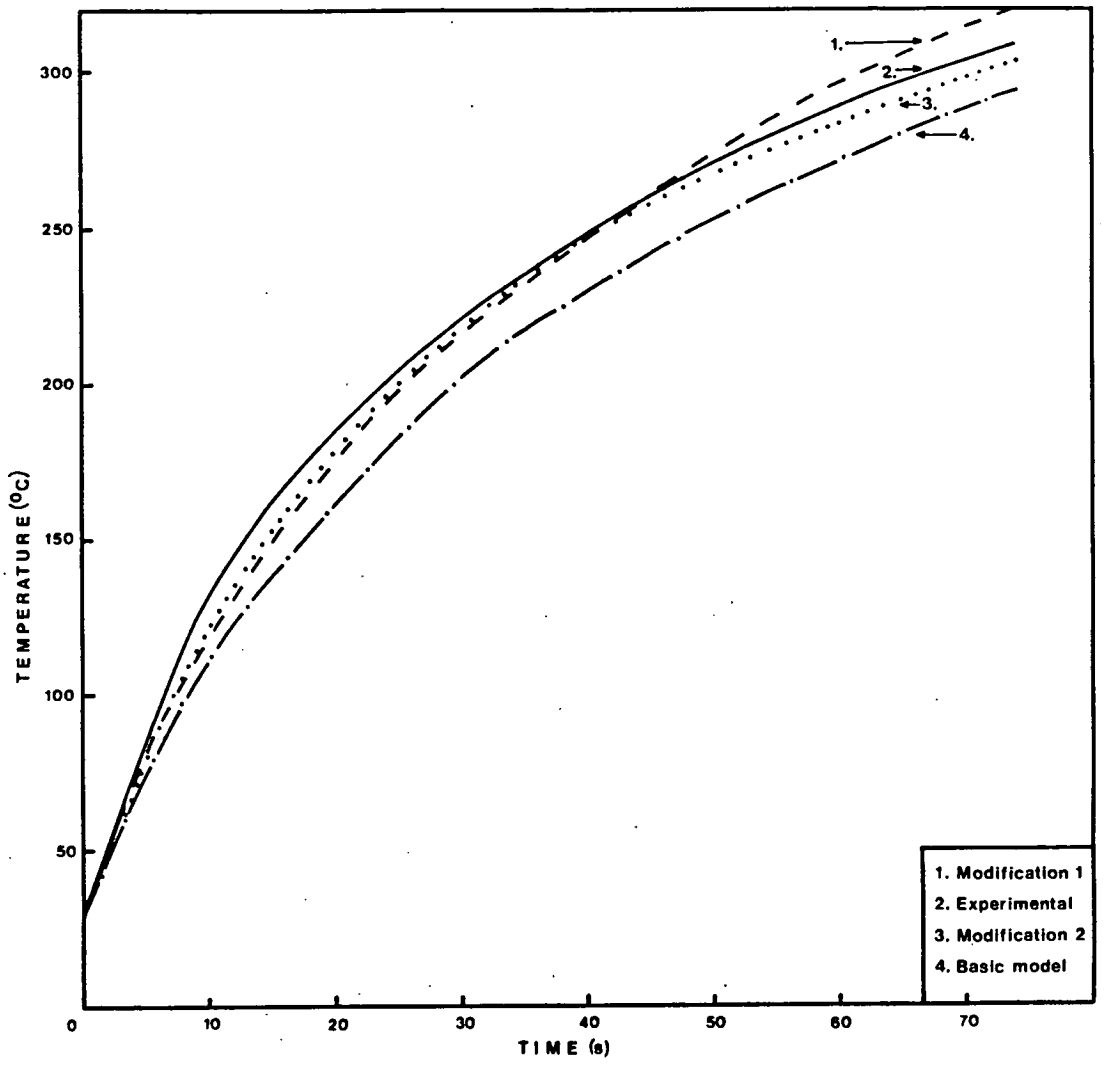

Figure 4.6 Comparison of experimental and theoretical surface temperature-time curves (PX @ 29kW/m^2)

Table 4.11

Results of mass loss experiments

(a) Perspex

HEAT FLUX (kW/m^2)	m''_{cr} ($g/m^2.s$)	m''_{fl} ($g/m^2.s$)	$\frac{m''_{cr}}{m''_{fl}}$
13	1.90(0.14)	0.96	2.0
"	**1.80(0.16)**	**1.00**	**1.8**
19	1.96(0.11)	0.95	2.1
"	**1.85(0.12)**	**0.93**	**2.0**
25	1.87(0.15)	0.99	1.9
"	**1.83(0.12)**	**1.04**	**1.8**
33	2.04(0.08)	-	-
"	**2.04(0.08)**	**-**	**-**

(b) Finnacryl

HEAT FLUX (kW/m^2)	m''_{cr} ($g/m^2.s$)	m''_{fl} ($g/m^2.s$)	$\frac{m''_{cr}}{m''_{fl}}$
13	1.95(0.13)	0.88	2.2
"	**2.05(0.09)**	**0.94**	**2.2**
19	2.04(0.09)	1.00	2.5
"	**1.94(0.19)**	**0.97**	**2.0**
25	2.15(0.18)	0.98	2.2
"	**1.89(0.08)**	**1.01**	**1.9**
33	1.92(0.19)	-	-
"	**1.92(0.19)**	**-**	**-**

Table 4.11 (cont.)

(c) Polyoxymethylene

HEAT FLUX (kW/m^2)	m''_{cr} ($g/m^2.s$)	m''_{fl} ($g/m^2.s$)	$\frac{m''_{cr}}{m''_{fl}}$
13	1.83(0.16)	0.82	2.2
"	**1.70(0.15)**	**0.85**	**2.0**
19	1.71(0.12)	0.85	2.0
"	**1.81(0.12)**	**0.9**	**2.0**
25	1.64(0.06)	0.90	1.8
"	**1.80(0.11)**	**0.95**	**1.9**
33	1.73(0.10)	-	-
"	**1.73(0.10)**	-	-

(d) Polypropylene

HEAT FLUX (kW/m^2)	m''_{cr} ($g/m^2.s$)	m''_{fl} ($g/m^2.s$)	$\frac{m''_{cr}}{m''_{fl}}$
13	1.03(0.06)	0.54	1.9
"	**1.12(0.08)**	**0.59**	**1.9**
19	1.13(0.08)	0.62	1.8
"	**1.16(0.10)**	**0.54**	**2.1**
25	1.10(0.11)	0.62	1.8
"	**1.22(0.07)**	**0.64**	**1.9**
33	1.2(0.08)	0.64	1.9
"	**1.2(0.08)**	**0.64**	**1.9**

Table 4.11 (cont.)

(e) Polyethylene[2]

HEAT FLUX (kW/m^2)	m''_{cr} ($g/m^2.s$)	m''_{fl} ($g/m^2.s$)	$\frac{m''_{cr}}{m''_{fl}}$
25	1.24(0.18)	-	-
"	**1.15(0.20)**	-	-
33	1.38(0.15)	-	-
"	**1.38(0.15)**	-	-

(f) Polystyrene

HEAT FLUX (kW/m^2)	m''_{cr} ($g/m^2.s$)	m''_{fl} ($g/m^2.s$)	$\frac{m''_{cr}}{m''_{fl}}$
13	0.93(0.05)	0.49	1.9
"	**0.99(0.06)**	**0.57**	**1.7**
19	1.01(0.08)	0.52	2.0
"	**1.04(0.07)**	**0.64**	**1.6**
25	1.07(0.06)	0.56	1.9
"	**1.03(0.06)**	**0.62**	**1.7**
33	0.91(0.04)	0.56	1.6
"	**0.91(0.04)**	**0.56**	**1.6**

1 Figures in bold refer to variable heater position/fixed temperature

2 Traces were irregular and extraction of data proved difficult.

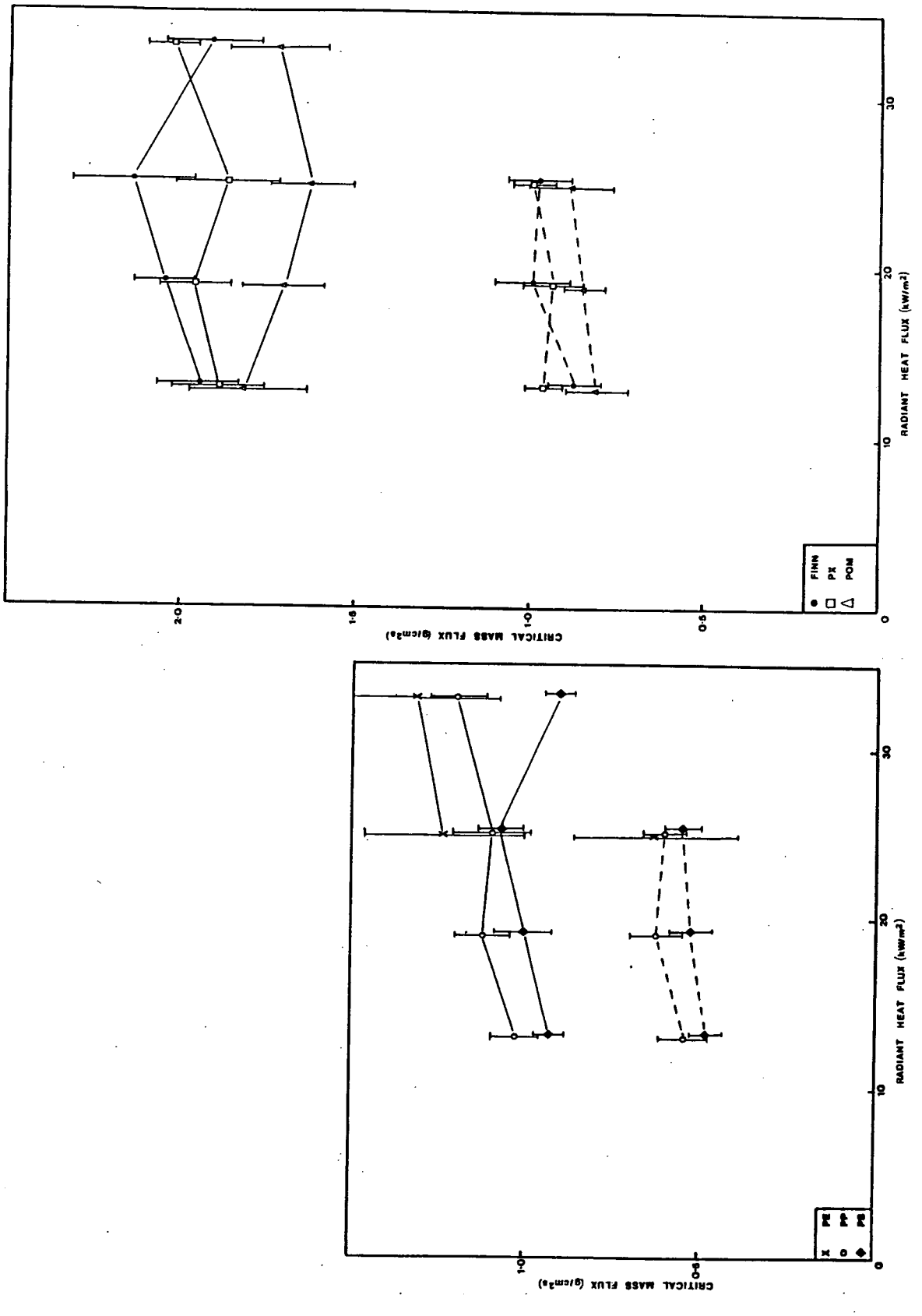

Figure 4.7 Critical mass flux at flashpoint and firepoint under fixed heater temperature/variable position regime

Firepoint ———, flashpoint - - -

Table 4.12

Activation energies of decomposition

MATERIAL	ACTIVATION ENERGY (kJ/mol)			$T_{5\%}$
	ZONE			
	1	2	3	
PX	58	77	63	293
FINN	42	89	57	277
POM	49	71	37	263
PP	34	64	29	288
PE	20	59	34	307
PS	-	92	72	320
PXFR	90	101	114	334
PPFR	78	124	89	350

Table 4.13

Limiting oxygen indices

MATERIAL	INDIVIDUAL TESTS (%)						MEAN
FINN	17.8	17.7	17.7	17.8	17.9	17.6	17.7(0.1)
PX	17.8	18.0	17.9	17.8	17.5	17.8	17.8(0.2)
PXFR	21.7	22.0	21.8	21.9	21.9	22.3	22.0(0.2)
POM	15.5	15.2	15.3	15.3	15.6	15.2	15.3(0.2)
PE	17.9	18.0	17.8	17.6	17.4	17.7	17.7(0.2)
PP	17.0	17.2	17.2	17.4	17.3	16.9	17.2(0.2)
PPFR	31.1	30.7	29.8	30.3	30.0	31.4	30.5(0.6)
PS	18.0	17.9	17.9	17.8	17.9	17.7	17.9(0.1)
PSFR	28.1	28.3	28.0	29.1	28.5	28.2	28.4(0.4)

Table 4.14

Effect of fire retardant on firepoint temperature

(a) POLYMETHYLMETHACRYLATE (Perspex / Perspex FR)

MATERIAL	HEAT FLUX (kW/m^2)	FIREPOINT TEMPERATURE(^{O}C) (A)	(B)
PX	14	288(2)	300(2)
"	17	312(1)	306(1)
"	20	306(4)	311(1)
"	24	307(3)	311(1)
"	30	306(3)	311(1)
"	37	312(3)	312(3)
PXFR	14	NI	NI
"	17	NI	NI
"	20	368(6)	373(5)
"	24	372(4)	370(6)
"	30	376(6)	372(5)
"	37	377(3)	377(3)

Table 4.14 (cont.)

(b) POLYPROPYLENE (Polypropylene / Simmona PPs)

MATERIAL	HEAT FLUX (kW/m^2)	FIREPOINT TEMPERATURE(^OC) (A)	(B)
PP	13	317(3)	328(3)
"	17	320(5)	329(2)
"	20	314(5)	330(5)
"	23	330(5)	334(4)
"	29	325(3)	341(6)
"	37	332(3)	332(3)
PPFR	13	NI	NI
"	17	NI	NI
"	20	NI	NI
"	23	NI	NI
"	29	392(12)	398(9)
"	37	407(10)	407(10)

Table 4.14 (cont.)

(c) POLYSTYRENE (Hyalite / Styron)

MATERIAL	HEAT FLUX (kW/m^2)	FIREPOINT TEMPERATURE(^{O}C) (A)	(B)
PS	14	-	360(7)
"	17	-	362(4)
"	20	-	367(4)
"	24	-	369(5)
"	29	-	365(4)
"	37	-	370(6)
PSFR	14	NI	NI
"	17	NI	NI
"	20	NI	NI
"	24	431(13)	430(9)
"	29	433(7)	441(8)
"	37	445(12)	445(12)

A refers to fixed heater position/variable temperature.

B refers to variable heater position/fixed temperature.

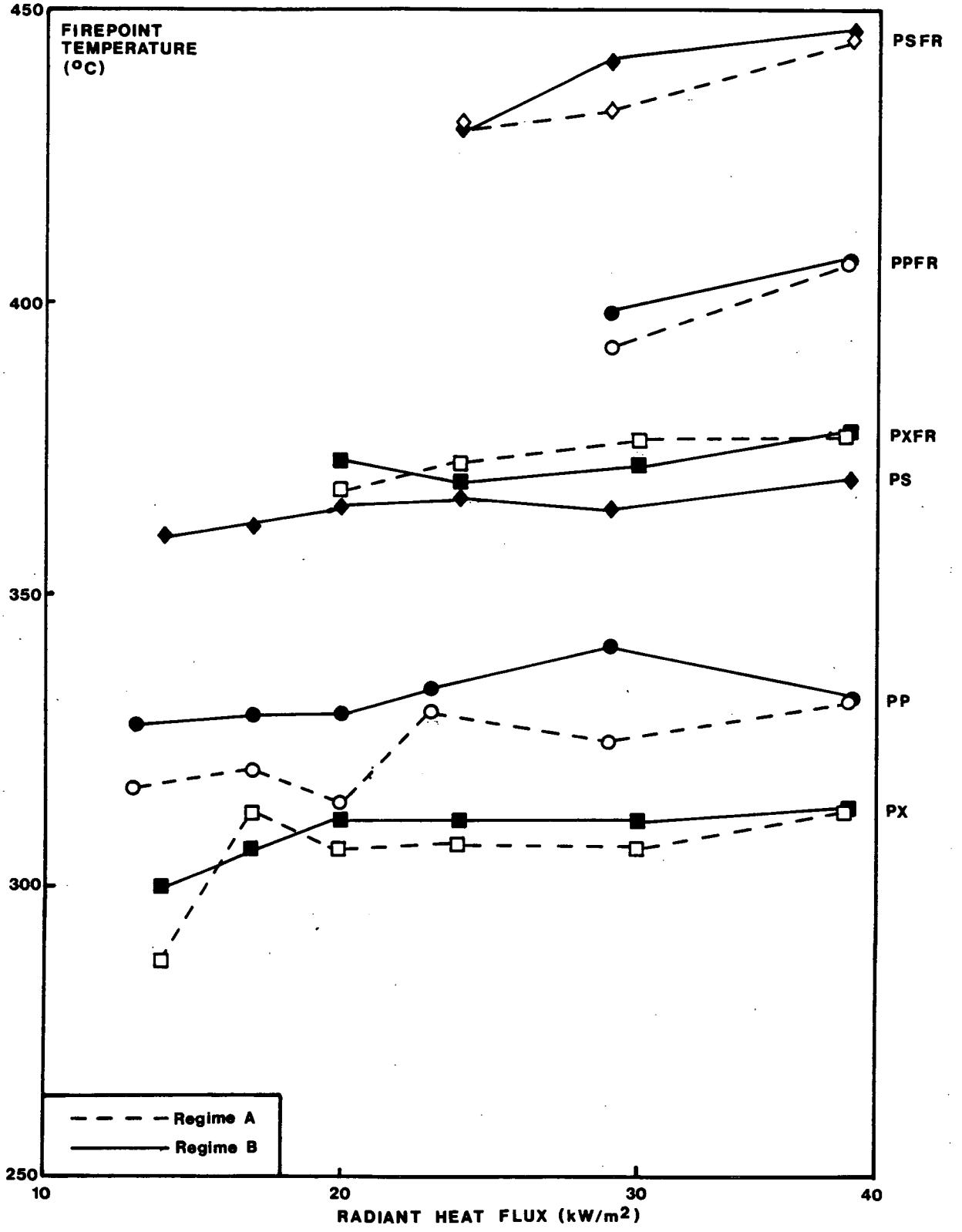

Figure 4.8 Comparison of firepoint temperatures of unmodified and fire retarded plastics

Table 4.15

Effect of fire retardant on critical mass flux

(a) POLYMETHYLMETHACRYLATE (Perspex / Perspex FR)

MATERIAL	HEAT FLUX (kW/m^2)	t_{ig} (s)	m''_{cr} ($g/m^2.s$)
PX	13	287(17)	1.90(0.14)
"	"	**223(8)**	**1.80(0.16)**
"	19	127(4)	1.96(0.11)
"	"	**109(6)**	**1.85(0.12)**
"	25	58(5)	1.87(0.15)
"	"	**52(3)**	**1.83(0.12)**
"	33	30(2)	2.04(0.08)
"	"	**30(2)**	**2.04(0.08)**
PXFR	13	NI	NI
"	"	**NI**	**NI**
"	19	352(23)	4.48(0.37)
"	"	**281(21)**	**3.46(0.26)**
"	25	194(13)	4.32(0.33)
"	"	**184(14)**	**4.17(0.23)**
"	33	89(4)	5.19(0.40)
"	"	**89(4)**	**5.19(0.40)**

Table 4.15 (cont.)

(b) POLYPROPYLENE (Polypropylene / Simmona PPs)

MATERIAL	HEAT FLUX (kW/m^2)	t_{ig} (s)	$\dot{m}''_{cr}$ ($g/m^2.s$)
PP	13	442(21)	1.03(0.06)
"	"	**302(27)**	**1.12(0.08)**
"	19	172(13)	1.12(0.11)
"	"	**146(5)**	**1.16(0.10)**
"	25	91(7)	1.10(0.11)
"	"	**75(5)**	**1.22(0.07)**
"	33	57(5)	1.20(0.08)
"	"	**57(5)**	**1.20(0.08)**
PPFR	13	NI	NI
"	"	**NI**	**NI**
"	19	NI	NI
"	"	**NI**	**NI**
"	25	285(12)	2.34(0.22)
"	"	**269(10)**	**2.88(0.24)**
"	33	90(7)	3.58(0.34)
"	"	**90(7)**	**3.58(0.34)**

Table 4.15 (cont.)

(c) POLYSTYRENE (Hyalite / Styron)

MATERIAL	HEAT FLUX (kW/m^2)	t_{ig} (s)	m''_{cr} ($g/m^2.s$)
PS	13	610(38)	0.93(0.05)
"	"	**496(18)**	**0.99(0.06)**
"	19	209(17)	1.01(0.08)
"	"	**183(9)**	**1.04(0.07)**
"	25	120(5)	1.07(0.06)
"	"	**110(6)**	**103(0.06)**
"	33	74(3)	0.91(0.04)
"	"	**74(3)**	**0.91(0.04)**
PSFR	13	NI	NI
"	"	**NI**	**NI**
"	19	NI	NI
"	"	**NI**	**NI**
"	25	291(16)	4.85(0.41)
"	"	**268(12)**	**4.42(0.6)**
"	33	124(6)	5.98(0.51)
"	"	**124(6)**	**5.98(0.51)**

1 Figures in bold refer to variable heater temperature/fixed position (regime A)

2 NI signifies no sustained ignition within 30 minutes.

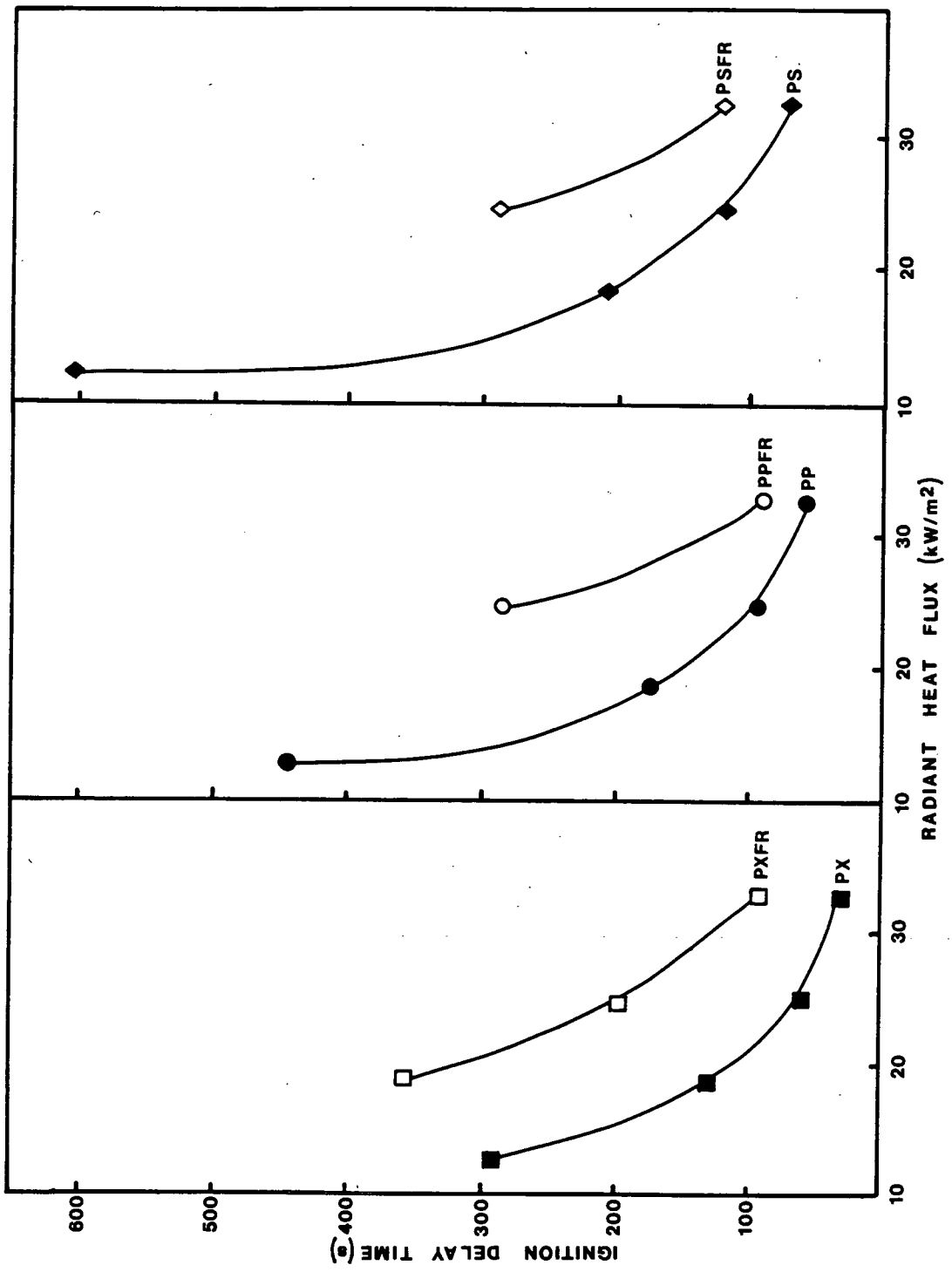

Figure 4.9 Comparison of ignition delay times of unmodified and fire retarded plastics

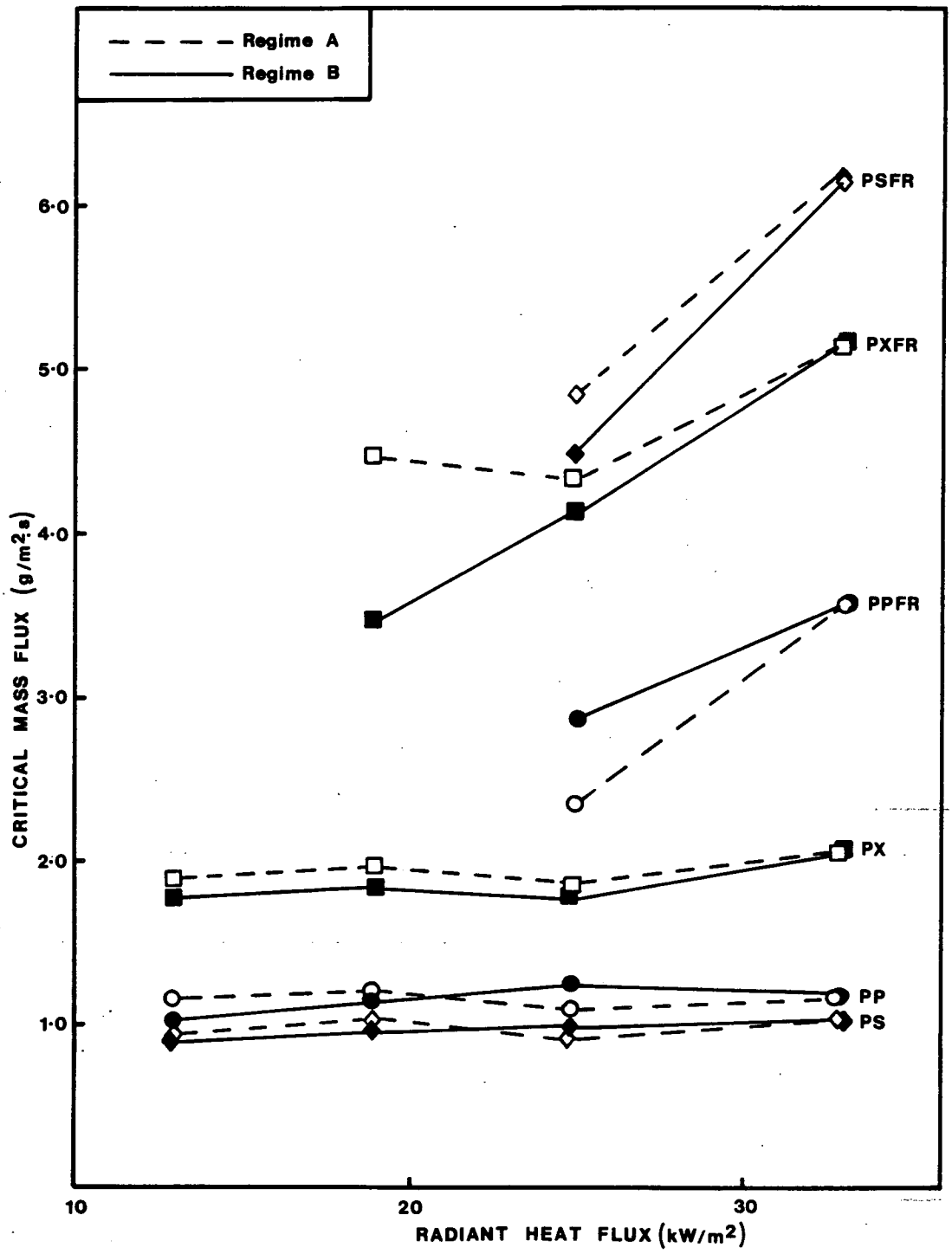

Figure 4.10 Comparison of critical mass flux of unmodified and fire retarded plastics

CHAPTER 5

DISCUSSION

CHAPTER 5
DISCUSSION

5.1 INTRODUCTION

Methods for characterising the ignition of combustible solids have been under study for several years. The "firepoint" concept has been assumed to be as applicable to combustible solids as it is to combustible liquids. For a liquid, the firepoint is achieved when the bulk liquid temperature reaches some critical level at which the vapours can be ignited to give a steady developing flame at the surface. The equivalent definition for solids is based on a minimum surface temperature below which sustained flame cannot be established at the surface.

The initial objective of the present study was to investigate the surface temperature at the firepoint for several commonly used thermoplastics. Surprisingly, this had not previously been investigated systematically and it was felt that the broad data base resulting from this work would lead to a better understanding of the ignition process and would allow existing models of piloted ignition to be tested.

The related concept of critical mass flux at ignition was also considered. Once again, a search of the literature revealed little systematic experimental data on mass loss rates at ignition of plastics other than the studies carried out by Tewarson and Pion (1978) for the National Bureau of Standards and limited work on polymethylmethacrylate and polypropylene carried out previously at Edinburgh University. Consequently, it was decided to determine mass fluxes at firepoint for the thermoplastics referred to in Appendix B, under a range of radiant heat fluxes from 13-33kW/m^2. These results were compared with existing

data and were used to seek validation for Rasbash's work on the "firepoint equation".

Additional experimental work included the application of thermal analysis techniques (TGA) to enable the calculation of activation energies of the decomposition processes. Limiting oxygen indices (LOI), generally accepted to be a satisfactory indication of "flammability", were also measured.

Effectiveness of fire retardancy was considered. The extent of protection afforded by a given treatment is generally assessed qualitatively by comparison in a standard test of the treated material and the parent untreated material. This information is highly specific and cannot be utilised to predict behaviour of different materials in fires. In an attempt to provide more generally applicable information on effectiveness of retardants, three pairs of thermoplastics and their fire retardant modifications were compared on the basis of firepoint temperature, ignition delay time, critical mass flux and limiting oxygen index.

5.2 FIREPOINT TEMPERATURE

5.2.1 Technique

The first series of experiments involved the measurement of the exposed surface temperature of seven common thermoplastics at the instant of ignition (subsequently referred to as the "firepoint temperature") over a range of radiant heat fluxes produced by various radiant sources. Rear surface temperature and ignition delay time were also determined.

Figure 2.10 shows a typical temperature-time curve while Figure 5.1 shows an enlargement of that portion of the temperature-time curve which lies between

flashpoint and firepoint.

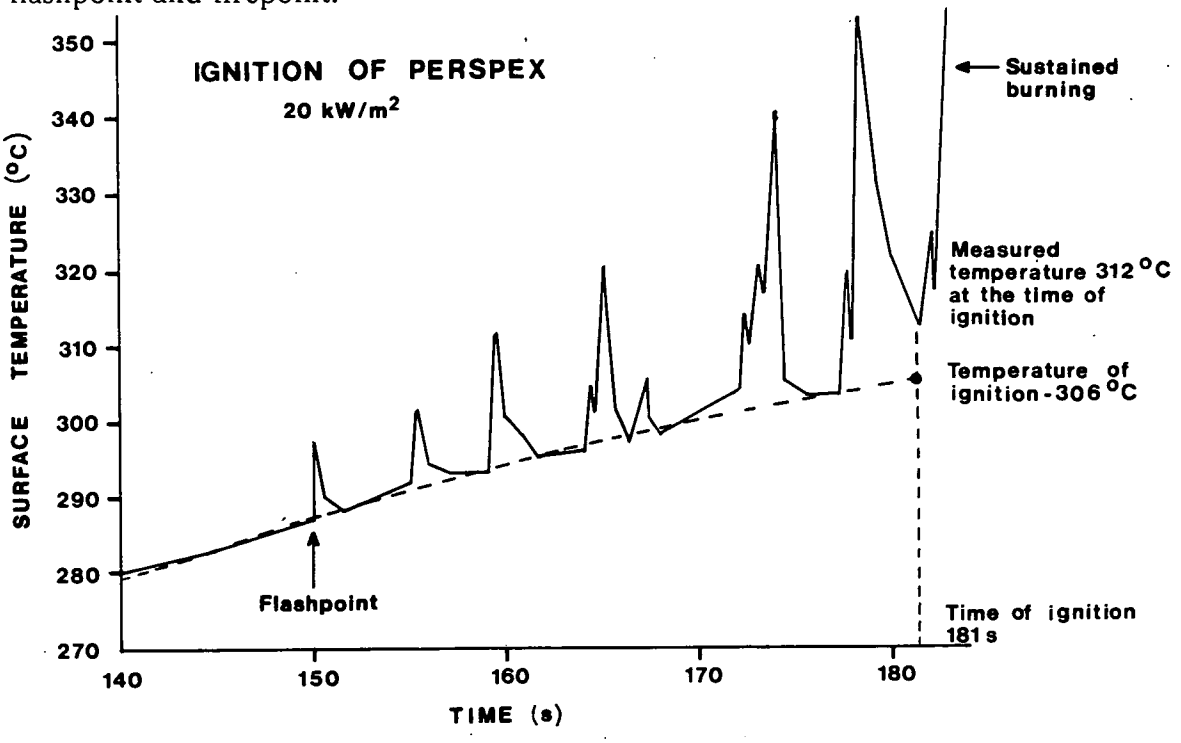

Figure 5.1 Enlargement of temperature-time trace.

It should be noted that the extrapolated surface temperature (the result of external radiation only) is significantly less than the momentary rises in temperature caused by the flashes which, nevertheless, did not initiate sustained flaming. Therefore, it may be deduced that sustained flaming requires that the surface temperature caused by external radiation alone should reach some critical value. Hence, any contribution to surface temperature from gas phase exothermicity cannot be included in the determination of the critical surface temperature. This is consistent with the concept of critical mass flux at ignition and implies that the critical flowrate of volatiles at ignition is produced by the solid indepth. The heat contribution from the flashes is small and is restricted to a thin surface layer which quickly loses heat by reradiation and conduction into the bulk of the solid. Rate of surface temperature rise is faster for higher heat fluxes and hence, the separation between flashing and sustained ignition will decrease

with increasing heat flux. Consequently, the surface temperature may not have time to reach equilibrium with external radiation and there will be difficulty in distinguishing the crossover point from flashing to sustained ignition. All temperatures quoted in this work are based on extrapolated surface temperature values. Thus, in Figure 5.1, 306°C rather than 312°C is the ignition temperature.

Measurements made in the Edinburgh University (E.U.) ignition apparatus (Figures 2.1 and 2.2) were subsequently repeated in the ISO Ignitability Test apparatus (Figures 2.7 and 2.8) at the Fire Research Station, Borehamwood. Firepoint temperatures (T_{ig}), rear face temperatures at ignition (T_{rear}) and ignition delay times (t_{ig}) for both sets of apparatus are quoted as the mean value of a minimum of six replicates with one standard deviation in parenthesis and are presented in Table 4.2. Failure to obtain temperature measurements at low heat fluxes for some materials was caused by difficulty in maintaining thermocouple junction contact at the sample surface for the duration of the heating period, as explained previously. These problems were exacerbated in the ISO tests by the larger sample area which required a length of unsupported thermocouple wire approximately three times greater than that required for the E.U. samples. In addition, there was a tendency for the larger samples to buckle upwards during heating which caused uncertainty about precise location of the thermocouple junction.

A consequence of the above observations is that reproducibility of firepoint temperature results tended to be lower at low heat fluxes than at higher heat fluxes (as indicated by increased standard deviations). However it should also be noted that at high heat fluxes with correspondingly rapid surface temperature rise, factors such as frequency of pilot application and precise identification of the

ignition point are crucial to the accuracy of firepoint temperature determination. Hence, optimum reliability would be expected at intermediate heat flux levels. Results obtained in the ISO Ignitability apparatus in general show a greater spread across the range of heat fluxes and more experiments were required in order to obtain six acceptable traces. On average, the success rate for acceptable traces was 1 in 1.35 for the E.U. apparatus and 1 in 1.9 for the ISO apparatus. This is indicative of the difficulties associated with temperature measurement in larger samples.

5.2.2 Is Critical Fire Point Temperature a Valid Concept?

The purpose of measuring surface temperature in these experiments was to establish the validity of applying a surface "firepoint temperature" to the definition for the critical condition for piloted ignition. Comparison of results from the E.U. and ISO test rigs (Figure 4.3) gives a first indication of the validity of the underlying assumption. In fact, despite significant differences between times to ignition at comparable heat fluxes in the two experimental rigs (Figure 4.2), there was no systematic difference between the two sets of firepoint temperature data. The effect of the intensity of radiant flux on T_{ig} appears to be slight for all materials tested except polymethylmethacrylate. In certain cases, there was an apparent gradual increase in the firepoint temperature with increase in heat flux. The experiments with Perspex in the ISO apparatus were carried out by Beyler (1985) using thermocouples constructed from 0.1mm diameter wires rather than 0.05mm as used in the other experiments. These results show that for the two highest heat fluxes in the range, the firepoint temperature of Perspex is more than $15^{o}C$ in excess of the average value over the complete range. This is thought to be attributable to absorption of significant amounts of radiation by the larger

thermocouples resulting in a higher temperature than actually exists at the specimen surface being recorded. This effect was not observed in experiments using the smaller diameter wires.

Table 5.1 shows the averaged value with one standard deviation of all the measured firepoint temperatures within the heat flux range quoted. The agreement between the averaged firepoint temperatures as measured in the two pieces of apparatus was particularly good for polypropylene and Finnacryl and within $10^{o}C$ for all other materials. However, there was a discrepancy of approximately $30^{o}C$ between the firepoint temperature of the unidentified brand of polymethylmethacrylate and that of Perspex and Finnacryl as measured in the E.U. apparatus.

Table 5.1

Average firepoint temperatures

MATERIAL	E.U. APPARATUS		ISO APPARATUS	
	Heat Flux Range(kW/m^2)	Ignition Temp.(^{o}C)	Heat Flux Range(kW/m^2)	Ignition Temp.(^{o}C)
POM	21-38	282(5)	20-50	292(4)
FINN	18-38	309(6)	20-50	308(7)
PMMA	18-29	279(3)	-	-
PX	17-38	310(2)	20-50	317(12)
PP	17-41	333(4)	20-50	336(6)
PE	19-39	363(3)	-	-
PS	19-40	364(5)	20-50	357(5)

The E.U. tests with PMMA (unidentified) used samples from a batch of material purchased in 1980. Results obtained in this study confirmed measurements of firepoint temperature made by Deepak and Drysdale (1983) in a previous investigation using samples from the same batch of material. However, these results were considerably lower than the firepoint temperatures obtained for Finnacryl and Perspex in both the E.U. and ISO apparatus. Thus, it would appear that the formulations of various brands of polymethylmethacrylate are sufficiently different as to cause variations in both firepoint temperature and ignition delay time. It has not been possible to confirm this with the manufacturers although a similar conclusion was reached by Kashwagi et al. (1986) in their work on PMMA degradation characteristics.

The hydrocarbon polymers (PS, PP, PE) have higher firepoint temperatures than either of the oxygenated polymers (PMMA, POM). With the exception of polystyrene, the measured firepoint temperatures of the polymers tested appear to reflect their relative thermal stabilities. Madorsky (1964) places these five polymeric types in the following order of ascending stability in a nitrogen atmosphere:

$$POM < PMMA < PS < PP < PE$$

which compares with the ascending firepoint temperatures:

$$POM < FINN = PX < PP < PE = PS$$

Since the plastics were all of commercial origin, it is possible that the discrepancy for PS is attributable to some "impurity" such as unreacted initiator or monomer, ultraviolet absorber, plasticiser, etc, which could influence decomposition. Alternatively, the greater influence of oxygen induced pyrolysis (a fast exothermic process) in the decomposition of PS over the remaining plastics could account for

the discrepancy.

The Effect of Radiant Intensity

With the exception of PMMA, there would appear to be no pronounced trend in firepoint temperature at various radiant heat fluxes other than a slight increase with increasing heat flux. If the volatiles are being produced from subsurface layers, this observation is consistent with the fact that the depth of the heated zone at ignition, as obtained from Equation 5.1, decreases with increasing heat flux and, consequently, higher surface temperatures are required to provide the same flow of volatiles.

$$x = (\alpha t)^{\frac{1}{2}} \qquad (5.1)$$

However, the scatter of data is large and more data would be required to establish whether or not this is a real effect.

This trend, if it does indeed exist, is in opposition to that found by Atreya et al. (1986) for wood in which a char layer develops at the surface (particularly at low heat fluxes) prior to ignition which tends to cause an increase in the firepoint temperature. However, with the exception of polymethylmethacrylate, these effects are quite small for both wood and thermoplastics. Thus, to a first approximation, the concept of definition of ignition by a critical firepoint temperature appears to be valid. However, there are certain constraints to the above statement which are discussed in greater detail in the next section.

5.2.3 Limitations of Firepoint Temperature Concept

There are circumstances when the use of a critical surface temperature criterion will predict ignition when in fact it will not occur. For example, a material under prolonged exposure to a flux less than the critical flux for piloted ignition may become fully exhausted or alternatively develop a thick layer of char. A

subsequent increase in the incident flux might cause the surface temperature to exceed the critical value, but ignition may no longer be possible.

Polymethylmethacrylate (all three brands) exhibits a significantly lower T_{ig} at the lowest heat flux (12.5-13kW/m^2) in the range applied. This observation is not unique to the present series of experiments; the same trend was observed for Persex in the ISO ignitability apparatus at 12.5kW/m^2 (Beyler (1985)) and Deepak and Drysdale (1983) found a similar decrease in T_{ig} for PMMA (unidentified) at a heat flux of 12kW/m^2. The decomposition of PMMA is thought to occur by a relatively simple process of random scission followed by "unzipping" to produce a yield of more than 90% methylmethacrylate monomer. Hence, it is most unlikely that the depressed firepoint temperature observed at low heat flux levels can be attributed to a change in the decomposition mechanism, and alternative explanations must be considered.

1. **Detachment/sinking of thermocouple:** Visual inspection would seem to preclude this possibility but, in addition, the results were too reproducible for this to be a significant factor. Furthermore, depressed firepoint temperature at low heat flux was not observed for any of the other materials tested, several of which were considerably less viscous than PMMA at high temperature

2. **Cooling of the thermocouple junction by rising bubbles of relatively cool monomer vapour:** Bubble formation in PMMA has been reported to commence at temperatures around 260^{o}C (Wichman (1986)). If vapour was able to escape rapidly to the surface from the lowest level of bubbling, then some degree of cooling would occur but it does not seem likely that this mechanism would be adequate to explain surface cooling of more than 30^{o}C.

3. **Formation of vapours at depth:** PMMA is the only polymer of those tested to exhibit significant bubble formation in the heated subsurface layer (Wichman (1986)). This is primarily because the boiling point of the decomposition product (methylmethacrylate monomer) is low (100^{o}C) by comparison with the decomposition temperature of the polymer. Under conditions of low heating rate, a matrix of trapped bubbles forms in the subsurface layers which are sufficiently fluid to allow bubbles to grow, distort upwards and finally to merge and create a network of channels

venting to the surface through which volatiles formed at depth may pass.

Kashiwagi and Ohlemiller (1982) have shown that explanation 3 causes an effective increase in the surface area of the sample, thereby increasing the total rate of production of decomposition products. The depth of the heated layer at ignition (Equation 5.1) which increases in direct proportion to the square root of the heating time, t_{ig}, will also contribute to this behaviour. This is shown qualititively in Figure 5.2 where the structure of the subsurface bubbles should be noted.

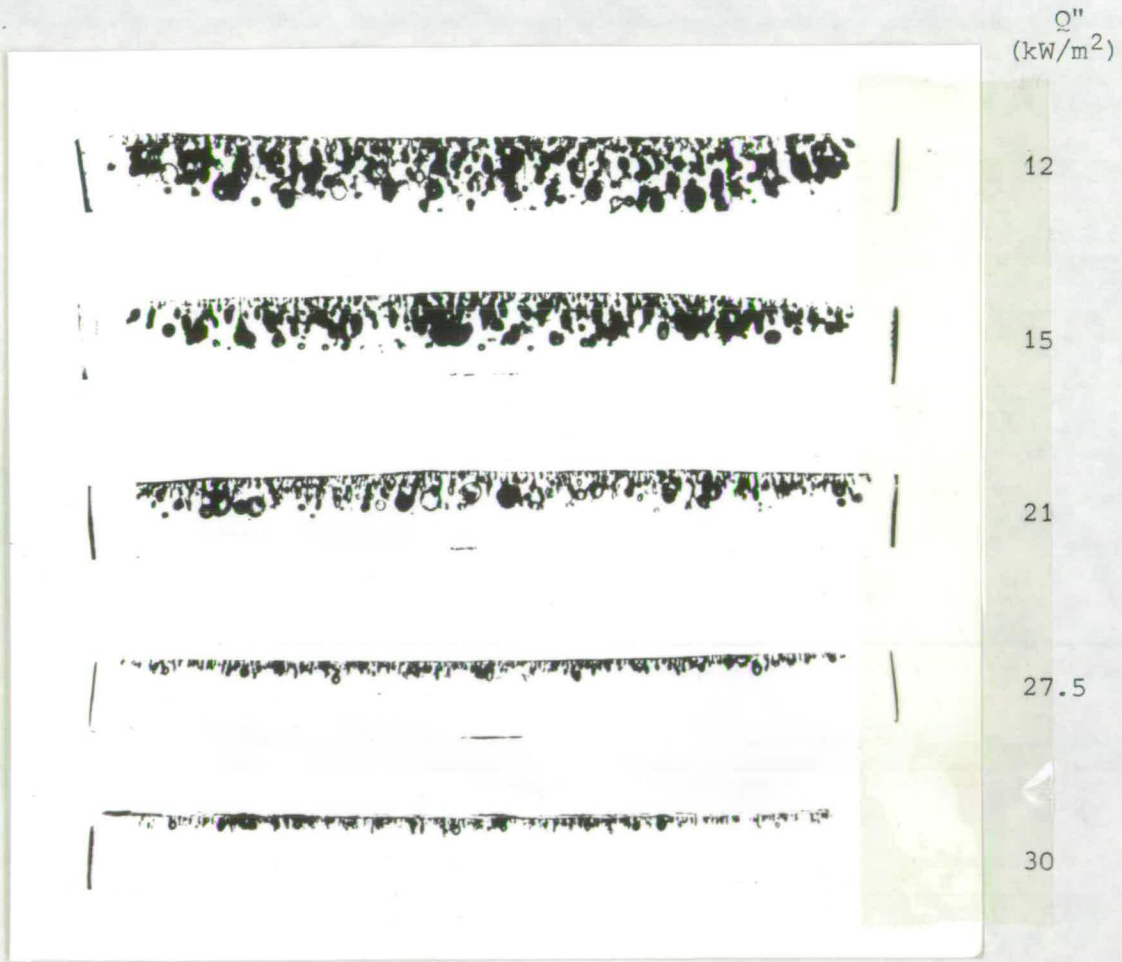

Figure 5.2 Bubble formation in subsurface layers of PMMA after exposure to radiation

Of the remaining four plastics, only polypropylene has been studied at reduced

heat flux because of the problem of thermocouple detachment. No significant decrease in firepoint temperature at the lowest heat flux was detected for polypropylene which is consistent with the fact that hydrocarbons do not tend to form subsurface bubbles.

The firepoint temperatures obtained in this study for Perspex are very different from the surface temperatures at piloted ignition reported by Kashiwagi (1979a) (360-400^{o}C). In his experiments, monochromatic radiation (10.6μm) from a divergent CO_2 laser beam was directed onto the horizontal sample surface at heat flux levels in excess of 70kW/m^2. In an attempt to account for this observed discrepancy in firepoint temperature, a few experiments were carried out in which the E.U. apparatus was modified by the incorporation of a laser as described previously, to produce a rig similar to that of Kashiwagi. Samples of Perspex were exposed to a diverged beam from a 12 W c.w. CO_2 laser. The maximum irradiated area was only 1.8cm^2 and the flux was non-uniform: an average flux of 34kW/m^2 (as determined by the heat flux meter) was used in this section of the work. The results are summarised and included in Table 4.7.

The ignition delay time of Perspex exposed to a radiant heat flux of 34kW/m^2 from the laser was approximately six times greater than that observed using the conical heater as the source. The firepoint temperature was slightly increased but not sufficiently to emulate Kashiwagi's results. At this point, it was recognised that these experiments were not strictly comparable with previous experiments in that the laser beam was irradiating only a small area of a larger surface (Figure 5.3).

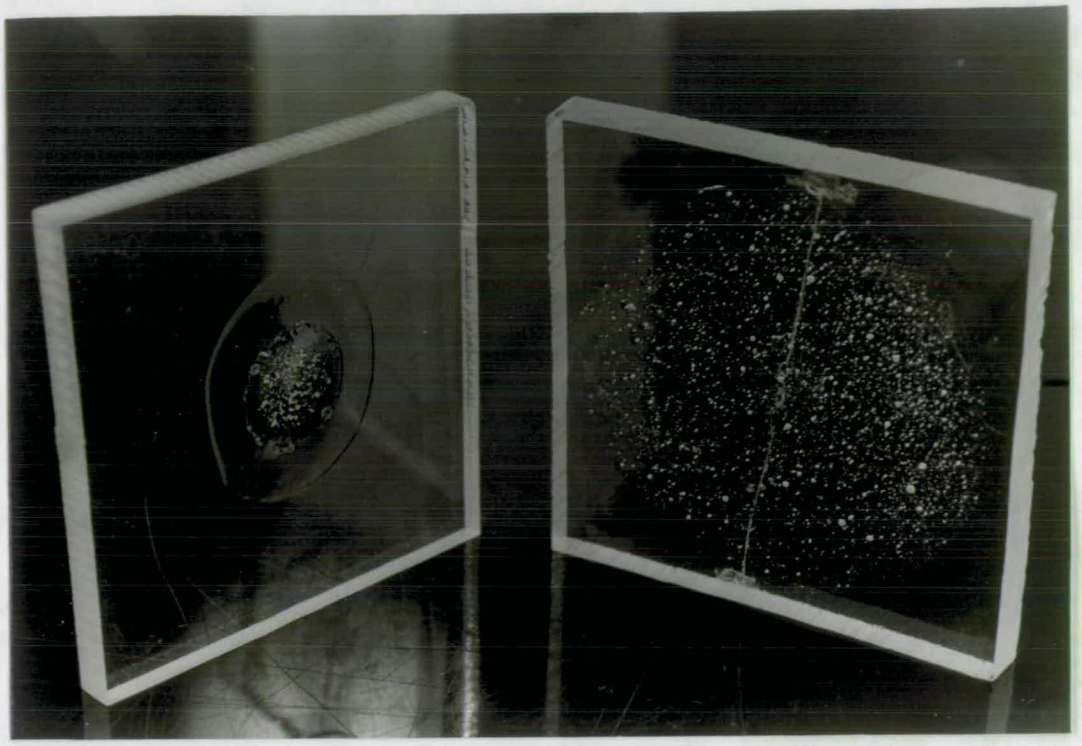

Figure 5.3 Comparison of samples exposed to conical heater and laser

Effect on Ignition of Sample Dimensions

A 65mm sample of PX was wrapped in aluminium foil, placed in the holder and a small central area of sample exposed by removing a 19mm square of foil. A thermocouple was attached in the usual way and the surface exposed to 34kW/m^2 from the conical heater. In a few experiments, the temperature of the foil was monitored and found never to exceed 100^{o}C during an experiment. The surface temperature at ignition was found to be significantly higher (338^{o}C) than measured previously. Essentially the same result was obtained when a 19mm square sample of Perspex which had been flush-mounted in the centre of a 65mm square piece of Kaowool board, itself covered with aluminium foil, was exposed to 34kW/m^2 from the conical heater. Significantly, when this experiment was repeated using the laser as the source of radiation a value for $T_{ig} = 334 \pm 5^oC$ was obtained.

These unexpected findings suggested that some factor other than temperature (and the rate of release of fuel vapours) was influencing the stabilisation of the nascent flame at the surface. Since high values of T_{ig} were obtained when the region surrounding a small area of exposed surface was (relatively) cool, experiments were carried out in which a 19mm square sample of Perspex was embedded in a piece of Kaowool board (65mm square) which had been painted black to enhance absorption of radiation when subjected to 34kW/m^2 from the conical heater. Both surface temperature at ignition (305±5^{0}C) and ignition delay time were found to be significantly reduced.

A tentative explanation of this observation has been made based on the stability of the developing flame at the surface following ignition. This nascent diffusion flame is likely to be tenuous and easily destroyed by any disturbance to the boundary layer. The influence of air entrainment through the plume boundary will progressively increase as the heated area is reduced and this could hinder establishment of flame. It may be possible to explain this simply in terms of dilution of flammable volatiles to the extent that volatile concentration falls below the lower flammability limit, but it seems more likely that the problem will require a theoretical analysis of the complex flow field associated with the boundary layer at a horizontal heated surface.

The question of the validity of carrying out experiments with samples 60mm in diameter then arises. Fortunately, it is possible to compare the present results directly with results obtained using the ISO Ignitability Test apparatus which exposes samples 150mm in diameter. These two sets of results for firepoint temperature are in reasonable agreement which indicates that the factor causing an increase in firepoint temperature for small irradiated areas is not significant in

the 60mm diameter samples used in the majority of these experiments.

The effect of area of irradiation on ignition was first studied by Simms et al. (1957). Simms (1960) has studied the general problem of area effect on ignition in some detail. The effect is observed to be smaller when irradiances are high than when they are low. The exact magnitude of the effect is also apparently dependent on the specimen's thermophysical properties. For specimens $0.01m^2$ or larger, however, the increase in ignition time is typically only 10% over what would be seen with a specimen of infinite area.

Kashiwagi's Results

In Kashiwagi's experiments (1979a,b) the area of irradiation was 20-30mm in diameter. While this could account for his values of T_{ig} being 20-30^{o}C higher than those reported in Table 4.2, it cannot explain a discrepancy of approximately 100^{o}C. Consequently, the reason for this lack of agreement must lie elsewhere.

Although Kashiwagi's data refer to higher radiant heat fluxes (70-179kW/m^2) than used in the present study, there is no obvious reason why this should influence the firepoint temperature at piloted ignition to the extent observed. At these high fluxes, significant attenuation of the incident radiation by absorption by the evolved products was observed considerably before the volatiles were ignited by the hot wire ignition source. Thus, one would expect longer ignition delay times than might have been predicted on the basis of incident heat flux levels alone but an increase in firepoint temperature would not be expected. Attenuation was unlikely to be important in the present experiments where the highest flux was 41kW/m^2. Kashiwagi (1979b) using a conical heater, found negligible attenuation within 120 seconds at a flux of 40kW/m^2. Ignition times of less than 90 seconds

were recorded at the highest fluxes for all materials used in the present study (Table 4.2).

Thus, it would appear that it is possible to ignite the fuel vapours and establish a diffusion flame at the surface of PMMA when the surface temperature and concentration of vapours are significantly lower than in Kashiwagi's experiments. The explanation for this conflict most probably lies in the form of ignition source used in the latter work. This consisted of 250μm platinum wire, maintained at 950°C, stretched parallel to and 15mm above the sample surface. The temperatures required to ignite flammable vapour/air mixtures have been shown to increase inversely with the area of the hot pilot surface (Powell (1969), Laurendeau (1982)). Coward and Guest (1927) found that temperatures in excess of 1100°C were necessary to ignite methane/air mixtures by a heated platinum strip (1 x 12 x 100mm) in a static system and so it is unlikely that a wire heated to 950°C would have been sufficient to ignite the fuel vapours in Kashiwagi's experiments. Indeed, Kashiwagi may have simply been inducing the process of spontaneous ignition which would account for the fact that he observed little difference between piloted and spontaneous ignition. In addition, his results (360-410°C) were in reasonable agreement with those of Setchkin (1949) (430,450°C) for spontaneous ignition. It is significant that in a more recent study, Kashiwagi et al. (1986) have used a platinum spiral (6mm in diameter) as the ignition source and report values of 275°C for vertical samples of Plexiglas (PMMA, Rohm-Haas Inc.) and Lucite (PMMA, DuPont Inc.) at 18kW/m^2 (conical heater). These are more consistent with the present results and with flash ignition temperatures quoted by Setchkin (1949) (280,300°C).

The observations made in this section imply that while the concept of critical

firepoint temperature for solids is attractive because of its simplicity in mathematical applications, great care must be taken in its use. Thus, although definition of ignition by critical surface temperature may be acceptible for certain simple models involving "standard" materials with large areas of exposure, it may be totally unsuitable for small samples of materials which behave in a non uniform manner when heated, ie those which char, delaminate, bubble, etc.

5.3 IGNITION DELAY TIME AND CRITICAL RADIANT HEAT FLUX

5.3.1 Theory

If heat losses are neglected and a material is assumed to be inert and semi-infinite, then the time to ignition based on the attainment of a minimum critical surface temperature (T_{ig}) can be approximated by the following expression (Carslaw and Jaeger (1959)):

$$t_{ig} = (\pi k\rho c/4)(T_{ig}-T_o)^2/Q''^2 \qquad (5.2)$$

In fact, when this theory is applied to the present results, gross underestimates of ignition delay time are obtained, particularly at low heat fluxes. In the solution of equation 5.2, it is assumed that (i) $k\rho c$ is constant and independent of temperature; (ii) surface reradiation loss is zero; (iii) there is no energy associated with any phase change or condensed phase process; and (iv) all materials have identical absorption characteristics. However, for polymers, (i) $k\rho c$ varies with temperature (ii) the surface reradiation loss is not negligible and increases with temperature (iii) surface as well as condensed phase processes can significantly influence the ignition of polymeric materials (iv) absorption characteristics of polymers vary greatly.

Neglect of reradiation in equation 5.2 is probably the most significant inadequacy.

If reradiation ($\varepsilon\sigma T^4$) is incorporated into the heat conduction equation, then the approximate expression for ignition delay time becomes

$$t_{ig} = (\pi k\rho c/4)(T_{ig}-T_o)^2/(\bar{\alpha}\dot{Q}''-\varepsilon\sigma T_{ig}^4)^2 \qquad (5.3)$$

Theoretical ignition delay times derived from equation 5.3 are more consistent with measured ignition delay times than are those derived from equation 5.2 (see Table 5.2) but underestimation still occurs. In order to achieve better predictive results, it is clear that a more advanced model of ignition is required.

Table 5.2

Experimental and theoretical ignition delay times for Perspex

RADIANT HEAT FLUX (kW/m^2)	EXPERIMENTAL		THEORETICAL	
	T_{ig} (^oC)	t_{ig} (s)	t_{ig} (s) (Eqn. 5.2)	t_{ig} (s) (Eqn. 5.3)
37.5	312	39	15	30
24	311	115	35	93
12.5	284	671	108	470

Although equations 5.2 and 5.3 are not totally realistic, they do indicate that "ease of ignition" is not entirely a function of ignition temperature. This is well illustrated by the fact that POM has a firepoint temperature approximately 30^oC lower than that of PMMA but the ignition delay time is almost twice that of PMMA under equivalent conditions. This is, to a certain extent, due to the difference in thermal inertia ($k\rho c$) of the two materials (POM, $772W^2s/m^4K^2$ and PMMA, $301W^2s/m^4K^2$). Hence for any given heat flux ($\dot{Q}''$), the ratio $t_{ig}(PX)/t_{ig}(POM)$ should be constant and equal to the ratio

$(k\rho c)(T_{ig}-T_0)^2(PX)/(k\rho c)(T_{ig}-T_0)^2(POM)$. The latter ratio is calculated as 0.48 while the average of $t_{ig}(PX)/t_{ig}(POM)$ over a range of heat fluxes is 0.43. Several other pairs of plastics have been considered and it is found that the agreement between ratios is better for some combinations than others (see Table 5.3). It is of interest to note that with the exception of pairs in which one of the materials is polystyrene, the variation between ratios is within 20%. This observation is consistent with the analogous position of polystyrene when firepoint temperatures were compared with thermal stabilities (Section 5.2.1).

Table 5.3

Ratios of ignition delay times and thermal inertias

MATERIAL PAIR (A)/(B)	$t_{ig}(A)/t_{ig}(B)$	$\frac{k\rho c(T_{ig}-T_o)^2(A)}{k\rho c(T_{ig}-T_o)^2(B)}$
PX/POM	0.43	0.48
PX/PP	0.64	0.71
PX/PS	0.49	1.28
POM/PP	1.49	1.48
POM/PS	1.15	2.69
POM/PE	0.88	0.71
PP/PS	0.77	1.82
PP/PE	0.58	0.48

The concept of a critical firepoint temperature for solids implies that for a given heat transfer environment, there exists a minimum radiation intensity (critical radiant heat flux) below which ignition is not possible. Hence, in theory, it should

be possible to select materials which will fail to ignite under a maximum anticipated incident heat flux in a particular design environment.

Under high levels of radiation with correspondingly short ignition delay times, heat losses are relatively unimportant. However, as the incident heat flux is reduced, convective and reradiative losses increase in importance until they reach a maximum at the critical radiant heat flux. Assuming a limiting steady state at ignition for a semi-infinite solid, this is given by

$$\bar{\alpha}\dot{Q}''_{min} = h(T_{ig}-T_o) + \varepsilon\sigma T_{ig}^4 + \dot{m}''_{cr}.L_v \qquad (5.4)$$

Evaluation of equation 5.4 using experimental values of T_{ig} and $\dot{m}''_{cr}$, values of $\bar{\alpha}_{av}$ as derived by Hallman et al (1977) and values of L_v as derived by Tewarson and Pion (1978) produces theoretical values of $\dot{Q}''_{min}$ as shown in Table 5.4. However, there are inherent problems with the theory on which equation 5.4 is based. Firstly, "real" materials cannot be assumed to be semi-infinite except at the highest heat flux levels (see Table 4.2) and hence, rear face heat losses may be significant. In addition, there is the problem of defining "non-ignition" in practical terms. In the present work, ignition times of up to one hour were observed for PMMA at 10kW/m^2. Simms and Law (1967) observed ignition times of 40-60 minutes for wood samples. The current ISO Ignitability test protocol requires the termination of tests after 15 minutes, if no ignition is observed within that time. Quintiere et al. (1983) apparently terminated their tests after 20 minutes. In the present investigation, rear surface temperature measurements indicated that even after one hour at 10kW/m^2 the specimen had not achieved thermal equilibrium. This indicates that in practical terms, the definition of a minimum incident heat flux for ignition must be influenced to a certain extent by an arbitrary decision as to the cut-off point beyond which a material will be

deemed non-ignitable at a specific heat flux.

Attempts to determine a critical heat flux for piloted ignition by extrapolation of Q" versus $1/t_{ig}^{\frac{1}{2}}$ using a correlation based on the semi-infinite solution to the linearised heat transfer problem have proved unsatisfactory due to the non-linear nature of the plots. The only acceptable method of determining critical heat flux at present is experimentally, using a bracketing method. This requires the experimental determination of two heat fluxes, one at which ignition will not occur and one at which ignition does occur. A binary bracketing method is then used to refine the determination of the minimum incident heat flux required for ignition. Results for the materials used in this study are given in Table 5.4.

Table 5.4

Critical radiant heat flux

MATERIAL	CRITICAL INCIDENT HEAT FLUX(kW/m^2)			
	Eqn 5.4	Extrapolation of t_{ig} data		Bracketing
		E.U.	ISO	ISO
PX	13.7	9.5	9.5	10-11.2
FINN	13.8	12	8	9-10
POM	12.8	9.5	9.5	11-12
PP	13.9	10.5	10	10-12.5
PE	16.3	13	16	15-20
PS	16.3	8.5	13.5	13-15

An acceptable method of reducing heat loss from the rear surface of horizontal samples is by improving the insulating properties of the backing board. The

E.U. tests use 25mm thick Kaowool board (density 215kg/m^3) while the ISO Ignitability test protocol requires the use of a 10mm thick non-combustible insulating board with a density of 825± 125kg/m^3. The effect of insulating properties of the backing board on times to ignition is discussed in a later section.

5.3.2 Factors Affecting Ignition Delay Time

Whilst there was little discernible difference between fire point temperatures measured in the E.U. rig and those measured in the ISO Ignitablity rig, the same could not be said of ignition delay times. In general, for a given polymer, times to ignition were longer in the ISO test rig than in the E.U. rig, probably because of differences in experimental arrangement. Several differences were identified (Table 2.1) and subsequently investigated in greater detail using the E.U. rig.

Effect on Ignition of Variation in Nature and position of pilot

A series of experiments to measure T_{ig} and t_{ig} at a heat flux level of 25kW/m^2 using different pilot source types and positions was carried out with Finnacryl. Results for three pilot source types (central stationary H_2 flame, small moving H_2 flame and central electric spark) at each of three positions (0.5, 1.0 and 2.0cm above the sample surface) were compared (Table 4.3). At a position of 0.5cm above the sample surface there was no significant difference between the results for the moving H_2 pilot flame and the electric spark; however the stationary flame produced a shorter ignition delay time and a higher fire point temperature. The time to flashpoint was also faster with a central stationary flame than with either of the other pilot types but the flames so produced were restricted to the area of sample surface directly below the pilot flame. At ignition, a small flame was established at the centre of the sample and subsequently spread towards the sample edge. With the other two pilot types, the sample surface was engulfed by

flame at the instant of ignition. Thus it may be deduced that the stationary H_2 pilot flame contributes to the localised temperature rise at the centre of the sample by providing an additional source of radiation. At 1.0cm above the sample surface, the moving H_2 flame and electric spark produced similar results to the 0.5cm setting while the stationary pilot flame again produced a shorter ignition delay time although the effect was less pronounced than previously. At 2.0cm above the sample surface both ignition delay time and firepoint temperature were slightly increased for all three pilot types although no significant difference could be detected between them. A lesser number of flashes of flame were observed prior to ignition at this pilot position.

It would appear from the above observations that the optimum pilot source is: (i) sufficiently energetic to initiate ignition, (ii) situated in the zone of maximum volatile concentration and (iii) non-radiating and does not contribute to sample heating. Both the moving H_2 flame and the electric spark at a position of 1.0cm above the sample surface apparently meet these criteria and have been used successfully in different phases of this work.

Effect on Ignition of Airflow

No appreciable difference was detected between measured values of T_{ig} and t_{ig} obtained for Finnacryl and polypropylene under a radiant heat flux of 25kW/m^2 with and without activation of the extract system (Table 4.4). This is not entirely unexpected since the airflow induced by the extract system over the cross sectional area of the extract hood is relatively small. It is possible that a difference in ignition time and temperature would be observed if results under stationary air conditions were compared with those under conditions of substantial forced airflow around the sample. Such experimental conditions are, unfortunately,

outside the scope of the present apparatus.

However, measurements have been made in the Ohio State University (OSU) apparatus to investigate influence of airflow on ignition (Babrauskas and Parker (1987)). Horizontal specimens of black polymethylmethacrylate were exposed to a heat flux of 35kW/m^2. An airflow of 12 l/s through the combustion chamber produced an ignition time of 209 seconds. When the airflow rate was doubled to 24 l/s, the ignition delay time increased to 403 seconds. One interpretation of this observation is that the phenomenon of ignition can be visualised as the attainment of the lower flammability limit in the volume of volatiles close to the specimen surface. High flow rates tend to dilute this volume and, thus, delay ignition. Alternatively, it is possible that the airflow simply cools the surface and reduces its rate of pyrolysis.

Effect on Ignition of Sample Mounting

In the E.U. experiments, the sample is completely enclosed by a stainless steel holder and hence, has no exposed edges. Conduction of heat from the holder to the sides of a relatively small sample creates an enhanced rate of heating which could account for a shorter time to ignition in the E.U. tests than in the ISO tests where the sample restraint system is such that the edges are exposed. This was verified by comparing edge temperatures, firepoint temperatures and ignition delay times for enclosed and exposed samples in the E.U. apparatus as explained in Section 2.2.3. When the sample edges were exposed, ignition was delayed and the edge temperature remained lower than the surface temperature for the duration of the experiment. When the sample was totally enclosed by the sample holder a shorter ignition delay time was recorded and the edge temperature equalled that of the surface before the end of the experiment. Edge effects would

be expected to become increasingly significant with decreasing sample size as the ratio of edge length:sample area increases.

Effect on Ignition of Varying the Radiant Source

One of the major differences between the E.U. and ISO apparatus is the method by which radiant heat flux is varied. In the E.U. tests, the range of radiant heat fluxes was achieved by setting the conical heater to its maximum temperature (1050K) and varying its height above the sample (Figure 2.3). Consequently, the spectral output, which is dependent on the temperature of the radiator, is constant over the heat flux range applied. In the ISO rig, the heat flux was varied by changing the temperature of the conical heater which was in a fixed position with its lower edge 4cm above the sample surface. Hence the source emits a different spectral distribution for each intensity within the range of heat fluxes. This would be unimportant if the polymer surface behaved as a blackbody with an absorptivity of unity, independent of wavelength, but the materials used in this study show pronounced banded absorption (Figure 1.6).

In an attempt to investigate the relationship between spectral distribution of the source and absorption characteristics of the sample, a series of experiments was carried out in the E.U. rig in which the radiant heat flux was varied as it is in the ISO test procedure. The relevant data for T_{ig} and t_{ig} relating to Perspex and polypropylene are shown in Table 4.6 alongside corresponding data obtained at constant heater temperature (variable position). The time to ignition is apparently sensitive to relatively small changes in the spectral distribution of the source (Figure 4.5(a) and (b)).

This observation was confirmed by means of the final version of the E.U

computer model which allowed distinction between the efficiencies of comparable radiant heat fluxes produced by blackbody radiators at different temperatures to be made (Table 5.5).

Table 5.5

Dependency of theoretical ignition delay time on source temperature(PX)

RADIANT FLUX (kW/m^2)	HEATER TEMP. (^oC)	THEORETICAL t_{ig} (s)
30	1000	82
30	800	72
30	600	64
30	400	61

Table 5.5 indicates that the theoretical rate of surface temperature rise is faster when radiation is provided by a low temperature source close to the sample surface than when it is provided by a high temperature source at a greater distance from the surface. Additional experiments were then carried out in which samples of black ICI Perspex were exposed to four different heater temperature/heater position combinations each producing a resultant heat flux of $25kW/m^2$ and firepoint temperatures and ignition delay times were measured. Similar measurements were then made for colourless ICI Perspex at the same heater settings. The results are quoted in Table 4.9.

For black Perspex, heater temperature has little effect on either firepoint temperature or ignition delay time. However, for colourless Perspex, the firepoint

temperature remains fairly constant but ignition delay time is observed to decrease with decreasing heater temperature. Black Perspex appears to be essentially a blackbody absorber and consequently, changes in the spectral distribution of radiation incident on its surface are unimportant provided that the net intensity of radiation remains constant. Colourless Perspex, on the other hand, has a strongly banded absorption spectrum and its absorption of radiation is enhanced if the emission peak maximum coincides with a strong PMMA absorption band. Hence some spectral distributions provide more effective surface heating than others of equal intensity.

Similar results have been reported by Hallman et al. (1972, 1976). They observed that colourless PMMA (Rohm-Haas, "Plexiglas") achieved its firepoint more rapidly when exposed to radiation from a benzene flame (T=1200K) than to that from a tungsten lamp (T=2500K) at equivalent irradiances. This was attributed to the fact that PMMA absorbs strongly only at wavelengths greater than 2μm, while of the two sources of radiation, the tungsten lamp has its emission maximum at 1μm and the flame shows a strongly banded spectrum at wavelengths greater than 2μm. These authors defined an average absorptivity coefficient as described in Chapter 1 (equation 1.34), ie

$$\bar{\alpha}_{av} = \frac{\int_{\lambda 1}^{\lambda 2} \bar{\alpha}_\lambda e_\lambda . d\lambda}{\int_{\lambda 1}^{\lambda 2} e_\lambda . d\lambda} \qquad (5.5)$$

where $\bar{\alpha}_\lambda$ is the (effective) monochromatic absorptivity and e_λ is the monochromatic emissive power of the source (assumed to be blackbody) at wavelength, λ, and showed this to decrease as the temperature of the source was increased. This observation is consistent with the results for PX and PP shown in Tables 4.6(a) and (b), respectively, where times to ignition are slower under the

constant heater temperature/variable heater position regime.

The effect of changes in the spectral distribution of the source on firepoint temperature is less obvious. The firepoint temperature of Perspex, with the exception of the lowest heat flux used ($13kW/m^2$) where T_{ig} showed a marked decrease with reduced heater temperature, was essentially independent of source temperature within the scatter of the data. Results for polypropylene show values of T_{ig} under conditions of constant heater temperature to be consistently higher than those obtained with a variable heater temperature (constant position). However the data show considerable scatter due to problems of thermocouple attachment and this may not be a real effect.

Effect on Ignition of Sample Dimensions

The effect of area of exposure of a specimen on ignition has already been alluded to in section 4.2.3. In addition, the sample thickness influences ignition. If the requirement for thermal thickness is taken to be:

$$x > 2(\alpha t)^{\frac{1}{2}} \qquad (5.6)$$

where α is thermal diffusivity ($k/\rho c$) then, clearly, the majority of the present work relates to samples which were not thermally thick for the duration of the experiment (see Table 4.2). This would partly account for observed discrepancies between theoretical predictions and experimental results. Comparison of T_{ig} and t_{ig} values for 6mm, 3mm and 1mm thick samples of Perspex exposed to a radiant heat flux of $24kW/m^2$ indicated that ignition delay time increased as thickness decreased but the fire point temperature appeared to be independent of sample thickness. Only the 6mm samples were thermally thick at this radiation level. The high standard deviation in results for 1mm samples is attributed to the severe

sample distortion which occured during heating.

An important ramification of thermally thin samples is the influence that the insulating properties of the backing board have on heat losses from the rear surface of the sample. This was clearly illustrated by comparing T_{ig} and t_{ig} values for 6mm, 3mm and 1mm Perspex samples backed by 25mm thick Kaowool board (density 215kg/m^3) with equivalent samples backed by 10mm thick Supalux (density 800kg/m^3) under a radiant heat flux of 25kW/m^2. Within the scatter of the data, firepoint temperatures for all thicknesses remained constant independent of the backing material. Little difference was observed in ignition delay times for 6mm samples (thermally thick) but for 3mm and 1mm samples, substantially faster ignition times were obtained from the samples backed by Kaowool board. When Q" was reduced to 17kW/m^2 and the experiment repeated for 6mm samples, faster ignition times were observed in samples backed by Kaowool board. This indicates that improved insulation, ie low thermal inertia, reduces time to ignition in those experiments for which the specimen was not effectively semi-infinite for the duration of the pre-ignition period ($x < 2(\alpha t)^{\frac{1}{2}}$). Thus, a possible contributory factor for the variation in times to ignition between the E.U. and ISO tests is identified.

5.4 THEORETICAL MODEL FOR IGNITION

Table 4.10 compares experimental and predicted firepoint temperatures at the highest and lowest heat fluxes for which firepoint temperatures are available in the ranges considered for various thermoplastics. The theoretical figures are derived from the model described in Chapter 3 using a time interval of 1 second, an increment thickness of 1mm, $\bar{\alpha}_{av}$ data as derived by Hallman et al.(1977) and

data on physical properties from commercial literature.

In general, the basic version of the model underestimates firepoint temperatures at high heat fluxes and overestimates at low heat fluxes. When modifications are made to incorporate diathermancy effects, good agreement between theoretical and experimental results is obtained at heat fluxes of 37-40kW/m^2 (less than 2% variation for all materials considered except PS) but at lower heat fluxes, overestimation of both the firepoint temperature and the rear face temperature occurs. This is not entirely unexpected since the model neglects the energetics of pyrolysis processes which become progressively more significant with decreasing radiant heat flux (see Table 5.6).

$$\%\ \text{of absorbed radiation required for volatile production.} = \frac{\dot{m}''_{cr}.L_v.100}{\bar{\alpha}_{av}\dot{Q}''} \qquad (5.7)$$

Table 5.6

% of absorbed radiation required for volatile production at ignition

MATERIAL	% AT 33kW/m^2	% at 13kW/m^2
PX	11.8	27.9
FINN	11.1	28.6
POM	13.8	37.2
PP	8.5	18.5
PE	10.5	-
PS	7.1	16.8

Experimental results indicated that the nature of the emission spectrum from the

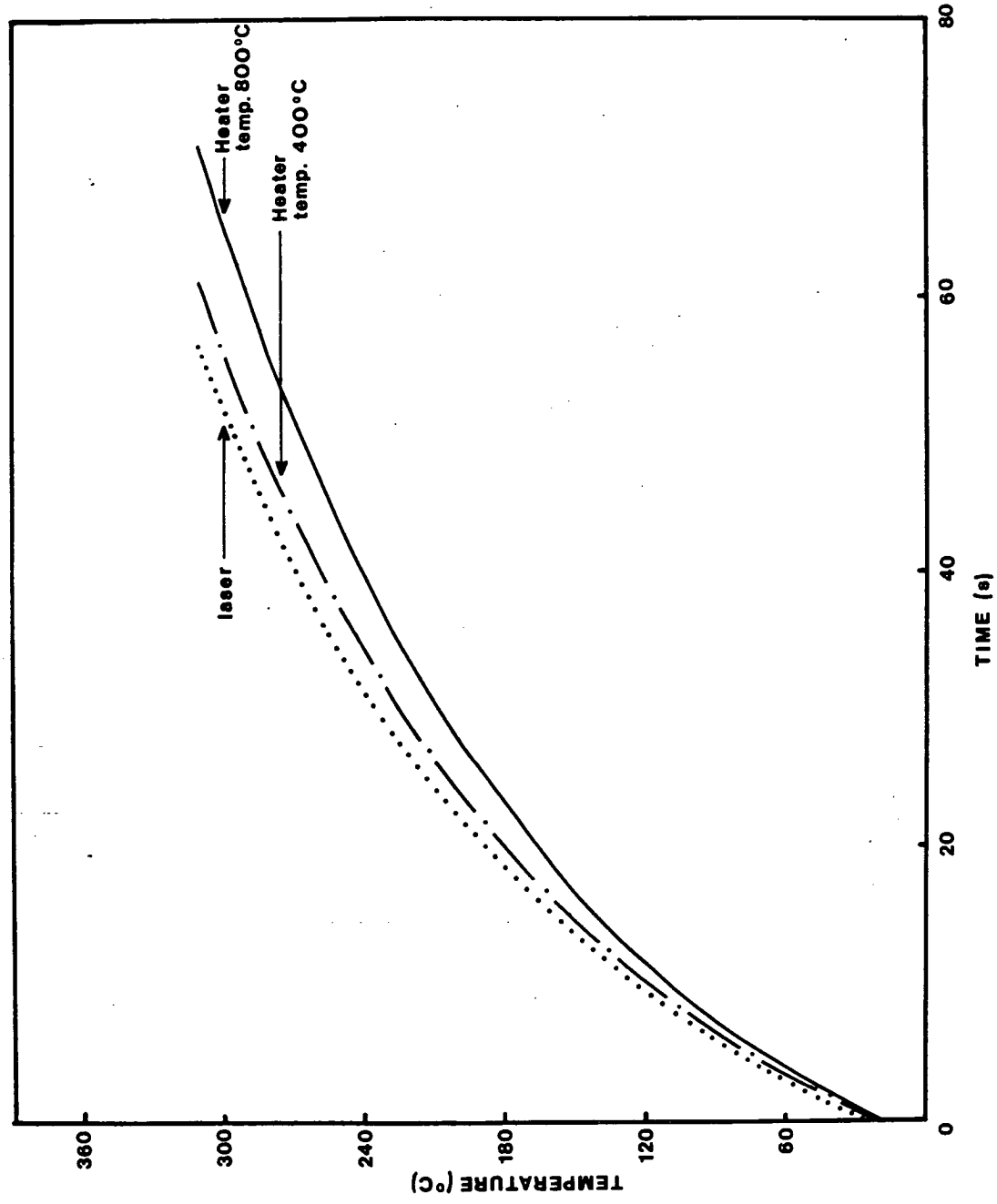

Figure 5.4 Theoretical temperature-time curves for Perspex exposed to 30kW/m^2 from various sources

* Based on full size samples attaining a temperature of 310^{0}C

source influenced ignition. Hence, the model was further modified as described previously, to take this into account. Figure 5.4 shows theoretical temperature-time curves for Perspex exposed to blackbody source temperatures of $400^{o}C$ and $800^{o}C$, respectively and also CO_2 laser radiation, each producing a radiant heat flux of $30kW/m^2$. If the firepoint temperature is assumed to be independent of nature of source as the experimental results indicate, then the theoretical predictions of ignition delay time under different source characteristics are consistent with experimental observations.

5.5 MASS LOSS MEASUREMENTS

5.5.1 Critical Mass Flux

The concept of a critical mass flux at the firepoint was first proposed by Bamford et al. (1946) in a study of the ignition of vertical slabs of wood by direct flame impingement. Koohyar et al. (1968b) reported experimental values of $m"_{cr}$ for vertical samples of wood varying from 1 to $22g/m^2.s$. These results were subsequently analysed by Melinek (1969) who quoted a mean value of $5.1g/m^2.s$. The only available experimental value of $m"_{cr}$ for wood is that of $2.2g/m^2.s$ obtained for white pine by Drysdale and Mazhar (1979). This is consistent with theoretical values deduced by Bamford et al. (1946) ($2.5g/m^2.s$) and by Atreya and Wichman (1986) ($1.8\ g/m^2.s$).

Tewarson and Pion (1976) concluded that sustained burning of thermoplastic materials could not be achieved if the mass flow rate of volatiles was less than a certain critical value ($m"_{cr}$). Tewarson and Pion (1978) subsequently reported values for $m"_{cr}$ for several materials under conditions of "natural" and "forced" convection (Table 5.8). Deepak and Drysdale (1983) reported measured values of

m''_{cr} for horizontal samples of PMMA. Rasbash (1975) derived m''_{cr} values from data on the extinction of fires involving PMMA and POM reported by Magee and Reitz (1974) (vertical samples).

In the present study, mass fluxes at flashpoint (m''_{fl}) and firepoint (m''_{cr}) were measured for horizontal samples of the six plastics identified in Appendix B, using the apparatus described in section 2.2.1. The results are summarised in Table 4.11.

"Flashpoint" was observed as the surface temperature of the sample approached the firepoint condition. This behaviour is comparable with that of combustible liquids: at low levels of heating, several flashes of flame were observed prior to ignition (PX:16 flashes at 13kW/m^2) whereas, at the highest heat flux applied (33kW/m^2), sustained ignition was achieved without any preliminary flashes. Mass flux measurements at the flashpoint were reproducible to within 10% generally and appear to be independent of both radiant intensity and the method by which it was varied ((a) constant heater position/variable temperature or (b) constant heater temperature/variable position).

The mass flux at the firepoint would also appear to be essentially independent, within the limits of experimental error, of both the intensity of radiant flux in the range 13-33kW/m^2 and the method by which it was varied ((a) or (b) above). A statistical analysis of the results largely confirmed this, although, the increase in m''_{cr} with increasing radiant heat flux for polypropylene and polystyrene under method (a) was just significant at the 5% level.

The lack of dependence of m''_{cr} on radiant heat flux for PMMA is in marked contrast to the observed dependence of the firepoint temperature at low heat flux.

Thus, m''_{cr} for PMMA does not decrease at the lowest heat flux as does the measured value of T_{ig} (Table 4.2). This provides strong evidence in favour of the hypothesis that the coalescence of many subsurface bubbles formed during prolonged heating creates a significant increase in the surface area resulting in an enhanced rate of production of volatiles (Section 5.2.3). The results for polyethylene at the two lower heat fluxes had to be discarded because of the large scatter of data. This inconsistency arose from polyethylene's tendency to form a surface char layer which tended to seal the surface and cause the volatiles to break through in an erratic manner, resulting in standard deviations of more than 25%. However, at the highest heat flux ($33kW/m^2$), ignition occured before the char layer became well established. Results for m''_{cr} at this heat flux are fairly reliable and agree satisfactorily with the data for the other two hydrocarbon polymers (PP and PS).

The polymers tested fell into two distinct groups according to their composition. The hydrocarbon polymers (PP,PS and PE) have values of m''_{cr} around $1g/m^2.s$ while those for the oxygenated polymers (FINN,PX and POM) have values close to $2g/m^2.s$. The reproducibility of the experiments was generally within 8-10%. These groupings, which occur in both flashpoint and firepoint mass flux values, are similar to those observed for firepoint temperatures where the hydrocarbon polymers exhibit the higher values (Table 5.1). The lower values of m''_{cr} at these higher firepoint temperatures suggest a significant difference between the properties of the decomposition products of the hydrocarbon polymers and those of the oxygenated polymers. Table 5.7 shows the heats of combustion and volatilisation of the thermoplastics used in this study. ΔH_c values for the hydrocarbon polymers are approximately double those for the oxygenated

polymers.

Table 5.7

Heats of combustion and volatilisation at 25°C

MATERIAL	$-\Delta H_c$ (kJ/g)	L_v (kJ/g)
PMMA	24.89	1.62
POM	15.46	2.43
PP	43.31	2.03
PE	43.28	2.32
PS	39.85	1.76

The stoichiometric concentration for oxygenated fuels is always higher than that for an equivalent hydrocarbon fuel,eg compare methanol, CH_3OH ($189g/m^3$) with methane, CH_4 ($68g/m^3$). Thus a significantly higher flowrate of volatiles from the oxygenated polymer is necessary to achieve the stoichiometric concentration.

Assuming that the firepoint corresponds to a super-stoichiometric concentration at the surface and that the flashpoint relates to the lower flammability limit, then one would expect a relationship between mass flux at the firepoint (m''_{cr}) and that at the flashpoint (m''_{fl}). Zabetakis (1965) has reported that the ratio of the stoichiometric concentration to the lower limit concentration for a range of flammable gases and vapours is approximately 1.8. Table 4.11 indicates that the ratio m''_{cr}/m''_{fl} for the materials tested lies between 1.8 and 2.2 (except for polystyrene).

The values of m''_{cr} reported by Tewarson and Pion (1978) (Table 5.8) for the

materials used in this study under conditions of "natural" convection are approximately twice as great as those reported here (Table 4.11), although a similar grouping of polymer types is observed. The sensitivity of the firepoint temperature to the boundary layer conditions has already been alluded to in the discussion of the effect of sample area on T_{ig}. It is probable that the airflow patterns in Tewarson and Pion's apparatus are completly different from those in the E.U. mass loss apparatus and may, in the case of Tewarson and Pion's experiments, cause flame instability which can only be overcome by increasing the flow of volatiles. This would require higher surface temperatures at the firepoint, but unfortunately, it is not possible to confirm this because Tewarson and Pion did not make surface temperature measurements. However in a limited series of experiments using the E.U. mass loss apparatus, the critical mass flux of volatiles at the firepoint for 19mm square samples of Perspex flush mounted in foil covered Kaowool board and exposed to a radiant heat flux of 34kW/m^2 was found to be 3.2±0.35g/m^2.s. This is consistent with the observed elevation of firepoint temperature when small Perspex samples flush mounted in foil covered Kaowool board were exposed to radiation from both conical heater and laser and provides further evidence for the sensitivity of ignition to boundary layer conditions.

There are several differences between Tewarson and Pions's apparatus and experimental procedure and the present work. Firstly, Tewarson used a sample area of approximately 0.0083m^2, compared with 0.0025m^2 in this study. They placed the samples on a water-cooled load cell assembly mounted inside a silica glass tube on the outside of which there were four coaxially placed tungsten filament heaters (2477K, 1.16μm spectral peak). The pilot source was a small pre-mixed CH_4/air flame approximately 1.0cm above the surface and situated at

the edge of the sample. Their scenario for ignition is shown in Figure 5.5.

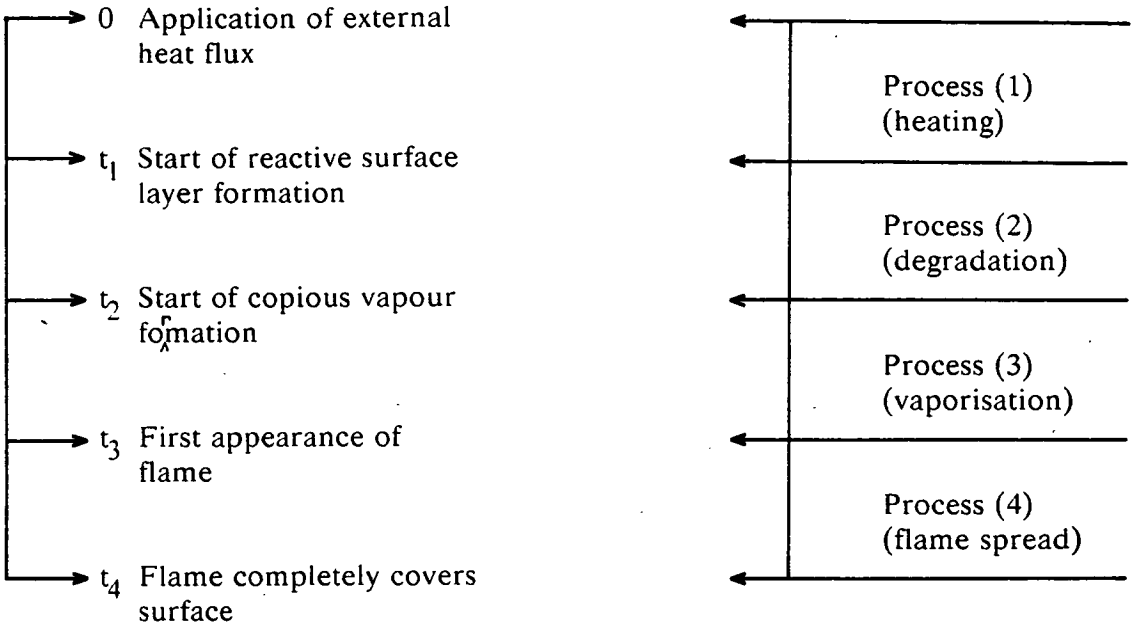

Figure 5.5 Ignition scenario (Tewarson and Pion (1978))

The mass flux at the ignition point is the average mass flux across a fixed surface area. It is the minimum rate of volatilisation, averaged across the surface, that will support flaming and allow the flame to produce sufficient heat to enable it to spread across the surface. The implication of this theory is that m''_{cr}, measured under conditions of piloted ignition, will be dependent on the mass flux profile across the sample surface. This in turn will be influenced by such factors as dilution effects around the periphery of the buoyant plume and non-uniform heating of the sample surface due to heat losses through exposed sample edges. These effects will increase with increasing sample area.

Tewarson and Pion (1978) identify a finite time between "appearance of flame" (t_3) and "flame completely covers surface" (t_4) and their values of critical mass flux at ignition are based on the average value of the mass loss rate during this

time interval (Process (4)). It is possible that a higher mass flux of volatiles was being produced at the centre of the sample than at the edges and that a centrally positioned pilot source would have initiated ignition sooner resulting in lower m''_{cr} values being recorded.

In the E.U. tests with a centrally positioned pilot source, flame was observed to cover the sample surface at the instant of sustained ignition, hence, critical mass flux was determined at a specific discrete time rather than being averaged over a time interval as in Tewarson's experiments. It would appear that the smaller sample area and enclosed sample edges in the E.U. tests resulted in uniform temperature rise across the sample surface and, consequently, an essentially constant volatile release rate over the total exposed area. Additional experiments were carried out in the E.U. rig under a radiant heat flux of 29kW/m^2 using larger samples (100mm x 100mm) of Finnacryl with edges exposed to compare central and edge pilot positions. The pilot source situated in the latter position produced critical mass fluxes around 3.0 g/m^2.s, ie approximately 50% higher than those obtained previously. In addition, a finite time interval was detected between first appearance of sustained flame and total flame cover. With a centrally positioned pilot, little difference was detected from the original E.U. mass loss measurements.

The reasons for the differences between the present results and those of Deepak and Drysdale (1983) are less clear. The experimental configurations were similar, although in Deepak's work, the sample was surrounded by a vertical water-cooled tube. It was not possible to emulate Deepak's apparatus precisely in the E.U. rig but instead the Supalux collar (L in Figure 2.19) was replaced by a short length of water-cooled cylinder (150mm in diameter) resting on the horizontal barrier

shown as "G" in Figure 2.19. Tests carried out on Finnacryl at 30kW/m^2 indicated that m''_{cr} was approximately 30% higher for this configuration. The only explanation for this is that the change in air flow pattern in the vicinity of the surface would affect the heat transfer coefficient.

It is of interest to note that the present values of m''_{cr} for PMMA and POM are similar to the value predicted for wood by Atreya and Wichman (1987). Such agreement would appear quite logical on the basis that wood is also an "oxygenated polymer". In addition, since the flammable volatiles from wood are effectively diluted by carbon dioxide and water vapour, the critical mass flux for wood might be expected to be greater than that for PMMA or POM.

The variation in m''_{cr} results from various sources indicates that the critical mass flux of volatiles at ignition is dependent to a certain extent on experimental parameters. These include such variables as airflow, oxygen concentration, sample orientation and scale. Therefore, while it is relatively easy to measure a critical flowrate, m''_{cr}, for a range of geometrical and aerodynamic conditions, this value has little practical use unless some theoretical framework exists to enable results to be generalised and meaningfully compared. One such framework has been proposed by Rasbash (1975).

5.5.2 Rasbash's Firepoint Equation

Rasbash (1975) suggested that piloted ignition is dependent on a critical flowrate of volatiles and that a critical surface temperature is a secondary consideration.

The Critical Mass Flux, m''_{cr}

Spalding (1955) introduced the concept of the B-number. This dimensionless mass transfer number characterised the rate of burning through the following

relationship (equation 5.8) and was not constant but depended on the conditions under which the material was burned.

$$m'' = \frac{h}{c}\ln(1+B) \qquad (5.8)$$

Rasbash proposed that the definition of a critical mass flux allowed a critical B-number to be defined as

$$m''_{cr} = \frac{h}{c}\ln(1+B_{cr}) \qquad (5.9)$$

The Critical B-Number, B_{cr}

The B-number is defined by A/H_f where $A = m_{O2}.\Delta H_c/r + c(T_o-T_s)$ (basically, the heat of combustion of air) and H_f is heat transfer to the fuel surface by convection from the flame, per unit mass of fuel transported from the fuel to the flame. At the firepoint, H_f becomes H_{fc} where $H_{fc} = \phi\Delta H_c$. Hence,

$$B_{cr} = \frac{A}{\Phi\Delta H_c} \qquad (5.10)$$

Combination of equations 5.9 and 5.10 gives

$$\Phi = \frac{A}{\Delta H_c \exp(m''_{cr}c/h) - 1} \qquad (5.11)$$

The ϕ Factor

Equation 5.11 provides a means by which ϕ (maximum fraction of heat of combustion that the flame reaction zone can lose to the fuel surface by convection, without extinction of the flame) may be determined. This kinetic parameter is inversely related to the critical mass flux and may prove an effective guide to flammability allowing results for different materials and configurations to be generalised and meaningfully compared.

Heat Balance at the Firepoint

Under critical conditions for piloted ignition,

$$S = (\phi \Delta H_c - L_v) m''_{cr} + Q''_{ext} - Q''_{loss} \geq 0 \qquad (5.12)$$

where S is net sensible heat entering the fuel in unit time, Q''_{ext} is heat transfer to the burning fuel surface other than by convection from the flame and Q''_{loss} is heat transfer from the burning fuel surface to the environment. For sustained ignition and flame spread, net heat entering the fuel (S) must equal or exceed zero. Tewarson and Pion (1978) applied Equation 5.11 to their m''_{cr} values and reported ϕ values for several materials (Table 5.8).

Table 5.8

Mass loss results of Tewarson and Pion (1978)

MATERIAL	FORCED CONVECTION		NATURAL CONVECTION	
	m''_{cr} (g/m²s)	ϕ	m''_{cr} (g/m²s)	ϕ
PMMA	4.4	0.28	3.2	0.27
POM	4.5	0.43	3.9	0.45
PP	2.7	0.24	2.2	0.26
PE	2.5	0.27	1.9	0.27
PS	4.0	0.21	3.0	0.21

When this was repeated for the present results using the value of h/c ($10 g/m^2.s$) recommended by Rasbash and applied by Tewarson and Pion, all the ϕ values were higher than the maximum possible value (0.45). Assuming that the use of Equation 5.11 is valid in the present context, and that ϕ must not exceed about 0.45, one or more of the data used in the derivation of ϕ must be incorrect. Since

the numerator of B_{cr} is, effectively, the "heat of combustion of air" and ΔH_c is the heat of combustion of the volatiles, both of which are known with reasonable precision, it would seem probable that the uncertainty lies in the value selected for h/c. Rasbash (1975) based his determination of the average heat transfer coefficient (h) on heat losses by natural convection from a flat horizontal plate. Tewarson and Pion confirmed the same figure ($10g/m^2$) experimentally for "natural" convection. However, Al-Arabi and El-Riedy (1976) reported a significant variation of h for horizontal plates (450mm square) maintained at 100^oC, in which the local value fell from around $10W/m^2.K$ near the edge, passed through a minimum ($4W/m^2.K$) 30mm from the edge and approached a value of $7W/m^2.K$ towards the centre. In the present experiments, the surface approximated to a horizontal plate, measuring 100mm x 120mm, although the airflow pattern close to the surface was influenced by the presence of the cylindrical draught shield around the sample. It is possible that in the present experiments, the heat transfer coefficient near the centre of the sample was considerably less than $10W/m^2.K$. Assuming that this was indeed the case, then adopting an arbitrary value of $h=5W/m^2.K$ and applying Equation 5.11 produces values for ϕ between 0.20 and 0.48 (Table 5.9) for the six materials tested which are much more compatible with Rasbash's hypothesis.

Table 5.9

ϕ values from E.U. Results

SAMPLE	r	ΔH_c (J/g)	T_{ig} (^oC)	m''_{cr} ($g/m^2.s$)	A	ϕ
PX	1.91	24890	310	1.94	2743.3	0.23
FINN	1.91	24890	309	2.02	2744.3	0.22
POM	1.07	15460	282	1.73	3101.5	0.48
PP	3.42	43310	333	1.11	2626.0	0.24
PE	3.43	43280	363	1.31	2594.0	0.20
PS	2.53	39850	364	0.98	3323.0	0.39

Data

$T_o = 17^oC$ $\quad A = m_{O2}.\Delta H_c/r + c(T_o - T_s)$

$h = 5W/m^2.K$ $\quad \phi = A/(\Delta H_c.\exp(m''_{cr}c/h)-1)$

$c = 1J/g.K$

$m_{O2} = 0.233$

Evaluation of ϕ values enables the application of equation 5.12 to predict whether or not a material will achieve sustained burning under a given heat flux.

In view of the observed uncertainties in the measurement of m''_{cr}, it is clear that the only way forward is to gain a better understanding of boundary layer behaviour associated with various sample configurations. This will enable more accurate prediction of the convective heat transfer coefficient and will increase understanding of the process of flame stabilisation at the firepoint. Additional factors which will have to be considered include:

1. The strength of the buoyant plume above the surface which is determined by the temperature of the surface and will influence the rate of dilution of the fuel vapours and, hence, the measured m''_{cr} values.

2. Heat transfer from the nascent flame to the fuel surface which is assumed to be by convection. However, it may not be justifiable to ignore radiative heat transfer if the polymer in question absorbs strongly at wavelengths corresponding to the H_2O and CO_2 emission bands. POM absorbs much more strongly at 10.6μm (one of the principle CO_2 bands) than does PMMA. This would have the effect of reducing m''_{cr}(POM) relative to m''_{cr}(PMMA).

3. Any air movement around the sample would influence the boundary layer, increase the effective heat transfer coefficient and hence, increase m''_{cr}. Comparison of Tewarson and Pion's results for "forced" and "natural" convection show greater values of m''_{cr} for forced convection in which air was flowing vertically round the sample during experiments.

5.5.3 Thermogravimetric Analysis

Thermal analysis studies were carried out on eight materials (PX, FINN, POM, PP, PE, PS,PXFR and PPFR) under normal atmospheric conditions as described in Chapter 2. The repeatability of the method was checked by analysing six PX samples of equal mass and determining the activation energy of degradation (Table 5.10) as described in Appendix E.

Table 5.10

Repeatability of TGA measurements

Perspex

SAMPLE N^0	E_A (kJ/mol) (zone 2)
1	75
2	80
3	79
4	83

5	72
6	70

Mean = 77±5 kJ/mol

There are many methods available for determination of kinetic parameters from TGA data (see Flynn and Wall (1966)), however, in this work the Broido method was used in view of its simplicity of application (Appendix E).

Thermal analysis results showed that for most of the plastics studied, degradation in air proceeded via three distinct zones. Each zone represented the sum of a series of consecutive reactions, the number occuring being dependent on experimental conditions. The activation energies quoted for each zone are overall activation energies relating to the sum of reactions occurring within that zone. The zones were as follows:

1. Initial zone with relatively low degradation rate in which, typically, approximately 10% of the sample was degraded.
2. Intermediate zone with substantially higher activation energies and degradation rates in which, typically, approximately 60-70 % of the sample was degraded.
3. Final zone with activation energies and degradation rates slightly higher than those of the initial zone.

Unfortunately, due to the relatively small number and limited nature of experiments carried out, it is not possible to comment more specifically on the nature of the reactions occurring in these zones. However, work by Kashiwagi et al. (1985) on the degradation of PMMA indicates that multiple reaction stages in the decomposition of commercial PMMA are caused by impurities. When the samples are purified by reprecipitation from methylene chloride solution, only

one reaction zone is observed during decomposition. This suggests that thermal oxidative degradation may be considerably affected by small concentrations of impurities (eg unreacted initiator and monomer, plasticiser, uv absorber etc.).

Comparison of activation energies determined for the commercial grades of plastics used in this study shows considerable variation between plastics. However, on the basis of the present results, it is not possible to determine the extent to which this variation is attributable to structure and the extent to which it is attributable to presence of various impurities. E_A for the fire retarded modifications is higher in all zones than E_A for the unmodified parent polymer, although, the difference is greater for polymethylmethacrylate than for polypropylene. Standard polypropylene and polyethylene have similar activation energies which are considerably lower than those of PX, FINN, POM and PS. In general, no apparent correlations were found between structure and thermal analysis results in air. In retrospect, it would have been useful to repeat the thermal analysis measurements with a nitrogen atmosphere in place of air since thermal degradation appears to be considerably less influenced by sample impurities than does thermal oxidative degradation. Unfortunately, this was prevented by lack of time and facilities.

5.6 FIRE RETARDANCY

5.6.1 Ease of Ignition

Several material properties may be identified as influencing ease of ignition. For example, a material will be difficult to ignite if the heat of volatilisation is high and the heat of combustion is small or if the thermal inertia is high. Figure 5.6 shows the cycle for sustained ignition and indicates that the attainment of steady

burning depends on processes 1 to 4.

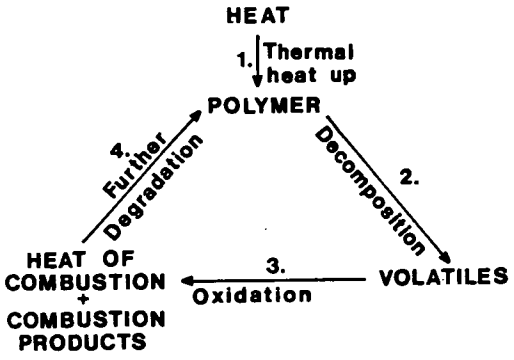

Figure 5.6 Combustion cycle

"Flammability" is frequently expressed in terms of the limiting oxygen index, which is the minimum percentage of oxygen in the surrounding atmosphere that will just support flaming combustion of a material in a candle-like orientation. The LOI test was carried out on the materials used in this study and results proved to be reliable and reproducible as shown by Table 4.13.

The importance of thermal degradation in relation to polymer flammability was assessed by seeking correlations between limiting oxygen index values and factors relating to thermal decomposition of polymers. Thermal stability of a material is frequently expressed in terms of temperature at which onset of degradation occurs (T_D), but in practice, this is often difficult to determine from TGA curves. A more convenient determination is the temperature at which a given small percentage (eg 5%) of the material has decomposed. This temperature ($T_{5\%}$) is much less sensitive to changes in rate of heating and sample size (Cullis and Hirschler (1983)). There is apparently a limited correlation between this criterion of polymer stability (data from TGA experiments) and limiting oxygen index of the polymer (see Table 5.11) although the correlation will be affected by the extent to which oxygen is involved during thermal decomposition of the various polymers.

Table 5.11

Comparison of $T_{5\%}$ degradation temperature and LOI

MATERIAL	$T_{5\%}$ (^{o}C)	LOI (%)
POM	263	15.3
FINN	277	17.3
PP	288	17.3
PX	293	17.8
PE	307	17.4
PS	320	17.9

On this basis, a correlation between heat of volatilisation and LOI would be predicted. However, Table 5.12 shows no such correlation.

Table 5.12

Comparison of heat of volatilisation and LOI

MATERIAL	L_v (kJ/g)[1]	LOI
PX	1.62	17.8
FINN	1.62	17.3
PS	1.76	17.9
PP	2.03	17.3
PE	2.32	17.4
POM	2.43	15.3

1 Results of Tewarson and Pion (1978)

Thus, it would appear that while very high thermal stability imparts a certain degree of resistance to combustion, there is little correlation generally between ease of polymer decomposition and the ease with which a polymer ignites and burns. This is indicative of the complexity of the combustion process of organic polymers.

5.6.2 Commercial Fire Retardants

An obvious way to produce a polymer resistant to fire is to design it initially so that it has a very high resistance to thermal decomposition. Thus, the combustion cycle (Figure 5.6) will be hindered at stage 2 and the burning process will not become self-sustaining. Unfortunately, the results of attempts to design inherently stable, non-flammable polymers tend to be expensive to produce and lack the desired physical properties for processability.

In practice, the solution to the problem of polymer flammability does not lie in the development of new, thermally stable polymers, rather it is in the modification of existing common polymers so that they exhibit satisfactory performance upon exposure to fire. Fire retardants can be divided into two types: (i) **reactives**, which are chemically bound to the substrate during polymerisation in a separate step and (ii) **additives**, which are blended with the substrate during manufacture. The three fire retardant systems investigated in this study fall into the latter group. Fire retardants act by interfering with one or more stages in the combustion cycle by either (i) increasing the thermal capacity and acting as a "heat sink" (eg hydrated alumina in polyesters); (ii) altering the decomposition mode of the solid to promote char formation and formation of low flammability volatiles (eg phosphates on wood); (iii) releasing chemical species into the the volatiles which inhibit gas phase reactions (eg halogenated compounds in hydrocarbons) or (iv)

providing a protective layer on the exposed surface (eg intumescent paint on wood).

In the present work, three plastics were compared with their fire-retardant modifications (Figure 5.7) on the basis of ignition delay time, firepoint temperature, critical mass flux at ignition and limiting oxygen index.

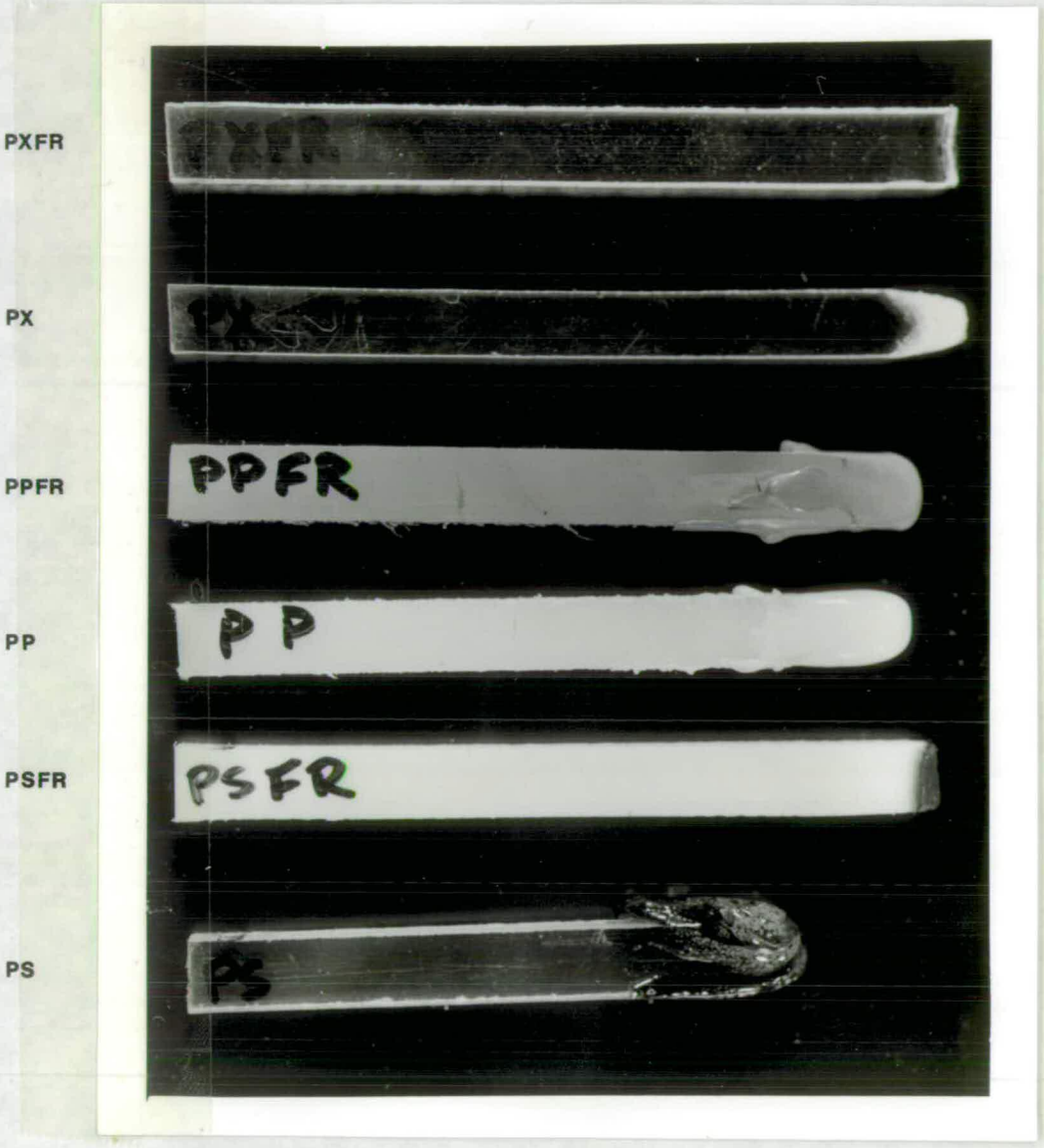

Figure 5.7 Samples exposed to butane flame for 120 seconds

The materials are listed in Table 5.13 together with the available information on the nature of the fire-retardant system.

Table 5.13

Fire Retardant Modifications

MATERIAL	IDENTIFIER	ORIGIN	RETARDANT
Polymethyl-methacrylate (Perspex FR)	PXFR	ICI	Chlorinated organo-phosphorus cmpd. 15%P, 27%Cl
Polypropylene (PPs)	PPFR	Simmona	Organic bromine + antimony trioxide
Polystyrene (Styron)	PSFR	Dow Chemicals	Organic bromine + antimony trioxide

Antimony appears relatively ineffective when used in isolation as a fire retardant. Antimony trioxide melts at 1550^{o}C, a temperature too high to render it an effective fluxing agent in the manner of phosphorus and hence, it is principally used as a synergist with the halogens (Hilado (1982)). The synergistic relationship between antimony oxides and halogen compounds has been extensively researched (see Gann, Dipert and Drews (1986)). The initial studies were primarily concerned with determining optimum antimony oxide to halogen and antimony oxide/halogen to polymer ratios for specific flame retardant applications. This combination has been used successfully for a range of polymer substrates such as cellulosics, PE,PP,PS and epoxies which all have different decomposition mechanisms. The efficiency of this system is dependent on flame inhibiting reactions occuring in the vapour phase and hence, is directly related to the volatilisation of antimony as oxyhalide or trihalide. Therefore, the flame retardancy effect should be independent of polymer substrate. For organohalogen compounds which undergo intramolecular dehydrohalogenation, the principal

route to the generation of volatile antimony containing species has been proposed as

$$R\text{-}CH_2\text{-}CHX\text{-}R \text{ --------> } R\text{-}CH{=}CH\text{-}R + HX$$

$$6HX + Sb_2O_3 \text{ --------> } 2SbX_3 + 3H_2O$$

Phosphorus based flame retardants can be active in condensed or vapour phase or operate by both mechanisms simultaneously. Condensed phase activity for phosphorus containing flame retardants has been reported for PET, rigid polyurethane foams and PMMA (Kuryla and Papa (1975), Avondo, Vovelle and Delbourgo (1978), Brauman (1980)), as well as for cellulosics. In all cases, flammable gas generation was reduced and char formation enhanced.

In general, data for haloalkyl/phosphorus systems suggest that halogen and phosphorus act independently (Benbow and Cullis (1975), Avondo, Vovelle and Delbourgo (1978)). Upon heating, the phosphorus containing compounds decompose to yield phosphorus acids and non volatile derivatives which must exert their main flame retardancy effects on the solid state chemistry. The volatile halogen containing fragments are vapour phase active and must account for retardancy effects observed in the flame chemistry.

Limiting oxygen index can show whether fire retarding additives act primarily in the condensed phase or in the gas phase (Fenimore and Jones(1966)). If an additive interferes with polymer decomposition, ie condensed phase, then its effect should be independent of the nature of the supporting gaseous oxidant although it would be expected to change with substrate structure. However, if the additive affects flame reactions, its influence will depend upon the oxidising atmosphere (eg replacement of O_2 by N_2O), but will be essentially independent

of the nature of the polymer.

Table 5.14 shows the percentage increase in LOI and firepoint temperature and the averaged percentage increase in ignition delay time (data from Tables 4.14 and 4.15) achieved when the flame retardant systems listed in Table 5.13 are present.

Table 5.14

% increase in LOI, t_{ig} and T_{ig} caused by fire retardants

PROPERTY	PX/PXFR	PP/PPFR	PS/PSFR
LOI	24%	77%	56%
t_{ig}	203%	135%	105%
T_{ig}	20%	20%	19%

Comparison of percentage increases in firepoint temperature and ignition delay time indicates that the degree of retardancy achieved in polypropylene and polystyrene is more or less equivalent for the two fire retardant systems. For polymethylmethacrylate, although the percentage increase in firepoint temperature is comparable to that of polystyrene and polypropylene, the average percentage increase in ignition delay time is considerably greater. The percentage increase in LOI for the three plastics shows substantial variation. It may be deduced from these figures that the organic bromine/antimony system present in both PPFR and PSFR acts predominantly in the vapour phase (substantial effect on LOI) by inhibiting flame reaction. The greater percentage increase in LOI for PPFR (77%) over PSFR (56%) is probably attributable to the observation that PPFR tended to melt, flow and drip much more readily than the parent polymer.

In the candle like orientation of the oxygen index test, this provides an effective mode of heat loss from the area of polymer exposed to the flame, thus inhibiting flame stabilisation (M^{c}Ilhagger and Hill (1987)). This effect was not observed for PSFR.

The chlorinated organophosphorus compound present in PXFR causes a percentage increase in LOI of only 24%. Since the overall retardancy achieved by this compound on the basis of increase in T_{ig} and t_{ig} is apparently as great as if not greater than the retardancy achieved by the bromine/antimony systems discussed previously, it would appear that vapour phase reactions contribute only in part to the total flame retardancy effect of chlorinated organophosphorus compounds. In addition, condensed phase reactions must play a significant role. This supposition is supported by the observation of char formation in PXFR which does not occur in standard PX.

The firepoint temperatures of the flame retarded grades are approximately 60-80^{0}C higher than the unmodified parent material which is consistent with the observation that higher heat fluxes are necessary before these materials will ignite and burn. It is possible that the degree of retardancy imparted by a particular treatment could be assessed on the basis of resultant increase in firepoint temperature rather than on the oxygen index test which is currently used for this purpose. Obviously, more data are required to test this hypothesis.

Firepoint temperature, in isolation, does not give any information about mode of action of the retardant. However, the firepoint equation (Rasbash (1975)) discussed in Section 5.5.2 indicates that critical mass flux is dependent on heat of combustion and reactivity of the volatiles. Table 4.15 shows that a significant

difference exists between the critical mass fluxes at firepoint for each plastic and its fire retarded modification. The difference of a factor of at least two between the values of m''_{cr} for modified and unmodified polymer suggests that the properties of the volatiles have been affected.

Gas phase active fire retardants achieve their effect by releasing species which inhibit gas phase reactions. Such species reduce the rate of reaction which causes a decrease in rate of heat release. Consequently, less cooling is required to quench the flame and as a result, lower values of ϕ (the maximum fraction of the heat of combustion that the flame reaction zone can lose to the fuel surface by convection without extinction of the flame) would be expected.

Application of equation 5.11 ($\phi = A/(\Delta H_c(\exp(m''_{cr}c/h)-1))$) provides a means of calculating ϕ for the three fire retarded plastics studied. Unfortunately, little data are available on the heats of combustion of fire retarded plastics and so ΔH_c values for the parent unmodified plastics have been used in this calculation. Critical mass flux and firepoint temperature at the highest heat fluxes considered in this study were used to calculate ϕ. The values thus obtained were considerably lower than for the equivalent unmodified parent plastics (Table 5.15).

Table 5.15

ϕ values for unmodified and fire retarded plastics

MATERIAL	Φ VALUE	
	Unmodified	Fire retarded
Polymethylmethacrylate	0.23	0.06
Polypropylene	0.22	0.06
Polystyrene	0.42	0.04

Thus, if accurate data on heats of combustion and stoichiometric ratios for fire retarded materials were available, m''_{cr} values enabling the calculation of ϕ values could be considered as a possible means of comparing effectiveness of different fire retardant treatments.

CHAPTER 6

CONCLUSIONS

AND SUGGESTIONS FOR FURTHER WORK

CHAPTER 6
CONCLUSIONS AND FURTHER WORK

6.1 CONCLUSIONS

6.1.1 Surface Temperature

Although there are experimental difficulties associated with the measurement of the surface temperature of combustible polymers, values of T_{ig} can be obtained with reasonable precision by use of very fine thermocouples and careful technique.

There appears to be little dependence of T_{ig} on intensity of radiant heat flux other than a slight increase in T_{ig} with increasing heat flux for a few of the materials tested. An exception, however, was noted in the case of PMMA (all brands) which showed a significant decrease in T_{ig} at the lowest heat flux used ($13kW/m^2$). This was attributed to the pronounced bubble formation at depth observed in PMMA after long heating times, resulting in an effective increase in surface area for the degradation process. This would enable the super-stoichiometric volatile concentration required for ignition to be achieved more rapidly than when degradation was confined to a thin surface layer. The above observation was given further credence by the mass loss experiments on PMMA which showed no equivalent dependence of m''_{cr} on level of incident irradiation. In addition, the theoretical firepoint temperature obtained from the heat transfer computer model on the basis of experimental ignition delay time was in good agreement with the measured value for an incident heat flux of $13kW/m^2$.

Limited experiments on Perspex and polypropylene, where the spectral characteristics of the source were varied, have shown that within the scatter of

results, firepoint temperature is independent of the spectral distribution of the source. However, a dependency of T_{ig} on area of ignition when the area exposed does not exceed approximately $4cm^2$ was detected. This implies that the stabilisation of flame, corresponding to attainment of the firepoint condition, is very sensitive to the surrounding flow field. Thus, it is to be expected that measured firepoint temperatures will be affected by factors such as sample orientation and induced airflow.

While the definition of piloted ignition by a critical surface temperature is by no means totally realistic, it is a useful concept for application to simple predictions of piloted ignition of "standard" materials under specific experimental conditions. Thus, for a horizontal sample of a material with an area of exposure in excess of approximately $4cm^2$ which neither bubbles, chars nor deforms and whose degradation products are generated exclusively from a thin surface layer, it is reasonable to assume that piloted ignition will occur when the sample surface attains some specific temperature irrespective of intensity or nature of incident irradiation.

Firepoint temperature measurement, per se, is not a particularly useful parameter in the classification of materials on the basis of fire hazard because there is no relationship between "ease of ignition" and firepoint temperature. However, development of increasingly sophisticated computer models for ignition has made accurate determination of surface temperature for a range of materials very neccessary for heat transfer calculations. In addition, it seems possible that increase in measured firepoint temperature could be used as a means of assessing the efficiency of various concentrations of fire retardants in plastics rather than the limiting oxygen index test used at present.

6.1.2 Ignition Delay Time

Ignition delay time is considerably more sensitive to a variety of material and environmental parameters than is firepoint temperature. These parameters include intensity and spectral distribution of the imposed radiative heat flux, thermal inertia of the fuel and any factors affecting the sample boundary conditions which determine heat loss. Thus, time to ignition is dependent on both sample area and thickness, and for low heat fluxes with correspondingly long ignition delay times (or for thin samples) where the sample has ceased to be thermally thick, nature of the sample backing board is significant.

Times to ignition proved sensitive to the relationship between spectral distribution of the source and the absorption spectrum of the "target". Significant effects on ignition delay time have been observed over the range of source temperatures from 400-800^{o}C. These results suggest that radiation from the hot layer at ceiling level in a compartment fire will cause ignition of neighbouring materials significantly faster than would an equivalent level of radiation from a diffusion flame. Understanding of this source/sample interrelationship is relevant not only to improving theoretical predictions of ignition but also to meaningful interpretation of the results of standard fire tests which utilise a variety of radiant sources.

6.1.3 Small Scale Fire Tests

Many of the fire tests currently in use are based on the determination of such parameters as ignition delay time, critical incident heat flux and flame spread rate for small samples under a fixed set of experimental conditions. The problems of scaling up the results of these tests has already been alluded to in Chapter 1. However, further problems arise in that various tests purporting to measure the

same parameter, frequently produce widely varying results. The present work has attempted to identify potential inconsistencies in these tests.

Generally, if a material is to be given a pass/fail rating or if minimum conditions for ignition are to be determined, then the low heat flux/long heating time situation is being considered. Under these conditions, it is probable that the samples will have ceased to be thermally thick before the end of the test and thus, factors such as sample thickness and nature of backing material will influence the results. Therefore, it is important that materials are able to be tested in such a form as to be representative of their end use assembly in terms of thickness, adhesives and backing materials used, etc.

Most tests examine materials in one fixed orientation, generally either vertical or horizontal, but there are few facilities within any single test to compare various orientations. Many materials melt and drip extensively in the vertical orientation. Initially, this may have a beneficial effect in the fire situation in that the flow of hot molten material away from the source of heat provides an effective mode of heat dispersal. Latterly, however, after ignition has occurred, the tendency to melt and drip will result in droplets of molten material falling onto items not previously involved in the fire. Thus, a material selected for use in the vertical orientation on the basis of its performance in a small scale horizontal test could prove to be considerably more hazardous than predicted. The ideal test would allow materials to be positioned in any orientation thus, emulating all material usages from floor covering to ceiling panel. The closest approach to this ideal at present is the cone calorimeter test (Babrauskas and Parker (1987)) designed to be usable with vertical or horizontal samples. An additional advantage of the cone calorimeter is that it allows simultaneous measurements of ignition delay time,

heat release, mass loss and smoke within one test which provides an element of uniformity across a range of results.

The ISO ignitability test is used to determine ignition delay time of horizontal samples only, at a range of radiant heat fluxes from 10-50kW/m^2. The sample baseboard is required to have an oven dry density of 825±125kg/m^3 and a nominal thickness of 6mm. The radiant heat flux is varied by adjusting the temperature of a fixed position radiant heater between approximately 400^{o}C and 1000^{o}C. This has the effect of altering the spectral distribution of the source considerably between the highest and lowest heat fluxes. Thus substantial variations in sample absorption/source emission interactions are observed over the range of heat fluxes considered.

In the well developed real fire situation, radiation from the soot tends to dominate and for such grey body radiation, the temperature will typically be in the vicinity of 1000^{o}C. Hence, a radiant electrical heater at a temperature of 1000^{o}C produces a similar spectral output to that produced by the well developed fire. Therefore, it would seem logical in the test situation to represent real fire conditions as closely as possible by maintaining the electrical heater at a fixed temperature of 1000^{o}C and varying the radiant heat flux by adjusting the heater position.

The observed variation in ignition delay times between the E.U. apparatus and the ISO ignitability apparatus illustrates one of the major problems of small scale testing, namely reproducibility of results between tests. This emphasises the need for a sound understanding of the processes involved in ignition and the factors which affect these processes before the results of small scale tests can be

interpreted meaningfully. Current developments in our understanding of fire dynamics suggest that ultimately, it should be possible to assess fire hazard of materials by means of standard detailed theoretical models. These models would utilise measured fundamental material properties and the problem of inter-test variations would be circumvented.

6.1.4 Mass Loss Experiments

The critical flowrate of fuel volatiles from horizontal samples of nine thermoplastics have been determined under both constant heater temperature/variable position and variable heater temperature/constant position regimes. It has been shown that the values derived are essentially independent of the nature of the spectral output but that they are sensitive to the boundary layer conditions existing at the surface. This is consistent with the observation that firepoint temperature is sensitive to boundary layer conditions since an increase in surface temperature corresponds to an increase in mass flux. This is illustrated by comparison of T_{ig} and m''_{cr} values for fire retarded and equivalent unmodified plastics.

Measurement of critical mass fluxes is not easy. The system is very susceptible to external vibration and buoyancy induced air movement and so smooth mass loss-time curves are not readily obtained. Calculation of rate of mass loss requires determination of the gradient of the mass loss-time curve at a particular time. For the unmodified materials which produced regular cubic type curves, this was achieved by means of a computerised curve fitting routine and subsequent differentiation to obtain m''_{cr} at t_{ig}. For the fire retarded plastics, further inaccuracies were introduced because the mass loss-time curves were too irregular to be approximated to cubic expressions and so gradients were calculated

manually by eye.

In spite of the difficulties encountered, results reproducible to within 10% were obtained for critical mass flux at both flashpoint and firepoint. A difference of approximately two exists between the present results and those of Tewarson and Pion (1978). It is proposed that this is due to the difference in boundary layer conditions existing at the surface in the two sets of apparatus. It will, thus, be necessary to derive accurate values for the convective heat transfer coefficient at the surface in order to enable the ignition condition to be analysed in detail.

The "firepoint equation" (Rasbash (1975)) appears to provide a necessary framework to enable mass loss data on materials obtained in various experimental rigs to be meaningfully compared. ϕ appears to be a useful indicator of the propensity of a material to achieve sustained burning. It is observed that ϕ values for fire retarded plastics are considerably lower than those of their unmodified equivalents.

The present results indicate that while a certain minimum surface temperature is a necessary requirement for piloted ignition, this is probably merely a function of the minimum conditions required to produce the critical volatile concentration for establishment of flame. Thus, it is proposed that critical mass flux provides a more rigorous definition for piloted ignition than does critical firepoint temperature.

The results of thermogravimetric analysis proved inconclusive mainly because there was insufficient time available to study the plastics involved in detail under a variety of experimental conditions. More useful information would have been provided by examining degradation under a variety of heating rates and under

conditions of isothermal heating. A nitrogen atmosphere or, alternatively, purification of the samples would have provided data less dependent on the nature of the impurities present in the samples

6.1.5 Theoretical model

The theoretical model used in this work was based on the numerical solution of simple heat transfer equations and the criterion of critical firepoint temperature to define ignition. Reasonable accuracy in theoretical predictions was obtained over the range of heat fluxes by application of the final version (modification 2) of the model which allowed the effect of variation in heater temperature to be considered. It is expected that more accurate predictions would be obtained if the effect of degradation processes was included in the model. Initially, it was hoped to achieve this by combining mass loss and surface temperature data. However, this did not prove feasible since the agreement between times to ignition in the two experimental rigs was poor.

6.2 SUGGESTIONS FOR FURTHER WORK

(1) Improved knowledge of boundary layer behaviour and the ability to derive accurate values for the convective heat transfer coefficient would enable more meaningful interpretation of ignition data and would permit accurate application of the firepoint equation (Rasbash (1975)). The effect of boundary layer conditions on ignition should be further investigated by examination of the ignition of samples in orientations other than horizontal and by consideration of the effect of substantial induced airflow on ignition.

(2) The present study utilised relatively low level radiant heat fluxes. The effect of substantially higher radiant heat fluxes on the parameters measured in this

work should be considered. Radiant heat fluxes in excess of 150kW/m^2 (more representative of real fire conditions) are envisaged. It would also be of interest to repeat the present measurements of T_{ig} and m''_{cr} using a convective heat source rather than a radiant source.

(3) Development of a data logging system in conjunction with the present experimental techniques would enable the simultaneous collection and processing of data. A multi-input computerised system would allow more channels to be monitored than are at present by the chart recorder system. Thus, a greater range of information could be obtained with higher accuracy than is obtained by manual processing of chart recorder outputs.

(4) The theoretical model could be improved by incorporation of degradation effects which would require the simultaneous measurement of surface temperature and rate of mass loss from t_0 to t_{ig}. Adaptation of the model to apply critical mass flux as the criterion for ignition would make the model more applicable to non-standard materials.

(5) It is hoped to broaden the current data base of ignition properties by measurement of firepoint temperatures and critical mass fluxes of a variety of foamed and cellulosic materials.

APPENDICES

APPENDIX A - GLOSSARY

APPENDIX B - MATERIALS USED

APPENDIX C - RADIATION FUNCTIONS

APPENDIX D - COMPUTER PROGRAMS

APPENDIX E - KINETIC PARAMETERS FROM TGA

APPENDIX F - PUBLICATIONS ARISING FROM WORK

APPENDIX G - REFERENCES

APPENDIX A
GLOSSARY

Critical mass flux is the minimum flow rate of volatiles at the point of ignition required to support sustained burning.

Firepoint is the limiting condition for establishment of flame at the surface of a combustible liquid or solid expressed as a bulk or surface temperature, respectively.

Flashover is that point in a compartment fire at which a localised fire spreads very rapidly to involve all combustible materials in the conflagration.

Flashpoint is the minimum bulk or surface temperature of liquid or solid fuels, respectively, at which the vapour/air mixture at the surface is flammable.

Flashing ignition refers to the period between attainment of flashpoint and firepoint and describes the intermittent bursts of flame observed at the surface during this time.

Ignition is the initiation of the self-sustaining combustion process.

Ignition delay time is the time interval between initial exposure to heat source and ignition.

Piloted ignition requires that the mixture of fuel vapours and air in the vicinity of the fuel surface is within the flammability limits and that an independent source of heat (such as pilot flame, spark, electrically heated filament) is available to initiate combustion.

Spontaneous ignition occurs when the flammable volatile/air mixture in addition

to being within the flammability limits, is also in such a condition as to automatically react in an accelerating exothermic manner to yield a flame without the aid of a pilot source. Much higher temperatures are required for spontaneous ignition to occur: Surface temperatures in excess of 400-500^{o}C are likely.

Sustained flaming ignition is that in which the flaming extends beyond termination of exposure and results in more or less complete consumption of the fuel.

Transient flaming ignition may be defined as that ignition (piloted or spontaneous) in which flames promptly self-extinguish when the external heat source is removed.

APPENDIX B
MATERIALS USED IN PROJECT

Generic name: Polymethylmethacrylate

Trade name: PERSPEX

Identifier: PX

Manufacturer: Imperial Chemical Industries

Supplier: Amari Plastics, Glasgow

Thermal conductivity: 0.17W/m.K

Specific heat capacity: 1.5J/g.K

Density: $1.18 \times 10^6 g/m^3$

Structure

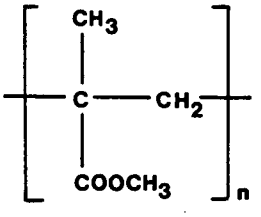

IR absorption spectrum

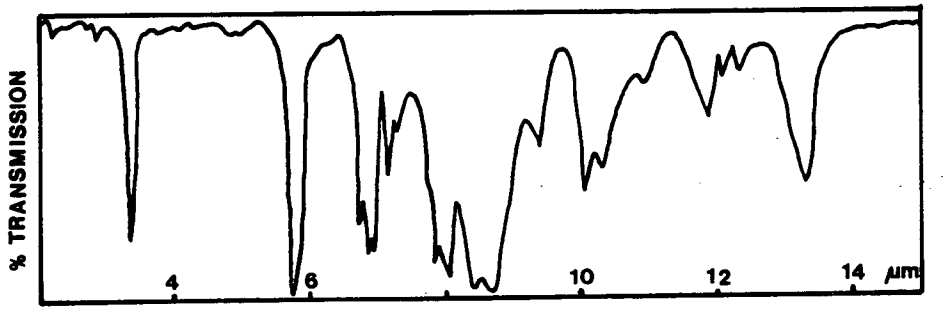

Generic name: Polymethylmethacrylate

Trade name: FINNACRYL

Identifier: FINN

Manufacturer: Lohja Corporation, Finland

Supplier: Easter Road Plastics, Edinburgh

Thermal conductivity: 0.21W/m.K

Specific heat capacity: 1.46J/g.K

Density: $1.19 \times 10^6 g/m^3$

Structure

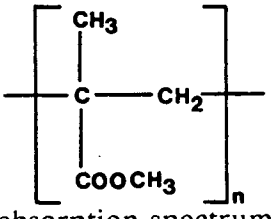

IR absorption spectrum

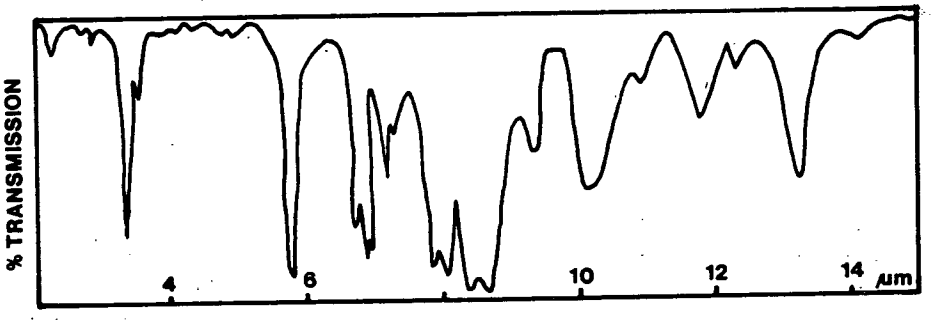

Generic name: Polyoxymethylene

Trade name: DELRIN

Identifier: POM

Manufacturer: Dupont

Supplier: G.H. Bloore Ltd., Manchester

Thermal conductivity: 0.37W/m.K

Specific heat capacity: 1.47J/g.K

Density: $1.42 \times 10^6 g/m^3$

Structure

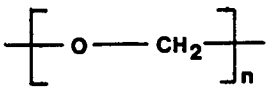

IR absorption spectrum

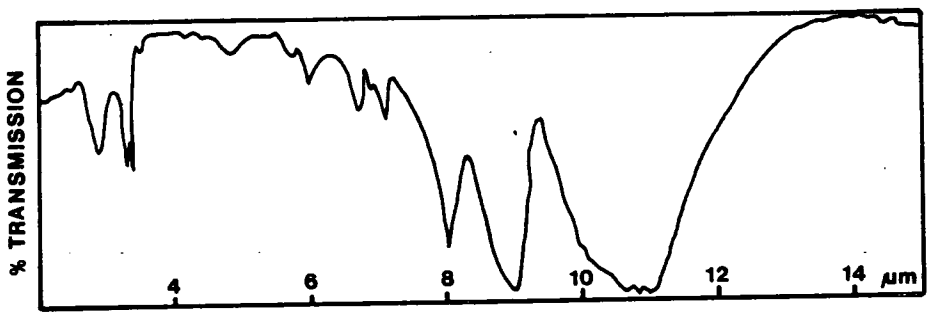

Generic name: Polyethylene

Trade name: POLYTHENE

Identifier: PE

Manufacturer: Courtalds Acetate P.L.C.

Supplier: G.H. Bloore Ltd., Manchester

Thermal conductivity: 0.33W/m.K

Specific heat capacity: 2.1J/g.K

Density: $9.2 \times 10^5 g/m^3$

Structure

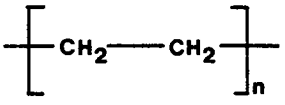

IR absorption spectrum

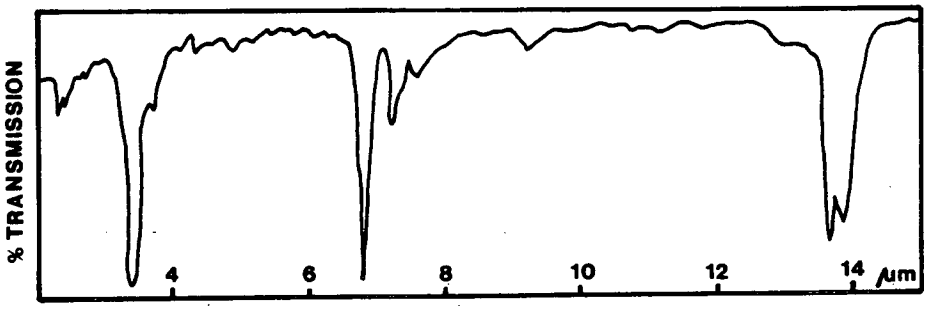

Generic name: Polypropylene

Trade name: POLYPROPYLENE

Identifier: PP

Manufacturer: Courtalds Acetate P.L.C.

Supplier: G.H. Bloore Ltd., Manchester

Thermal conductivity: 0.21W/m.K

Specific heat capacity: 1.93J/g.K

Density: $9.05 \times 10^5 g/m^3$

Structure

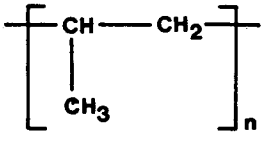

IR absorption spectrum

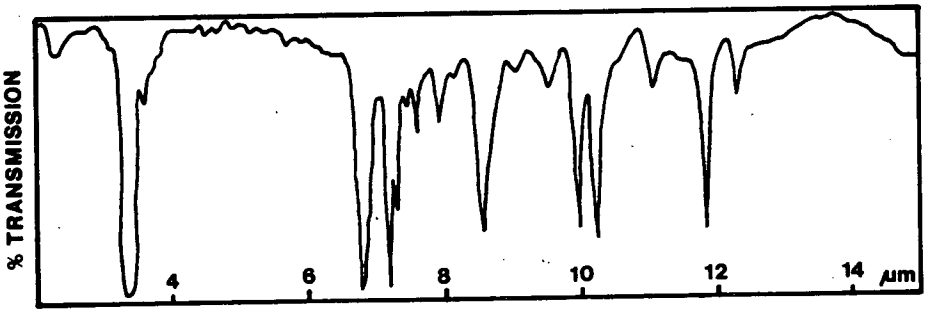

Generic name: Polystyrene

Trade name: HYALITE

Identifier: PS

Manufacturer: BASF

Supplier: G.H. Bloore Ltd., Manchester

Thermal conductivity: 0.12W/m.K

Specific heat capacity: 1.34J/g.K

Density: $1.04 \times 10^6 g/m^3$

Structure

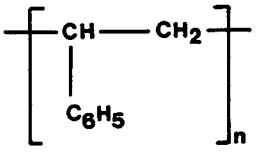

IR absorption spectrum

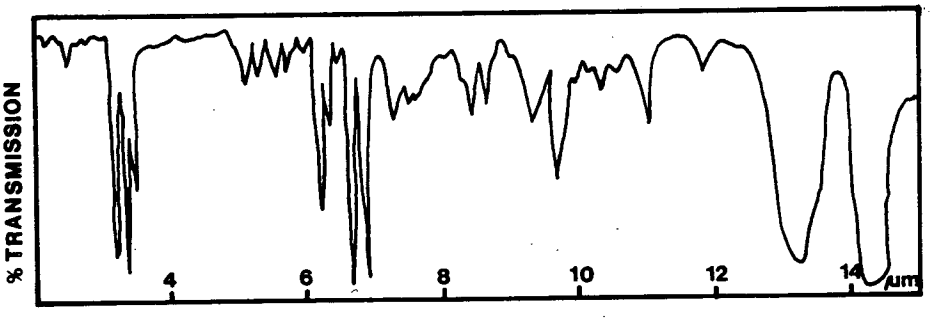

Fire Retarded Modifications

Generic name: Fire retardant polymethylmethacrylate

Trade name: PERSPEX FR

Identifier: PXFR

Manufacturer: Imperial Chemical Industries

Supplier: Amari Plastics, Glasgow

Fire retardant system: Chlorinated organophosphorus compound (15%P, 27%Cl)

Generic name: Fire retarded polypropylene

Trade name: PPs

Identifier: PPFR

Manufacturer: Simmona, West Germany

Supplier: Easter Road Plastics, Edinburgh

Fire retardant system: Organic bromine and antimony trioxide

Generic name: Fire retarded polystyrene

Trade name: STYRON

Identifier: PSFR

Manufacturer: Dow Chemicals, Switzerland

Supplier: Dow Chemicals

Fire retardant system: Organic bromine and antimony trioxide

APPENDIX C
RADIATION FUNCTIONS

*

λT	$\frac{E_{\lambda b} \times 10^5}{\sigma T^5}$	$\frac{E_{b(0-\lambda T)}}{\sigma T^4}$	λT	$\frac{E_{\lambda b} \times 10^5}{\sigma T^5}$	$\frac{E_{b(0-\lambda T)}}{\sigma T^4}$	λT	$\frac{E_{\lambda b} \times 10^5}{\sigma T^5}$	$\frac{E_{b(0-\lambda T)}}{\sigma T^4}$
1000	.0000394	0	7200	10.089	.4809	13400	2.714	.8317
1200	.001184	0	7400	9.723	.5007	13600	2.605	.8370
1400	.01194	0	7600	9.357	.5199	13800	2.502	.8421
1600	.0618	.0001	7800	8.997	.5381	14000	2.416	.8470
1800	.2070	.0003	8000	8.642	.5558	14200	2.309	.8517
2000	.5151	.0009	8200	8.293	.5727	14400	2.219	.8563
2200	1.0384	.0025	8400	7.954	.5890	14600	2.134	.8606
2400	1.791	.0053	8600	7.624	.6045	14800	2.052	.8648
2600	2.753	.0098	8800	7.304	.6195	15000	1.972	.8688
2800	3.872	.0164	9000	6.995	.6337	16000	1.633	.8868
3000	5.081	.0254	9200	6.697	.6474	17000	1.360	.9017
3200	6.312	.0368	9400	6.411	.6606	18000	1.140	.9142
3400	7.506	.0506	9600	6.136	.6731	19000	.962	.9247
3600	8.613	.0667	9800	5.872	.6851	20000	.817	.9335
3800	9.601	.0850	10000	5.619	.6966	21000	.702	.9411
4000	10.450	.1051	10200	5.378	.7076	22000	.599	.9475
4200	11.151	.1267	10400	5.146	.7181	23000	.516	.9531
4400	11.704	.1496	10600	4.925	.7282	24000	.448	.9589
4600	12.114	.1734	10800	4.714	.7378	25000	.390	.9621
4800	12.392	.1979	11000	4.512	.7474	26000	.341	.9657
5000	12.556	.2229	11200	4.320	.7559	27000	.300	.9689
5200	12.607	.2481	11400	4.137	.7643	28000	.265	.9718
5400	12.571	.2733	11600	3.962	.7724	29000	.234	.9742
5600	12.458	.2983	11800	3.795	.7802	30000	.208	$.976_5$
5800	12.282	.3230	12000	3.637	.7876	40000	.0741	$.988_1$
6000	12.053	.3474	12200	3.485	.7947	50000	.0326	$.994_1$
6200	11.783	.3712	12400	3.341	.8015	60000	.0165	$.996_3$
6400	11.480	.3945	12600	3.203	.8081	70000	.0092	$.998_1$
6600	11.152	.4171	12800	3.071	.8144	80000	.0055	$.998_7$
6800	10.808	.4391	13000	2.947	.8204	90000	.0035	$.999_0$
7000	10.451	.4604	13200	2.827	.8262	100000	.0023	$.999_2$
						∞	0	1.000_0

* From Dunkle (1954)

APPENDIX D
COMPUTER PROGRAMS

Key to Variables

AB	Surface absorptivity
ALF	Thermal diffusivity
CAP	Specific heat capacity
CND	Thermal conductivity
DT	Timestep duration
DX	Element thickness
EM	Emissivity
EX	Experimental ignition delay time
FO	Fourier number
FPT	Experimental firepoint temperature
H	Convective heat transfer coefficient
I	Number of elements in slab
J	Number of timesteps corresponding to ignition
K	Timestep

LCV	Convective heat losses
LR	Radiative heat losses
N	Element
Q	Incident radiant heat flux
RHO	Density
SIG	Stefan–Boltzmann constant
T	Temperature
TIM	Time
VAR	% variation
ZO	Ambient temperature

BASIC MODEL

The basic model allows application of a simple heat transfer calculation to an inert slab and enables determination of theoretical temperature profiles after exposure to a given level of radiation for a period of time equal to the experimentally determined ignition delay time at that radiation level. No account is taken of degradation kinetics, diathermancy, temperature dependence of thermal properties or emission/absorption interactions.

Program Listing

```
 10 REM BASIC HEAT TRANSFER MODEL
 20 PRINT"-----------"
 30 PRINT"BASIC MODEL"
 40 PRINT"-----------"
 50 PRINT""
 60 PRINT"ENTER DATA AS REQUESTED"
 70 PRINT""
 80 PRINT"1. MATERIAL?"
 90 INPUT PM$
100 PRINT""
110 PRINT"2. DENSITY (KG/M3)?"
120 INPUT RHO
130 PRINT""
140 PRINT"3. HEAT CAPACITY (KJ/KG.K)?"
150 INPUT CAP
160 PRINT""
170 PRINT"4. THERMAL CONDUCTIVITY (KW/M.K)?"
180 INPUT CND
190 PRINT""
200 ALF=CND/(RHO*CAP)
210 THI=CND*RHO*CAP
220 PRINT"5. SURFACE ABSORPTIVITY?"
230 INPUT AB
240 PRINT""
250 PRINT"6. INCIDENT RADIANT HEAT FLUX (KW/M2)?"
260 INPUT Q
270 PRINT""
280 PRINT"7. EXPERIMENTAL IGNITION DELAY TIME (S)?"
290 INPUT EX
300 PRINT""
310 PRINT"8. FIREPOINT TEMPERATURE (C)?"
320 INPUT FPT
330 PRINT""
340 PRINT"9. AMBIENT TEMPERATURE (C)?"
350 INPUT ZO
360 PRINT""
370 PRINT"10. ELEMENT THICKNESS (M)?"
380 INPUT DX
390 PRINT""
400 PRINT"11. DURATION OF TIME INTERVAL (S)?"
410 INPUT DT
420 PRINT""
430 FO=ALF*DT/(DX^2)
440 IF FO<0.5 THEN 470
450 PRINT"TIMESTEP TOO LARGE, REASSIGN VALUE"
460 GOTO 400
470 PRINT"12. NUMBER OF ELEMENTS IN SLAB?"
480 INPUT I
490 PRINT""
```

```
500 J=EX/DT
510 REM CONSTANTS
520 SIG=5.67E-11
530 H=0.01
540 EM=AB
550 EMS=EM*SIG
560 CA=DT/(RHO*CAP*DX)
570 CB=CND/DX
580 DIM TIM(J),T(I,J)
590 FOR K=0 TO J
600 FOR N=1 TO I
610 T(N,K)=ZO
620 NEXT N
630 NEXT K
640 PRINT""
650 VDU2
660 PRINT"------------------------------------------------"
670 PRINT"FIREPOINT TEMPERATURE CALCULATION FOR ";PM$
680 PRINT"------------------------------------------------"
690 PRINT"DENSITY = ";RHO;" KG/M3"
700 PRINT"HEAT CAPACITY = ";CAP;" KJ/KG.K"
710 PRINT"THERMAL CONDUCTIVITY"
720 PRINT"SURFACE ABSORPTIVITY = ";AB;
730 PRINT""
740 PRINT"INCIDENT RADIANT HEAT FLUX = ";Q;" KW/M2"
750 PRINT"ELEMENT THICKNESS = ";DX;" M"
760 PRINT"TIME INTERVAL DURATION = ";DT;" S"
770 PRINT""
780 PRINT"********************************************"
790 PRINT""
800 FOR K= 1 TO J
810 TIM(K)=K*DT
820 FOR N=1 TO I
830 IF N=1 THEN 870
840 IF N=I THEN 910
850 T(N,K)=T(N,K-1)+CA*CB*(T(N-1,K-1)-2*T(N,K-1)+T(N+1,K-1))
860 GOTO 920
870 LR=EMS*(T(1,K-1)+273)^4
880 LCV=H*(T(1,K-1)-ZO)
890 T(1,K)=T(1,K-1)+CA*(Q*AB-LR-LCV-CB*(T(1,K-1)-T(2,K-1)))
900 GOTO 920
910 T(I,K)=T(I,K-1)+CA*(CB*(T(I-1,K-1)-T(I,K-1))-H*(T(1)-ZO))
920 NEXT N
930 NEXT K
940 PRINT"THEORETICAL FIREPOINT TEMPERATURE=";INT(T(1,J)+0.5
950 PRINT"CORRESPONDING REAR FACE TEMP.=";INT(T(I,J)+0.5
960 VAR=((T(1,J)-FPT)/FPT)*100
970 PRINT""
980 PRINT"% VARIATION FROM MEASURED TEMP. = "INT(VAR+0.5);"%"
990 VDU3
1000 END
```

Input

```
ENTER DATA AS REQUESTED

1. MATERIAL?
?PERSPEX

2. DENSITY (KG/M3)?
?1180

3. HEAT CAPACITY (KJ/KG.K)?
?1.5

4. THERMAL CONDUCTIVITY (KW/M.K)?
?.00017

5. SURFACE ABSORPTIVITY?
?0.85

6. INCIDENT RADIANT HEAT FLUX (KW/M2)?
?24

7. EXPERIMENTAL IGNITION DELAY TIME (S)?
?115

8. FIREPOINT TEMPERATURE (C)?
?311

9. AMBIENT TEMPERATURE (C)?
?17

10. ELEMENT THICKNESS (M)?
?.001

11. DURATION OF TIME INTERVAL (S)?
?1

12. NUMBER OF ELEMENTS IN SLAB?
?6
```

Output

```
-----------------------------------------
FIREPOINT TEMPERATURE CALCULATION FOR PERSPEX
-----------------------------------------
DENSITY = 1180 KG/M3
HEAT CAPACITY = 1.5 KJ/KG.K
THERMAL CONDUCTIVITY = 1.7E-4 KW/M.K
SURFACE ABSORPTIVITY = 0.85

INCIDENT RADIANT HEAT FLUX = 24 KW/M2
ELEMENT THICKNESS = 1E-3 M
TIME INTERVAL DURATION = 1 S

**************************************

THEORETICAL FIREPOINT TEMP. = 301 C
CORRESPONDING REAR FACE TEMP. = 100 C

% VARIATION FROM MEASURED FIREPOINT TEMP. = -3%
```

MODIFICATION 1.

In this version of the model, the basic program described previously was adapted to take account of diathermancy. It was assumed that instead of radiation being reflected as in the basic version of the program, any radiation not absorbed by the surface element was transmitted and partially absorbed by successive elements at depth. As previously, theoretical surface temperatures were determined at the time corresponding to experimental ignition delay time.

Program Listing

```
 10 REM BASIC HEAT TRANSFER MODEL
 20 PRINT"RATE OF SURFACE TEMPERATURE RISE"
 30 PRINT"--------------------------------"
 40 PRINT""
 50 PRINT" ENTER VARIABLES AS REQUESTED"
 60 PRINT""
 70 PRINT"1. SELECT MATERIAL FROM MENU"
 80 PRINT""
 90 PRINT"1. PERSPEX              2. FINNACRYL
100 PRINT"3. POLYOXYMETHYLENE     4. POLYPROPYLENE
110 PRINT"5. POLTETHYLENE         6. POLYSTYRENE
120 PRINT"7. OTHER
130 PRINT""
140 INPUT AN
150 GOTO 950
160 PRINT"2. INCIDENT RADIANT HEAT FLUX (KW/M2)?"
170 INPUT Q
180 PRINT""
190 PRINT"3. EXPERIMENTAL TIME TO FIREPOINT (S)?"
200 INPUT EX
210 PRINT""
220 PRINT"4. EXPERIMENTAL FIREPOINT TEMPERATURE (C)?"
230 INPUT FPT
240 PRINT""
250 PRINT"5. AMBIENT TEMPERATURE (C)?"
260 INPUT ZO
270 PRINT""
280 PRINT"6. NUMBER OF LAYERS IN SLAB?"
290 INPUT I
300 PRINT"   INCREMENTAL THICKNESS (M)?"
310 INPUT DX
320 PRINT""
330 PRINT"7. DURATION OF TIMESTEP (S)?"
340 INPUT DT
350 J=EX/DT
360 W=I*DX
370 ALF=CND/(RHO*CAP)
380 FO=ALF*DT/(DX^2)
390 IF FO<0.5 THEN 420
400 PRINT"TIMESTEP TOO LARGE, REASSIGN DT VALUE"
410 GOTO 330
420 REM CONSTANTS
430 SIG=5.67E-11
440 H=0.01
450 FR=DT/(RHO*CAP*DX)
460 FC=CND/DX
470 DIM TIM(J),T(I,J)
480 TIM(J)=0
490 T(I,J)=0
500 FOR K=0 TO J
510 FOR N=1 TO I
```

```
520 T(N,K)=ZO
530 NEXT N
540 NEXT K
550 THI=CND*RHO*CAP
560 PRINT""
570 PRINT""
580 VDU2
590 PRINT"TEMPERATURE PROFILE FOR ";PM$
600 PRINT"-----------------------------------"
610 PRINT"THICKNESS = ";W;" M"
620 PRINT"DENSITY = ";RHO;" KG/M3"
630 PRINT"HEAT CAPACITY = ";CAP;" KJ/KG.K"
640 THERMAL CONDUCTIVITY = ";CND;" KW/M.K"
650 PRINT"THERMAL DIFFUSIVITY = ";ALF;" M2/S"
660 PRINT"THERMAL INERTIA = ";THI;" KW2.S/M4.K2"
670 PRINT"INCIDENT RADIANT HEAT FLUX = ";Q;"KW/M2"
680 PRINT"EXPERIMENTAL FIREPOINT TEMPERATURE = ";FPT;" C"
690 PRINT""
700 FOR K=1 TO J
710 TIM(K)=K*DT
720 FOR N=1 TO I
730 IF N=1 THEN 780
740 IF N=I THEN 830
750 D=FC*(T(N-1,K-1)-2*T(N,K-1)+T(N+1,K-1))
760 T(N,K)=FR*(D+Q*EM*(1-EM)^(N-1))+T(N,K-1)
770 GOTO 850
780 LR=EM*SIG*(T(1,K-1)+273)^4
790 LCV=H*(T(1,K-1)-ZO)
800 A=Q*EM-LR-LCV
810 T(1,K)=T(1,K-1)+(A+FC*(T(2,K-1)-T(1,K-1)))*FR
820 GOTO 850
830 B=FC*(T(I-1,K-1)-T(I,K-1))-H*(T(I,K-1)-ZO)
840 T(I,K)=T(I,K-1)+FR*(B+Q*EM*(1-EM)^(I-1))
850 NEXT N
860 NEXT K
870 VAR=((T(1,J)-FPT)/FPT)*100
880 PRINT"*******************************************"
890 PRINT""
900 PRINT"THEORETICAL FIREPOINT TEMP.=";INT(T(1,J)+0.5);"C"
910 PRINT"CORRESPONDING REAR TEMP.=";INT(T(I,J)+0.5)
920 PRINT"% VARIATION FROM MEASURED TEMP.=";INT(VAR+0.5);"%"
930 VDU3
940 END
950 IF AN=1 THEN 1020
960 IF AN=2 THEN 1080
970 IF AN=3 THEN 1140
980 IF AN=4 THEN 1200
```

```
 990 IF AN=5 THEN 1260
1000 IF AN=6 THEN 1320
1010 IF AN=7 THEN 1380
1020 PM$="PERSPEX"
1030 EM=0.85
1040 RHO=1180
1050 CAP=1.5
1060 CND=.00017
1070 GOTO 160
1080 PM$="FINNACRYL"
1090 EM=0.85
1100 RHO=1190
1110 CAP=1.46
1120 CND=.00021
1130 GOTO 160
1140 PM$="POLYOXYMETHYLENE"
1150 EM=0.92
1160 RHO=1420
1170 CAP=1.47
1180 CND=.00037
1190 GOTO 160
1200 PM$="POLYPROPYLENE"
1210 EM=0.87
1220 RHO=905
1230 CAP=1.93
1240 CND=.00021
1250 GOTO 160
1260 PM$="POLYETHYLENE"
1270 EM=0.92
1280 RHO=920
1290 CAP=2.1
1300 CND=.00033
1310 GOTO 160
1320 PM$="POLYSTYRENE"
1330 EM=0.75
1340 RHO=1040
1350 CAP=1.34
1360 CND=.00012
1370 GOTO 160
1380 PRINT"MATERIAL?"
1390 INPUT PM$
1400 PRINT"SURFACE ABSORPTIVITY?"
1410 INPUT EM
1420 PRINT"DENSITY (KG/M3)?"
1430 INPUT RHO
1440 PRINT"HEAT CAPACITY (KJ/KG.K)?"
1450 INPUT CAP
1460 PRINT"THERMAL CONDUCTIVITY (KW/M.K)"
1470 INPUT CND
1480 GOTO 160
```

Input

```
ENTER VARIABLES AS REQUESTED

1. SELECT MATERIAL FROM MENU

1. PERSPEX              2. FINNACRYL
3. POLYOXYMETHYLENE     4. POLYPROPYLENE
5. POLYETHYLENE         6. POLYSTYRENE
7. OTHER
?1

2. INCIDENT RADIANT HEAT FLUX (KW/M2)?
?24

3. EXPERIMENTAL TIME TO FIREPOINT (S)?
?115

4. EXPERIMENTAL FIREPOINT TEMPERATURE (C)?
?311

5. AMBIENT TEMPERATURE (C)?
?17

6. NUMBER OF LAYERS IN SLAB?
?6
   INCREMENTAL THICKNESS (M)?
?.001

7. DURATION OF TIMESTEP (S)?
?1
```

Output

```
TEMPERATURE PROFILE FOR PERSPEX
-------------------------------
THICKNESS = 6E-3 M
DENSITY = 1180 KG/M3
HEAT CAPACITY = 1.5 KJ/KG.K
THERMAL CONDUCTIVITY = 1.7E-4 KW/M.K
THERMAL DIFFUSIVITY = 1.124E-7 M2/S
THERMAL INERTIA = 0.321 KW2.S/M4.K2
INCIDENT RADIANT HEAT FLUX = 24 KW/M2
EXPERIMENTAL FIREPOINT TEMPERATURE = 311 C

****************************************

THEORETICAL FIREPOINT TEMPERATURE = 331 C
CORRESPONDING REAR TEMP. = 134 C
% VARIATION FROM MEASURED TEMP. = 6%
```

MODIFICATION 2.

In this version of the model, the effect of the interrelationship between source emission and sample absorption spectra is taken into account. The spectra are translated into a series of narrow strips corresponding to small wavelength increments. For each wavelength increment, the fraction of the total energy of radiation contained within that increment is multiplied by the incident radiant heat flux and by the corresponding monochromatic absorptivity to give the radiant heat flux absorbed by the increment. The total heat flux absorbed by the sample is given by the summation of the incremental heat fluxes between an upper and lower wavelength limit. If the wavelength range chosen contains less than 95% of the total energy of radiation then the run is aborted and alternative wavelength limits should be set. Heat losses by reradiation from the exposed surface are calculated in a similar manner, assuming that $\alpha_\lambda = e_\lambda$. Diathermancy was also included in this version.

Information on radiation functions and monochromatic absorptivities were entered in the form of DATA statements which were subsequently READ into arrays. As previously, the temperature of every element at the end of each timestep interval was computed but in this version, the theoretical time for the sample to reach the experimentally determined firepoint temperature was calculated.

Program Listing

Preliminary part of program similar to MODIFICATION 1. up to line 500

```
 730 GOTO 10000
 740 DIM D(M-1)
 750 FOR K=0 TO J
 760 FOR N=1 TO I
 770 T(N,K)=ZO
 780 NEXT N
 790 NEXT K
 800 FOR K=1 TO J
 810 TIM(K)=K*DT
 820 FOR N=1 TO I
 830 IF N=1 THEN 930
 840 IF N=I THEN 1020
 850 TV=0
 860 CON=FC*(T(N-1,K-1)-2*T(N,K-1)+T(N+1,K-1))
 870 FOR B=1 TO M-1
 880 V(B)=A(B)*((1-A(B))^(N-1))*Q
 890 TV=TV+V(B)
 900 NEXT B
 910 T(N,K)=T(N,K-1)+(FR*(CON+TV/(M-1)))
 920 GOTO 1090
 930 TLR=0
 940 FOR B=1 TO M-1
 950 D(B)=A(B)*((T(1,K-1)+273)^4)*SIG
 960 TLR=TLR+D(B)
 970 NEXT B
 980 LC=H*(T(1,K-1)-ZO
 990 P=SUM-TLR/(M-1))-LC
1000 T(1,K)=T(1,K-1)+(P+FC*(T(2,K-1)-T(1,K-1)))*FR
1010 GOTO1090
1020 G=FC*(T(I-1,K-1)-T(I,K-1))-H*(T(I,K-1)-ZO)
1030 ST=0
1040 FOR B=1 TO M-1
1050 S(B)=A(B)*((1-A(B))^(I-1))*Q
1060 ST=ST+S(B)
1070 NEXT B
1080 T(I,K)=T(I,K-1)+FR*(G+ST/(M-1))
1090 NEXT N
1100 TS=T(1,K)
1110 PRINT""
1120 PRINT"T(1,K) =":T(1,K)
1130 IF TS<FPT THEN 1190
1140 LET KA=K
1150 FTIME=DT*KA
1160 VDU2
1170 PRINT"THEORETICAL IGNITION TIME FOR ":PM$
1180 PRINT"----------------------------------------"
1190 PRINT"RADIANT HEAT FLUX=":Q:" KW/M2)"
1200 PRINT"EXPERIMENTAL FIREPOINT TEMPERATURE=":FPT:" C"
1210 PRINT"EXPERIMENTAL IGNITION DELAY TIME IS":EX: " S"
1220 PRINT""
1230 PRINT"RANGE OF WAVELENGTHS CONSIDERED IS ":U:" TO ":L:" MICRONS"
1240 PRINT"WAVELENGTH INCREMENT IS ":DW:" MICRONS"
1250 PRINT""
```

```
 1260 PRINT"**************************************"
 1270 PRINT""
 1280 PRINT"THEORETICAL TIME TO IGNITION IS ":FTIME:" S"
 1290 PRINT"THEORETICAL REAR FACE TEMP. AT IGNITION IS ":T(I,KA):" S"
 1300 VAR=INT((((FTIME-EX)/EX)*100)+0.5)
 1310 PRINT"% VARIATION BETWEEN THEORY AND EXPERIMENTAL TIMES IS ":VAR
 1320 GOTO 1350
 1330 NEXT K
 1340 VDU3
 1350 END
10000 DIM X(30),Y(30)
10010 FOR N1=0 TO 30
10020 READ X(N1)
10030 NEXT N1
10040 FOR N1=0 TO 30
10050 READ Y(N1)
10060 NEXT N1
10070 SUM=0
10080 PRINT"ENTER UPPER AND LOWER LIMIT WAVELENGTHS (MICRONS)"
10090 INPUT U,L
10100 PRINT"WAVELENGTH INTERVAL (MICRONS)?"
10110 INPUT DW
10120 M=((U-L)/DW)+1
10130 DIM E(M),W(M),A(M-1),EQ(M-1),EQA(M-1)
10140 DIM V(M-1),S(M-1)
10150 PRINT"HEATER TEMPERATURE (DEG C)?"
10160 INPUT HC
10170 HR=HC*9/5+32+459.67
10180 FOR B=1 TO M-1
10190 READ A(B)
10200 NEXT B
10210 W(1)=L
10220 FOR B=2 TO M
10230 W(B)=W(B-1)+DW
10240 NEXT B
10250 FOR B=1 TO M
10260 IT=INT(W(B)*HR/1000)
10270 E(B)=(((Y(IT+1)-Y(IT))/(X(IT+1)-X(IT)))*(W(B)*HR-X(IT)))+Y(IT)
10280 NEXT B
10290 FOR B=1 TO M-1
10300EQ(B)=(E(B+1)-E(B))*Q
10310 TEQ=TEQ+EQ(B)
10320 EQA(B)=EQ(B)*A(B)
10330 SUM=SUM+EQA(B)
10340 NEXT B
10350 IF TEQ/Q>.95 THEN 10380
10360 PRINT"INSUFFICIENT WAVELENGTH RANGE"
10370 GOTO 1210
10380 GOTO 740

DATA STATEMENTS FOR RADIATION FUNCTIONS

DATA STATEMENTS FOR POLYMER MONOCHROMATIC ABSORPTIVITIES
```

Input

```
SELECT MATERIAL FROM PX, FINN, POM, PP, PE, PS OR OTHER
?PX

RADIANT HEAT FLUX (KW/M2)?
?24

FIREPOINT TEMPERATURE OF PERSPEX EXPOSED TO 24 KW/M2 = ?
?311

EXPERIMENTAL IGNITION DELAY TIME AT THIS HEAT FLUX (S)?
?115

INCREMENTS IN SLAB?
?6

INCREMENTAL THICKNESS?
?.001

TIME INTERVAL DURATION (S)?
?1

ENTER UPPER AND LOWER LIMIT WAVELENGTHS (MICRONS)
?12,.2

WAVELENGTH INTERVAL (MICRONS)?
?.2

HEATER TEMPERATURE (DEG C)?
?800
```

Output

```
THEORETICAL IGNITION DELAY TIME FOR PERSPEX
-------------------------------------------
RADIANT HEAT FLUX = 24 KW/M2
EXPERIMENTAL FIREPOINT TEMPERATURE = 311 C
EXPERIMENTAL IGNITION DELAY TIME = 115 S

RANGE OF WAVELENGTHS CONSIDERED IS 0.2 TO 12 MICRONS
WAVELENGTH INCREMENT IS 0.2 MICRONS

**************************************************

THEORETICAL TIME TO IGNITION IS 117 S
THEORETICAL REAR FACE TEMP. AT IGNITION IS 112 C
% VARIATION BETWEEN THEORETICAL AND EXPERIMENTAL IGNITION TIMES IS 2%
```

APPENDIX E
DETERMINATION OF KINETIC PARAMETERS FROM TGA

It is possible to monitor the degradation reactions of solids by continuous weighing. A thermal balance is well suited to this task. From Broido (1969), W_t, the weight at any time, t, is related to the fraction of the number of initial molecules not yet decomposed, y, by the equation

$$y = N/N_0 = (W_t - W_\infty)/(W_0 - W_\infty) \quad \text{(E1)}$$

The reaction rate under isothermal pyrolysis is given by:-

$$dy/dt = -ky^n \quad \text{(E2)}$$

where the rate constant, k, varies with temperature according to the Arrhenius equation:

$$k = A.\exp(-E_A/RT) \quad \text{(E3)}$$

If temperature is assumed to be a linear function of time, $T = T_0 + ut$, equations E1-E3 may be combined to give:

$$dy/y^n = -(A/u)\exp(-E_A/RT)dT \quad \text{(E4)}$$

Equation E4 represents the curve for such a reaction from a temperature T_0 at which y=1. Therefore

$$\int_y^1 dy/y^n = A/u\int_{T_0}^{T}\exp(-E_A/RT)dT \quad \text{(E5)}$$

Assuming a first order reaction, ie n=1 and $\int_y^1 dy/y = \ln(1/y)$

$$\ln(1/y) = A/u\int_{T_0}^{T}\exp(-E_A/RT)dT \quad \text{(E6)}$$

assuming that $\exp(-E_A/RT) \simeq (T_m/T)^2\exp(-E_A/RT_m)$

$$\ln(1/y) = (A/u)T_m^2\exp(-E_A/RT)\int_{T_0}^{T} dT/T^2 \quad \text{(E7)}$$

Integrating and taking logs of both sides gives:

$$\ln\ln(1/y) = -(E_A/R)(1/T) + \text{const.} \quad \text{(E8)}$$

Hence activation energy can be determined from a plot of $\ln\ln(1/y)$ versus 1/T derived from TGA data.

APPENDIX F
PUBLICATIONS ARISING FROM THIS WORK

- Thomson, H.E. and Drysdale, D.D. (1987). "Flammability of plastics I: Ignition temperatures." Fire and Materials, **11**, 163-172

- Thomson, H.E. and Drysdale, D.D. (1987). "Piloted ignition of plastics." Paper presented at IOP Short Meetings, Series N^{O}4, Institute of Physics

- Thomson, H.E. and Drysdale, D.D. (1987). "Ignition of fire retarded plastics." Paper presented at Flame Retardants '87, Tara Hotel, London

- Thomson, H.E. and Drysdale, D.D. (1988). "Flammability of plastics II: Critical mass flux at firepoint." Paper to be presented at Second International Symposium on Fire Safety Science, Tokyo, Japan

- Thomson, H.E. , Drysdale, D.D. and Beyler, C.L. (1988). "An experimental evaluation of critical surface temperature as a criterion for piloted ignition of solid fuels." Fire Safety Journal, in press

APPENDIX G
REFERENCES

- Akita, K. (1978). in Jellinek, H.H.G. (Ed): Aspects of Degradation and Stabilization of Polymers. Ch.10, p.514, Elsevier Scientific Publishing Company, Amsterdam.

- Al-Arabi, M. and El-Reidy, M.K. (1976). "Natural convection heat transfer from isothermal horizontal plates of different shapes." International Journal of Heat and Mass Transfer, **19**, 1399-1406.

- Alvares, N.J. (1963). "Measurement of temperatures of the thermally irradiated surface of alpha-cellulose." USNRDL-TR-735.

- Alvares, N.J. (1975). "Some experiments to delineate the conditions for flashover in enclosure fires." International Symposium on Fire Safety of Combustible Materials, Edinburgh. p.375-383.

- Alvares, N.J. and Martin, S.B. (1971). "Mechanisms of ignition of thermally irradiated cellulose." 13th Symposium (International) on Combustion, p.905-914. The Combustion Institute, Pittsburgh.

- Alvares, N.J., Blackshear, P.L. and Murty, K.A. (1969). "The influence of free convection on the ignition of vertical cellulosic panels by thermal irradiation." Central States Section, Combustion Institute Meeting, University of Minnesota.

- American Society for Testing and Materials (1976). "Methenamine pill test." ASTM D2859-76.

- American Society for Testing and Materials (1977). "Rate of burning of plastics in a vertical position." ASTM D568-77.

- American Society for Testing and Materials (1977). "Rate of burning and/or extent of burning of self-supporting plastics in a horizontal position." ASTM D635-77.

- American Society for Testing and Materials (1977). "Ignition properties of plastics." ASTM D1929-77.

- American Society for Testing and Materials (1977). "Standard method for measuring the minimum oxygen concentration to support candle-like combustion of plastics." ASTM D2863-77.

- American Society for Testing and Materials (1978). "Standard test method for flashpoint and firepoint by the Cleveland Open Cup method." ASTM D92-78.

- American Society for Testing and Materials (1978). "Flammability of materials using a radiant heat energy source." ASTM E162-78.

- American Society for Testing and Materials (1978). "Flooring radiant panel test." ASTM E648-78.

- American Society for Testing and Materials (1979). "Surface burning characteristics of building materials (Steiner tunnel test)." ASTM E84-79a.

- American Society for Testing and Materials (1979). "Behaviour of materials in a vertical tube furnace at 750^{0}C." ASTM E136-79.

- American Society for Testing and Materials (1980). "Standard test method for flashpoint by the Pensky-Martens closed tester." ASTM D93-80.

- Atreya, A., Carpentier, C. and Harkleroad, M. (1986). "Effect of sample orientation on ignition and flame spread." Fire Safety Science - Proceedings of the First International Symposium, p.97-109.

- Atreya, A. and Wichman, I. (1987). "Heat and mass transfer during piloted ignition." Second ASME-JSME Thermal Engineering Joint Conference, Hawaii. Submitted to ASME Journal of Heat Transfer.

- Avondo, C., Vovelle, C. and Delbourgo, R. (1978). "The role of phosphorus and bromine in flame retardancy." Combustion and Flame, **31**, 7-16.

- Babrauskas, V. and Parker, W.J. (1987). "Ignitability measurements with the cone calorimeter." Fire and Materials, **11**, 31-43.

- Bamford, C.H., Crank, J. and Malan, D.H. (1946). "On the combustion of wood." Proceedings of the Cambridge Philosophical Society, **42**, 166-182.

- Beckel, S.A. and Matthews, R.D. (1984). "Ignition of polyoxymethylene." Combustion and Flame, **57**, 71-86.

- Benbow, A.W. and Cullis, C.F. (1975). "The combustion of flexible polyurethane foams: mechanisms and evaluation of flame retardance." Combustion and Flame, **24**, 217-230.

- Beyler, C.L. (1985). Unpublished results.

- Brauman, S.K. (1980). "Ammonium polyphosphate, a model system." J. Fire Retard. Chem., **7**, 61-68.

- British Standards Institution (1968). "Fire propagation test for materials." BS476 Part 6: 1968.

- British Standards Institution (1976). "Surface spread of flame test for materials." BS476 Part 7: 1976.

- British Standards Institution (1977). "International thermocouple reference tables." BS4937 Part 4: 1977.

- British Standards Institution (1978). "Methods of testing plastics." BS2782 Part 5: 1978.

- British Standards Institution (1979). "Method of test for ignitability." BS476 Part 5: 1979.

- British Standards Institution (1987). "Method of measuring the ignitability of products subjected to thermal irradiance." BS476 Part 13: 1987.

- Burgoyne, J.H., Roberts, A.F. and Alexander, J.L. (1967). "The significance of open flashpoints." J. Institute of Petroleum, **53**, 338-341.

- Broido, A.J. (1969). J. Polymer Sci., **7**, 1761-1768

- Burgoyne, J.H. and Williams-Leir, G. (1949). "Inflammability of liquids." Fuel, **28**, 145-149.

- Carslaw, H.S. and Jaeger, J.C. (1959). "Conduction of Heat in Solids." 2nd Edition, Oxford University Press.

- Clark, F.R.S. (1983a). "Ignition of polymethylmethacrylate slabs using a small flame." J. Polymer Science: Polym. Chem. Ed., **21**, 2323-2334.

- Clark, F.R.S. (1983b). "Ignition of low density polyethylene slabs by a small flame." J. Polymer Science: Polym. Chem. Ed., **21**, 3225-3232.

- Clark, F.R.S. (1984a). "The role of oxygen in the ignition of polystyrene by a small flame." J. Polymer Science: Polym. Chem. Ed., **22**, 263-268.

- Clark, F.R.S. (1984b). "Radiative ignition of thermoplastic and char forming materials." Fire and Materials, **8**, 196-198.

- Comeford, J.J. (1972). "The spectral distribution of radiant energy of a gas fired radiant panel and some diffusion flames." Combustion and Flame, **18**, 125-132.

- Coward, H.F. and Guest, P.G (1927). J. Amer. Chem. Soc., **49**, 2479

- Croft, D.R. and Lilley, D.G. (1977). "Heat transfer calculations using finite difference equations." London Applied Science Publishers, London.

- Cullis, C.F. and Hirschler, M.M. (1983). "The significance of thermoanalytical measurements in the analysis of polymer flammability." Polymer, **24**, 834-840.

- Dawes, S. (1983). Unpublished results.

- Deepak, D.D. and Drysdale, D.D. (1983). "Flammability of solids: An apparatus to measure the critical mass flux at the firepoint." Fire Safety Journal, **5**, 167-168.

- Delmonte, J. and Azam, M.A. (1943). "Ignition points of plastic materials." Mod. Plast., **20**, 188.

- de Ris, J.N. (1969). "Spread of a laminar diffusion flame." 12th Symposium (International) on Combustion, p.241-252. The Combustion Institute, Pittsburgh.

- de Ris, J.N. (1979). "Fire radiation - a review." 17th Symposium (International) on Combustion, p.1003-1016. The Combustion Institute, Pittsburgh.

- Devarall, L.I. and Lai, W. (1969). "A criterion for thermal ignition of cellulosic materials." Combustion and Flame, **13**, 8-12.

- Drysdale, D.D. (1985). "An Introduction to Fire Dynamics." John Wiley & Sons.

- Drysdale, D.D. and Mazhar, M. (1979). "Critical flowrates of fuel vapours under conditions of pilot ignition." Paper presented at Interflam'79, Guildford.

- D'Souza, M.V. and M^{c}Guire, J.H. (1977). "ASTM E84 and the flammability of foamed thermosetting plastics." Fire Technology, **13**, 85-94.

- Dunkle, R.V. (1954). Trans. ASTM, **76**, 549

- Emmons, H.W. (1974). "Fire and fire protection." Scientific American, **231**, 21-30.

- Fang, J.B. (1975). "Fire build up in a room and the role of interior finish materials." National Bureau of Standards Technical Note, No.879.

- Fenimore,C.P. and Jones,G.W. (1966). "Modes of inhibiting polymer flammability." Combustion and Flame, **10**, 295-301.

- Fenimore, C.P. and Martin, F.J. (1966). "Flammability of polymers." Combustion and Flame, **10**, 135-139.

- Fernandez-Pello, A. and Williams, F.A. (1977). "A theory of laminar flame spread over flat surfaces of solid combustibles." Combustion and Flame, **28**, 251-277.

- Flynn, J.H. and Wall, L.A. (1960). J. Res. Nat. Bur. Stand., Section A, **70A**, 487

- Fons, W.L. (1950). "Heating and ignition of small wood cylinders." Industrial and Engineering Chemistry, **42**, 2130-2133.

- Frey, A.R. and T'ien, J.S. (1979). "A theory of flame spread over a solid fuel including finite chemical kinetics." Combustion and Flame, **36**, 263-289.

- Gann,R.G., Dipert, R.A. and Drews, M.J. (1986). "Flammability" Encyclopedia of Polymer Science and Engineering, 154-210

- Gardon,R. (1953). "Temperatures attained in wood exposed to high intensity radiation." Fuels Research Laboratory Technical Report No.3, Massechusetts Institute of Technology, Cambridge, Mass.

- Glassman, I. and Dryer,F. (1981). "Flame spreading across liquid fuels." Fire Safety Journal, **3**, 123-138.

- Hallman, J.R. (1971). "Ignition characteristics of plastics and rubber." Ph.D. Thesis, University of Oklahoma.

- Hallman, J.R., Welker, J.R. and Sliepcevich, C.M. (1972). "Ignition of polymers." S.P.E. Journal, **28**, 43-47.

- Hallman, J.R., Welker, J.R. and Sliepcevich, C.M. (1974). "Polymer surface reflectance - absorptance characteristics." Polymer Eng. and Sci., **14**, 717-723.

- Hallman, J.R., Welker, J.R. and Sliepcevich, C.M. (1976). "Ignition times for polymers." Polym.-Plast. Technol. Eng., **6**, 1-56.

- Hallman, J.R., Welker, J.R. and Sliepcevich, C.M. (1977) in "Characterisation of Metal and Polymer Surfaces, Vol.II, Polymer Surfaces." p.429-446. Academic Press, Inc. New York.

- Hallman, J.R., Welker, J.R. and Sliepcevich, C.M. (1978). "Radiation absorption for polymers: The radiant panel and carbon arcs as radiant heat sources." J. Fire and Flamm., **9**, 353-366.

- Havens, J.A. (1968). "Thermal decomposition of wood." Ph.D.Thesis, University of Oklahoma.

- Henriques, F.C. (1947). "Studies of thermal injury, viz, the predictability and significance of thermally induced rate processes leading to irreversible epidermal injury." Arch. Path. (Lab. Med.), **43**, 489-502.

- Heseldon, A.J.M. (1976). "Radaition characteristics of the radiator cone of the ISO Ignitability Test." ISO/TC92/SC1/WG2 N56.

- Heselden, A.J.M. and Wraight, H.G.H. (1984). "Results of inter-laboratory trials with the ISO ignitability test." International Standards Organisation, ISO/TC 92/SC 1/WG 2 N32.

- Hilado, C.J. (1982). "Flammability Handbook for Plastics." Technomic Publishing Company, Conneticut.

- Hirata, T., Kashiwagi, T. and Brown, J.E. (1985). "Thermal and oxidative degradation of polymethylmethacrylate: Weight loss." Macromolecules, **18**, 1410-1418

- Holman, J.P. (1976). "Heat transfer.", 4th edition, M^{c}Graw-Hill, New York.

- Hunter, L.W. and Hoshall, C.H. (1980). "An ignition test for plastics." Fire and Materials,**4**, 201-202.

- Hunter, L.W., Schacke, H., Grunfelder,G and Fristrom, R.M. (1977). "Surface temperature measurements in the moving wire technique." Combustion Science and Technology, **15**, 41-48.

- International Standards Orgnisation (1986). "Fire tests - reaction to fire - ignitability of building products." ISO 5657-86.

- Kanury, A.M. (1972). "Ignition of cellulosic solids - a review." Fire Reasearch Abstracts and Reviews, **14**, 24-52.

- Kanury, A.M. (1977). "Ignition of cellulosic solids: Minimum pyrolysate mass

flux criterion." Combustion Science and Technology, **16**, 89-90.

- Kanury, A.M. and Blackshear (1970). Combustion Science and Technology, 2, 5-12.

- Kashiwagi, T. (1974). "A radiative ignition model of a solid fuel." Combustion Science and Technology, **8**, 225-236.

- Kashiwagi, T. (1979a). "Experimental observation of radiative ignition mechanism." Combustion and Flame, **34**, 231-244.

- Kashiwagi, T. (1979b). "Effects of attenuation of radiation on surface temperature for radiative ignition." Combustion Science and Technology, **20**, 225-234.

- Kashiwagi, T. (1982). "Effects of sample orientation on radiative ignition." Combustion and Flame, **44**, 223-245.

- Kashiwagi, T., Inaba, A. and Brown, J.E. (1986). "Differences in PMMA degradation characteristics and their effects on its fire properties." Proceedings of the First International Symposium on Fire Safety Engineering, p.483-493.

- Kashiwagi, T., Macdonald, B.W., Isoda, H. and Summerfield, M. (1971). "Ignition of a solid polymeric fuel in a hot oxydising gas stream." 13th Symposium (International) on Combustion, The Combustion Institute, Pittsburgh. p.1235-1247

- Kashiwagi, T. and Ohlemiller, T.J. (1982) "A study of oxygen effects on non-flamming transient gasification of PMMA and PE during thermal irradiation." 19th Symposium (International) on Combustion, The Combustion Institute, Pittsburgh. p.815-823.

- Kindelan, M. and Williams, F.A. (1975). "Theory for endothermic gasification of a solid by constant energy flux." Combustion Science and Technology, **10**, 1-19.

- Kindelan, M. and Williams, F.A. (1977). "Gas phase ignition of a solid with indepth absorption of radiation." Combustion Science and Technology, **16**, 47-58.

- Kishore, K. and Mohandas, K. (1982). "Laboratory test methods for the evaluation of flammability of polymers." J. Macromol. Sci. - Chem., **A18**, 379-393.

- Kishore, K. and Mohandas, K. (1982b). "Ignition behaviour of polystyrene." Combustion Science and Technology, **29**, 299-304.

- Koohyar, A.N., Welker, J.R. and Sliepcevich, C.M. (1968a). "An experimental technique for the ignition of solids by flame irradiation." Fire Technology, **4**, 221-228.

- Koohyar, A.N., Welker, J.R. and Sliepcevich, C.M. (1968b). "The irradiation and ignition of wood by flame." Fire Technology, **4**, 284-294.

- Kuryla, W.C. and Papa, A.J. (1975). "Flame Retardancy of Polymeric Materials." Vol.3, Marcel Dekker, Inc., New York.

- Laurendeau, N.M. (1982). "Thermal ignition of methane-air mixtures by hot - surfaces: a critical examination." Combustion and Flame, **46**, 29-49. Lawrence, E.K. (1950). "Analytical study of flame initiation." Ph.D. Thesis, Dept. of Chem. Eng., Massachusetts Institute of Technology, Mass.

- Lawson, D.I. and Simms, D.L. (1952). "The ignition of wood by radiation." British J. Applied Physics, **3**, 288-292.

- Linan, A. and Williams, F.A. (1971). Combustion Science and Technology, **3**, 91.

- Linan, A. and Williams, F.A. (1972). "Radiant ignition of a reactive solid with in-depth absorption." Combustion and Flame, **18**, 85-97.

- Lygate, J.F. (1979). "The determination of mass flux under critical conditions." MSc thesis, University of Edinburgh.

- Lyons, J.W. (1970). "The Chemistry and Use of Fire Retardants." John Wiley & Sons, Inc., New York.

- M^{c}Ilhagger, R. and Hill, B.J. (1987). "The influence of extrusion conditions on the burning and smoke characteristics of polypropylene film." Plastics and Rubber Proc. Appl., **7**, 179-183.

- Madorsky, S.L. (1964). "Thermal Degradation of Organic Polymers." Interscience, John Wiley, New York.

- Magee, R.S. and Reitz, R.D. (1974). "Extinguishment of radiation augmented plastic fires by water sprays." Factory Mutual Research Technical Report No.22357-1.

- Malhotra, H.L. (1975). "The philosophy and design of fire tests." International Symposium on Fire Safety of Combustible Materials, p.149-155, Edinburgh.

- Martin, S.B. (1965). "Diffusion controlled ignition of cellulosic materials by intense radiation energy." 10th Symposium (International) on Combustion, p.877. The Combustion Institute, Pittsburgh.

- Melinek, S. (1969). Fire Research Note 755, DSIR and FOC, Joint Fire Research Organisation.

- Mutoh, N., Hirano, T. and Akita, K. (1979). "Experimental study on radiative ignition of PMMA." 17th Symposium (International) on Combustion, p.1183-1190, The Combustion Institute, Pittsburgh.

- Niioka, T. and Williams, F.A. (1979). "Relationship between theory and experiment for radiant ignition of solids." 17th Symposium (International) on Combustion, p.1163-1171, The Combustion Institute, Pittsburgh.

- Ohlemiller, T.J. and Summerfield, M. (1971). "Radiative ignition of polymeric

materials in oxygen/nitrogen mixtures." 13th Symposium (International) on Combustion, p.1087-1074, The Combustion Institute, Pittsburgh.

- Patten, G.A. (1961). "Ignition temperatures of plastics." Modern Plastics, **38**, 119,120,122,180.

- Powell, F. (1969). "Ignition of gases and vapours: a review of ignition of flammable gases by friction and impact." Industrial and Engineering Chemistry, **61**, 29-37.

- Quintiere, J. (1981). "A simplified theory for generalising results from a radiant panel rate of flame spread apparatus." Fire and Materials, **5**, 52-60.

- Quintiere, J., Harkelroad, M. and Walton, W. (1983). "Measurement of material flame spread properties." Combustion Science and Technology, **32**, 67-89.

- Rasbash, D.J. (1975). "Relevance of firepoint theory to assessment of fire behaviour of combustible materials." International Symposium on Fire Safety of Combustible Materials, Edinburgh, p.169-178.

- Rasbash, D.J. and Drysdale, D.D. (1983). "Theory of fire and fire processes." Fire and Materials, **7**, 79-88.

- Rasbash, D.J., Drysdale, D.D. and Deepak, D. (1986). "Critical heat and mass transfer at pilot ignition and extinction of a material." Fire Safety Journal, **10**, 1-10.

- Roberts, A.F. and Quince, B.W. (1973). "A limiting condition for the burning of flammable liquids," Combustion and Flame, **20**, 245-251.

- Robertson, A.F. (1979). "A flammability test based on proposed ISO spread of flame test." Third Progress Report, Intergovernmental Maritime Consultative Organisation, IMCO FP/215.

- Rockett, J.A. (1974). "Mathematical modelling of radiant panel test methods." Fire Safety Research, National Bureau of Standards, NBS SP 411 (1974)

- Ryan, L.R., Penzias, G.J. and Tourin, R.H. (1961). "An Atlas of Infrared Spectra of Flames, Part 1, Infrared spectra of hydrocarbon flames in the 1-5μm region." Office of Aerospace Research (USAF), Bedford, Mass.

- Sauer, F.M. (1956). "The charring of wood during exposure to thermal radiation - correlational analysis for semi-infinite solids." U.S. Dept. of Agriculture Forest Service, Division of Fire Research, Berkeley, California.

- Schoenborn, E.M. and Weaver, D.S. (1947). "Ignition temperatures of rigid plastics." ASTM Bulletin, **146**, 80-87.

- Setchkin, N.P. (1948). "Discussion of paper on the ignition temperature of rigid plastics." ASTM Bulletin, **151**, 66-69.

- Setchkin, N.P. (1949). "A method and apparatus for determining the ignition

characteristics of plastics." J. Research, National Bureau of Standards, **43**, 591-608.

- Simmons, R.F. and Wolfhard, H.G. (1957). "Some limiting oxygen concentrations for diffusion flames in air diluted with nitrogen." Combustion and Flame, **1**, 155-161.

- Simms, D.L. (1960). "Ignition of cellulosic materials by radiation." Combustion and Flame, **4**, 293-300.

- Simms, D.L. (1962). "Damage to cellulosic solids by thermal radiation." Combustion and Flame, **6**, 303-318.

- Simms D.L. (1963). "On the pilot ignition of wood by radiation." Combustion and Flame, **7**, 253-261.

- Simms, D.L. and Coiley, J.E. (1963). "Some radiation characteristics of a gas fired panel." British J. Applied Physics, **14**, 292-294.

- Simms, D.L. and Law, M. (1967). "Ignition of wet and dry wood by radiation." Combustion and Flame, **11**, 377-388.

- Simms, D.L., Law, M., Hinkley, P.L. and Pickard, R.W. (1957). "The effect of size of irradiated area on the spontaneous ignition of materials." Fire research Note, No.307.

- Simms, D.L. and Miller, J. (1955). "Some characteristics of a gas fired panel." Fire Research Note, No.217.

- Smith, W.K. and King, J.B. (1970). "Surface temperature of materials during radiant heating to ignition." J. Fire and Flammability, **1**, 272-288.

- Spalding, D.B. (1955). "Some Fundamentals of Combustion.", Butterworths, London.

- Stokes, H.N. and Weber, H.C.P. (1917). "Effects of heat on celluloid and similar materials." Technologic papers of the Bureau of Standards, No.98.

- Tewarson, A. and Pion, R.F. (1976). "Flammability of plastics. I Burning intensity." Combustion and Flame, **26**, 85-103.

- Tewarson, A. and Pion, R.F. (1978). "The flammability characterisation of polymeric materials - I piloted ignition." Factory Mutual Research Serial, U1 1A6R1 RC.

- Thomson, H.E. and Drysdale, D.D. (1987). "Flammability of plastics. I Ignition temperatures." Fire and Materials, **11**, 163-172.

- Troitzsch, J. (1982). "International Plastics Flammability Handbook." Hanser Publishers, Munich.

- U.K. Fire Statistics (1984). Home Office, London.

- Walton, W. and Twilley, W. (1984). "Heat release and mass loss rate

measurements for selected materials." NBSIR 84-2960, 1984.

- Weatherford, W.D. and Sheppard, D.M. (1965). "Basic studies of the mechanism of ignition of cellulosic materials." 10th Symposium (International) on Combustion, p.897-910, The Combustion Institute, Pittsburgh.

- Welker, J.R. (1970). "The pyrolysis and ignition of cellulosic materials: A literature review." J. Fire and Flammability, **1**, 12-29.

- Wichman, I.S. (1986). "A model describing the steady state gasification of bubble-forming thermoplastics in response to an incident heat flux." Combustion and Flame, **63**, 217-229.

- Williams, C.C. (1953). "Damage initiation in organic materials exposed to high intensity thermal radiation." Massachusetts Institute of Technology, Fuels Research Laboratory, Technical Report No.2, Cambridge, Mass.

- Wraight, H.G. (1971). "A robust heat flux meter for use in experimental fires." J. Physics E., **4**, 786

- Zabetakis, M.G. (1965). "Flammability characteristics of combustible gases and vapours." U.S. Bureau of Mines, Bulletin 627.